UNCLASSIFIED

AD 444184

DEFENSE DOCUMENTATION CENTER

FOR

SCIENTIFIC AND TECHNICAL INFORMATION

CAMERON STATION, ALEXANDRIA, VIRGINIA

UNCLASSIFIED

FINAL REPORT ON ADVANCED ANTENNA

DESIGN TECHNIQUES

1 JUNE 1962 THROUGH 30 SEPTEMBER 1963

GER 11246
Report No. 4

11 October 1963
Copy No. 11

Contract DA-36-039 SC-90746

DA Project No. 3A99-12-001

U. S. Army Electronics Research and Development Laboratory
Fort Monmouth, New Jersey

GOODYEAR AEROSPACE CORPORATION

AKRON, OHIO

FINAL REPORT ON ADVANCED ANTENNA DESIGN TECHNIQUES

1 JUNE 1962 THROUGH 30 SEPTEMBER 1963

GER 11246 — 11 October 1963
Report No. 4 — Copy No. ____

Prepared by

D. D. Collins and J. C. Bell Jr.

Contract DA-36-039 SC-90746
and Modification No. 1 Dated 6 Sept 1963

Signal Corps Technical Requirements No. SCL-4346
dated 23 October 1961, as amended by Contract
Article I - Statement of Work dated 31 May 1962

DA Project No. 3A99-12-001

U. S. Army Electronics Research and Development Laboratory
Fort Monmouth, New Jersey

GOODYEAR AEROSPACE CORPORATION

AKRON, OHIO

Objective: To assess the particular needs of two broad categories of application (1) space vehicle antennas and (2) ground-based tracking antennas, and to conduct design studies leading to the generation of new concepts, materials, techniques, and practical designs for lightweight and economical antenna systems. To demonstrate the feasibility of the three most promising concepts with suitable models.

TABLE OF CONTENTS

TABLE OF CONTENTS (Continued)

TABLE OF CONTENTS (Continued)

LIST OF ILLUSTRATIONS

LIST OF ILLUSTRATIONS (Continued)

REF ENGINEERING PROCEDURE S 017

LIST OF ILLUSTRATIONS (Continued)

LIST OF ILLUSTRATIONS (Continued)

LIST OF ILLUSTRATIONS (Continued)

LIST OF ILLUSTRATIONS (Continued)

LIST OF ILLUSTRATIONS (Continued)

LIST OF TABLES

PART 1. PURPOSE

The purposes of this contract are to assess the particular needs of two broad categories of antenna applications, (1) space vehicle (satellite) antenna systems and (2) ground-based tracking antennas including radomes, and to conduct design studies leading to the generator of new concepts, materials, techniques, and practical designs for lightweight and economical antenna systems. These studies will lead to the design and fabrication of models for the three most promising concepts, which will be utilized to demonstrate feasibility of these concepts.

For space vehicle antenna systems, the goal is to develop concepts and practical designs for large aperture appendage arrays and discrete radiators which will provide the best stowage to final dimension ratio, lowest possible weight, and lowest cost.

For ground-based tracking antennas, the goal is to develop concepts and practical designs for large aperture collimators, large arrays, and sub-array elements of minimum weight and low cost which can be simply and economically assembled and erected on site.

This program effort was broken down into six discrete phases as follows:

<u>Phase I - System Parameter Investigation</u>

This phase established the system parameters for antenna designs consistent with the specified requirements. Specifically, this phase established the size of the antennas to be studied as well as the power requirements, the environmental conditions, and the structural design parameters.

Phase II - Concept Generation and Preliminary Evaluation

During this phase, various antenna system concepts were generated and given a preliminary evaluation. The concepts that appeared most desirable from the standpoint of meeting the established requirements and economy were selected for further study. This phase essentially represented the most creative part of the program. Many concepts were considered which include completely new approaches to the problem as well as new advances to the present state-of-the-art.

Phase III - Preliminary Analysis and Concept Selection

During this phase, the concepts selected for further study in Phase II were given a preliminary analysis. Based on this analysis, the space and ground concepts were further weeded out until only the most promising of each remained. From these, one space vehicle antenna concept and two ground-based antenna concepts were selected for detail design study, analysis, and model fabrication.

Phase IV - Detail Study and Analysis

During this phase, a more detail study and analysis of the selected concepts were made. Study and analysis included electrical design, performance and accuracy aspects, structural analysis, and detail mechanical and structural design considerations. Also, materials and fabrication techniques were investigated during this phase.

Phase V - Models

During this phase, models of the three selected designs, consisting of one space vehicle antenna and two ground-based antennas, were designed, fabricated and evaluated. These models were designed and fabricated for purposes of adequately demonstrating the feasibility of all unique or advanced state-of-the-art techniques or concepts employed.

Phase VI - Reports

The reporting was carried out concurrent with Phases I through V and included 10 monthly letter-type reports, three formal quarterly reports, and one formal final report as required by the contract.

Figure 1 shows the work program broken down into phases and shows the time span utilized for each phase.

The following programs related to the objectives of this contract were under way at Goodyear Aerospace Corporation during the course of the program:

(1) Goodyear Aerospace supported development program to evaluate foams and their application techniques in conjunction with process improvement for utilization of foams for producing antenna reflector surfaces. Strength, dimensional stability, and durability required for antenna reflector surfaces were considered.

(2) Goodyear Aerospace supported process development program to perfect and evaluate a technique for producing very accurate contoured antenna reflector surface by applying exothermic plastic material in thin layers over a rough reflector surface, utilizing a precision tool sweep method. The final reflective surface will be obtained by metal spraying or application of reflective paint to the hardened plastic surface.

(3) U.S. Air Force - RADC Contract AF30(602)2753 Pseudo-Hardened Emergency Antenna Installation - Study Program. The purpose of this study program was to determine the feasibility of an air-supported, integrated radome-antenna configuration wherein a portion of the surface of the air-supported radome serves as the antenna reflector requiring rotation of only the feed system for scanning operation. This

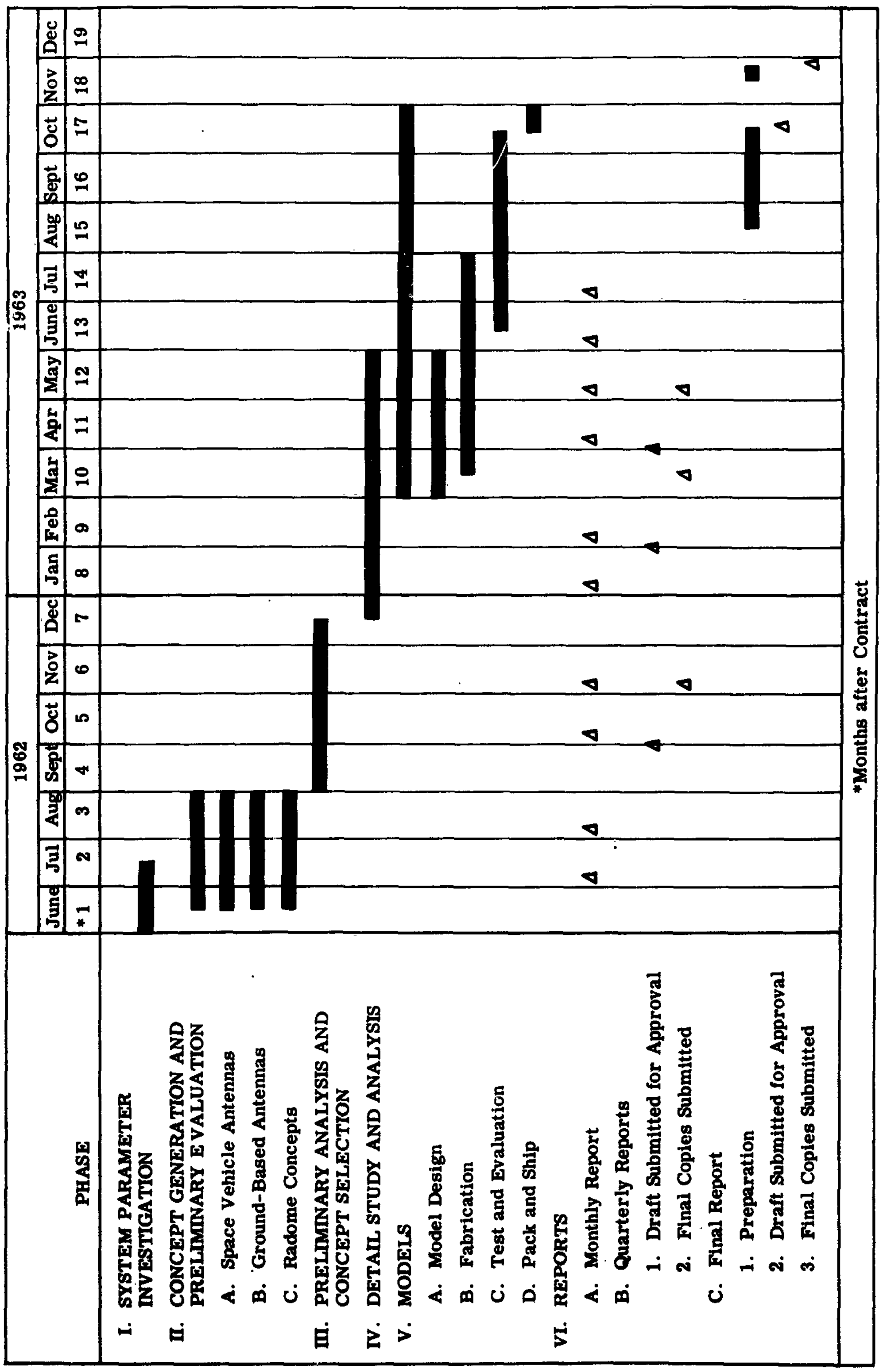

Figure 1. Work Program for Advanced Antenna Design Study Program

program involved design, fabrication, and antenna pattern testing of a scale model and development of design data for a full-scale concept.

(4) Contract with Airborne Instruments Laboratory to manufacture and erect two 17-foot diameter polyurethane foam radomes for use with airport ground control radar equipment.

(5) Goodyear Aerospace supported general design and application study program to prove feasibility and to establish general design criteria for microwave structures and antennas for space applications. The study is being supported with feasibility models and testing of materials, structures, rigidization techniques, and electrical characteristics.

(6) Subcontract with Sundstrand Corporation to design and produce an experimental preprototype 44.5-foot diameter solar collector for USAF Prime Contract AF33(616)-7128. The object of this program is to design and produce an inflatable foam-rigidized parabolic solar concentrator of flight prototype size. The preprototype model is intended for optical evaluation and testing under ground environmental conditions; however, the design approach will be such as to permit early development to meet space application requirements.

(7) U.S. Air Force - ASD Contract AF33(657)-10165 Solar Reflector Foaming Technology Program. A study and investigation of the technology for foaming solar reflectors in space environment.

(8) Goodyear Aerospace supported theoretical study program to develop new design criteria for very high performance reflector antennas. The objectives of this program are to establish detail design criteria for optimum feed illumination for minimum achievable side lobes, blockage effects, and interrelation of these with tolerances.

PART 2. ABSTRACT

This final report covers the entire advanced antenna design techniques study program. Space vehicle antenna systems and ground-based tracking antenna system parameters were studied, and requirements were established as design goals. Various types of antenna configurations were investigated to meet the established requirements. Those concepts appearing most desirable for meeting these requirements were evaluated and compared. Selection for further study was made to determine the three most promising concepts consisting of one space antenna and two ground-based antennas. Detail design, structural aspects, and performance for the three selected antennas were studied. New material applications were investigated, and new manufacturing techniques were developed. Design and fabrication of three models and evaluation of these to demonstrate the feasibility of the selected concepts are described.

Twelve space vehicle antenna concepts representing a wide range of types were investigated and evaluated from the standpoints of weight, cost, packageability, and advancement of erectable or expandable techniques. Seven concepts consisting of inflatable and expandable pencil-beam and fan-beam antennas were selected for further study. The study showed that the inflatable lenticular antenna, the inflatable paraboloid antenna, and the foldable metallic antenna (rigid-panel Swirlabola*) had the best potential over the maximum range of applicability. However, since similar inflatable antenna types were being studied for ground-based antennas, the rigid-panel Swirlabola was selected for the space antenna detail design study and model fabrication.

*A parabolic antenna reflector having petal-like reflector elements that unfold in a "swirl" fashion to form the parabolic reflector shape.

A 10-foot diameter, full-scale design was studied for space application, and a 3-foot diameter model was designed, fabricated, and evaluated. Evaluation of the model indicates that the folding petal (Swirlabola) concept was structurally and mechanically feasible, practical to manufacture, and capable of being deployed in space and of providing performance comparable to a rigid, close-tolerance parabolic reflector. It also has the unique capability of being quickly and easily folded into a reduced size cylindrical package for stowage within a space vehicle. Also, this antenna concept can be adapted for ground applications to provide a transportable, quick-erecting, ground antenna.

Twenty-two ground-based antennas concepts were studied, and nine of these having the best potential for meeting the program objectives were selected for further study, analysis, and evaluation. These consisted of inflatable reflector types, foam-rigidized reflector types, foldable-truss types, multiple-reflector arrays, and a circular hog-horn configuration. The nine antenna types were evaluated and compared with each other and with the Syncom antenna system relative to cost, packageability, weight, mobility, simplicity of erection, accuracy, performance, and growth potential. The inflatable paraboloid antenna and the inflatable lenticular antenna were selected for detail design study and model fabrication.

These two inflatable antenna designs were studied as Cassegrainian systems in sizes up to 40 feet in diameter. The studies included the structural, mechanical, and electrical design, and the fabrication of five-foot diameter scale models. A particular effort was made which resulted in the successful development of a flexible foldable r-f reflective surface as well as fabrication techniques of applying an accurately contoured flexible foam surface to the inflatable antenna structure.

The evaluation of the two inflatable antenna models demonstrated their capability of providing quickly erectable, lightweight, packageable antennas that will retain the desired parabolic shape when pressurized. Limited packaging and inflation tests have shown that these inflatable antennas can be packaged into a relatively small volume and reinflated and retain their original contour with no damage to the reflective surface.

To capitalize on these recent antenna developments, Goodyear Aerospace recommends that the next logical phase of the development will be to optimize the materials and fabrication techniques to be used in the design and fabrication of a larger prototype antenna model that can adequately demonstrate the electrical performance capabilities. In addition, this prototype should also demonstrate the packaging and erection capabilities under anticipated operational environmental conditions.

PART 3. PUBLICATIONS, LECTURES, REPORTS, AND CONFERENCES

A. CONFERENCES

A conference was held at Goodyear Aerospace on 27 June 1962 with Mr. F. J. Triolo,of the Asto Electronics Division of USAERDL, and Goodyear Aerospace engineering representatives. The purpose of the meeting was to present Goodyear Aerospace program organization and the planned approach for carrying out the program, and to resolve questions that had come up as a result of a detail review of the technical requirements.

The following points were generally agreed upon:

(1) The Syncom specification would be used as a general guide for ground-based tracking antenna requirements.

(2) Ground-based antenna types would receive the major emphasis throughout the program.

(3) This program would attempt to establish the relationship between system costs and system accuracies.

(4) High emphasis would be placed on light weight, quick and simple erection, transportability, and low cost.

(5) Models would be tested to demonstrate concept feasibility. Antenna pattern testing is considered beyond the scope of this program and therefore is not planned as a part of this program.

A conference was held at Goodyear Aerospace on 25 September 1962 with Mr. F. J. Triolo and Mr. F. Kansler, of the Astro Electronics Division of USAERDL, and Goodyear Aerospace engineering representatives. The purpose of the meeting was to review the results of the first quarter's work on the program, which included Phases I and II.

The established system parameters were reviewed. Also, the space vehicle and ground-based antenna concepts were reviewed in detail. The method for comparison and evaluation of the various antenna concepts was reviewed, and it was agreed that the Syncom antenna would be used as a basis or norm for evaluation of the ground-based concepts.

A conference was held at the U. S. Army Electronics Research and Development Laboratory, Fort Monmouth, New Jersey, on 19 December 1962 with Mr. F. J. Triolo and Mr. F. Kansler, of the Astro Electronics Division of USAERDL, and W. B. Koller, J. C. Bell Jr., and D. D. Collins, Goodyear Aerospace engineering representatives. The purpose of the meeting was to review the results of the second quarter's work on the program consisting of Phase III - Preliminary Analysis and Concept Selection.

The design configurations of the various space vehicle and ground-based antenna concepts were reviewed in detail. The procedure and results of the concept evaluation and selection were reviewed. Tentative selection of the rigid-panel Swirlabola space antenna and two inflatable AIRMAT* ground-based antennas for further detail study and model consideration was agreed upon. It was also agreed that ground-based antenna pedestal structures and drives would not be studied extensively, since most of the antenna concepts being considered could be adapted to utilize existing equipment such as the Syncom trailer-mounted pedestal and drive.

A conference was held at Goodyear Aerospace on 2 April 1963 with Mr. F. J. Triolo, of the Astro Electronics Division of USAERDL, and Goodyear Aerospace engineering representatives. The purpose of the meeting was to review the

*TM, Goodyear Aerospace Corporation, Akron, Ohio results of the third quarter's work on the program. The design analysis and design configuration for the full-scale and demonstration scale model space system Swirlabola antenna and the ground-based inflatable paraboloid and lenticular antennas were reviewed in detail. Model fabrication in process at the time was inspected. The desirability of continued effort, subsequent to the present program, to include electrical performance and environmental testing was discussed. It was agreed that Goodyear Aerospace would submit an unsolicited proposal for a recommended test program to determine and demonstrate the electrical performance and environmental capabilities of the inflatable ground-based antennas developed on the current program.

B. LECTURES

A paper entitled "Lightweight Erectable Space Antennas" (GER 11148) was presented at the International Symposium of the IEEE Professional Group on Antennas and Propogation held at Boulder, Colorado, on 9 July 1963 by James Roth, Goodyear Aerospace Corporation. Material for the paper, which was derived from this study contract, was approved by USAERDL prior to the presentation.

C. REPORTS

Progress charts showing forecast of monthly expenditures by principal elements of cost were submitted to the Signal Corps on 29 June 1962. Reference GAC letter X51-E58 of 29 June 1962.

The first monthly letter report was submitted to the Signal Corps on 3 July 1962. Reference GAC letter X51-Y1283 of 3 July 1962.

The second monthly letter report was submitted to the Signal Corps on 3 August 1962. Reference GAC letter X51-E-161 of 3 August 1962.

The first quarter financial report, DD-1097 Report, was submitted to the Signal Corps on 24 September 1962. Reference GAC letter X51-G7235 of 24 September 1962.

Draft copies of the first quarterly progress report (GER 10814) were submitted to the Signal Corps for review and approval on 1 October 1962. Reference GAC letter X51-A496 of 1 October 1962.

The third monthly letter report was submitted to the Signal Corps on 5 October 1962. Reference GAC letter X52-E338 of 5 October 1962.

The financial report, DD-1097 Report, for September 1962 was submitted to the Signal Corps on 19 October 1962. Reference GAC letter X51-Y1858 of 19 October 1962.

The fourth monthly letter report was submitted to the Signal Corps on 6 November 1962. Reference GAC letter X52-C495 of 6 November 1962.

Final approved copies of the first quarterly report (GER 10814) were distributed on 29 November 1962. Reference GAC letter X51-E462 of 26 November 1962.

The financial report, DD-1097 Report, for November 1962 was submitted to the Signal Corps on 26 December 1962. Reference GAC letter X51-AH1636 of 26 December 1962.

The fifth monthly letter report was submitted to the Signal Corps on 5 January 1963. Reference GAC letter X52-Y2236 of 5 January 1963.

The second quarter financial report, DD-1097 Report, was submitted to the Signal Corps on 24 January 1963. Reference GAC letter X51-Q209 of 24 January 1963.

Draft copies of the second quarterly progress report (GER 10979) were submitted to the Signal Corps for review and approval on 30 January 1963. Reference GAC letter X51-G7536 of 30 January 1963.

The sixth monthly letter report was submitted to the Signal Corps on 7 February 1963. Reference GAC letter X51-Q278 of 7 February 1963.

The financial report, DD-1097 Report, for January 1963 was submitted to the Signal Corps on 20 February 1963. Reference GAC letter X51-Q338 of 20 February 1963.

Final approved copies of the second quarterly report (GER 10979) were distributed on 8 March 1963. Reference GAC letter X51-Y2713 of 8 March 1963.

The financial report, DD-1097 Report, for February 1963 was submitted to the Signal Corps on 20 March 1963. Reference GAC letter X51-Y2793 of 20 March 1963.

Draft copies of the third quarterly progress report (GER 11045) were submitted to the Signal Corps for review and approval on 29 March 1963. Reference GAC letter X51-Y2859 of 29 March 1963.

The seventh monthly letter report was submitted to the Signal Corps on 9 April 1963. Reference GAC letter X51-S89 of 9 April 1963.

The financial report, DD-1097 Report, for March 1963 was submitted to the Signal Corps on 15 April 1963. Reference GAC letter X51-S111 of 15 April 1963.

The eighth monthly letter report was submitted to the Signal Corps on 9 May 1963. Reference GAC letter X51-Y3109 of 9 May 1963.

Final approved copies of the third quarterly progress report (GER 11045) were distributed on 10 May 1963. Reference GAC letter X51-Y2713 of 10 May 1963.

The financial report, DD-1097 Report, for April 1963 was submitted to the Signal Corps on 20 May 1963. Reference GAC letter X51-S331 of 20 May 1963.

The ninth monthly letter report was submitted to the Signal Corps on 7 June 1963. Reference GAC letter X51-0114 of 7 June 1963.

The financial report, DD-1097 Report, for May 1963 submitted to the Signal Corps on 19 June 1963. Reference GAC letter X51-0163 of 19 June 1963.

The tenth and last monthly letter report was submitted to the Signal Corps on 9 July 1963. Reference GAC letter X51-Z5049 of 9 July 1963.

The financial report, DD-1097 Report, for June 1963 was submitted to the Signal Corps on 23 July 1963. Reference GAC letter X51-AF22 of 23 July 1963.

The financial report, DD-1097 Report, for July 1963 was submitted to the Signal Corps on 28 August 1963. Reference GAC letter X51-T3161 of 28 August 1963.

PART 4. FACTUAL DATA

SECTION I. INTRODUCTION

This study and investigation program has covered two broad categories of antenna application: (1) space vehicle (satellite) antenna systems and (2) ground-based tracking antennas including radomes. The program effort was broken down into the six phases described in Part 1:

Phase I - System Parameter Investigation
Phase II - Concept Generation and Preliminary Evaluation
Phase III - Preliminary Analysis and Concept Selection
Phase IV - Detail Study and Analysis
Phase V - Models
Phase VI - Reports

The studies, investigations, and analyses have involved a somewhat parallel effort for the space vehicle and ground-based antenna systems in each phase of the work, with the major emphasis being placed on ground-based antennas. System parameters were investigated, and requirements were established as design goals. Various types of antenna configurations were investigated to meet these requirements. The concepts appearing most desirable for meeting the established requirements were evaluated and compared. Selection of the three most promising concepts was ultimately made, consisting of one space antenna and two ground-based antennas. Detail design, structural aspects, and performance of the three selected configurations were studied. Materials investigations and manufacturing techniques development were carried out. Scale models were designed, fabricated, and evaluated to demonstrate the feasibility of the selected concepts.

For better continuity of the subject matter, the factual data for the space vehicle antennas and the ground-based antennas are presented separately. Space vehicle antennas are covered in Sections II through VI, and ground-based antennas are covered in Sections VII through XI. Specific reference to the program phases has been omitted in this part of the report for clarity and for a more logical sequence, since the final results are independent of the phase of effort.

PART 4. FACTUAL DATA

SECTION II. SPACE VEHICLE ANTENNA SYSTEM PARAMETERS

A. GENERAL

To establish system parameters, the program technical requirements as specified in SCL-4346, dated 23 October 1961, were reviewed in detail along with the requirements for other space antenna systems. Tentative parameters and requirements, including frequency, environmental, mechanical, and electrical requirements, were established for space antennas. These requirements are considered general design goals and may change for specific antenna types or for a particular application.

B. SPACE VEHICLE ANTENNA SYSTEM REQUIREMENTS

Specific requirements are dependent upon the mission of the vehicle, the usage and performance requirements of the particular antenna system, and the configuration of the vehicle. Since these factors are not specified, no attempt was made to define specific detailed requirements. However, the following general requirements were established:

Frequency	1 to 10 kmc
Power (maximum)	100 watts
Size	4 to 30 feet, if appendage
Aperture Efficiency	At least 55 percent
Life	10, 000 hours

Space Temperature Limits . . . . A function of coatings and/or colorings:

+225°F desired to photolyze films

-200°F for wire in earth's shadow

Packaging Factor. . . . . Approximately 5 times molten vol, for wire/film

Surface Accuracies . . . . for 1 kmc: $\lambda/10 = \pm\ 1.18$ in. *

for 10 kmc: $\lambda/10 = \pm\ 0.118$ in. *

*Smaller tolerances than these (e. g., $\lambda/16$ - $\lambda/64$) primarily affect the side lobes, with minor significance for the antenna efficiency or radiated power in the main lobe. Since the side lobes are not normally as detrimental in space as in ground antennas, the surface tolerance of $\lambda/10$ is a reasonable choice for large appendage antenna reflectors. Other specific types require individual consideration.

C. SPACE VEHICLE ANTENNA MATERIALS AND ENVIRONMENT CONSIDERATIONS

1. General

In general, low ambient pressure, electromagnetic radiation, micrometeorites, and temperature extremes can contribute to the failure of an improperly designed space antenna. Consideration of these space environmental conditions in regard to material selection is discussed briefly in the following paragraphs.

2. Deployment Rigidization

The durability and usefulness of inflated space structures are greatly increased if after deployment the structures are rigidized in such a manner that it is not important to maintain the inflation pressure. One excellent technique is the use of wire rigidization of thin plastic films. The wires are spaced closely enough to appear electrically equivalent to a solid reflector at the radio frequencies in use, yet have less mass than a solid layer of metal, although adding stiffness to the structural shape. If these wires are stretched to their yield point during initial inflation, micrometeorite punctures or other deflative forces will have little effect. In many cases, it is desirable to eliminate the thin plastic film after rigidization of the structure to reduce environmental load effects. This can be accomplished by photolyzation and sublimation.

3. Low Ambient Pressure

The low ambient atmospheric pressure at altitudes above several hundred miles permits a much more rapid rate of evaporation of volatile materials than at atmospheric pressure. Since compounds with a high molecular weight have a lower vapor pressure, such materials as polyesters, e.g., Mylar, or epoxies, which have a uniformly high molecular weight, must be used for applications of long duration. For laminates of wire and photolyzable film, the adhesives used to bond the wires together for structural integrity after the film has disappeared must be carefully chosen. However, the high evaporation rate is not always a disadvantage since it permits, after antenna deployment, a fairly rapid discarding of any photolyzable film utilized.

4. Electromagnetic Radiation

By changing the chemical bonds within a substance, ultraviolet radiation on organic materials can alter the materials' physical properties. These basic changes can result in a higher or lower molecular weight of the material, depending on the basic monomers and the types of scissons that occur. The fact that ultraviolet radiation can reduce the molecular weight of certain plastic films will be used in selecting the film that is to be removed by photolyzation and sublimation.

Other types of radiation such as neutrons, X-rays, and gamma rays are relatively unimportant in deteriorating such materials as a wire grid.

5. Micrometeorites

Micrometeorites will gradually erode the wires on the antenna until the structure becomes unsound. For typical antenna structures under consideration, severance of the wires up to 25 percent is not expected to exert a significant effect on either their structural integrity or their microwave reflectance characteristics. If it is assumed that 25 percent severance of the wires will limit the operational life of a structure, conservative calculations indicate that the useful life of any of the antennas in space will be at least four years.

6. Temperature Extremes

High temperature increases the rate of change in polymeric materials and affects the tensile strength, elastic modulus, and creep-rupture properties of all materials. Therefore, the major thermodynamic considerations are (1) the temperature control required for the photolyzable film and (2) the inflation pressure control required for effective rigidization.

Surface temperatures can be determined by writing a thermal balance on an individual satellite (e.g., antenna in space) segment and on the satellite structure as a whole. The resulting equation for the maximum temperature is rather complex. For the purposes of this discussion, it is sufficient to consider the important design parameter to be the ratio of solar absorptivity (A_s) to surface emissivity (E_0).

At a temperature of $225^{\circ}F$, which is required to eliminate the film in a relatively short time, an A_s/E_0 of 1.3 is required. This can be attained by proper coloring of the film material.

The effect of temperature on the inflation pressure of the structure must be considered. Adequate stress is needed in the wire to produce yielding, but the shape must not be distorted beyond the allowable limit.

7. Other Considerations

For antennas on space vehicles at altitudes above 100 miles, the only external force is generally solar pressure. However, antenna structures with widely displaced masses have a significant torque in the structure if they are slewed rapidly and/or stopped abruptly.

The solar pressure is very small, only about 1.5×10^{-9} psi. It can be ignored as a deforming force on a wire grid antenna when the plastic film is photolyzed away, greatly reducing the absorbing and reflecting area.

Aerodynamic drag could have a very minor effect on the larger space antennas, but will also be reduced by the elimination of the plastic film. Therefore, the net effect of aerodynamic drag can be ignored over the expected effective life of the various antennas.

PART 4. FACTUAL DATA

SECTION III. SPACE VEHICLE ANTENNA SYSTEMS

A. GENERAL

Space vehicle antenna systems represent a broad area of application, depending upon the mission of the vehicle, the usage and performance requirements of the particular antenna system, and the configuration of the vehicle.

Missions could include communications, navigation, space probes, lunar base operations, space stations, reconnaissance, surveillance, meteorological satellites, early warning, space traffic control, and others.

The requirements for space antennas broadly classify four types:

(1) Broad-Coverage Antennas
(2) Medium-Beamwidth Antennas
(3) Pencil-Beam Antennas
(4) Fan-Beam Antennas

Mission time may be long or short. Loading due to gravity fields and steering may be light or severe. Type and degree of stabilization may vary. These requirements and the type of antenna would be dependent on the mission of the vehicle and the usage and performance requirements of particular antenna system. Since these are not defined for this study program, initial effort was directed toward the generation and investigation of space vehicle antenna concepts of a rather wide range of antenna types that were adaptable to expandable techniques, suitable for stowage in the space vehicle, and practical from the standpoint of

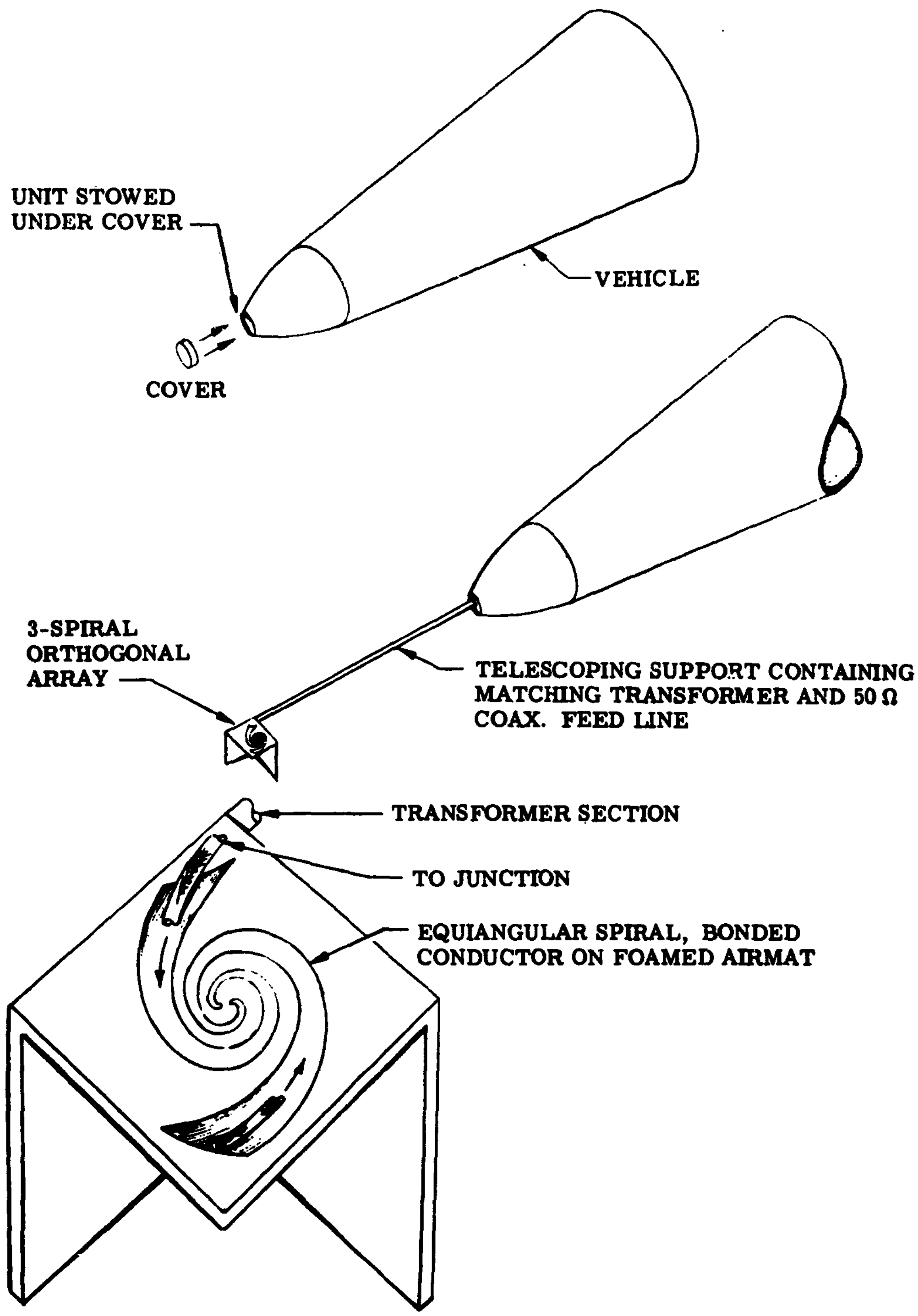

Figure 2. Broad-Coverage Three-Spiral Array

deployment in space. Pencil-beam antennas were considered to have the greatest range of applicability to the national space program and to offer the best potential for advancement of expandable techniques. For this reason, subsequent effort was concentrated on the development of concepts for expandable pencil-beam antennas.

Preliminary evaluations of the various concepts were made in regard to electrical performance and system operation. Some of the electrical performance factors considered are antenna gain and efficiency, operational frequencies, frequency bandwidths, pattern beamwidths, side lobe levels, and tolerance effects. System operation factors considered include circuit complexity, method of deployment, structural considerations, weight, and packageability.

B. SPACE VEHICLE ANTENNA CONCEPTS

1. Broad-Coverage Three-Spiral Array

This array, shown in Figure 2, consists of three equiangular, orthogonally positioned spirals. The spiral conductors are bonded or printed on an AIRMAT structural surface or a lightweight rigid-foam cube stowed within the vehicle under a blow-off cover. A broadband matching transformer section matches the function of the three spirals to a 50-ohm coaxial line. The array is deployed by extension of a telescoping support strut, which contains the coaxial feed and matching transformer. The size of a spiral array for 1 to 10 kmc frequency is a 6-inch cube, excluding the support strut. This type of array provides a pseudo-broad-coverage antenna system. Each spiral could provide circular polarization for a bandwidth of 10:1. The half power beamwidth of each spiral is approximately 80 degrees. The gain is approximately 0 db.

2. Medium-Beamwidth Antennas

a. Four-Helix Array. The four-helix array, shown in Figure 3, consists of a broadside array of four helical antennas supported above an aluminum ground

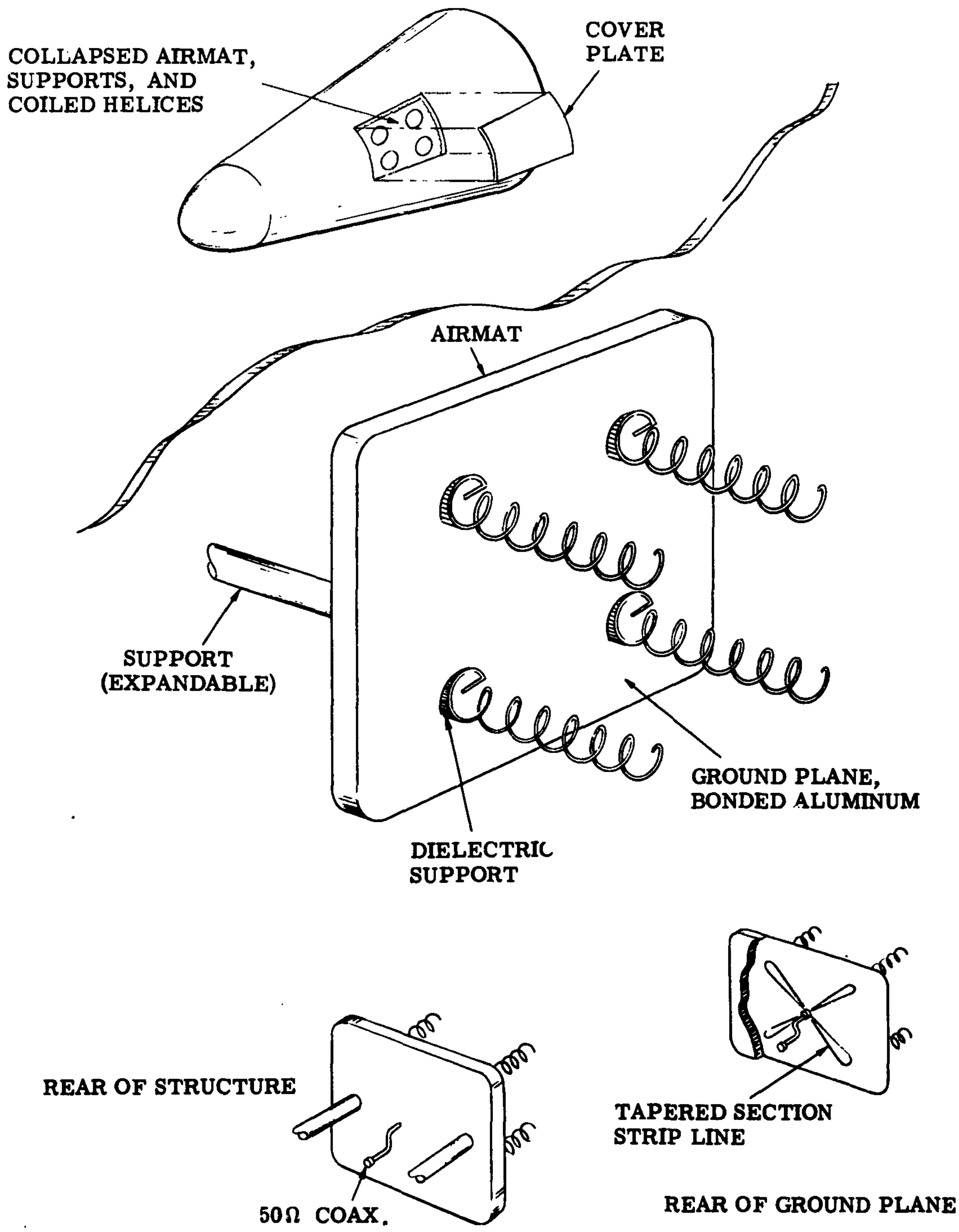

Figure 3. Four-Helix Array

plane which in turn is supported by an AIRMAT expandable structure. The input circuit consists of a coaxial feed connected to a strip-line transformer mounted at the back of the ground plane. This array is considered suitable for frequencies from 1 to 4 kmc. For 1 kmc the ground plane is 36 x 36 inches. The helices are 18 inches long with six turns. The array is stowed inside the vehicle under a cover plate. For deployment the cover plate is blown free, releasing the coiled helices, which spring into position. The unit is extended on foamed or telescoping supports at which time the AIRMAT support is inflated and foam-rigidized.

This array provides an antenna of medium beamwidth (20 degrees at half power), moderate gain (15 db) for frequencies from approximately 1 to 4 kmc. Above 4 kmc, the performance is degraded by tolerance effects and could be more suitably replaced with the conical horn concept described in paragraph b. The bandwidth is approximately 2:1 for both a suitable field pattern and impedance match. Radiated power is more than 90 percent of power input. Side lobe level is approximately 10 db.

Advantages are simplicity of structure and rather wide tolerance on all but the strip-line sections, which are the most critical items. The array may be oriented for circular or linear polarization. However, at look angles off the main beam axis, the ellipticity of circular polarization rapidly increases.

b. Conical Horn. This concept utilizes an expandable horn structure that may be formed into shape by any of the three methods of construction and deployment shown in Figure 4. The following methods are shown in Figure 4:

(A) Wire mesh horn whose aperture perimeter is attached to the inner surface of an inflatable sphere. Prior to launch, the horn and sphere are collapsed and stowed. For deployment, the sphere is inflated, stretching the wire mesh horn sufficiently to take a

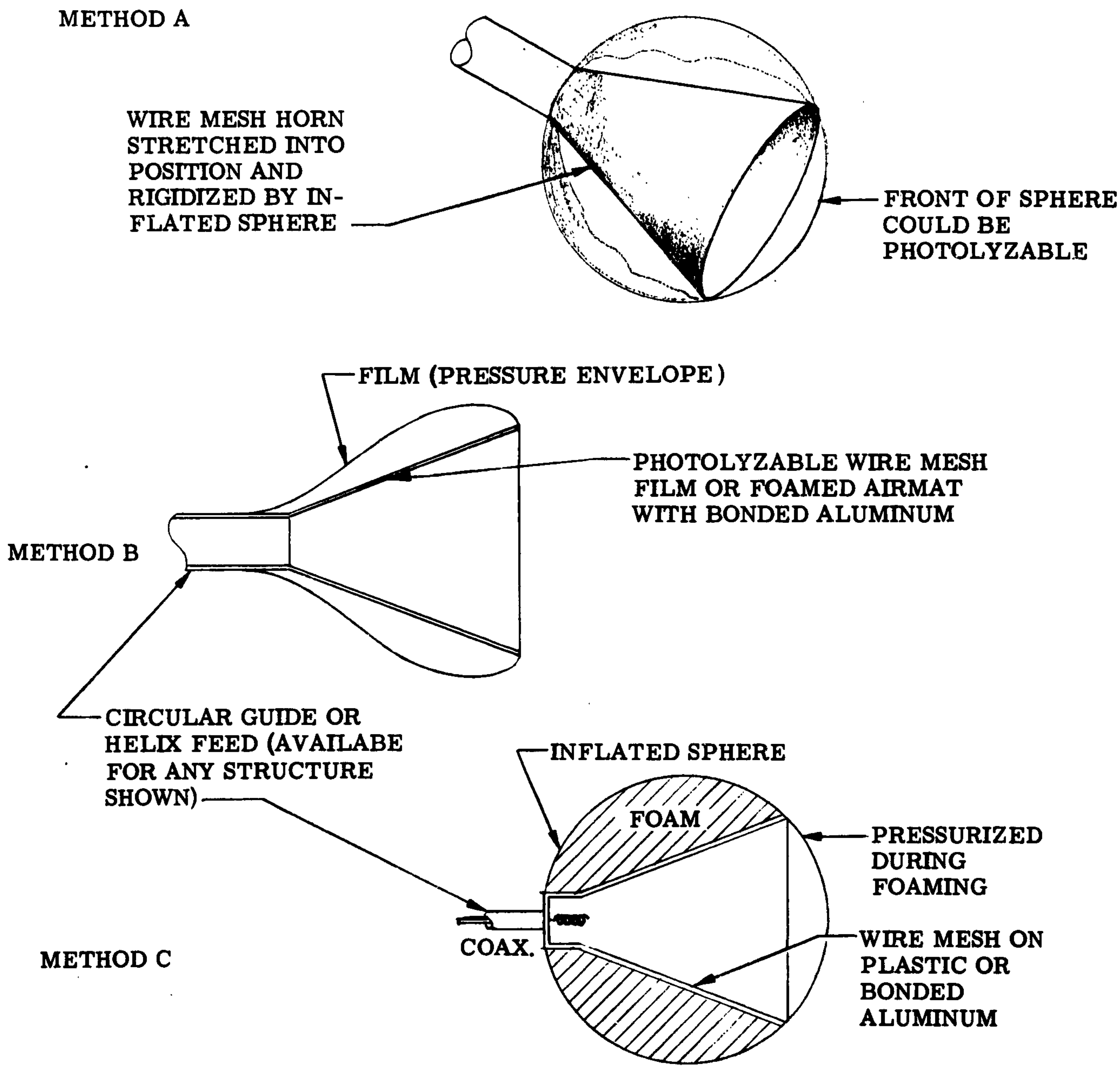

NOTE: ALL MAY BE PACKED IN ODD SHAPE PRIOR TO ERECTION.

Figure 4. Conical Horn

permenent set in position. The portion of the sphere covering the aperture of the horn may be photolyzable. The remainder of the sphere is of no consequence after horn erection.

(B) Horn-shaped structure with conducting surface on the inside to form a conical horn. The structure may be photolyzable wire mesh film on the inner surface and photolyzable film on the outer surface. An alternate structure, an example of which has been developed at Goodyear Aerospace, would be AIRMAT construction with bonded aluminum for the conducting surface. Either would be inflated from an irregularly shaped stowed position.

(C) Foamed horn whose aperture perimeter is attached to the inner surface of the sphere. The volume of the cone would be pressurized while foaming the volume between the cone and sphere to aid in maintaining the cone's shape. The cone's conducting surface may be wire mesh on plastic or bonded aluminum. After erection, the surface over the cone's aperture may be photolyzed.

The conical horn structures can be used from 1 to 10 kmc. From 1 to 4 kmc, a helical antenna can be used to excite the horn. Circular guide can be used over the 1 to 10 kmc range for producing either circular or linear polarization. Circular polarization with a circular guide limits the bandwidth to approximately 1.15 to 1; the other methods allow a bandwidth of approximately 1.5 to 1. Added circuit complexity is required by the circular guide - circular polarization combination, which requires a phase shifter. For 16 db gain, horn diameter and length are approximately 3 λ by 3λ or approximately 36 x 36 inches for 1-kmc frequency.

Advantages are simplicity of structure and rather wide tolerance, light weight, and small storage space requirements. The field pattern can be designed to have essentially no side lobes for a 36-inch-length horn with 16-db gain. The horn can be used either as an individual radiator, as an element of an array, or as the feed for a reflector.

c. Parabolic Cylinder. This antenna consists of a cylindrical parabolic surface reflector formed onto a section of the inner skin of the space vehicle with a line source slotted wave guide feed positioned just under the skin of the vehicle (see Figure 5). For erection, the reflecting surface merely swings out into position. An off-set feed could be used to minimize blockage. This system could be used for a pencil beam in one plane and either a pencil beam or broad beam in the other plane. Power gain for a 9-inch-wide, 4-foot-long reflector would be approximately 23 db at 3 kmc and 33 db at 10 kmc. The recommended frequency range for this reflector would be approximately from 3 to 10 kmc for the reflector, since the gain drops and the pattern broadens to an unsuitable degree at lower frequencies. A wider reflector could be used down to 1 kmc. The bandwidth of this system would be limited by the slotted wave guide feed and would be approximately 1.2:1. However, no other circuit components would be required other than the slotted wave guide feed.

3. Fan-Beam Antennas

a. Expandable Fan Beam. This concept, shown in Figure 6, provides an expandable antenna that is packaged as a part of the space vehicle payload and can be deployed in orbit. Each antenna has a cylindric-parabolic shape 20 to 40 feet in length and 10 to 50 feet in width.

The antenna is packaged for launch within the limits of a cylindrical envelope approximately 2 feet in diameter and 20 feet long and is mounted on the outer wall of the space vehicle.

The antenna design employs a solid metal parabolic rim (three places) that establishes the contour and supports the reflecting surface. These rims are

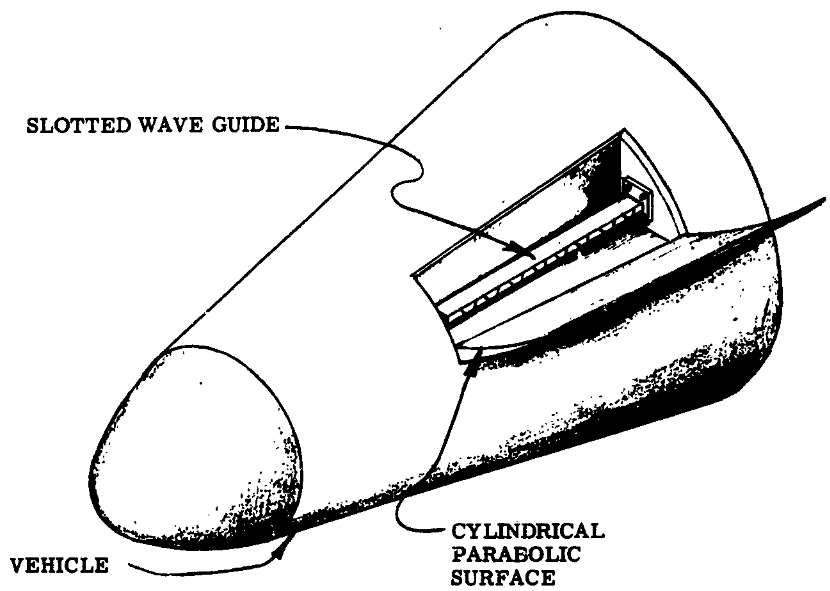

Figure 5. Parabolic Cylinder

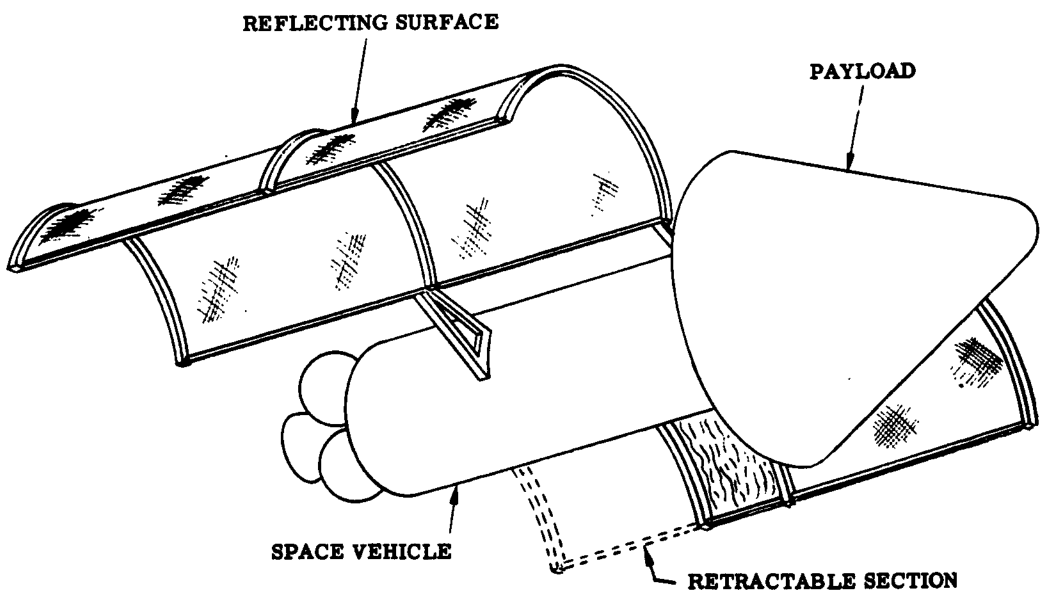

Figure 6. Expandable Fan-Beam Antenna

designed as a bow so that, when the ends are fixed a specified distance apart, the bow takes the desired parabolic shape. This is achieved by properly tailoring the cross sectional area of the bow. Two of the rims are held a fixed distance apart (approximately 20 feet) by three metallic tubes equally spaced around the parabola, and the third rim is extendable by three telescoping rods, thus permitting the 40-foot reflector length to be reduced to approximately 20 feet for packaging within the available space. The reflector material is considered to be a lightweight wire screen, 2 to 5 mil wire, supported on a photolyzable film. A slotted wave guide line source feed is envisioned, which would be of sufficient length to illuminate the extended length of the reflector. This would probably require employment of extendable or folding techniques. To package for launch, each reflector is "telescoped," coiled into a loose roll, and contained in a three-section jettisonable container. This type of antenna is suitable for operation over a frequency range from 1 to 10 kmc. The bandwidth of a particular antenna would be limited by the slotted wave guide feed and would be approximately 1.2:1. Gain would be approximately 33 db at 3 kmc.

b. Fan-Beam Pillbox. A "pillbox" antenna has the characteristics of a distinct and predictable fan-beam radiation pattern over a medium bandwidth of the base band (2 to 3 percent with moderate feed impedance variation) and can be scaled to operate anywhere within the 1 to 10 kmc region of interest. This concept, shown in Figure 7, consists of two parabolic reflectors formed by metal bows with flat parallel flexible wire mesh side panels. The bows provide spring tension to keep the flat parallel side panels straight and true. Bottom tension of the sides is maintained by inflated, wire-rigidized tubes, which also establish the desired flare of the aperture.

For storage, each antenna is coiled on a storage drum and restrained by a

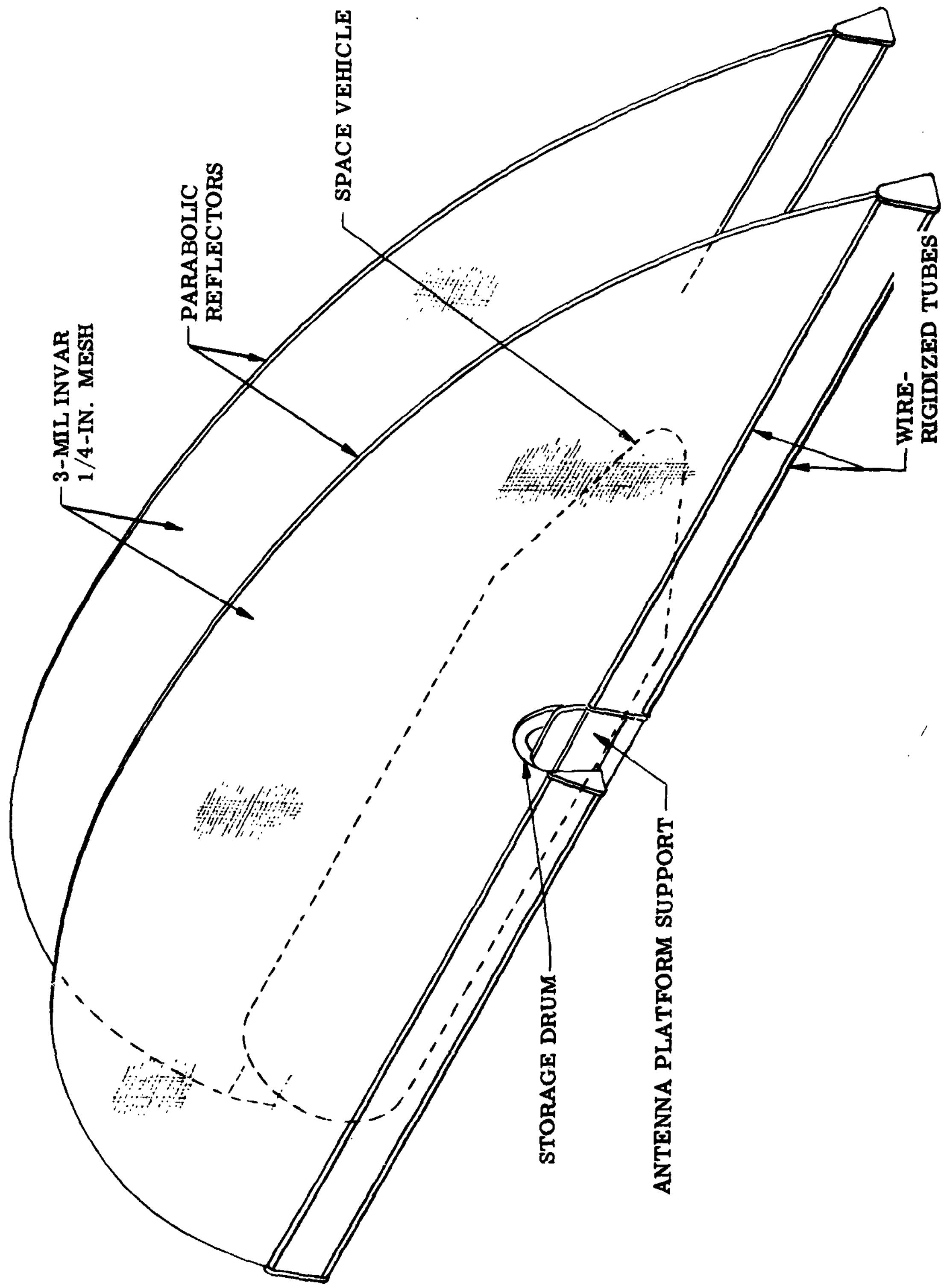

Figure 7. Fan-Beam Pillbox Antenna

jettisonable cover. The drum structure provides a rigid mount for the r-f feed and also serves as a support mount for the deployed antenna. For deployment, the drums are extended out from the sides of the space craft by air-motor rotation of an axial ball screw. The antennas are then automatically unfurled after release from the drum by spring action of the metal rims.

The bandwidth is limited by the feed to 25 percent or better of the base frequency band. The beamwidth would be approximately 1 degree along the long axis of the aperture and 14 degrees perpendicular to the antenna. For 10 kmc, the antenna would be approximately 50 feet wide, 12-1/2 feet high with 3 inches between the parallel faces, flaring to 10 inches at the aperture.

4. Pencil-Beam Antennas

a. Inflatable Torus-Supported Paraboloid (Pressure-Supported). This concept, shown in Figure 8, is a pencil-beam antenna consisting of an inflatable envelope having a parabolic face on one side, which serves as the reflector. The other face is a curved surface that closes the inflatable envelope and provides a cover for the feed. The envelope is supported at the periphery by an inflated torus, which in turn is supported by a tripod structure. The reflecting surface can be aluminized Mylar, wire grid, or reflective paint. This antenna depends on internal pressure to maintain rigidity.

The inherent tolerances for this type of antenna are in the order of ±0.25 to ±0.375 inch, the lowest accuracy for the space antennas being considered. This antenna is characterized by its applicability to only short-term missions, due to internal pressure requirement and to low steering load limitation. However, weights in the order of 0.15 to 0.25 lb/ft^2 of surface area can be achieved. Packaging ratios (ratio of packaged volume to total material volume) of about 3:1 are practical with this type of antenna. The weight includes the support and steering mechanism. Common f/D ratios are obtainable.

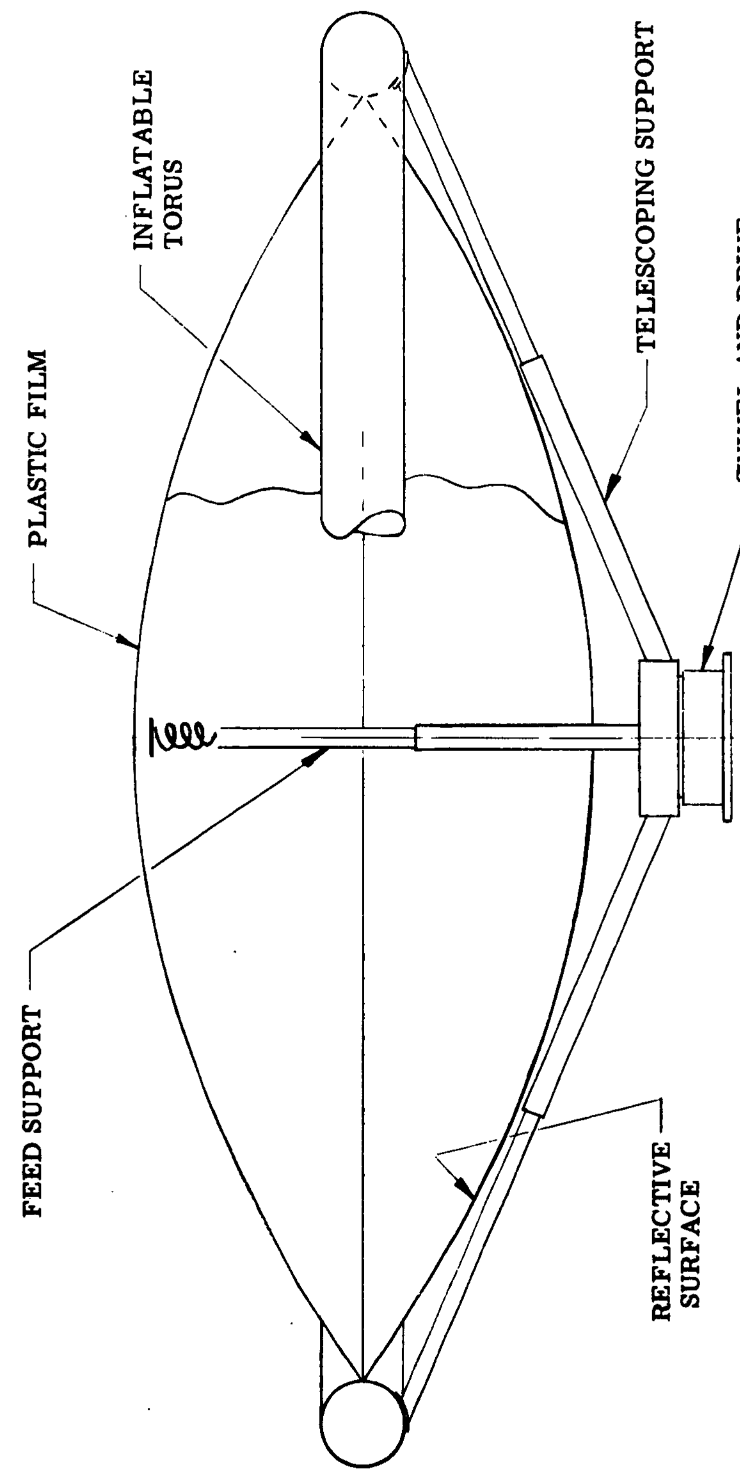

Figure 8. Inflatable Torus-Supported Parabolic Space Antenna

b. Inflatable Torus-Supported Paraboloid (Wire-Rigidized). This technique is similar to the pressure-supported paraboloid depicted in Figure 8. The antenna is composed of an inflatable lenticular-shaped envelope, the bottom surface of which is reflective, supported by an inflatable torus. However, since the antenna is intended for longer mission times, the reflecting surface and torus are composed of an Invar wire grid adhered to a thin plastic envelope. In deploying the antenna, the lenticular bag and torus are inflated to a pressure that uniformly yields the wires in the two envelopes, thus rigidizing without further need for internal pressure in a low g environment.

The antenna is characterized by longer mission times (in the order of days) and is intended for operation in a low g environment. Accuracies in the order of ±0. 25 to ±0. 375 inch are practicable.

Antenna weights of 0. 2 to 0. 3 lb/ft^2 of surface area are achievable, with packaging ratios of about 2. 5:1. Common f/D ratios are obtainable.

c. Wire-Mesh Swirlabola. The wire mesh Swirlabola, shown in Figure 9, is a high-gain, long-mission, steerable, pencil-beam antenna. This configuration provides curved radial ribs that extend from the hub to the outer periphery to support the reflector screen and establish the parabolic contour outboard of the hub. These ribs are pivoted at the hub rim, and having the approximate radius of the hub, nest circumferentially around the hub rim in the packaged condition. The screen material is a lightweight Invar wire mesh that is attached to the ribs; when packaged, it folds inward over the hub.

The reflector hub is a conventional structural arrangement that, in addition to providing the support mounting for the radial ribs, accomplishes the structural interface to the spacecraft and the structural mounting of the feed support. The primary structure consists of two perpendicular contoured ribs or beams that intersect at the center line and extend outward to a circumferential

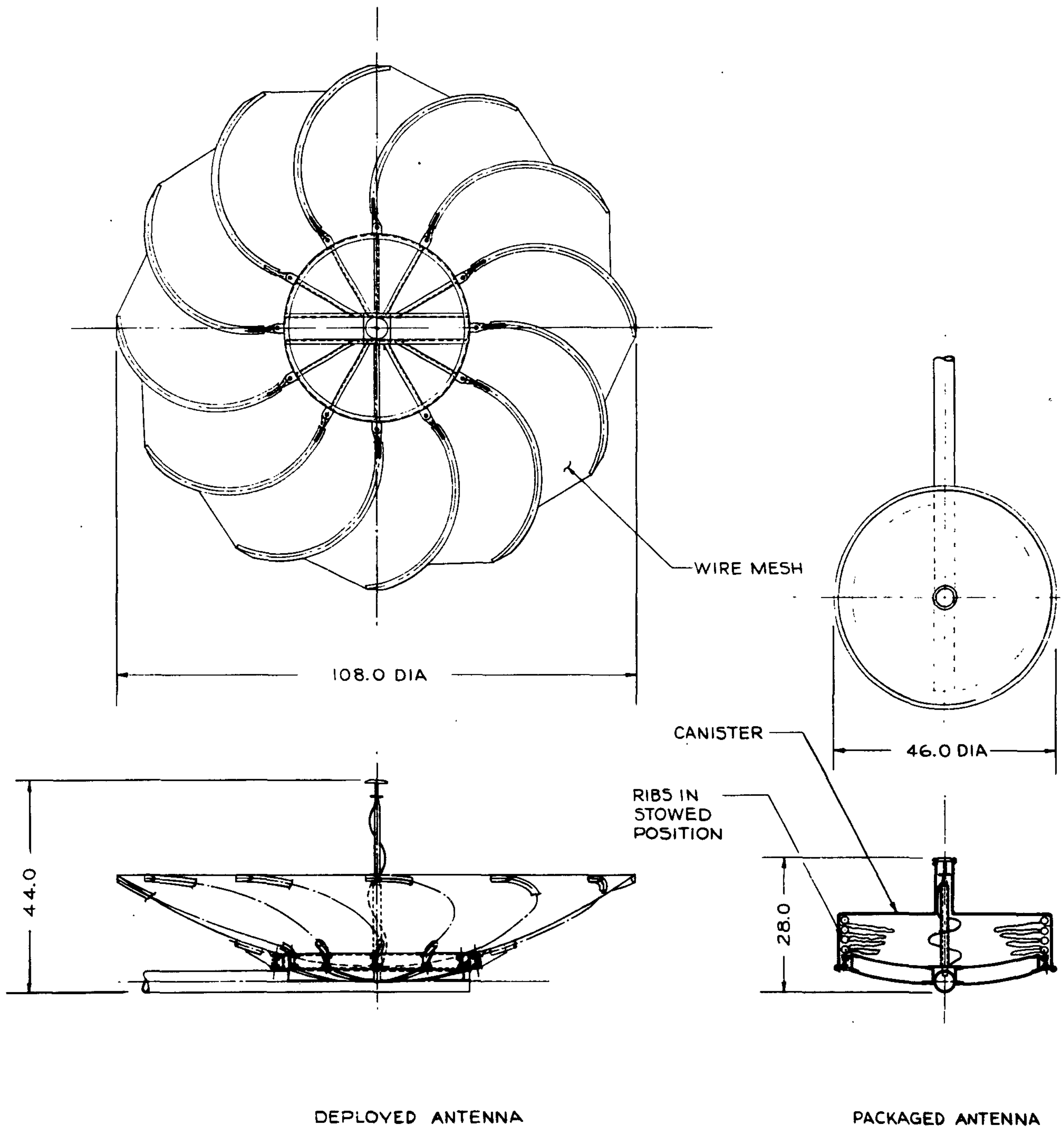

Figure 9. Wire-Mesh Swirlabola Antenna

rim. This rim, in addition to establishing the edge contour of the hub, provides the equally spaced pivot attach points for the outer ribs. Secondary contoured radial members extend from the center to the rim for contour control and structural backup of the hinge points. This structural frame supports the lightweight reflector screen.

The feed support is a single telescoping strut extending from the center of the reflector hub. The support is mounted to the hub at four points that incorporate adjustment provisions angularly, parallel to and normal to the focal axis of the antenna for alignment of the antenna electrical axis.

This antenna has been selected by Goodyear Aerospace for a high-gain space-probe antenna and is presently being developed further by Goodyear Aerospace under another contract.

As indicated, long missions with antenna steering requirements can be met with this approach. Accuracies on the order of ±0.10 inch are practicable. Weight is on the order of 0.35 lb/ft^2 with a packaging ratio of 2 or 3:1.

An attractive feature of this antenna is that it can be erected and boresighted prior to final packaging and launch.

d. Rigid-Panel Swirlabola. The rigid-panel Swirlabola is a high-gain, long-mission, steerable, pencil-beam antenna that is somewhat similar to the wire-mesh Swirlabola, with improved accuracy achieved by utilizing rigid panels in lieu of wire mesh to form the parabolic reflector surface. The antenna configuration (Figure 10) provides 12 curved radial ribs and rigid sandwich antenna surface leaves extending from a center hub to the outer periphery, which establish the parabolic contour outboard of the hub. These ribs are pivoted at the hub rim and, having the approximate radius of the hub, nest circumferentially around the hub rim in the packaged condition. The rib structure is

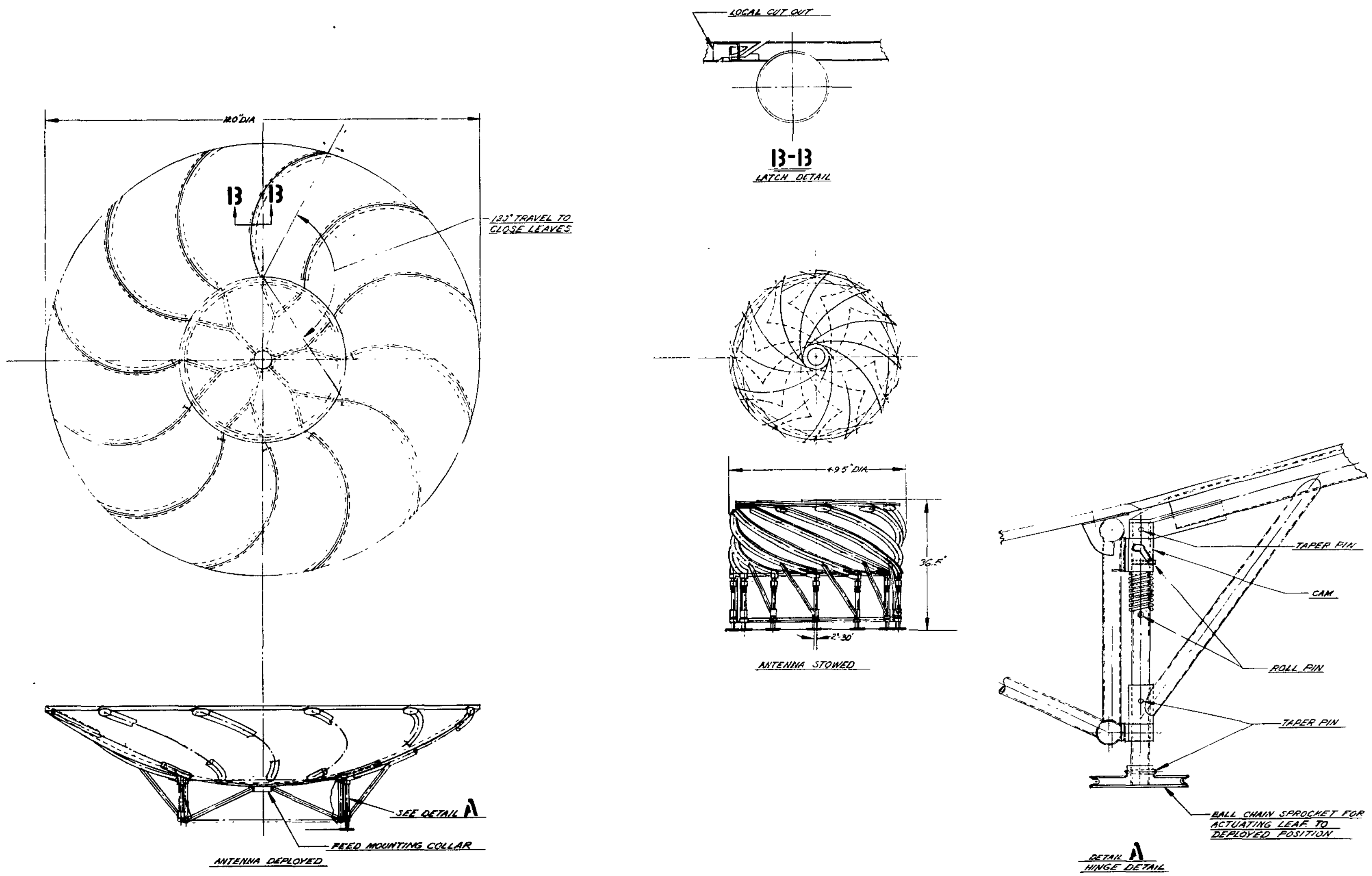

Figure 10. Rigid-Panel Swirlabola Antenna

fabricated of Invar tubes. The sandwich panels have Invar face sheets with aluminum or Invar honeycomb core. Two latches are provided to secure each leaf to its adjacent leaf (see Section B-B of Figure 10). The leaves are deployed by a ball chain that drives sprockets at each leaf hinge. The prime mover that drives the chain can be either a small electric drive or a pneumatic motor powered by compressed gas.

The hub structure will have a supporting space frame of welded Invar tubes and will include hinge fittings to support the hinged panels and their rotation mechanism. The hub structure will also provide mounting for the feed and the fixed portion of the reflector sandwich panel in the center or hub area.

The packaging container would be a conventional lightweight monocoque structure. It would be designed so that the canister cover would slip over the antenna and mount to the interface structure. The canister cover would be externally jettisonable in three sections. A circular clamp of wedge-type cross section would be used to secure the cover in the packaged state. Explosive bolts would tie the clamp sections together at each of the three cover section separation points. The three sections would be spring-loaded for positive reliable separation.

e. Lenticular AIRMAT Antenna. The lenticular design, shown in Figure 11, features a stable structure with good contour control that can be microwave-tested on the ground (1-g environment) with confidence that the same characteristics will be duplicated when it is deployed in the space environment.

The two prime contoured surfaces are paraboloids of revolution, 24 feet in diameter, modified by two closure surfaces along parallel chords 7-1/2 feet from the center to produce the 15 by 24 foot dimensions shown in the plan view.

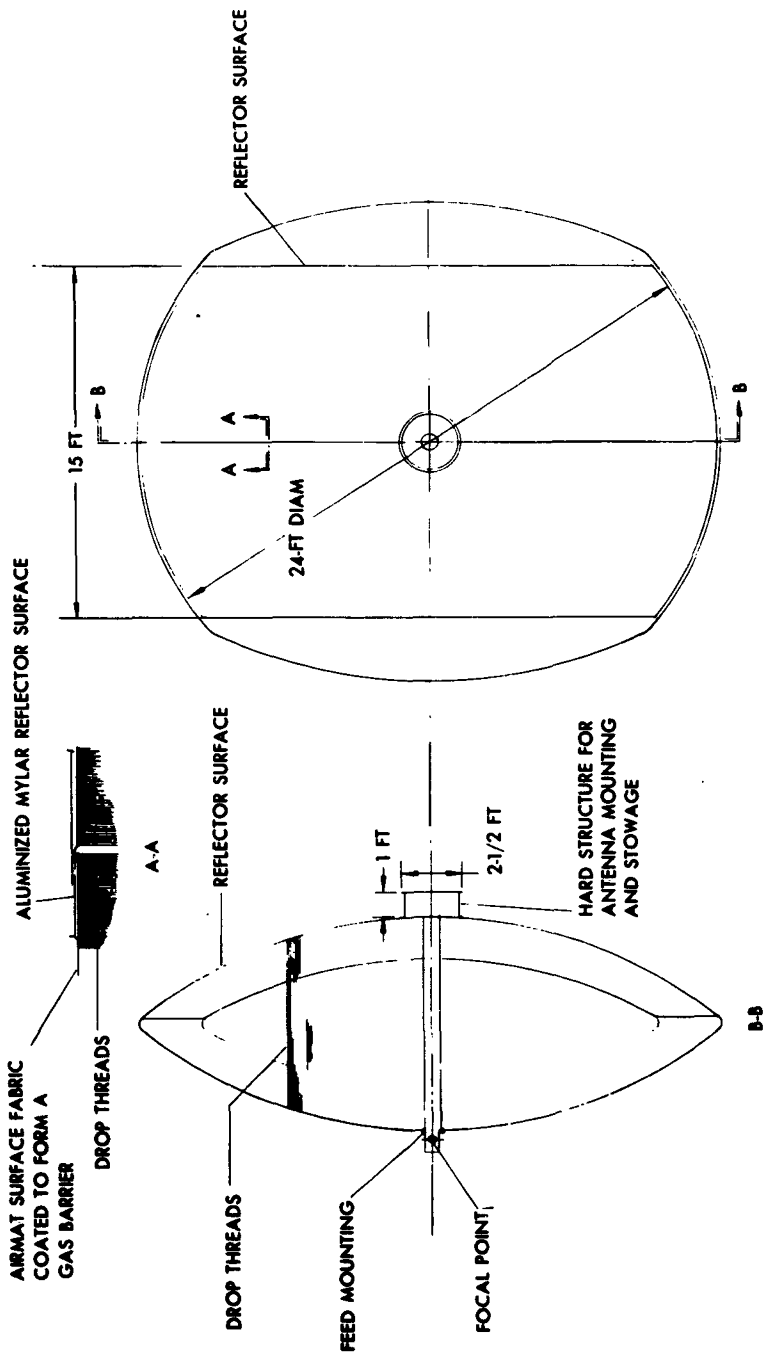

Figure 11. Lenticular AIRMAT Antenna

The drop threads shown in Section B-B are spaced as required for contour and surface accuracy and span the distance between the parabolic surfaces throughout the structure. The threads are woven into the cloth at each parabolic surface, securely fastening the entire structure together. The threads ensure excellent adherence to the required contour and add to the structure rigidity. This antenna is similar in general concept to the ground-based inflatable lenticular antenna shown in Section VIII.

The closure surface for the chord area removed from the 24-foot diameter will be made of patterned gores of Mylar. The juncture of each closure radius forms a corresponding tangency to the parabolic curves. This form is used to prevent the closures from influencing the parabolic surface when the envelope is inflated.

Mylar film is laminated as the outer cover of the fabric surfaces to form a barrier for the inflation gas and to increase the structural strength.

The Mylar forming the reflector surface would utilize a laminate of a 3-mil-thick aluminum foil or a coating of r-f reflective paint to produce the microwave reflecting surface. The balance of the antenna is reasonably transparent to microwaves.

As shown in Figure 11, the antenna feed is attached to the parabolic side away from the reflector surface.

The weight of this type of antenna is on the order of 0.2 lb/ft^2 reflecting surface area, including inflation system and feed weight. Tolerances of about ±0.15 to ±0.20 inch are practicable, depending on antenna size.

The antenna is applicable for short missions and can maintain rigidity under steering accelerations.

f. <u>AIRMAT Paraboloid Antenna.</u> This antenna utilizes a parabolic reflector fabricated from AIRMAT material as shown in Figure 12. The shape is a

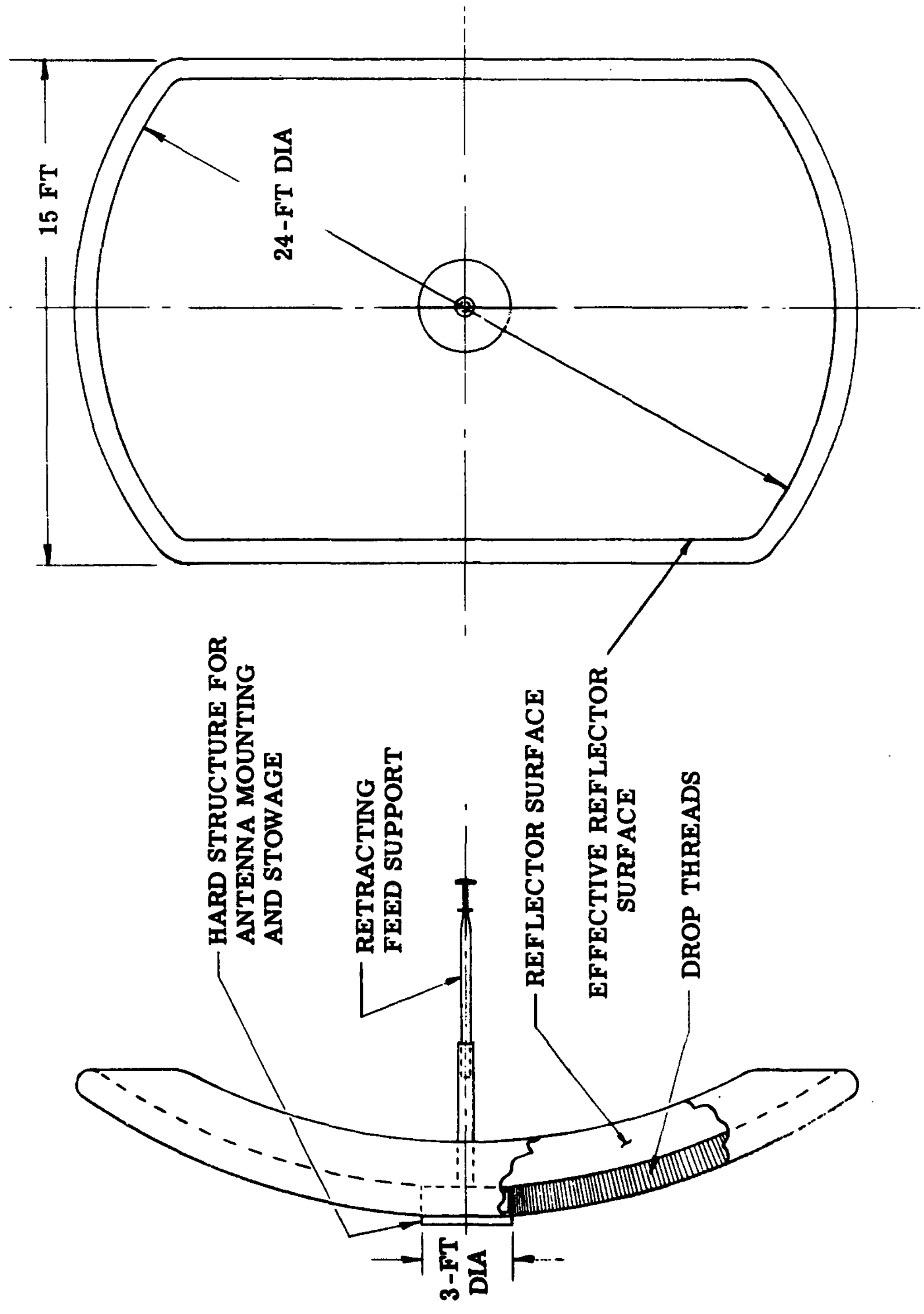

Figure 12. AIRMAT Paraboloid Antenna

paraboloid of revolution, 24 feet in diameter, modified by two closure surfaces along parallel chords 7-1/2 feet from the center to produce the 15 by 24 foot size shown. The contour is formed by fabricating together pie-shaped segments of single-contour AIRMAT. Reflecting material could be Mylar-aluminum foil laminate or r-f reflective paint. An extendable prime feed supported from rigid structure at the hub is visualized. This contoured AIRMAT reflector is similar in general concept to the ground-based inflatable paraboloid antenna shown in Section VIII.

The estimated weight of this antenna is about 0.2 lb/ft^2 of surface area. Practical tolerances are in the order of ±0.15 inch, depending on the over-all dimensions. Some improvement in contour accuracy could be realized, with some penalty in weight, by utilizing a flexible foam to smooth out the irregularities in the AIRMAT surface.

PART 4. FACTUAL DATA

SECTION IV. SPACE VEHICLE ANTENNA SYSTEM EVALUATION AND SELECTION

A. GENERAL

The analysis and evaluation effort was directed toward selecting antennas having the greatest applicability to the national space program. Full advantage was taken of parallel work by Goodyear Aerospace in the space antenna field. A companion Goodyear Aerospace supported general design and application study program was performed concurrently with this study program. The purpose of this companion program was to establish design criteria and develop erectable space antennas. Also, many requests for designs of erectable space antennas to meet specific requirements or specifications have been received and analyzed. In addition, Goodyear Aerospace is under contract to design and fabricate some of these antennas. As a result, the relative merits of various types of space antennas have been evaluated. Material requirements have been determined, and some antennas have been designed to meet these requirements; in the process, many concepts have been generated and analyzed. Some have been discarded, and others have been accepted for erectable antennas that meet the national space program requirements. For this reason, the need for the analysis and evaluation of many antenna types was minimized on this program.

As a part of this contract, it is required that models of the three most promising concepts, considering both space and ground applications, be designed and fabricated to demonstrate the feasibility of these concepts. Since it was previously agreed that the major program effort would be devoted to the ground-based antenna applications, it was decided that one space antenna and two ground-based antennas would be selected for the demonstration models.

The evaluation and analysis of the space vehicle antenna concepts and the final selection of the one concept for the demonstration model are presented in the following paragraphs.

B. CONCEPT EVALUATION AND SELECTION

The 12 antennas discussed in Section III were evaluated to select for further detail evaluation those antennas having the greatest range of applicability to the national space program and offering the best potential from the standpoints of weight, cost, packageability, and advancement of erectable or expandable techniques. Five of the concepts having the least capability of meeting these objectives were discarded from the evaluation and study program. However, some of those discarded have merit for certain specific applications. Generally, those concepts whose configuration would be dependent on the shape and structural design of a particular space vehicle were not selected for further detail evaluation. The following concepts were eliminated:

(1) Four-Helix Array
(2) Conical Horn Antenna
(3) Parabolic Cylinder Antenna
(4) Broad-Coverage Three-Spiral Array
(5) Expandable Fan-Beam Antenna

The considerations involved in the elimination of these antenna concepts are discussed in the following paragraphs.

The four-helix array was discarded because due to its basic simplicity, it has little to offer from a standpoint of advancing expandable or unfurlable techniques.

Also, due to tolerance effects, it is not adaptable to as wide a frequency range as some other concepts. The array is very applicable for specific applications of medium beamwidth and moderate gain in the 1 to 4 kmc range and where unfurlable techniques are not required.

The conical horn antenna is a versatile broad band antenna having the advantages of simplicity of structure, rather wide permissible tolerance, light weight, and good packageability. This concept was discarded, however, because it was not believed to be as applicable to the over-all national space efforts as are the parabolic types being considered.

The parabolic cylinder antenna offers a clean design that is amenable to ordinary engineering solution. The design configuration is, however, dependent on the shape and structural configuration of the particular space vehicle being considered, since it is permanently attached to the skin of the vehicle. Also, it is not adaptable to expandable or unfurlable techniques.

The broad-coverage three-spiral array was discarded because it is not as adaptable to erectable or expandable techniques as other concepts being considered.

The expandable fan-beam antenna was discarded because investigation has shown that, at microwave frequencies, this concept presents a serious problem in design of the feed. This expandable or extendable feed is complex and very heavy in comparison with the weight of the remaining antenna structure. There is, however, some promise for application of this concept at VHF and low UHF frequencies.

The seven antenna concepts selected for further evaluation consist of pencil-beam and fan-beam types which differ primarily in regard to mission time, achievable accuracy, and steerability:

(1) Inflatable Torus-Supported Paraboloid (Pressure-Supported)
(2) Inflatable Torus-Supported Paraboloid (Wire-Rigidized)

(3) Wire-Mesh Swirlabola
(4) Fan-Beam Pillbox
(5) Lenticular AIRMAT Antenna
(6) AIRMAT Paraboloid Antenna
(7) Rigid-Panel Swirlabola

These antenna types were conceived in response to a wide range of national space requirements. It is considered that all these concepts meet a cross section of these requirements for which erectable or inflatable techniques are applicable. Evaluation and selection were made on the basis of the following:

(1) Spectrum of applicability
(2) Weight per unit area as a function of tolerance, steerability, and lifetime
(3) Maximum permissible tolerance
(4) Probable cost

Actually, the selection is not so simple as indicated. This is due to the fact that a single requirement for an antenna specifies the lowest weight for a given tolerance, lifetime, steerability, cost, etc. Therefore, as an example, suppose that the interest is a short-life, low-tolerance, low-g antenna for the lightest weight possible, or suppose that a requirement exists for a long-life high-tolerance, high-g antenna for the lightest weight possible. For a specific requirement, there is no concern in regard to the applicability of the antenna at the other end of the spectrum. The one that best suits the requirement is chosen. However, here the interest is in choosing the antenna or antennas that are best or near best over the maximum range of applicability, and selection has been made on this basis.

The two inflatable torus-supported antenna concepts have a lower accuracy, shorter life, and lower steering capability than the other types considered and therefore have less over-all potential.

The wire-mesh Swirlabola has good accuracy, long life, and high steering load capability, as well as other attractive features, and is considered a good prospect. However, this antenna is presently being developed further under another contract, and for this reason, further development on this program is not warranted.

The lenticular AIRMAT antenna, the AIRMAT paraboloid antenna, and the rigid-panel Swirlabola were selected in the final evaluation as those holding the most promise for further detail study and model fabrication. However, the two AIRMAT concepts are quite similar to the ground-based inflatable lenticular and inflatable paraboloid antenna concepts, which were studied in detail for ground-based applications (see Section X), and therefore these two concepts were not selected for further study or model fabrication specifically for space application.

The rigid-panel Swirlabola antenna has long life and high steering load capability, has good reliability, is a structurally rugged design, is an excellent r-f reflector, and possesses better contour accuracy capability than the other types considered. Also, this antenna, with suitable modifications, has very good potential for mobile, quickly erectable, ground-based applications. The rigid-panel Swirlabola was selected as the one space vehicle antenna for further development, detail design study, and model fabrication.

PART 4. FACTUAL DATA

SECTION V. DETAIL STUDY AND ANALYSIS OF RIGID-PANEL SWIRLABOLA SPACE VEHICLE ANTENNA

A. GENERAL

Initial study established the following general design goals for the rigid-panel Swirlabola antenna:

(1) Simple mechanical structure to enhance reliability.
(2) Lightweight design with close tolerance contour control.
(3) Fabrication methods within the state-of-the-art.
(4) Efficient reflector for r-f energy.
(5) Structurally sound design to withstand handling, repeated erection and storage, launching, and deployment in space.
(6) Type of construction that will maintain mechanical strength and surface accuracies and offer an excellent lifetime with no aging problems.
(7) A solid-skin-type reflector surface with contour accuracies suitable for X-band operation which will be finished to minimize heat concentration on the feed.
(8) A structure fabricated primarily of Invar material to reduce any heating distortion. (Invar has a thermal expansion coefficient of only about 1/10 the value of steel and 1/20 of aluminum.)
(9) Design that permits all necessary alignment adjustments, check-outs, contour measurement, and deployment tests in the factory.

The following general requirements were established as a basis for the design study and analysis:

(1) The erected antenna will provide an essentially circular aperture with an approximate maximum diameter of 10 feet. Its aperture efficiency will be greater than 55 percent.

(2) The antenna will operate at X band. It will use a paraboloidal reflector with an f/D of 0.3 to 0.5.

(3) The reflector will have a tolerance of ± 1/12 inch to ± 1/24 inch from a true paraboloidal shape after fabrication and erection, whether in a 1-g or 0-g field at temperatures from -100 to +200^{o}F.

(4) The approximate unit weight of the combined aperture and feed system will be less than 1 lb/ft^2.

(5) The antenna will be capable of operating in a search mode, scanning at a high rate in a sector scan mode about one axis, or scanning slowly and uniformly.

(6) When packaged for stowage, the antenna will fit in the minimum volume, can be erected on the ground, and restowed for space erection.

Detail study and analysis was carried out along three major areas based on these general goals and requirements:

(1) Electrical Design
(2) Structural Analysis
(3) Mechanical Design

The results in these three major areas are discussed in the following paragraphs.

B. ELECTRICAL DESIGN

The electrical design for the most part is a straightforward problem since the antenna is the well known and much studied paraboloid. Its aperture efficiency requirement of more than 55 percent is consistent with common feeds and resulting illumination taper on the dish due to path taper of the diverging electromagnetic wave before collimation. Spill-over losses and transmission line component losses will reduce the antenna efficiency further. Two areas requiring investigation were surface tolerance effects and blockage effects.

Goodyear Aerospace has made studies of surface tolerance effects, enhancing the information available for this not so well-known problem. It has been found that the most applicable approach for these antennas under investigation is that suggested by Ruze (Reference 1, page 2. 40). For irregularities that seem to be distributed over a distance much larger than a wavelength, Ruze's approach leads to a gain reduction figure of

$$\frac{G}{G_0} = e^{-\bar{\delta}^2} \tag{1}$$

where

G_0 = unperturbed gain,

G = gain with phase errors,

and

$\bar{\delta}^2$ = mean squared phase error over the aperture.

The effects of elements that tend to block the collimated r-f energy are well known for objects in the center of the aperture. Recent fruitful investigations in this area at Goodyear Aerospace have considered the effects of objects that are distributed across the aperture. The theory (Reference 2) applicable to the performance of this antenna has been used.

Using these factors, the analysis of the rigid-panel Swirlabola resulted in specific surface tolerance requirements. The antenna's surface distortion at X band must be maintained within ± 1/12 to ± 1/24 inch, the latter being the upper design goal.

C. STRUCTURAL ANALYSIS

1. General

The analysis assumes the following constraints:

(1) X band
(2) Search angle - approximately 22 degrees
(3) Search velocity - 140 degrees/second

These requirements do not completely define the structural problems, but in conjunction with past experience, the requirements provide sufficient information to select the most efficient type of antenna and to approximate its weight and packaging volume.

The Swirlabola is ideally suited for this application. The conventional structure utilized presents a few problem areas. Past experience indicates that the strength required for accelerations, vibration, and shock during boost and in orbit can be met by careful attention to detail design.

The critical problems are associated with the close tolerances required for X band. This requires that deflections of the structure be kept small during the antenna operation. There are two major sources of deflection that must be corrected: those arising from thermal gradients and those arising from the angular accelerations required in the operating mode. These are subject to trade-offs, and a final design cannot be established until additional requirements are specified. For the present work, a particular design has been selected to provide a basis for discussing the principal trade-off areas and to establish the approximate weight and package volume of the antenna.

The general arrangement of the antenna is shown in Figure 10. The principal structural features include the use of Invar material throughout with 1/2-inch honeycomb panels and 3-inch-diameter ribs.

2. Thermal Deflections

Thermal studies of antennas show that for most missions the surfaces can be treated to control temperatures to acceptable limits. Reasonable limits are a total temperature change of $300^{O}F$ with temperature differentials across members of $100^{O}F$. For this reason, Invar material was selected for its low coefficient of thermal expansion. This coefficient is 0.9×10^{-6} per ^{O}F, which is approximately 1/10 and 1/20 the coefficient for steel and aluminum respectively.

The same material is used throughout so that uniform temperature changes will not introduce pointing or focusing errors. Similarity in shape is preserved, and the only effect is a small change in size. For a $300^{O}F$ temperature change, the change in size will amount to $300 \times 0.9 \times 10^{-6} \times 100 = 0.027$ percent.

Deflections from temperature gradients are a serious problem. Consider a cantilever beam of depth (h) and length (ℓ), initially straight at uniform temperature, then subjected to a temperature differential across the depth of magnitude (T). It can be shown that the deflection at the tip (δ) is

$$\delta = \frac{(\Delta T)\, C\ell^2}{2h} \tag{2}$$

where C is the coefficient of thermal expansion. One of the critical deflections is the tip of the rib. The rib is 46 inches long and 3 inches in depth; therefore,

$$\delta = \frac{(100)\,(0.9)\,(10^{-6})\,(46)^2}{(2)\;(3)} = 0.032 \text{ inch.}$$

Another critical deflection is the sandwich panel between the ribs. This is 1/2-inch thick and has a span of about 20 inches between ribs. Equation 2 may be used for this case if ℓ is considered equal to half of the span.

Then

$$\delta = \frac{(100)\ (0.9)\ (10^{-6})\ (10)^2}{(2)\ (1/2)} = 0.009 \text{ inch.}$$

These two deflections are acceptable for X band, whereas if the material were steel or aluminum, the resulting deflections would not be tolerable.

3. Search and Scan Deflections

The turnaround time in the search and scan operations will have a pronounced effect on the weight of the antenna. This is a primary trade-off area and will require considerable study. A study is presented herein.

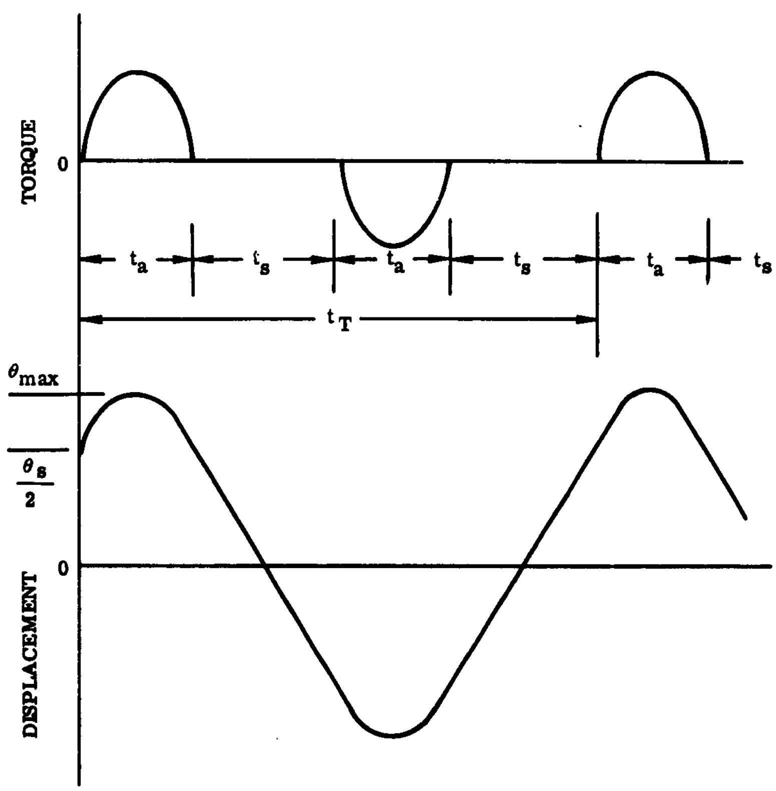

Figure 13. Typical Torque and Displacement Curves

It is assumed that a sine pulse torque is applied at each end of the stroke to achieve the turnaround. This will result in typical torque and displacement curves as shown in Figure 13. In order to examine the effect of turnaround time on the structure, it is necessary to determine the various quantities shown in Figure 13 in terms of a load factor (n) computed at the tip of the reflector for both the search and scan modes. The angle and velocity in the scan mode are taken as 1/10 of those in the search mode. The resulting expressions are tabulated in Table I, where r ≈ 5 feet, the distance from the axis of rotation to the tip of the reflector.

Table I. Torque and Displacement Parameters for Search and Scan Modes

ITEM	UNITS	SEARCH	SCAN
Scan Angle (θ_s)	degrees	22	2.2
Angular Velocity (W)	degrees/second	140	14
Angular Velocity (W)	radians/second	2.44	0.244
Sweep Time (t_s) $= \frac{\theta_s}{W}$	seconds	0 157	0.157
Turnaround Time (t_a) $= \frac{\pi Wr}{ng}$	seconds	1.19/n	0.119/n
Total Time (t) $= 2(t_a + t_s)$	seconds	0.314 + 1.119/n	0.314 + 0.119/n
Overshoot (θ_0) $= \frac{57.3 W^2 r}{ng}$	degrees	53/n	0.53/n
Maximum Travel (θ_{max}) $= \frac{\theta_s}{2} + \theta_0$	degrees	11 + 53/n	1.1 + 0.53/n

The results for the search and scan modes are plotted in Figures 14 and 15 respectively.

The structural parameters required to complete the analysis were determined for the particular structure selected. These calculations are quite conventional and are not included herein. The principal results are natural frequency with unsymmetrical mode, 32 cps; deflection of rib tip for n = 1, 0.0097 inch; and deflection of sandwich panel between ribs for n = 1, 0.0025 inch.

The major concern is the magnitude of the deflection while the antenna is sweeping across the search or scan angle. The deflection during this time is the residual deflection resulting from the half cycle sine pulse. This deflection depends on the static deflection, which is proportional to the load factor n, and to a response factor dependent on the ratio of the duration of the pulse to the natural period of vibration of the antenna. The response factor for this case is shown in Reference 3. The pulse time is t_a, which was shown in Figures 14 and 15 to be a function of n. The natural period of vibration is the reciprocal of the natural frequency and, for this case, equal to 1/32 or 0.031 second. The residual deflection for the search and scan modes is shown as a function of n in Figures 16 and 17 respectively.

D. MECHANICAL DESIGN

The mechanical design features for the rigid-panel Swirlabola are described in the following paragraphs. The configuration is essentially the same as described in Section III, except for the addition of more detail information resulting from further design study.

The antenna configuration (Figure 10) provides 12 curved radial ribs and antenna surface leaves extending from a center hub to the outer periphery, which establish the parabolic contour outboard of the hub. These ribs are pivoted at the hub rim and, having the approximate radius of the hub, nest circumferentially around the

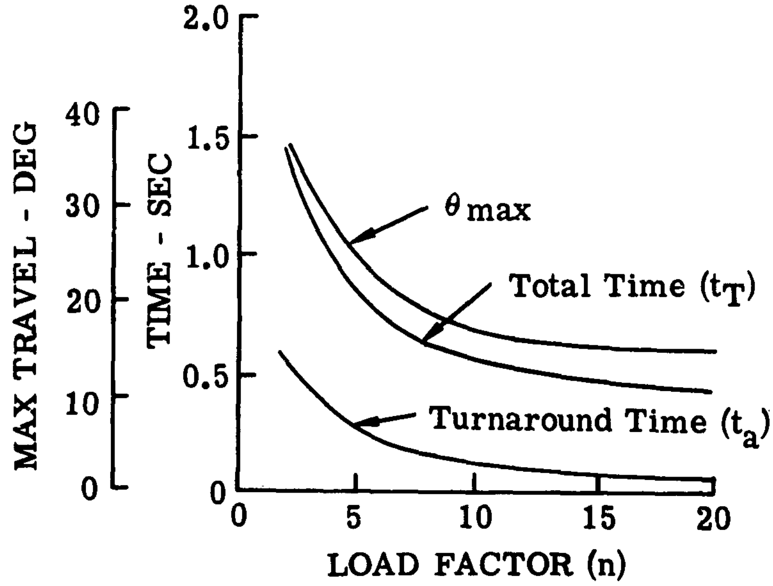

VALUES

n	t_a	t_T	θ_{max}
2	0.595	1.50	37
5	0.238	0.79	22
10	0.119	0.55	16
15	0.079	0.47	14.5
20	0.060	0.43	13.6

Figure 14. Turnaround Parameters versus Load Factor (Search Mode)

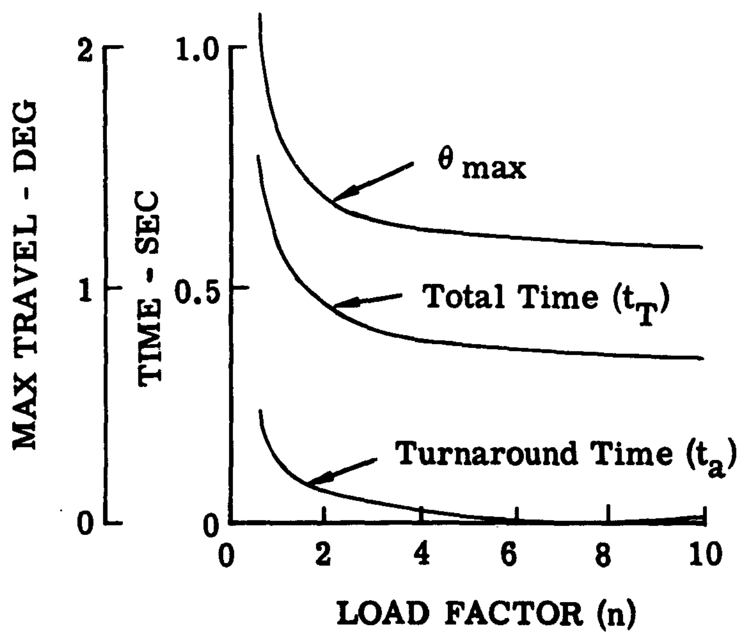

VALUES

n	t_a	t_T	θ_{max}
1/2	0.238	0.280	2.16
1	0.119	0.552	1.63
2	0.060	0.433	1.37
5	0.024	0.362	1.21
10	0.012	0.339	1.15

Figure 15. Turnaround Parameters versus Load Factor (Scan Mode)

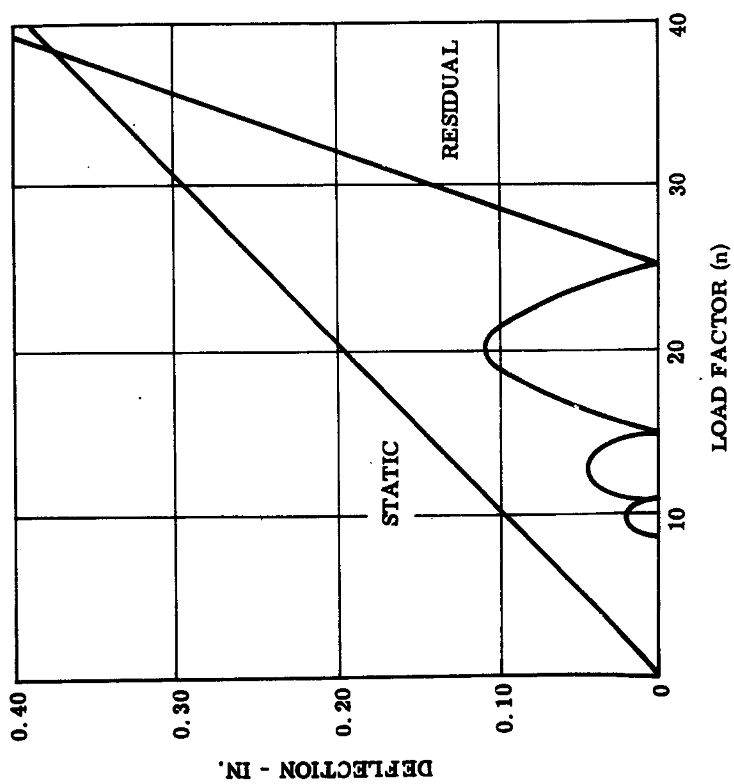

Figure 16. Residual Deflection for Search Mode

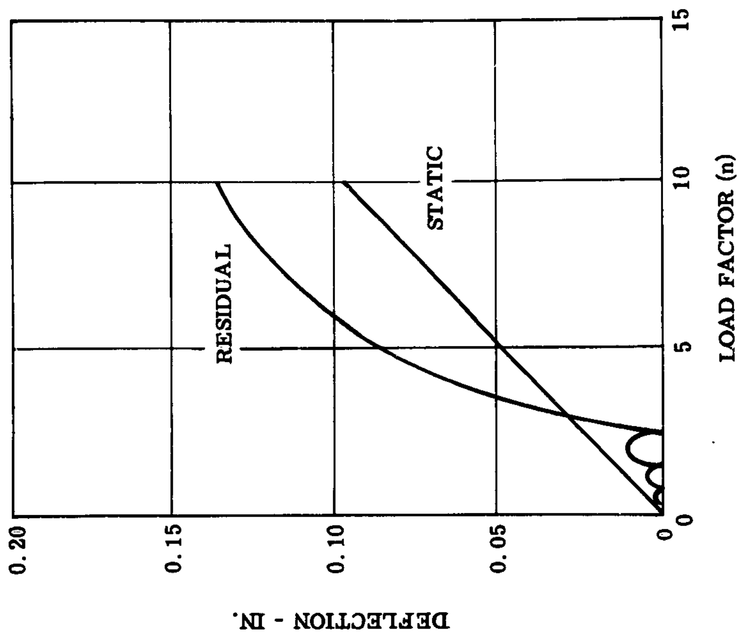

Figure 17. Residual Deflection for Scan Mode

hub rim in the packaged condition. The rib structure is fabricated of Invar tubes that are chem-milled to reduce the wall thickness as they approach the outer periphery of the reflector.

The outer leaves of the parabolic surface are fabricated of honeycomb sandwich. The sandwich has Invar face sheets with Invar or aluminum honeycomb core. The face sheets, core, and support rib are bound into one integral component. The leaves and ribs are hinged at the central hub (see detail A of Figure 10).

The top pillow block of the hinge also acts as a cam to control the displacement of the leaf during deployment. A compression spring holds the cam pin in the secured position after deployment. Two latches are provided to secure each leaf to its adjacent leaf (see Section B-B of Figure 10). These latches are located at the midpoint of the leaf and at the outboard extremity. The leaves are deployed by a ball chain that drives sprockets at each leaf hinge. The ball chain is spring-loaded to provide constant tension. The prime mover that drives the chain can be either a small electric drive or a pneumatic motor powered by compressed gas. Limit devices can be provided to define the end of travel of the mechanism.

The hub structure will have a supporting space frame of welded Invar tubes. Two tubes are rolled to a 44-inch diameter. Spacer tubes are then welded at each hinge point and have provisions for mounting the pillow blocks for precise position. The hinge center line is canted at $2^{o}3'$ so that the folded leaves of the reflector surface will nest on top of each other (see view of the stowed antenna, Figure 10).

The reflector surface for the hub is a honeycomb sandwich composed of Invar face sheets and Invar or aluminum foil honeycomb core. The sandwich, attached to the hub ring with Invar clips at each hinge location, will serve as the shear resistant member for the hub structure as well as the reflector surface. A spider of Invar tubes spans the distance from the outer ring lower tube to an Invar collar at the center of the reflector, which also serves as the mounting reinforcement for the feed.

E. CANISTER DESIGN CONSIDERATIONS

A conventional sealed monocoque construction of magnesium can be custom-designed to provide the antenna packaging envelope. It would be designed so that the canister cover would slip over the antenna and mount to the interface structure. The canister interface to payload either can be mounted to concentrated load points or can be uniformly distributed, whichever is most favorable to the payload structure.

The canister cover can be jettisonable externally in three sections. A circular clamp of wedge-type cross section would be used to secure the cover in the packaged state. Explosive bolts would tie the clamp sections together at each of the three cover section separation points. As it is mandatory that the covers be jettisoned and not foul with the canister contents, the three sections would be spring-loaded for positive reliable separation. The deployment of the canister cover would be initiated by a programmed signal.

Other prime considerations that will influence the canister design are as follows:

(1) The launch environment imposes the effects of shock, vibration, and inertial loads.

(2) The thermal effects at launch and aerodynamic heat effects must be investigated to determine the optimum insulation required for protection of the canister contents.

The canister detail design would be dependent on the configuration of the particular vehicle in which the antenna would be used and on the environmental conditions imposed by that vehicle. Therefore, the design of the canister was not pursued in further detail in this program.

PART 4. FACTUAL DATA

SECTION VI. MODEL DESIGN, FABRICATION, AND EVALUATION - RIGID-PANEL SWIRLABOLA SPACE VEHICLE ANTENNA

A. GENERAL

A reduced size scale model of the rigid-panel Swirlabola antenna was designed and fabricated for demonstrating the mechanical and structural feasibility and the packaging and deployment capabilities of the full-scale design configuration resulting from the detail design study described in Section V. The operating mechanism for the model was modified to provide manual deployment and retraction operation in order to reduce the complexity of the mechanism for purposes of economy and to facilitate the fabrication of the reduced-scale components. This simplification does not adversely affect the demonstration capability of the model. Upon completion, the model was evaluated relative to the structural and mechanical feasibility and operational capability of the full-scale design configuration for space vehicle application. Consideration was also given to utilization of the basic concept, with suitable structural modifications, for mobile, quick-erecting, ground antenna applications. The model design configuration, fabrication, and evaluation are discussed in the following paragraphs.

B. DESIGN CONFIGURATION

A scale factor of 3/10 was selected for the demonstration model. Thus, the diameter of the parabolic reflector is 36 inches as compared to 120 inches for the full-scale design. The f/D ratio is 0.35, the same as for the full-scale model.

The model general configuration is essentially the same as the full-scale design shown in Figure 10, except for the reduced size, modifications to the basic hub and operating mechanism, use of sheet stock for the petals in lieu of sandwich structure, and other minor simplification of details.

The basic central hub structure (see Figure 18) consists of a flat, circular, steel base plate, 11.50 inches in diameter. Twelve steel radial ribs are attached to a slotted hub fitting at the center of the hub. At their outer extremities the ribs support the hub rim to which 12 equally spaced petal hinge fittings are attached.

The center section of the reflector in the hub area is 13.05 inches in diameter and is made of 0.030-inch thick steel sheet formed to the center contour of the paraboloid. This center section of the reflector is supported by a shaft at the center of the hub.

The reflector outboard of the hub consists of 12 petals made of 0.030-inch thick steel sheet formed to the contour of the paraboloid. The petals are developed by dividing the paraboloid into 12 identical curved segments. The petals are separated by a curved cut having a radius approximately equal to the outside radius of the hub rim. The inner ends of these separation cuts are equally spaced around the circumference of the hub rim. The outer ends fall on the intersection points of the outer reflector circumference and 12 equally spaced radial lines that are offset 30 degrees from radial lines through the inner end points. Each petal is supported by a 5/16-inch diameter brass tubular rib. The ribs are curved in planform to approximately the same radii as the petal separation cuts and are contoured in elevation to match the parabolic curvature of the petal lower surfaces. The tubular ribs are bonded to each petal adjacent to the petal separation cuts. The ribs incorporate hinge fittings that attach to the 12 mating hinge fittings on the hub rim. Each petal assembly includes a lever arm, attached to the rib hinge fitting, which engages a radial slot in a rotatable ring located just inside the hub outer rim (see Figure 18). The rotatable ring imparts rotary motion to the petals for retraction and extension.

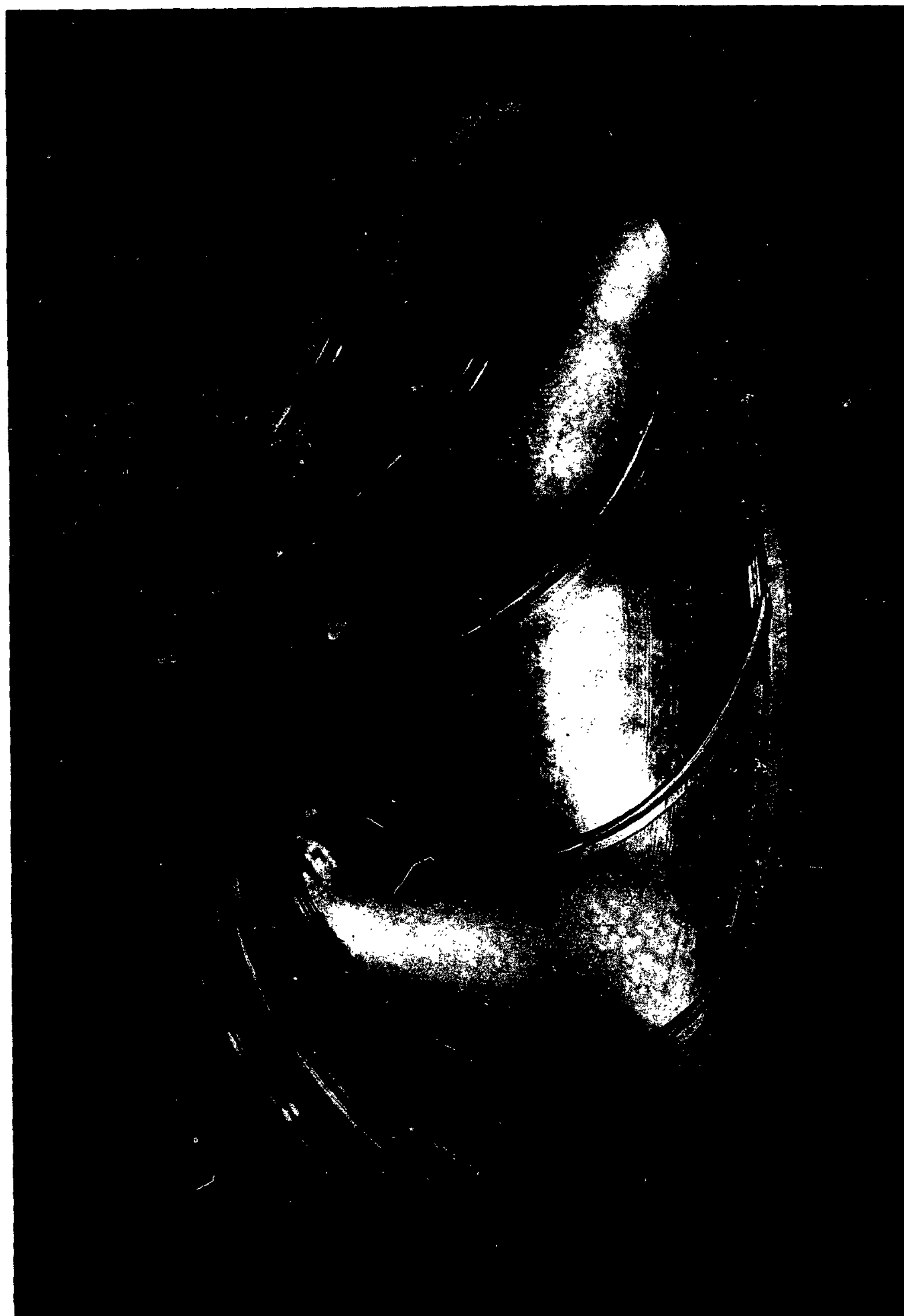

Figure 18. Rigid-Panel Swirlabola Model - Rear View on Assembly Mold

Actuation for extending the antenna from the packaged or stowed position to the operating position or vice versa is accomplished by three separate manual operations as follows:

(1) Two handles consisting of rods extending out from the rotating ring at the base of the antenna are rotated clockwise (viewed from front of antenna) to extend the reflector petals from the stowed to the deployed or operating position and are rotated counterclockwise to return the petals to the stowed position.

(2) A knob located on the underside of the antenna is attached to a threaded shaft in the center of the hub and is used to raise the center portion of the reflector to match the petal contour after the petals are in the operating position. Likewise, the center reflector portion must be lowered before retracting the petals.

(3) The simulated feed is a simple telescoping section and must be raised into the operating position by hand and pushed down into the stowage position.

Figure 19 shows the antenna in the stowed position. Figure 20 shows the petals in an intermediate position, and Figure 21 shows the antenna in the fully deployed or operating position.

The packaged diameter is 19 inches or 53 percent of the 36-inch diameter in the fully deployed or operating position. The over-all packaged height (height to top of feed) is approximately 8-1/8 inches as compared to 13-1/8 inches in the deployed position. The height from the bottom of the base plate to the top of the reflector is approximately 5-7/8 inches in the packaged position and 7-5/8 inches in the deployed position.

Small spring locks are provided on the lower surface of each petal near the periphery to interlock the petals together in the deployed position. The simulated

Figure 19. Rigid-Panel Swirlabola Model - Stowed Position

Figure 20. Rigid-Panel Swirlabola Model
Partially Extended Position

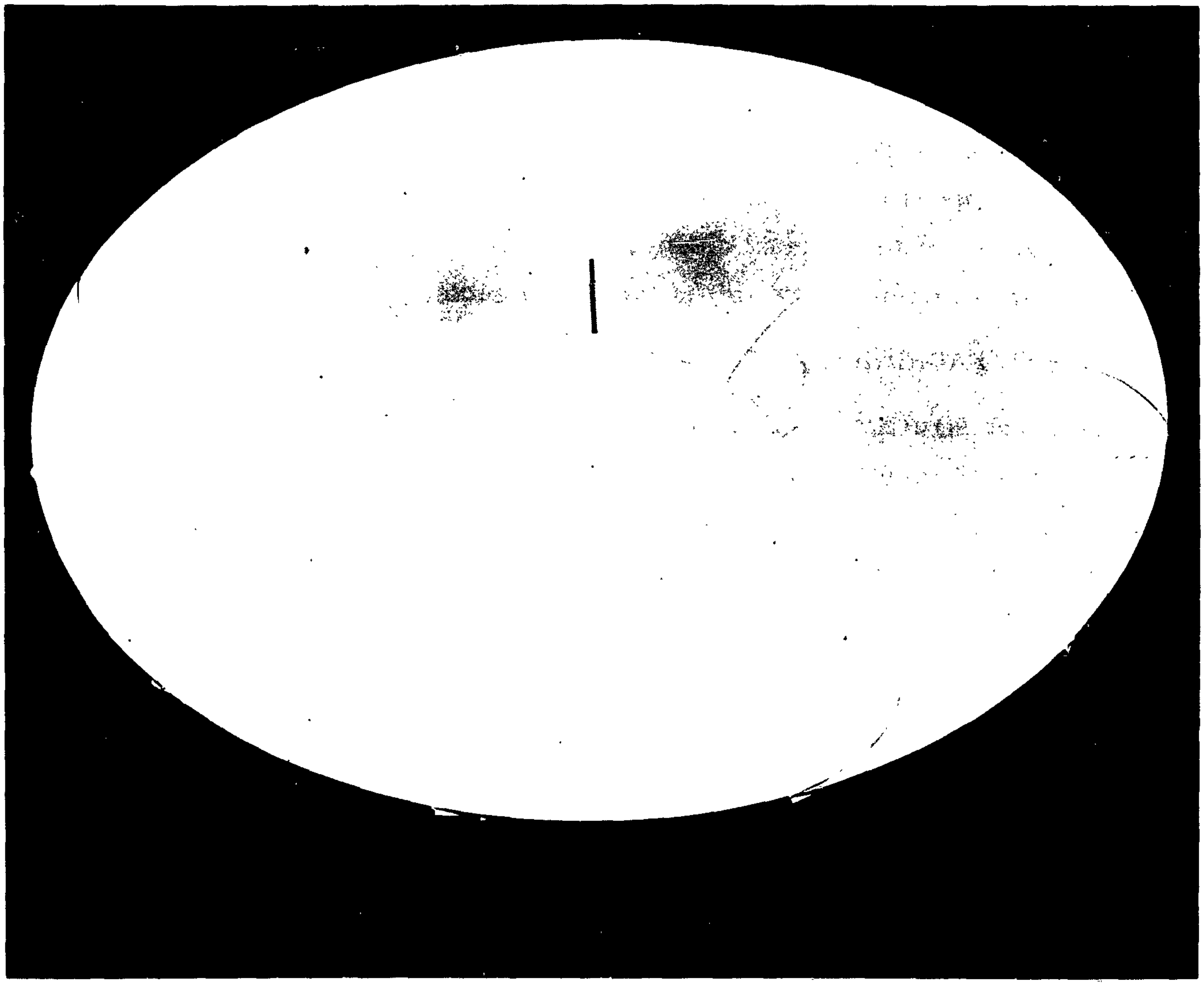

Figure 21. Rigid-Panel Swirlabola Model - Fully Deployed Position

locks employed on the model require some manual engagement; however, in a full-scale design, the petal position locks would be automatic at the end of the deployment cycle. This model was designed primarily to demonstrate space vehicle application; therefore, it was not considered necessary to provide automatic release of petal locks for retraction into the stowage position, since the space mission does not require repackaging after initial deployment. For this reason, the petal locks require manual disengagement prior to antenna stowage. The retraction mechanism, however, is fully reversible.

C. MODEL FABRICATION

The basic hub structure was manufactured utilizing conventional fabrication techniques. The 12 radial ribs were silver soldered to the slotted hub fitting in the center and to the rim at their outer ends. The radial ribs were attached to the base plates by means of spacer clips tack-welded to the base plate and bolted to the radial ribs (see Figure 18).

The reflector sections were made of sheet steel formed to the paraboloid contour by spinning. Three spinnings were made from 0. 030 steel sheet. The center portion of the reflector was cut from one spinning, and the 12 petals were cut from the other two. The first two spinnings were not stress-relieved after spinning, because it was expected that stress-relieving would cause undesirable distortion. No difficulty was encountered in making the center portion of the reflector from the first spinning. Seven petals were cut from the second non-stress-relieved spinning. After cutting, the petals, which extend to the outer extremities of the spinning, exhibited a marked tendency to spring back or flatten out. Hammer forming was necessary to restore the petals to the proper contour. In an effort to reduce the hand forming, the third spinning was stress-relieved. Five petals were cut from this spinning. The spring-back condition was practically eliminated, and only minimum hand forming was required to achieve proper contour. The petals made from the stress-relieved spinning are not as stiff as those made from the non-stress-relieved one; however, this reduced stiffness does not present a problem for the model. This condition would not exist in the full-scale design, since the petals would be made of sandwich material individually formed to accurate contour.

The hinged support ribs were made from brass tubing of 5/16 inch in diameter and 0.065 inch wall thickness. Each rib was hand formed to match the petal separation cut radius and the parabolic curvature of the back surface of the petals. Hinge fittings and actuation lever arms were silver soldered to the inner end of the ribs.

The petals and ribs were aligned and hand fit on a master form block, and the ribs were bonded in place on each petal with Epon 901 adhesive (see Figure 18).

D. MODEL EVALUATION

Evaluation of the completed model shows that the rigid-panel Swirlabola antenna concept is structurally and mechanically feasible and is practical to manufacture. The design will provide all the operational capabilities of a rigid, close-tolerance parabolic reflector with the unique capability of being quickly and easily folded or retracted into a reduced size cylindrical package for stowage within a space vehicle. Although the mechanism employed on the model was simplified for hand operation, it demonstrates smooth reliable operation for extending or retracting the reflector petals. Such a mechanism is readily adaptable to the application of powered drives for remote or automatic operation.

As stated previously, a packaged diameter of 19 inches (53 percent of the deployed diameter) was achieved for the model. Study of the model design indicates that the packaged diameter can be readily reduced to approximately 14 inches with no change in the operating mechanism by merely trimming the pointed tips of each reflector petal. This would produce a slight scalloping around the periphery at the split line between the petals. Trimming the petals in this manner would provide a minimum package diameter for stowage, but would be expected to cause some small increase in side-lobe level. For the purpose of this model, it was decided not to trim off the petal points, but rather to show the full circular reflector capability without the scalloping effect.

The petal alignment locks used on the model are simple spring clips that only simulate full-scale locks, which would be some type of positive spring-loaded latch mechanism. This lock simplification was made in the interest of economy because of the difficulty involved in proportionally scaling down a mechanism of this type. These simulated petal locks require some manual engagement when the antenna is extended into the deployed position. This is due, in part, to the spring-back condition encountered in the seven non-stress-relieved petals. This spring-back tends to cause some misalignment of the petals at the tips, preventing automatic engagement of some of the locks. Good contour characteristics are achieved when the petals are locked together.

The reflector for this model conforms closely to the contour of the parabolic tool used for its fabrication since the petals were individually checked to the tool contour. Also the petal-rib assemblies and linkage were assembled on the tool. Accurate duplication of tool contour was not the primary consideration for the sheet metal petals used in this model, since for any full-scale operational model, the petals would be made of sandwich material individually formed to accurate contour with adequate tooling. A detail contour measurement or comparison with the tool contour for this model would not yield significant information pertinent to the capability of a full-scale operational model; therefore, further contour checks were not made.

This antenna concept can be adapted for ground applications to provide a transportable quick erecting ground antenna that can be stowed and packaged for over-road or air transportation. Such an antenna can be easily and quickly erected for operation and can be quickly retracted, stowed, and moved to another site. Structural integrity necessary to withstand high wind loadings and transportation loads would require special consideration for the supporting rib structure and hinge design to provide the required rigidity and still permit the petals to overlap for storage.

The Swirlabola design can yield a stowed diameter in the order of 40 to 50 percent of the fully deployed reflector diameter. Size limitations for space vehicle application would be governed by weight and stowed package size requirements for the particular space vehicle involved. For ground-based applications, the package size limitations for air or over-road transportation would dictate the maximum size.

PART 4. FACTUAL DATA

SECTION VII. GROUND-BASED TRACKING ANTENNA SYSTEM PARAMETERS

A. GENERAL

The program technical requirements as specified in SCL-4346, dated 23 October 1961, were reviewed in detail along with the requirements for other ground-based antenna systems including Syncom in order to establish system parameters. As agreed early in the program, the Syncom specification was used as a general guide for establishing ground-based tracking antenna requirements. Tentative requirements were established, which include frequency band grouping, environmental, mechanical, and electrical requirements. These requirements were used as design goals in establishing and evaluating the design concepts for this program.

B. GROUND-BASED TRACKING ANTENNAS

The following tentative requirements were established for ground-based antennas in the 10 to 40 foot diameter size range:

(1) Frequency

Class I . . . . 0.1 to 2 kmc

Class II . . . . 5 (±0.5) kmc

Class III . . . . 9.5 (±0.5) kmc

(2) Environmental

(a) Wind - Operational 45 mph with added 15-mph gusts

Drive to stow . . . . 60 mph

Stowed . . . . 125 mph

REF. ENGINEERING PROCEDURE S 017
77.10 (5-63)

(b) Ice - Operation - 1/2-inch maximum ice or equivalent snow with 50 percent degradation in electrical performance

(c) Temperature. . . . $-80^{\circ}F$ (12 hours) to $+135^{\circ}F$ (4 hours)

(d) Humidity . . . . 5 percent at $+135^{\circ}F$

97 percent at $+80^{\circ}F$ to $+85^{\circ}F$

Condensation at all temperatures below $+80^{\circ}F$

(e) Salt Spray . . . . . . As encountered in coastal regions

(f) Rain . . . . Two inches continuous per hour

(g) Altitude . . . . 5000 feet above sea level

(3) Mechanical

(a) Size

Class I . . . . 20 to 40 feet

Class II . . . . 40 feet

Class III . . . . 30 to 40 feet

(b) Excursion

Azimuth . . . . 360 degrees continuous

Elevation . . . . ±95 degrees from zenith

(c) Velocity . . . . 8 degrees/second

(d) Acceleration

Azimuth and Elevation . . . . 6 degrees/second^2

(e) Life. . . . . 10,000 hours (minimum)

Total useful life . . . . 3 years

(f) Surface Accuracy - The deviation from theoretical contour shall not exceed the following under any combination of conditions for environmental requirements listed:

Class I	3 sigma, $\lambda/24 = \pm 0.246$ in.
Class II	3 sigma, $\lambda/24 = \pm 0.090$ in.
Class III	3 sigma, $\lambda/24 = \pm 0.050$ in.

PART 4. FACTUAL DATA

SECTION VIII. GROUND-BASED TRACKING ANTENNA CONCEPTS AND RADOMES

A. GENERAL

Many types of ground-based tracking antennas were investigated, and a preliminary evaluation of these concepts relative to electrical, structural, and over-all system performance was made to determine which concepts merit further investigation. The concepts generated and investigated include completely new approaches as well as new advances to the present state-of-the-art.

The initial effort was directed toward evolving concepts that offered a possibility, with further development, of improving ground-based antennas. Improvements sought included performance, economy, mobility, transportability, ease of erection, and ease of operation. Most of the concepts that evolved during the initial creative effort were investigated at least on a cursory basis to avoid missing a good approach. Advantages and disadvantages of the various concepts were compared so that they could be categorized either for further study and evaluation or discarded in favor of better concepts.

Since some of the ground-based antenna concepts developed for this program will require radomes to reduce environmental load conditions and to provide protection from the elements, it was considered desirable to assess available data on various types of radomes and to compile comparative information. Accordingly, a comparison study was made for five different types of radomes.

The antenna concepts generated and investigated during the initial creative stage of the program are described in this section of the report. Refinements, improvements, and modifications to some of these concepts have evolved during the course of the study program and will be discussed in subsequent sections of this report.

B. DESCRIPTION AND COMPARISON OF GROUND-BASED ANTENNA CONCEPTS

1. Introduction

Five different types of ground-based antennas, categorized relative to different types of microwave radiators, were investigated:

(1) Parabolic Antennas
(2) Spherical Antennas
(3) Fresnel Zone Plate Antenna
(4) Leaky Wave-Structure Antenna
(5) Circular Hog-Horn Antenna

Since the parabolic reflector is the most conventional and basically provides a very efficient antenna concept, the parabolic antenna was given considerable investigation. Therefore, a number of variations in parabolic antenna structures have evolved. Less consideration was given to each of the other types, since with the possible exception of the spherical reflector, they did not initially appear as promising as the parabolic antenna. The focal length to reflector diameter ratios (f/D) are on the order of 0.35 to 0.5 for typical systems.

2. Parabolic Antennas

a. General. The parabolic antennas included antennas that use a paraboloidal dish as a reflector. Therefore, a Cassegrain antenna was included in this group since its main reflector is a paraboloid.

The Cassegrain antenna uses a paraboloid as the main reflector with the feed in the hub at or near the vertex of the main reflector and a hyperbolic subreflector located in front of the paraboloid between the feed and the focus. The Cassegrain antenna permits a shorter axial length with associated reduced moment. Also, it permits greater flexibility in the design of the feed system and eliminates the necessity for long transmission lines, since the feed is located near the hub. The Cassegrain antenna normally offers an advantage in receiving low noise level signals because of the shorter transmission lines and reduced spill-over of energy in the back direction. The advantages of the Cassegrain antenna are normally gained at the expense of blockage plus an additional reflector surface.

Figure 22 shows a comparison of gain between the conventional and Cassegrain reflectors. Beamwidths and side lobes would be approximately the same, the Cassegrain reflector having slightly higher side lobes. Exact side lobe configurations cannot be discussed at this point, because the gain, side lobes, and beam width trade-off are functions of size, tolerance, blockage, and illumination, and these parameters will not be defined until the design of the specific system is investigated further.

Three different categories of ground-based parabolic antennas were studied. They include foam-rigidized systems, inflatable systems, and foldable rigid-structure systems.

Most antenna reflectors are designed to meet deflection requirements. The structure is analyzed to meet given deviations from contour. The total allowable deviation is divided in an arbitrary manner between structural deflections and manufacturing tolerances. The structural deflection is then divided into two parts: dead weight and live load deflections. The structure is sized to meet the allowable live load requirements, the reflector weight is estimated,

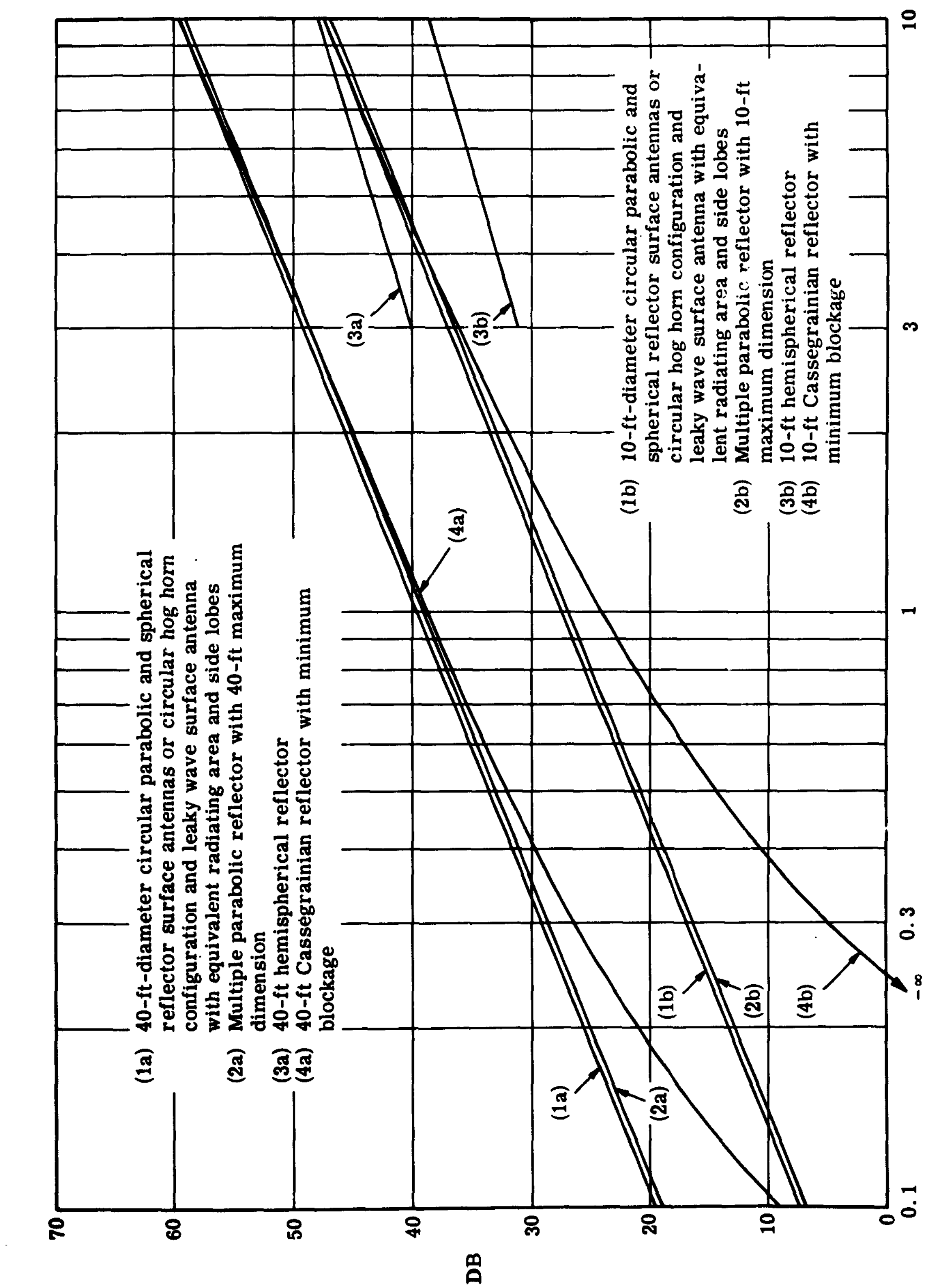

Figure 22. Maximum Gain Comparison of Various Antenna Configurations

and the dead weight deflections are then calculated. The distribution of the error is arbitrary and based on the judgement of the engineers doing the work.

Past work has shown that, when a circular reflector has the ability to carry hoop tension and compression, the deflections due to the symmetrical part of a loading are small and usually negligible. The anti-symmetrical part of the loading is carried by the radial structure and contributes most of the structural deflection. The shear deflection of the radial members is a function of the radius-to-depth ratio of the member and the shear modulus of the material from which it is constructed. These shear deflections, usually assumed negligible in more conventional beams, are often not negligible. This is particularly true when materials having a low shear modulus are used in the construction of the antenna.

The technique described in the preceding paragraphs are applicable to antennas that follow conventional design practice. Some of the concepts studied do not fit in this conventional category. These require the development of a method of analysis before accurate deflection calculations can be carried out.

Some of the factors that were considered in regard to electrical performance are antenna gain and efficiency, operational frequencies, frequency bandwidths, pattern beamwidths, side lobe levels, and tolerance effects. The system operation factors considered include relative circuit complexity and methods of scanning, as well as structural considerations. The parabolic antenna concepts and advantages and disadvantages of each are discussed in the following paragraphs.

b. Foam-Rigidized Antennas. The foam-rigidized antenna concept consists of an r-f reflecting surface supported by a rigidized-foam dish with an integrated metal framework. The reflector dish in this concept has a reflecting surface that is bonded to a thick layer of polyurethane foam, which is supported and stabilized by an encapsulated metal framework within it. Two manufacturing processes were investigated to determine the best method of fabricating an accurate parabolic antenna. While each of these processes is quite different, the final configurations are very similar.

In either process, the basic polyurethane foam dish is reinforced and supported by a metallic framework that is partially encapsulated in the foam. Both antenna types are made in segments to facilitate transportability, and the segments are bolted together on the site to form the complete reflector.

In one process, the reflecting surface is an aluminum foil - Mylar film laminate. The laminate is stretched over a male tool that has been made as accurately as possible ($\approx \pm 0.002$ inch) to the desired parabolic shape.

After the reflector surface has been formed to the shape of the tool, the back side of the reflector is foamed with a high-density foam and allowed to adhere and rigidize to maintain and support the reflector surface. The metallic support structure is then placed on top of the foam, and additional lower density foam is added to integrate the metallic support with the foam antenna dish. Figure 23 shows a 10-foot solar collector dish during the foaming operation. Utilizing this concept, once the original tooling was made, mass production of antennas would be inexpensive. Figure 24 shows the solar collector dish when completed.

For the second method, the foam antenna structure is first formed to the approximate contour, and onto this surface a thin layer of exothermic plastic material is applied by a special sweeping process being developed by Goodyear Aerospace. Figure 25 shows a preliminary 10-foot diameter reflector with its sweeping tool. In the final technique, a large precision turntable would be used to rotate the reflector or reflector segment to sweep

Figure 23. Solar Collector Dish during Foaming Operation

Figure 24. Completed Solar Collector Dish

Figure 25. Foam-Swept Antenna with Sweeping Tool and Dial Indicators

against a rigid, fixed-position, precision-contoured sweep template. This precision template sweeping process results in a very close tolerance, hard, durable surface. By addition of a metallic reflecting surface to the swept plastic contour using a metal spraying process, a highly accurate antenna surface is produced.

This sweeping process is not limited to foam-rigidized antennas, but is also applicable as a means of applying a very accurate surface to other more conventional antenna reflector structures.

Parallel, internally funded programs are being conducted at Goodyear Aerospace to develop and study both types of foam reflector structures. Results of these investigations will be reported in a subsequent section of this report.

These foam antenna concepts appear to have two basic advantages that are offered by either of the two methods for producing an antenna. They provide the following:

(1) A close-tolerance antenna reflector that meets the exacting requirements for satellite tracking and communication applications.

(2) Low cost. The processes for obtaining accurate reflector surfaces on the foam, as described, appear to offer an antenna of lower cost than the cost of producing an antenna of equal accuracy by other methods.

Surface contour stability under extreme environmental conditions may present a problem with this type of structure. The nature and extent of this problem were investigated under an internally funded development program and will be covered in a subsequent section of this report.

Foam-rigidized antennas closely fit the advanced antenna design program specifications defined by the contract work statement. The foam-rigidized antennas are expected to be supported by conventional pedestal-power assemblies. Tooling for the first alternate manufacturing process can be either rigid or inflatable. An in-the-field manufacturing operation may be somewhat difficult to optimize; however, it remains a possibility. In both antenna concepts, the dishes would be made in segments to facilitate transportability. Also, inflatable or foam-rigidized radomes of the types that will be mentioned later in this report could be used to provide shelter for on-the-site manufacture of at least smaller size antennas.

c. Inflatable Parabolic Antennas. Inflatable parabolic antennas offer the potential of obtaining a highly mobile antenna system with the capability of achieving operating efficiencies comparable to present conventional antennas. Various types of inflatable parabolic antenna concepts investigated in the early stages of the program are described in the following paragraphs.

(1) AIRMAT Paraboloid Antenna. The AIRMAT paraboloid antenna is a Cassegrain-type antenna concept that utilizes an inflatable AIRMAT

paraboloid main reflector. Figure 26 is an artist's sketch showing the basic construction features of this concept in a mobile configuration. The paraboloid antenna reflector, as initially envisioned, is formed by fabricating together pie-shaped segments of single-contour AIRMAT. The required surface contour accuracies are then obtained by foaming a flexible foam over the AIRMAT surface. The Cassegrain subreflector is supported by an air-inflated fabric cylinder. Nonreflective guy straps to the rim of the reflector stabilize the subreflector in the radial direction. Also, guy wires from the rim of the subreflector to the main reflector hub (not shown in Figure 26) stabilize the subreflector in the axial direction and provide a means for close control of the axial separation between the reflectors. Azimuth and elevation supports that are adaptable to any suitable pedestal can be provided. Movement in elevation is ±95 degrees from zenith and in azimuth is 360 degrees. In most cases, a radome would be used with this antenna to reduce environmental loads and to afford protection against the elements. The configuration shown in Figure 26 is specially mounted on a semitrailer for use as a transportable antenna. An inflatable radome is used with this concept, and the entire antenna system with its reflector, folding support pedestal, and radome can be packed into a relatively small package on the trailer bed.

Some of the basic advantages of this inflatable antenna system are:

(a) Packageability, which allows the antenna to be packaged into a single compact transportable unit.
(b) Ultralight weight feature, which allows ease of handling.
(c) Low inertia, which requires lower drive power and smaller, lighter bearings.
(d) Very quick erection and packaging.

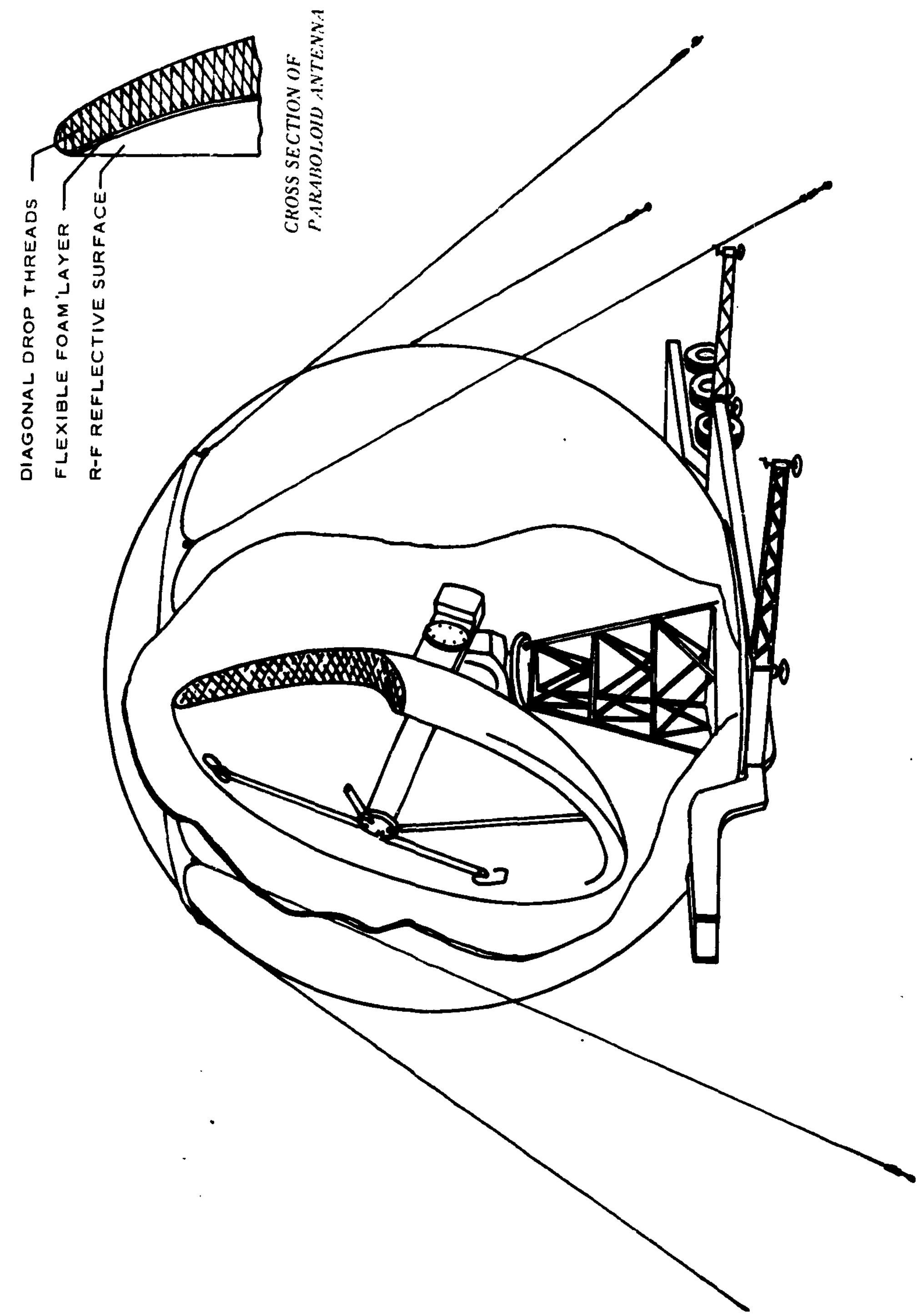

Figure 26. AIRMAT Paraboloid Antenna (Mobile Configuration)

(2) AIRMAT Vacuum-Supported Antenna. This antenna utilizes a vacuum instead of pressure to form the reflector surface. As shown in Figure 27, the basic antenna structure is formed by a curved AIRMAT structure that provides a ring support for the reflector surface. The reflector is a fabric diaphragm patterned to take the required parabolic shape when a vacuum is pulled between the AIRMAT support structure and the reflector skin. The reflective surface would be a Mylar - aluminum foil laminate or a sprayed-on flexible reflective coating.

This inflatable antenna has the same mobility, packageability, and light weight advantages as the previously described AIRMAT paraboloid antenna. In addition, this system will not have the problem of perfecting a noncreasing flexible-foam surface. The antenna concept, however, has some added complexity over the AIRMAT paraboloid, because it requires a vacuum source to maintain the reflector contour, in addition to the pressure supply for the AIRMAT.

(3) Lenticular AIRMAT Antenna. This antenna, shown in Figure 28, uses AIRMAT structure to form the reflector shape in a manner similar to that described for the AIRMAT paraboloid antenna. In this case, the AIRMAT is fabricated into a lenticular or convex lens shape with each side having identical parabolic contour. The rear surface is used as the r-f reflector and is formed to the required accuracy by foaming a flexible foam over the outside surface in a manner similar to that described for the AIRMAT paraboloid antenna. In this case, however, a thicker AIRMAT section is used, chosen to support the Cassegrain subreflector on the forward face at the correct distance from the main paraboloid reflector surface. Guy wires are used between the subreflector and rigid hub structure to accurately control the subreflector spacing. For this

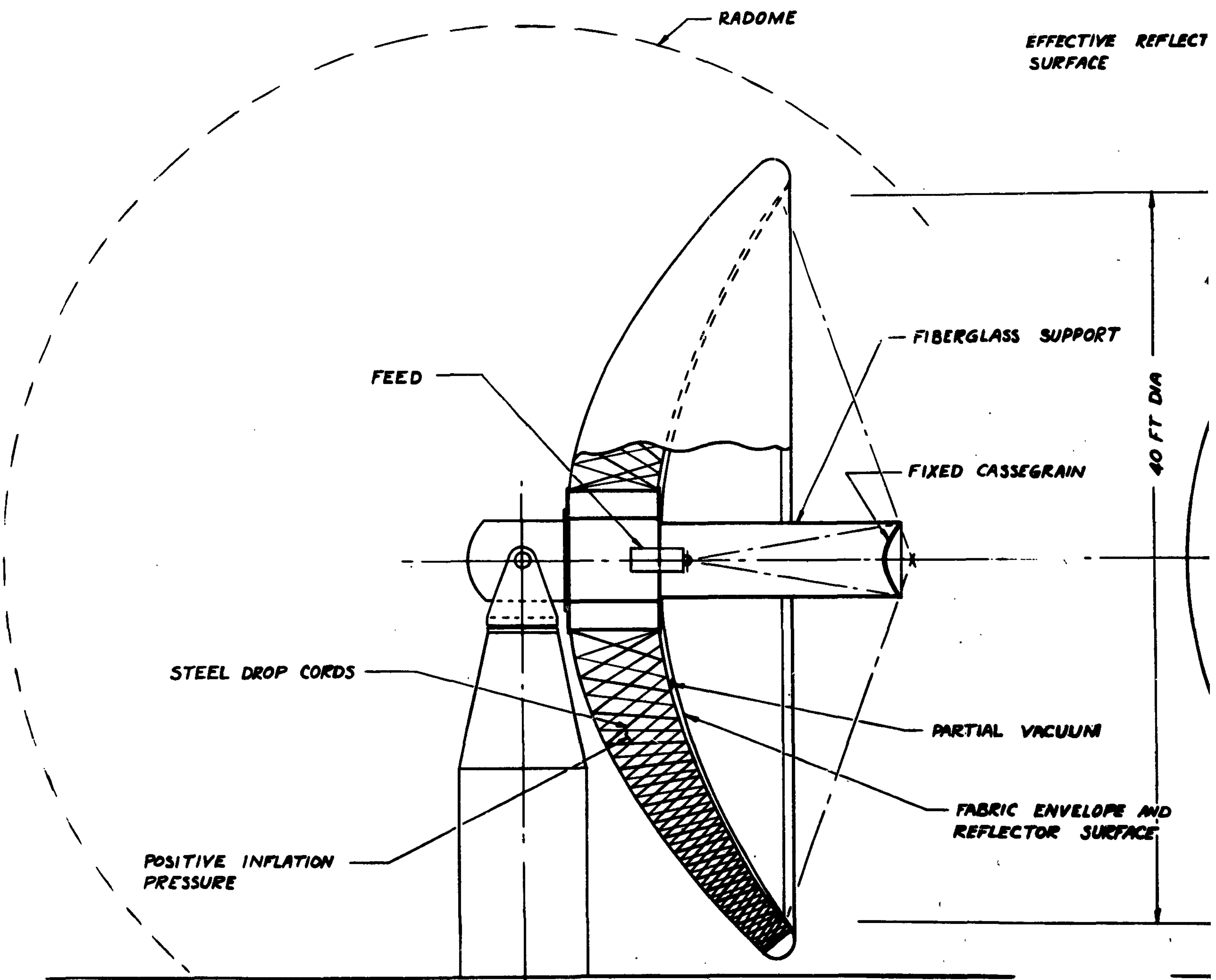
RADOME
EFFECTIVE REFLECT
SURFACE
FIBERGLASS SUPPORT
FEED
40 FT DIA
FIXED CASSEGRAIN
STEEL DROP CORDS
PARTIAL VACUUM
FABRIC ENVELOPE AND
REFLECTOR SURFACE
POSITIVE INFLATION
PRESSURE

1

2

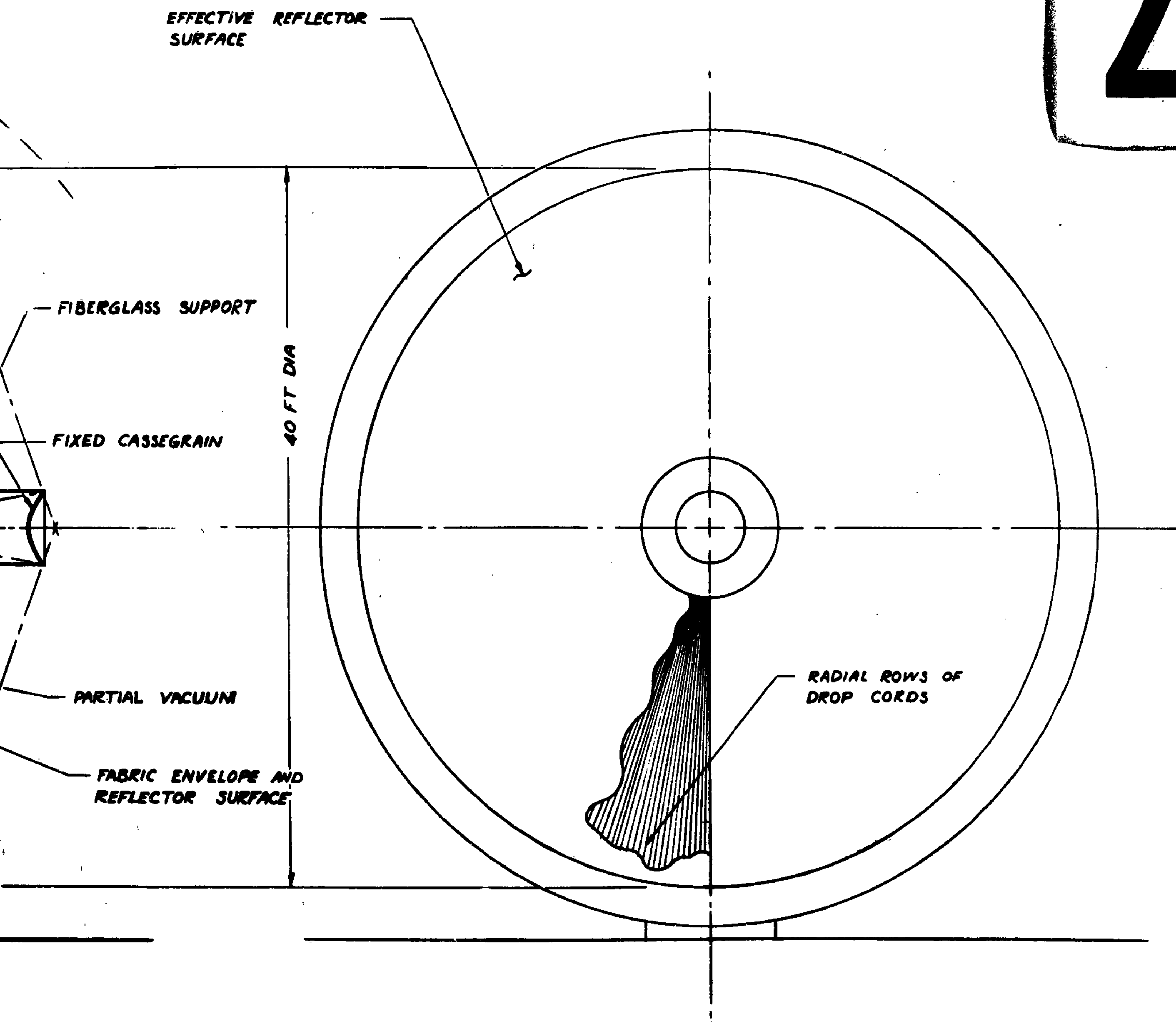

Figure 27. AIRMAT Vacuum-Supported Antenna

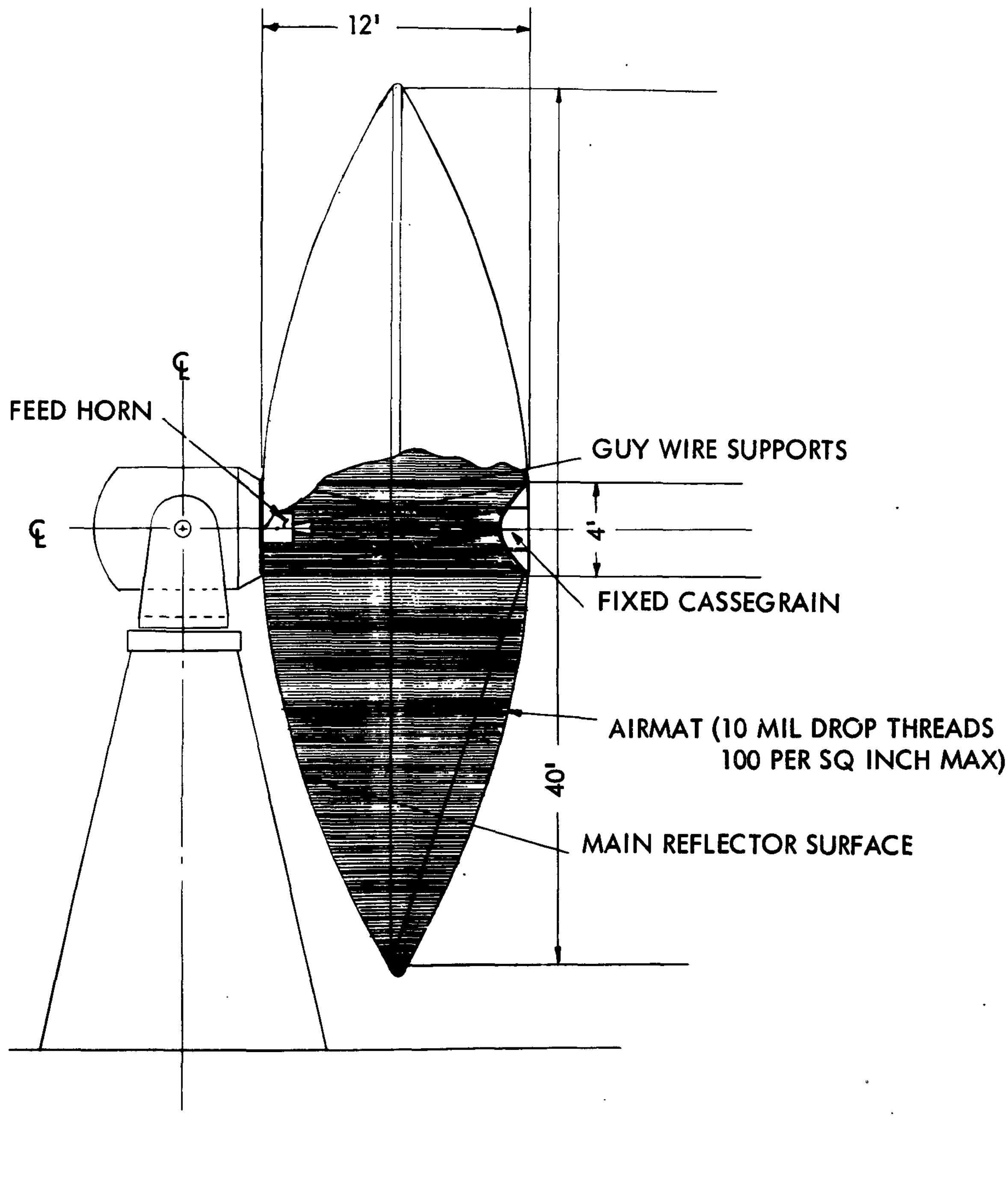

Figure 28. Lenticular AIRMAT Antenna

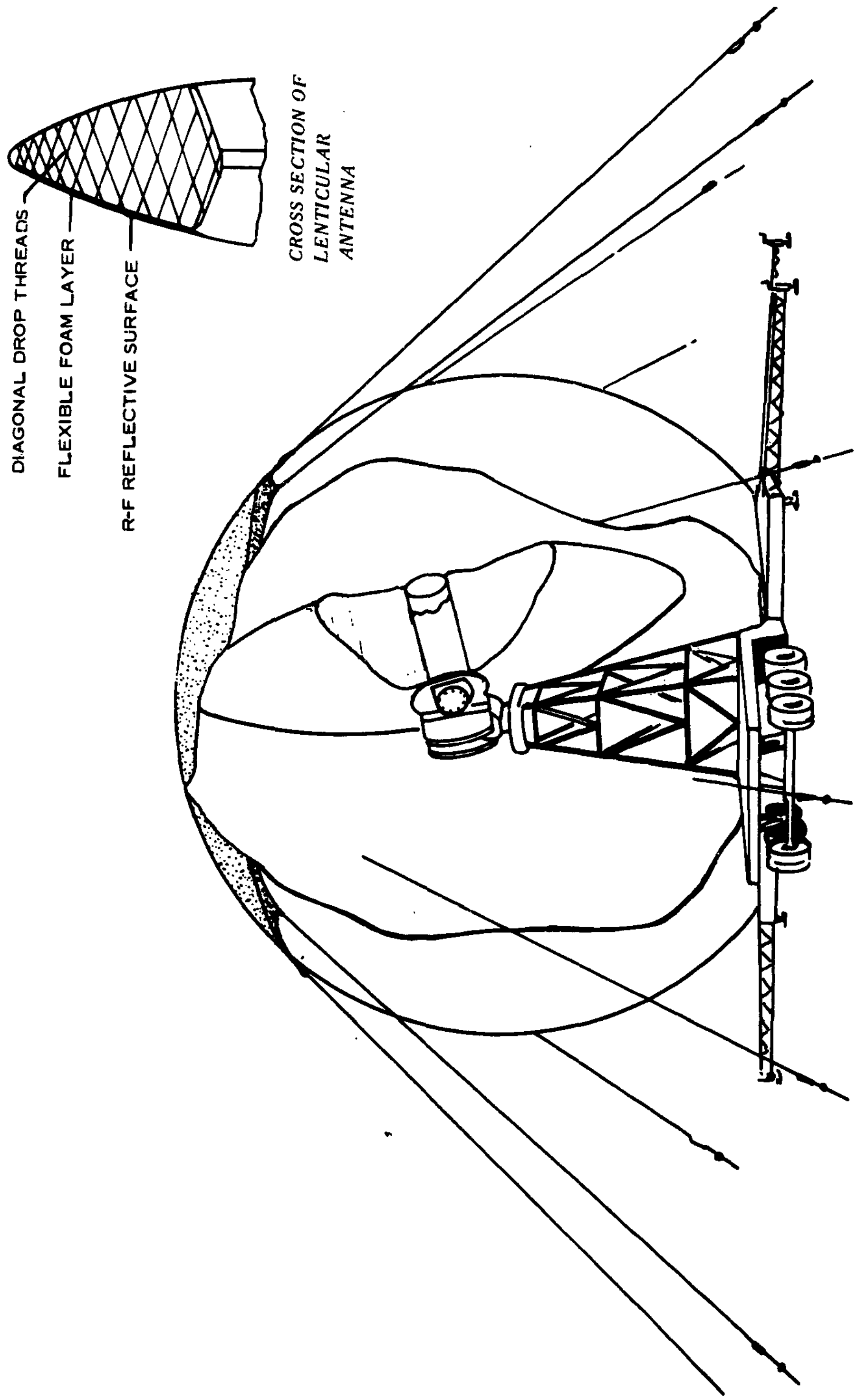

Figure 29. Lenticular AIRMAT Antenna System (Mobile Configuration)

concept, the r-f energy must be reflected through the AIRMAT structure. Evaluation of this problem and others is covered in another section of this report. Figure 29 shows a mobile configuration of this antenna.

This antenna has the same basic advantages as the AIRMAT paraboloid antenna.

(4) Torus-Supported Parabolic Antenna. The torus-supported parabolic antenna is an inflatable antenna mounted on a conventional pedestal. Figure 30 shows a preliminary layout of a 40-foot diameter paraboloid antenna. The torus supports the two identically contoured fabric skins to form an envelope that, when inflated, provides the reflector contour. The radial loads resulting from the internal pressure are counteracted by the inflated torus at the reflector's perimeter.

A Cassegrainian system appears the most compatible arrangement for this concept, because the weight of the feed is located close to the rotation axis, thus reducing the inertia of the reflector. The hyperbolic subreflector is mounted in the fiberglass support hub that is cantilevered from the main hub of the antenna.

For additional antenna stiffness, straps are attached in a bicycle-spoke arrangement from each side of the torus, crossing over to each side of the center hub.

Two different pressures are required to inflate this antenna. A relatively high pressure will be maintained in the torus, and a lower pressure will be utilized to form the parabolic reflector.

An inflatable radome will be used with this concept. Fiberglass cloth appears to be a good candidate material for the antenna because of its high strength and stiffness characteristics.

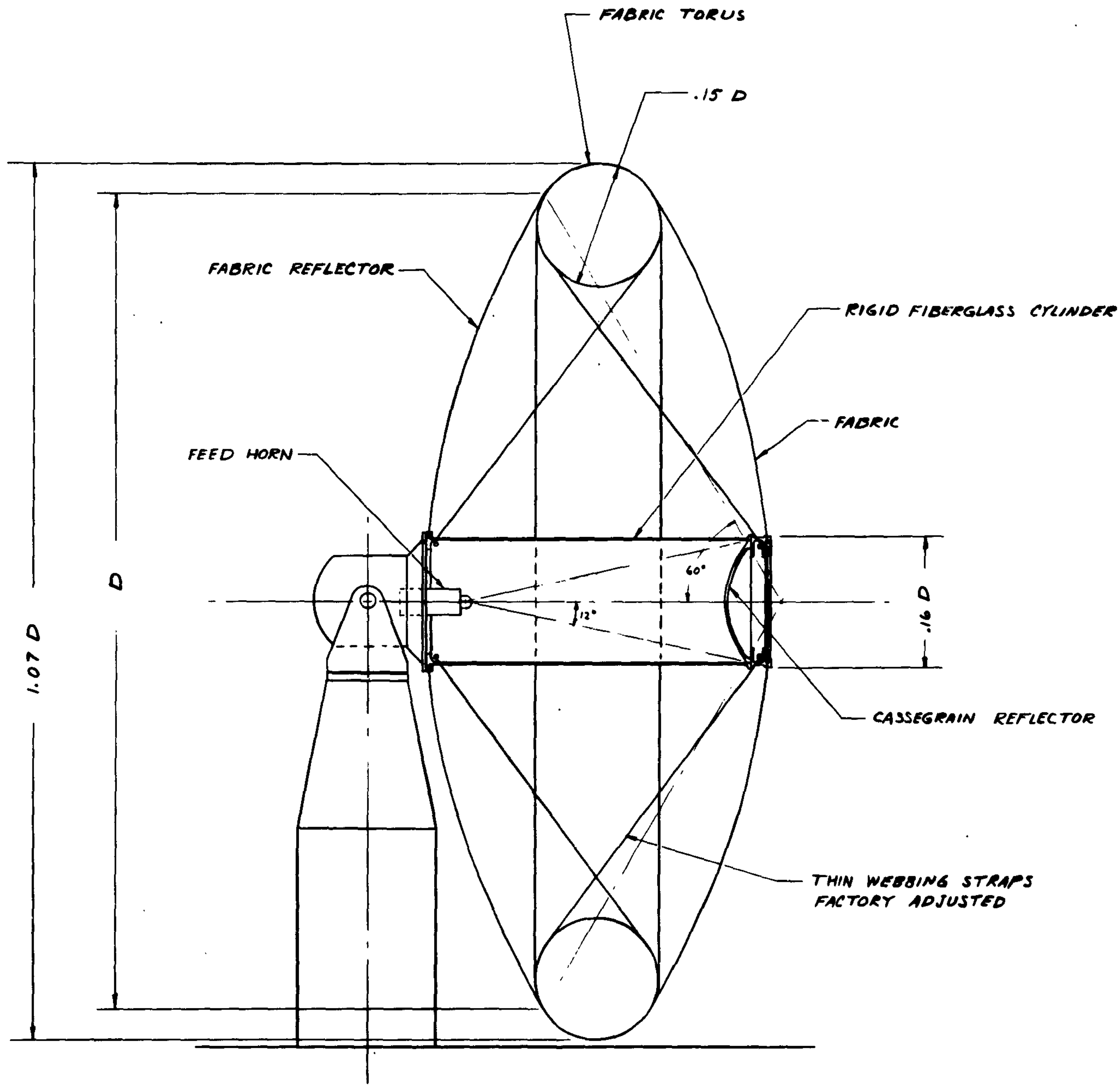

Figure 30. Torus-Supported Parabolic Antenna

The outstanding features of this concept are the easy and rapid erection advantages, the ease of mobility, and its low mass requiring lower drive power requirements.

Comparing this inflatable concept to the AIRMAT paraboloid, this concept has some inflatable structure ahead of the reflector as well as the fiberglass support tube, which will attenuate, reflect, absorb, and refract some microwave energy. Also, two different pressure systems must be monitored and regulated, whereas only one pressure must be maintained for the AIRMAT concept. The torus concept has an advantage in that it will be somewhat less costly to build than the AIRMAT concepts.

(5) Inflatable-Horn Antenna System. The inflatable-horn antenna concept utilizes a long f/D ratio parabolic reflector having a folded focal length. The structure is inflatable and is mounted on a single base. The radome is attached to the fixed portion of the base; the reflector system is attached to the rotating portion. This concept is shown in Figure 31. Both the reflector surface and the radome shape are maintained by air pressure. The entire pedestal, reflector, and reflector support system rotates 360 degrees in azimuth, and the reflector rotates 180 degrees in elevation to provide full tracking capability.

The following features of this concept are relative to rigid antennas:

(1) Lightweight structure resulting in ease of transportation, quick response to directional changes, and low drive power requirements.
(2) Quick assembly and erection.
(3) Electronic amplifiers and power equipment located in the base carriage; only readout, tuning, and manual direction control in a stationary position.

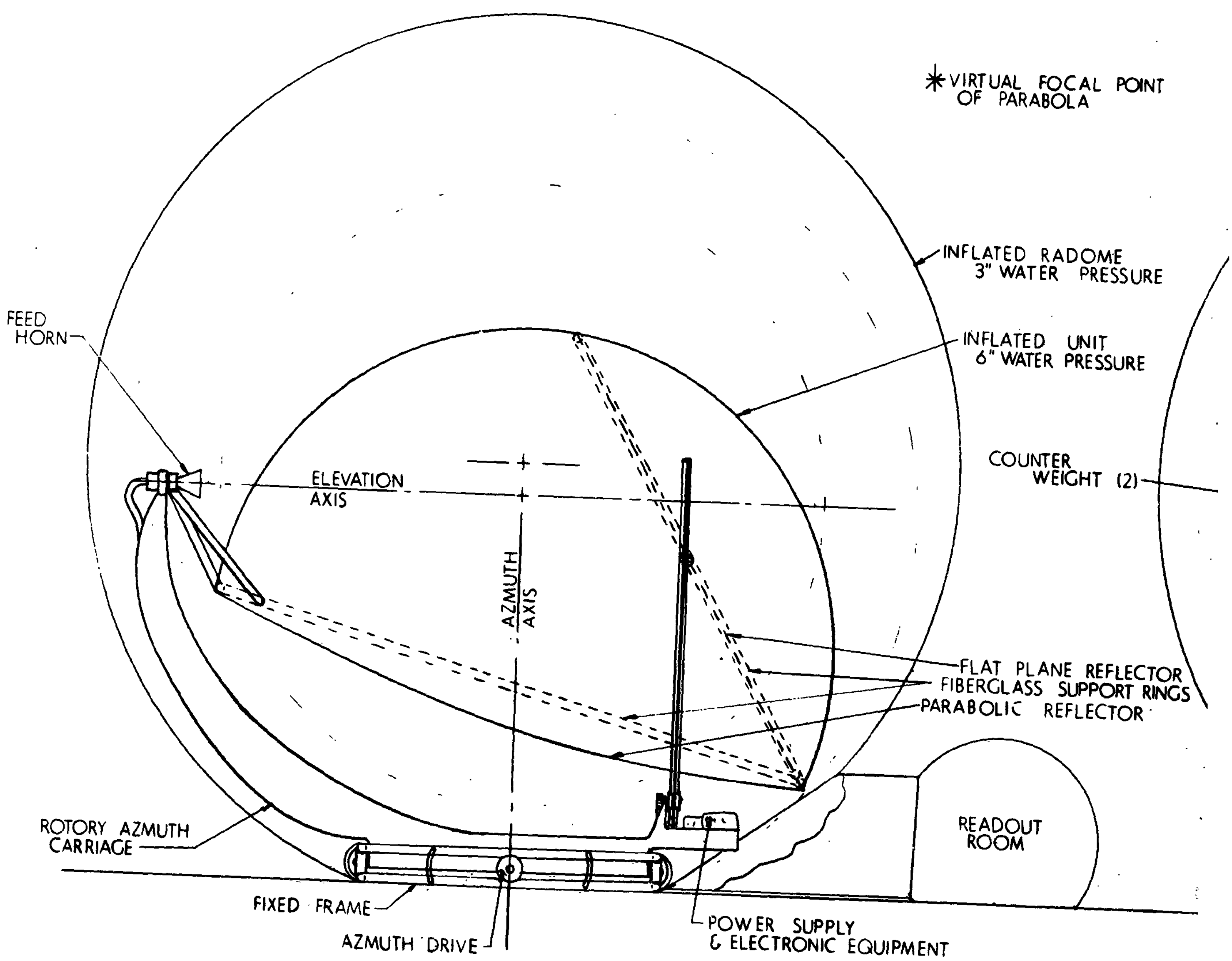

VIRTUAL FOCAL POINT OF PARABOLA
INFLATED RADOME 3" WATER PRESSURE
INFLATED UNIT 6" WATER PRESSURE
FEED HORN
ELEVATION AXIS
COUNTER WEIGHT (2)
AZMUTH AXIS
FLAT PLANE REFLECTOR
FIBERGLASS SUPPORT RINGS
PARABOLIC REFLECTOR
READOUT ROOM
ROTORY AZMUTH CARRIAGE
FIXED FRAME
AZMUTH DRIVE
POWER SUPPLY & ELECTRONIC EQUIPMENT

1

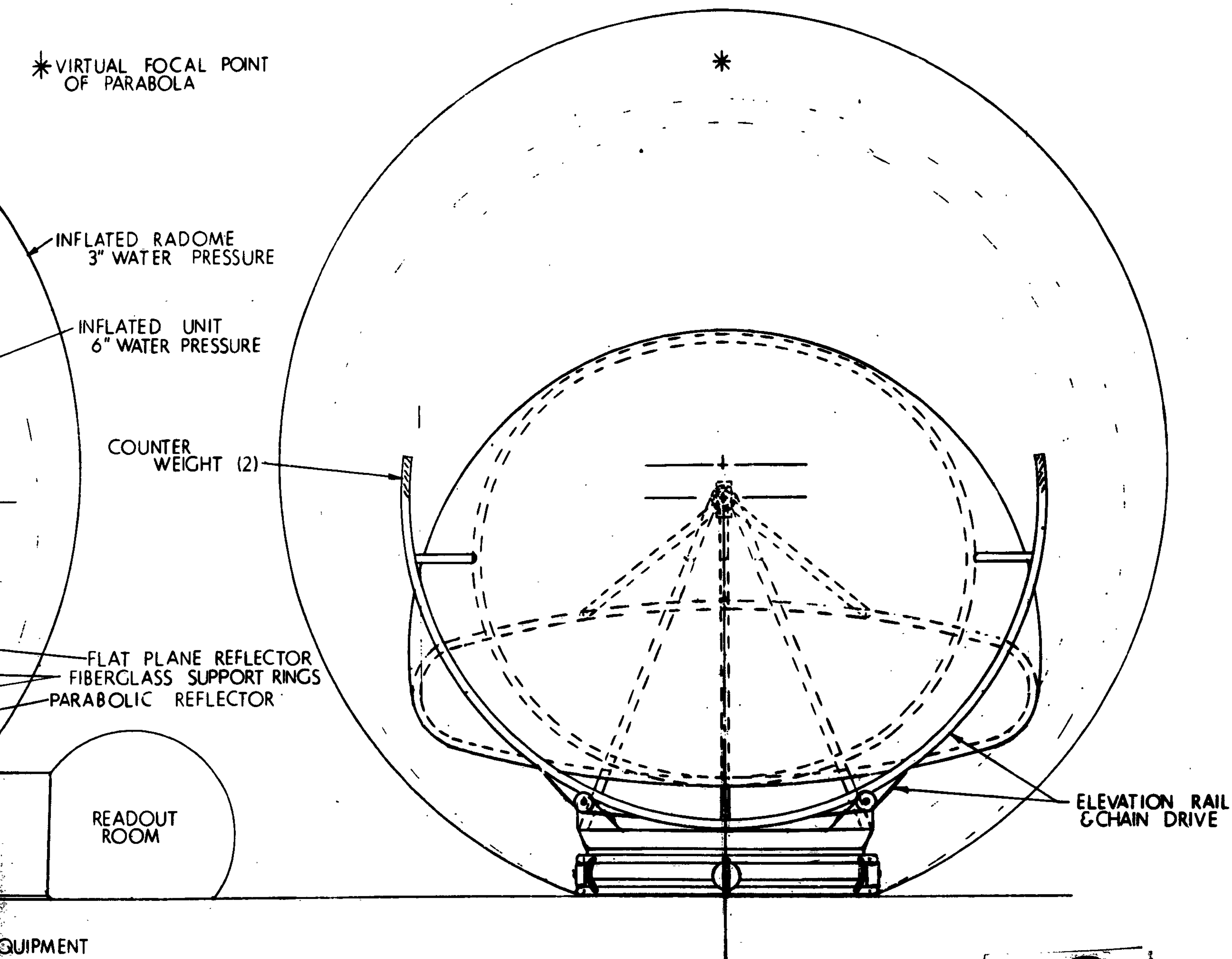

Figure 31. Inflatable-Horn Antenna

2

A typical folded reflector design considered employs a plane reflector surface that reflects the transmitted power from the feed horn into a 30-foot diameter parabolic surface with a long f/D ratio.

The plane reflector surface consists of a fabric surface supporting an array of parallel wires. This array (5-mil wires at 1/8-inch spacing) is bonded on the fabric surface and is positioned parallel to the polarization of the transmitted power from the feed horn and parallel to the struts supporting the plane surface.

The parabolic surface, which utilizes a dual-screen reflector, is formed by a pressurized envelope of fabric cloth and fiberglass rigid rings. The parabolic surface dual screen reflector is designed to twist the polarization of the energy reflected from the plane reflector. The dual screen is made up of a crossed wire screen on the bottom separated by a layer of flexible foam from a second screen made up of parallel wires. The parallel array of grid wires, however, is bonded to the fabric surface at a 45-degree angle to the parallel wires of the plane surface.

The purpose of the plane reflector is to fold the focal point from the normal parabolic focal point to allow the feed horn to be located at the edge of the parabola. This folding allows the over-all height of the antenna system to be reduced. Linear polarization is transmitted parallel to the plane surface wires and is reflected into the parabolic surface. Orthogonal linear polarization is reflected from the polarization twisting parabolic surface. Thus, the first reflector becomes transparent to the outgoing beam of the parabola. The position and surface tolerances on the plane and parabolic surface will be a major factor that will limit the gain that can be achieved with this configuration.

A structure of aluminum tubing supports the reflector. The structure is a semiconical configuration; the apex is supported by a bearing around the feed horn. The base of the structure is a sector ring. This structure rotates about a horizontal center line through the feed horn to provide elevation rotation. The reflector structure in turn is supported by the carriage, which provides azimuth rotation.

The radome used with this antenna is a coated-fabric sphere approximately 44 feet in diameter. This is the required size for clearance of the reflector and its support frame in the event of possible distortion due to high wind loads.

The advantages of the inflatable-horn antenna over rigid-type antennas are similar to other inflatable antennas. The advantages over other inflatable antennas, though, would be difficult to establish. The inflatable-horn antenna does not have the low noise ratio that is characteristic to the rigid metallic-horn antenna. Also, the rigid components, even though they may be folded somewhat, do limit the packaging flexibility of the concept.

(6) Deep-Dish Inflatable Antenna. The deep-dish inflatable antenna consists of an inflatable paraboloid closed off with a spherical cap as shown in Figure 32. The antenna is supported near the vertex by the same structure that supports the ring-shaped feed horn. Additional support can also be provided to the paraboloid by the support yoke; however, it is recognized that local attachments will tend to dimple the surface until the load is dispersed into the fabric envelope. A continuous support attachment to the yoke would require the yoke positioning to be very accurate. This positioning could probably be accomplished.

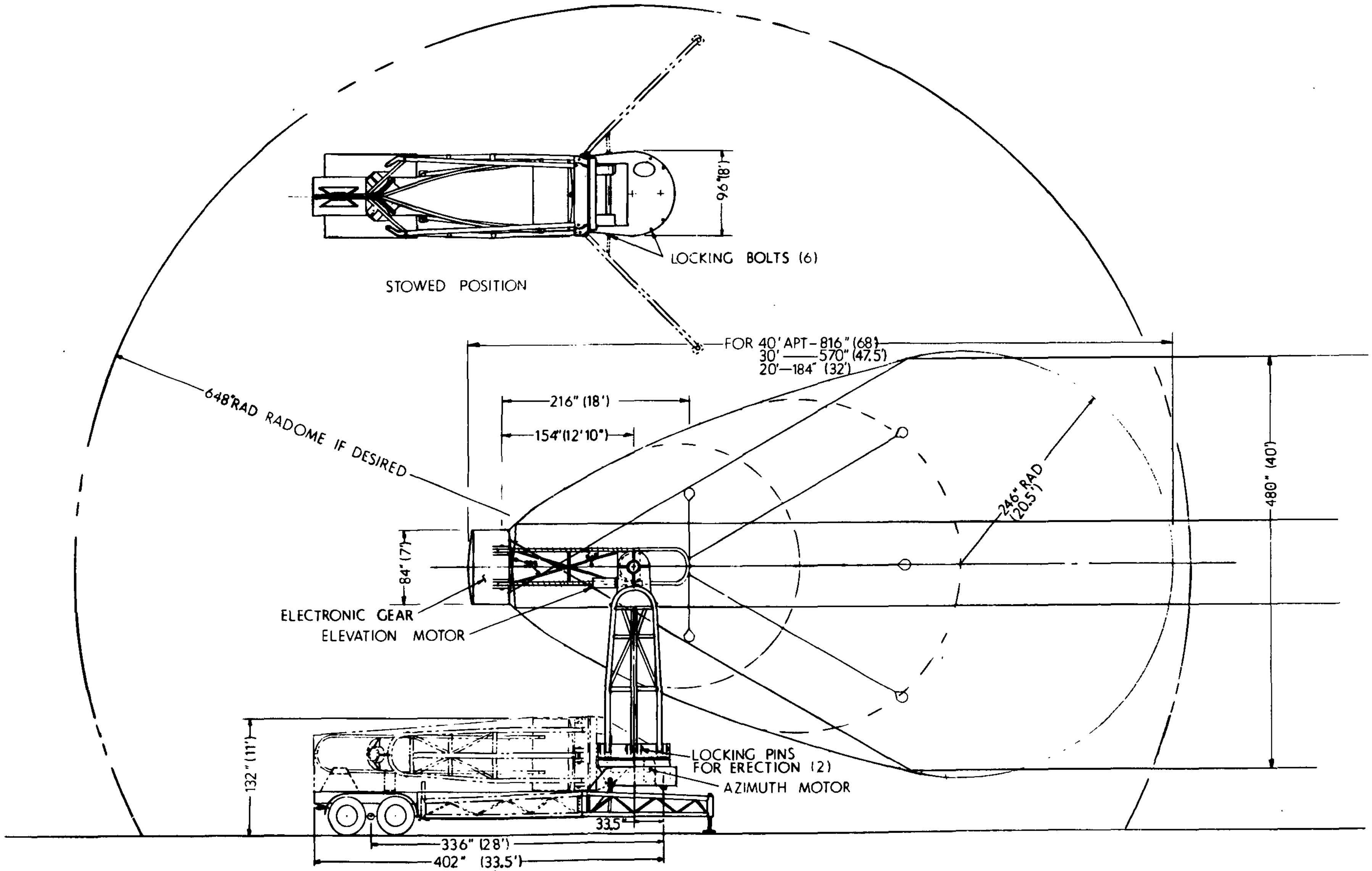

Figure 32. Deep-Dish Inflatable Antenna

The elevation pivot is located at the center of gravity of the feed-horn reflector unit.

The yoke is mounted on a turntable that provides azimuth positioning.

The turntable is part of a truck trailer, which houses the whole unit. For transport, the reflector is turned to the vertical position, then deflated. The fabric then lies in loose folds between the jaws of the yoke. After the fabric is secured, the yoke is folded hydraulically to rest compactly on the trailer bed. This trailer-pedestal concept is illustrated on this antenna, but it could be used with other antenna concepts as well. Radiation from the ring reflector passes through the parabola focal point and on to the reflective surface where it is reflected and collimated into a parallel beam.

Because of its shape, the deep-dish reflector inherently can hold a fairly accurate surface in the unloaded position. On the other hand, a greater surface accuracy is required, since the forward part of the reflector must reflect the received radar signal over a greater distance to the focal point, thus causing greater dispersion of the signal at the focal point. These two features may tend to cancel each other.

Because the feed horn is heavy relative to the coated fabric reflector, this attach point is relatively close to the parabola vertex. Hence, there is a large overhang of the antenna. This cantilevered overhang, coupled with the relatively small envelope circumference at the attach point, leads to large gravity and inertia bending moments at the attach point.

To preclude the excessive deflections that would be caused by environmental wind loads, a radome would be used for this concept.

The advantages of this antenna include low weight characteristics as compared to rigid structures and simplified construction techniques for the reflector.

The basic problem here is that this inflatable antenna probably has the most severe static and dynamic deflection characteristics of any of the concepts considered, and will have severe r-f design and bandwidth problems.

d. Foldable-Antenna Support Trusses. Two types of folding trusses were investigated. The types studied include a radially folding truss and an umbrella-type folding truss.

Folding-truss-type structures were investigated because of the need for fast erection. Obviously, to make any rigid structure foldable, one must pay in terms of weight, cost, and complexity. These items must be considered as trade-offs for reduced erection time if this is a major requirement.

Both folding truss concepts were designed to be used with a multiple-segment dish concept so that the dish as well as the support structure would be packageable.

One such foldable truss studied was a radially folding truss. This support truss, shown in Figure 33, consists of a central hub to which are hinged the radial cantilever beams that support the antenna dish. Ring segments are used to position the trusses in the radial position. To fold the support truss, the trusses can be rotated about the hub in a plane perpendicular to the parabolic axis.

In this manner, half the radial members can be pivoted forward and half rearward to make a 40-foot long pack that can be transported and then

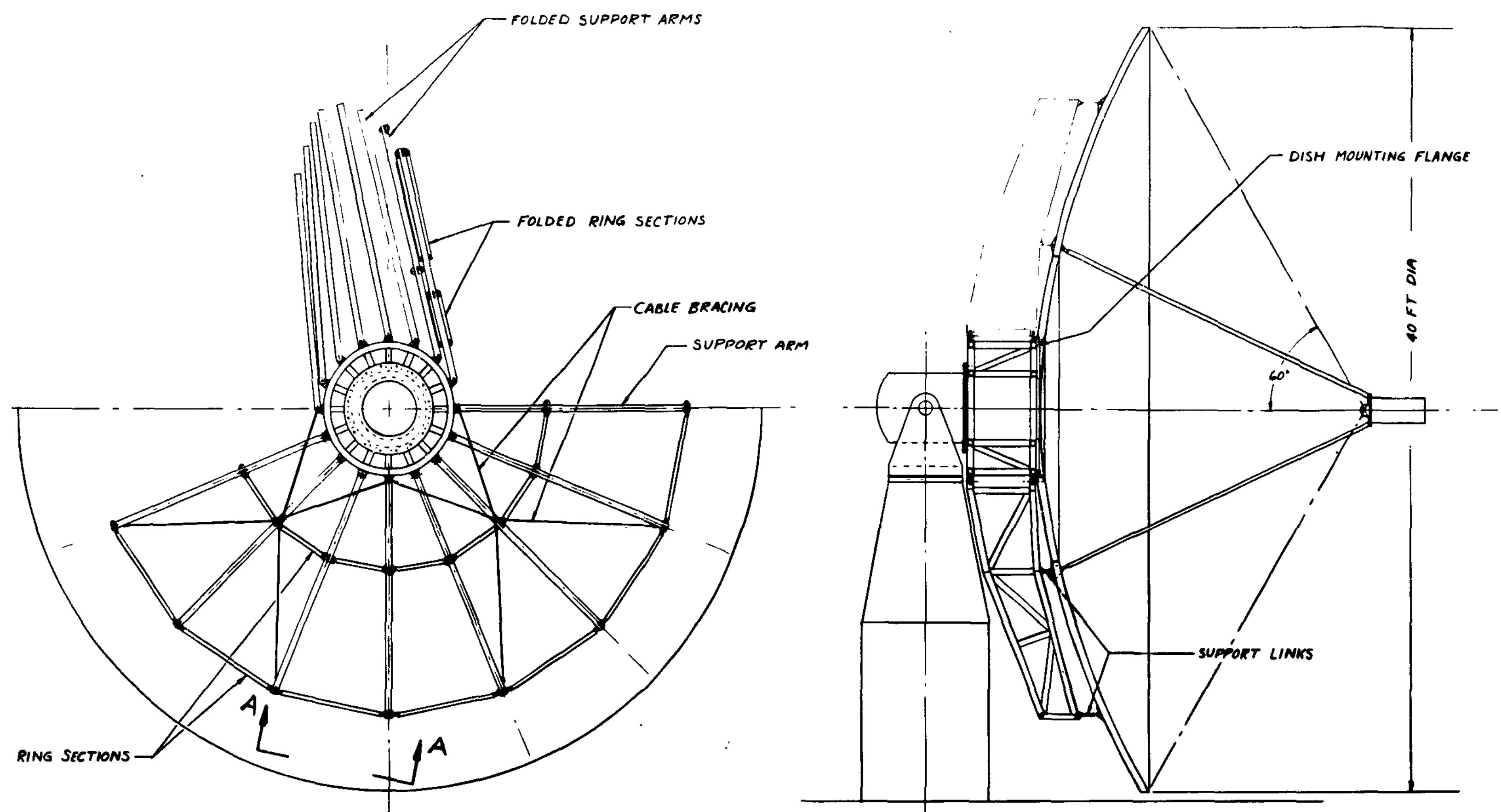

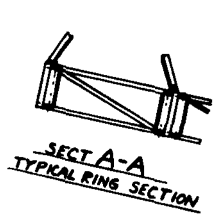

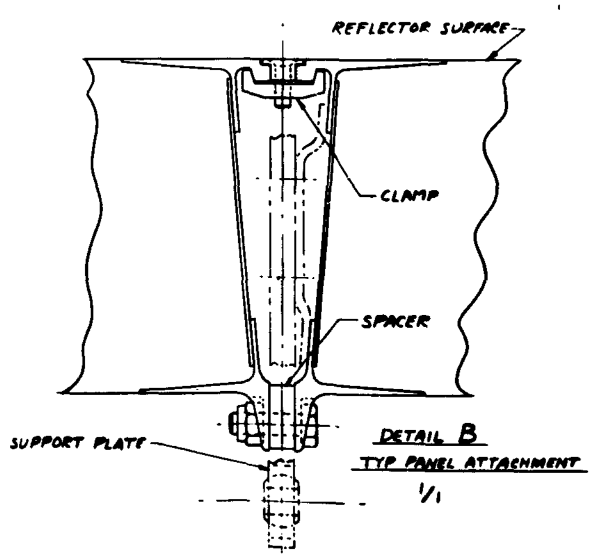

NOTES:

1. REFLECTOR DISH IS CONSTRUCTED OF THICK-SECTION F
2. PANELS (EXCEPT CENTER PANEL) ARE OF ALUMINUM BO OR FIBERGLASS SANDWICH WITH PAPER HONEYCOMB CC
3. SUPPORT LINKS TO BACK UP STRUCTURE ARE BALL ENDE REACT FORCES IN AXIAL DIRECTION ONLY. LENGTH O LINK IS FACTORY ADJUSTED TO GIVE PROPER CONTOU
4. DISH TORQUE AND SHEAR ARE REACTED AT MOUNTING
5. TORQUE ON BACK-UP STRUCTURE IS REACTED BY CABLE SYSTEM. CABLES ARE FACTORY ADJUSTED, REQUIRING TENSIONING OF ONLY TWO CLOSING CABLES.
6. RING SECTIONS ARE FACTORY ADJUSTED.
7. CENTER DISH PANEL IS AN ALUMINUM SPINNING.
8. F/D = 0.433

1

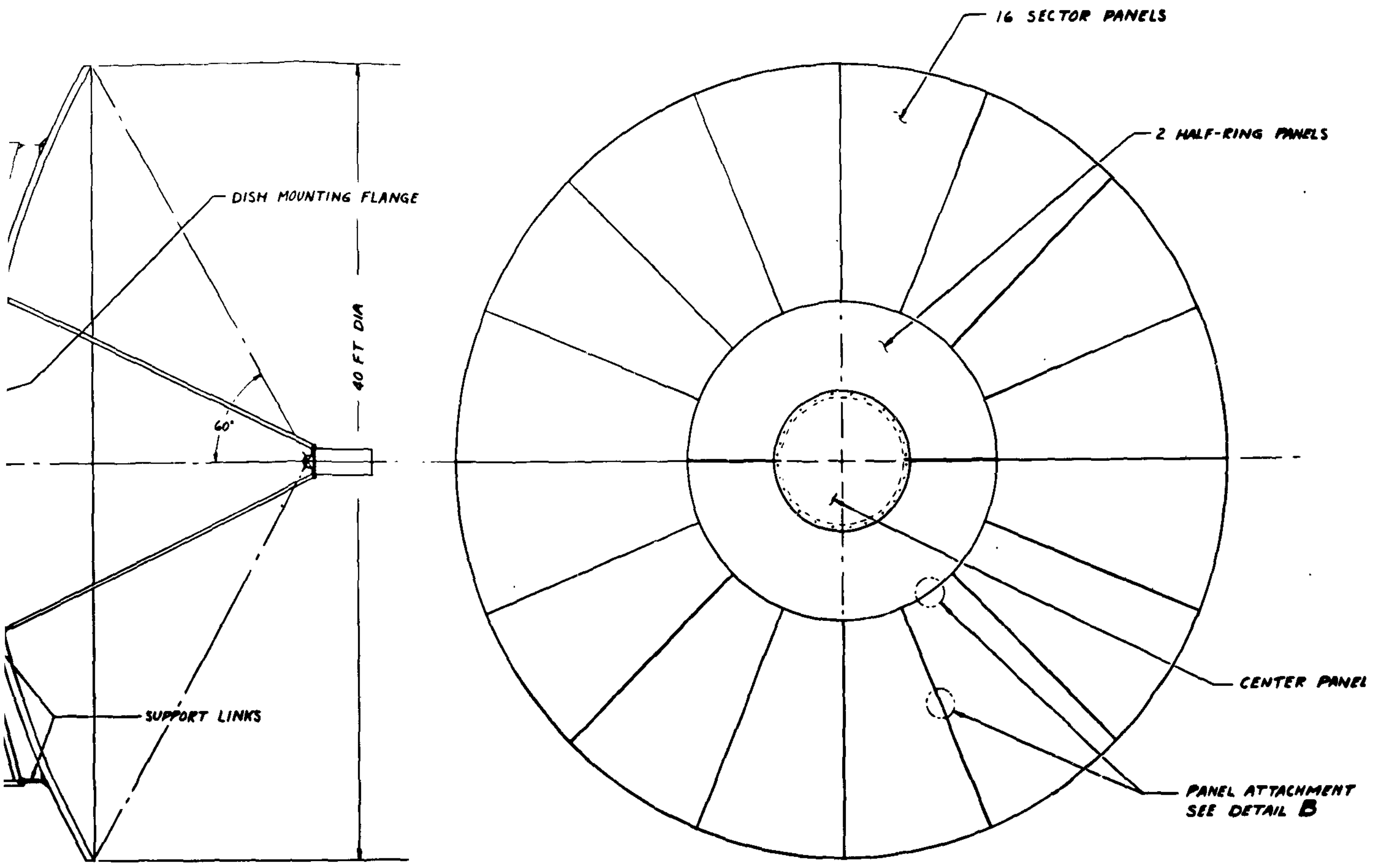

:TOR DISH IS CONSTRUCTED OF THICK-SECTION PANELS.
LS (EXCEPT CENTER PANEL) ARE OF ALUMINUM BONDOLITE,
IERGLASS SANDWICH WITH PAPER HONEYCOMB CORE.
)RT LINKS TO BACK UP STRUCTURE ARE BALL ENDED TO
I FORCES IN AXIAL DIRECTION ONLY. LENGTH OF EACH
IS FACTORY ADJUSTED TO GIVE PROPER CONTOUR.
TORQUE AND SHEAR ARE REACTED AT MOUNTING FLANGE.
UE ON BACK-UP STRUCTURE IS REACTED BY CABLE BRACE
'M. CABLES ARE FACTORY ADJUSTED, REQUIRING FIELD
IONING OF ONLY TWO CLOSING CABLES.
SECTIONS ARE FACTORY ADJUSTED.
ER DISH PANEL IS AN ALUMINUM SPINNING.
0.433

12

Figure 33. Radially Folding Support Truss

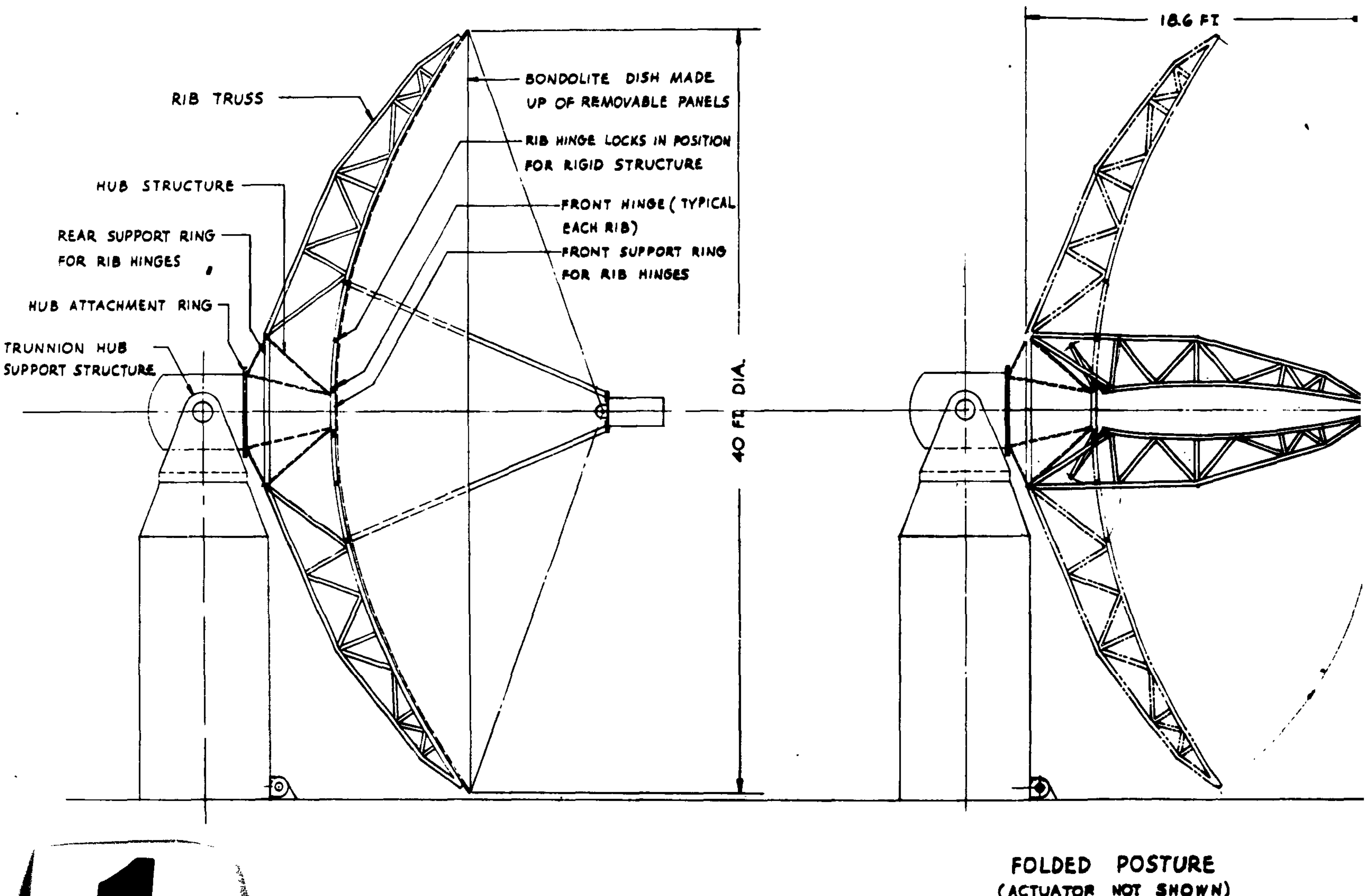

Figure 34. Umbrella-Type Folding Truss (Sheet 1)

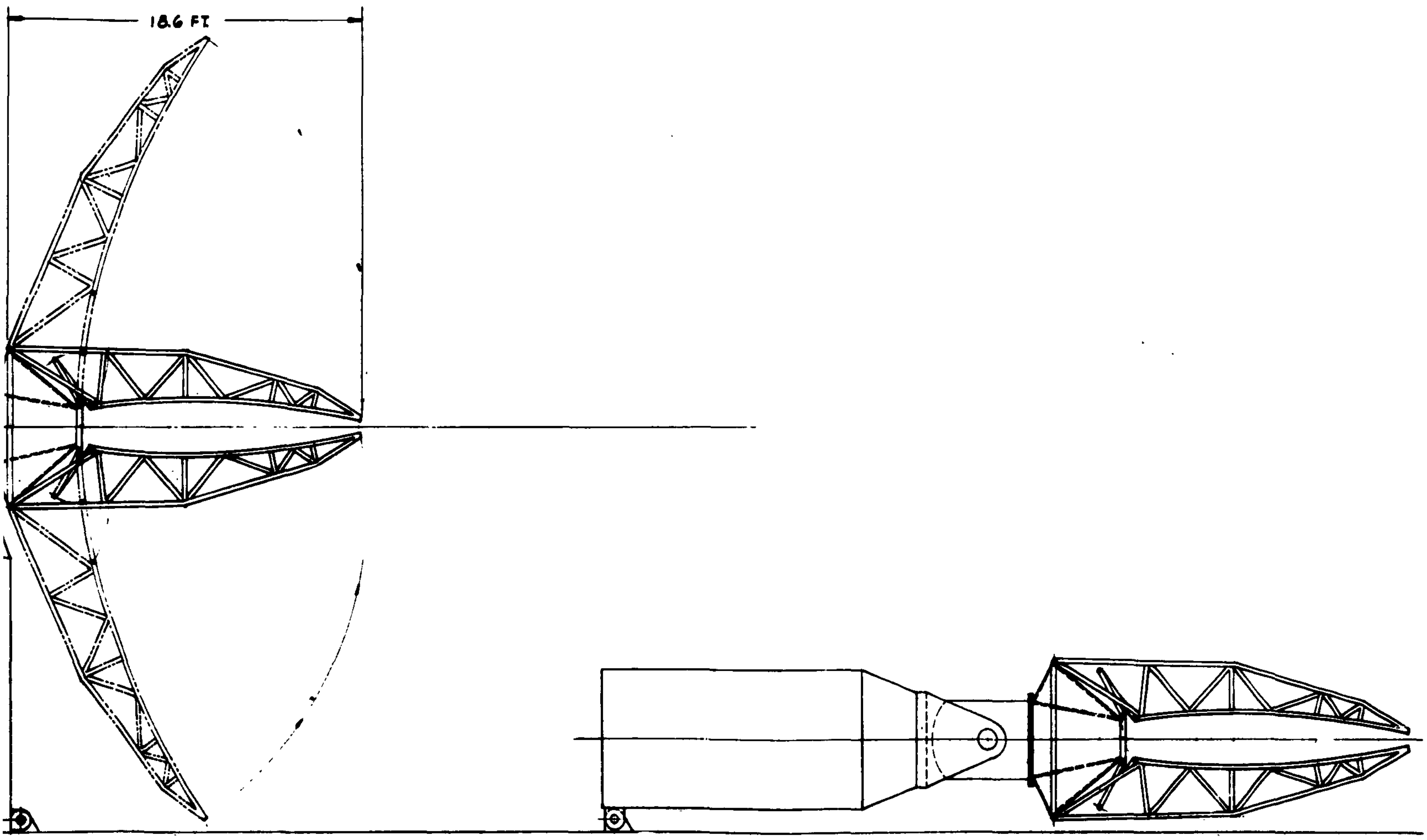

OLDED POSTURE
:TUATOR NOT SHOWN)

RECLINED POSTURE
(ACTUATOR NOT SHOWN)

12

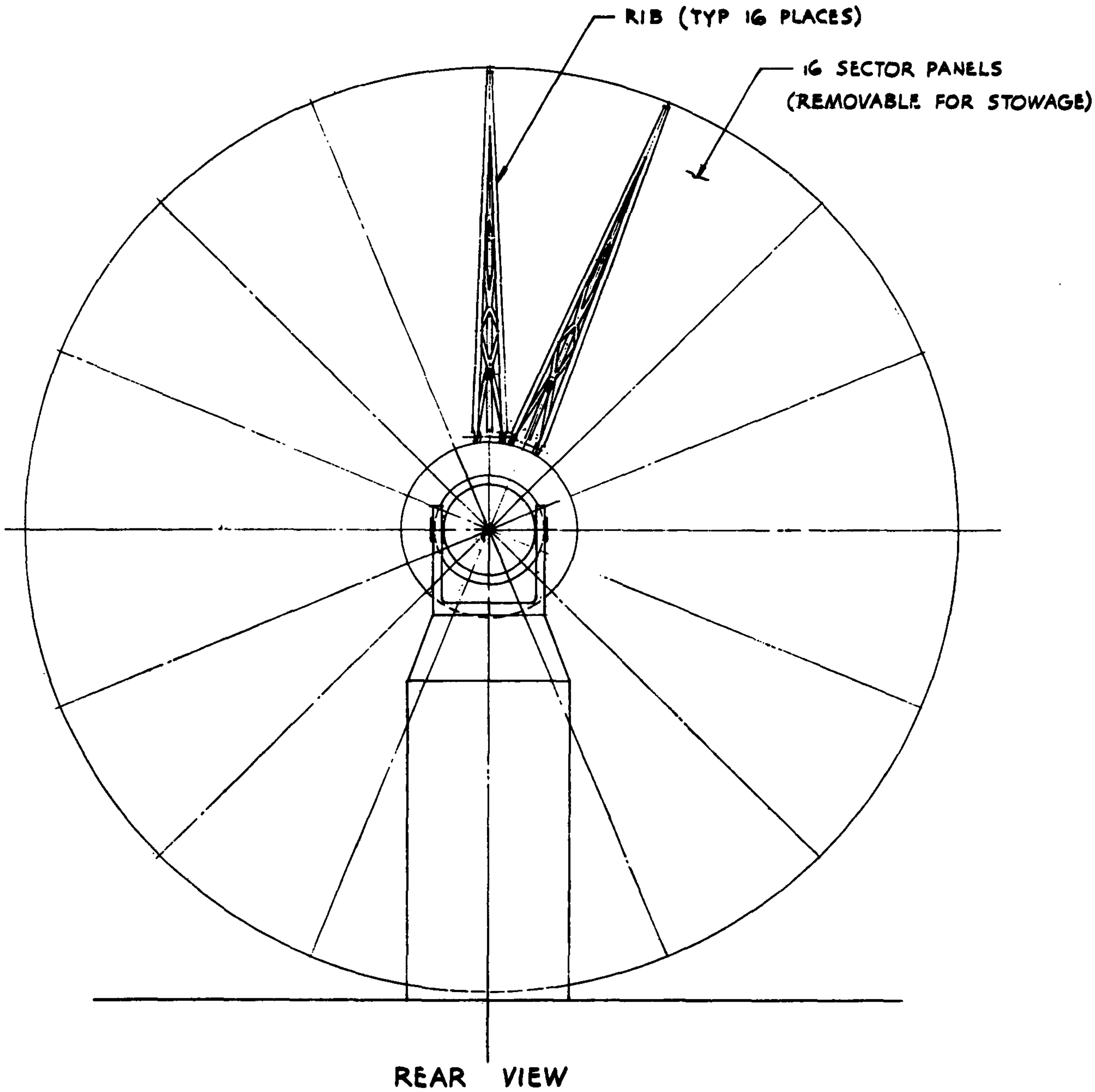

Figure 34. Umbrella-Type Folding Truss (Sheet 2)

erected quickly on the site. A typical erection procedure is explained in the following paragraph.

During transport, the hub and entire back-up structure remain assembled to the pedestal and folded in a compact unit. At erection on the site, the back-up structure is erected by swinging the radial beams into place, positioning them by the ring segments, and then attaching and tensioning the four closing cables of the cable brace system. The back-up structure is then ready to receive the dish segments. The two half-ring panels of the dish are bolted to the mounting flange, and the mating edges are attached as shown in Detail B of Figure 33. The 16-sector panels are then assembled successively onto the two half-ring panels by clamping and bolting all edges as shown in Detail B. The sectors are attached to the back-up structure by connecting the support links to them. These links, adjusted to length at the factory, hold the dish in proper contour with little or no in-the-field adjustment. Since the bolt spacers, as shown in Detail B, are also factory-adjusted and fixed in place, no adjustment of the reflector should be necessary in the field.

Another type of foldable truss considered was an umbrella-type folding truss (see Figure 34). The folding of the trusses in this case is not in the same plane but rather toward the axis of the paraboloid. This design may compact a little better than the previous one, since it will fold to about half the length of the other. The design uses a truss that is triangular in cross section with the single chord member in contact with the back of the parabolic reflector sections. This configuration was chosen to provide roll stability.

e. <u>Multiple-Reflector Array Antenna</u>. A multiple-reflector antenna system was investigated, since deflection and manufacturing tolerances can be held

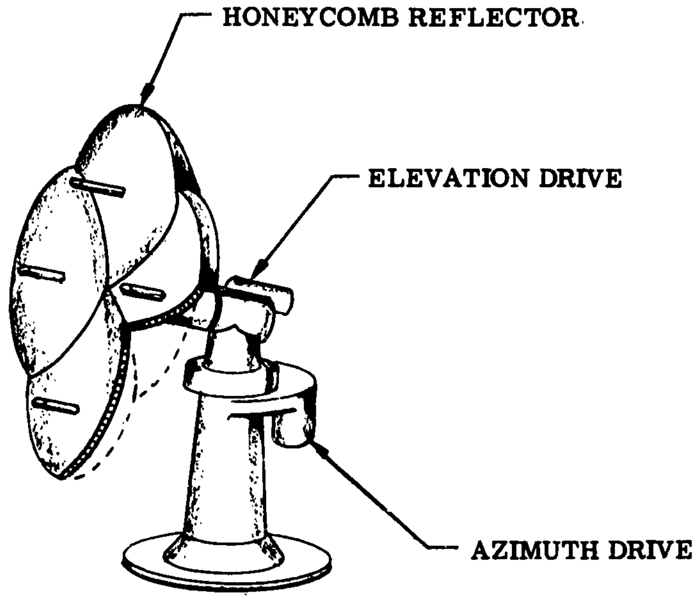

Figure 35. Four-Element Multiple-Reflector Antenna

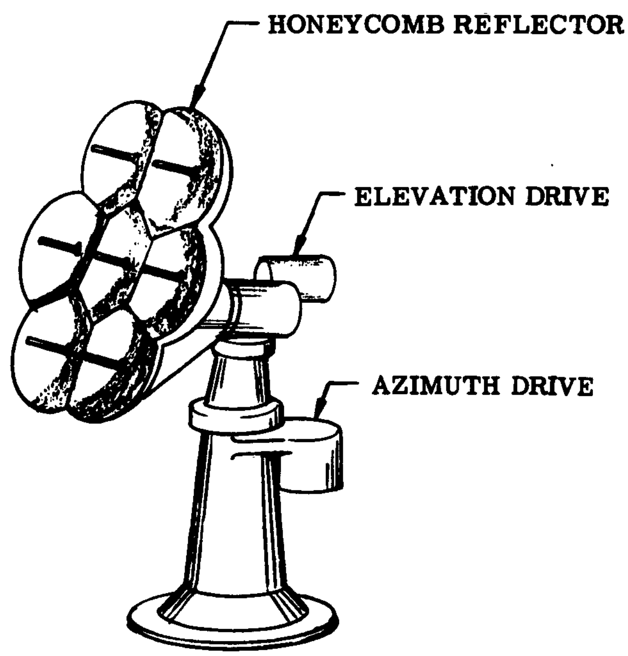

Figure 36. Seven-Element Multiple-Reflector Antenna

better on small reflectors than on large reflectors. Therefore, since an array of paraboloids can be used to obtain approximately the same gain as a single paraboloid of nearly the same diameter, this concept offers good possibilities. The depth of the multiple-reflector array is less than that of the corresponding single reflector. This unit would therefore require less bulky supports and could scan mechanically, using smaller drive units. Multiple reflectors consisting of several adjoining parabolic surfaces as shown in Figures 35 and 36 result in a-20 db and -16 db side lobe level for a 4-element and 7-element array respectively by the frequency sensitive technique of setting the beamwidth equal to that of a large single reflector. The multiple-reflector assembly could also consist of individual reflectors with synchronized drive units as shown in Figure 37.

The gain of a multiple reflector (four or more parabolic sections) is approximately 1 decibel below that of a single parabola with the same diameter reflecting surface (see Figure 22). The structure could be adapted to the 100 mcs to 10 kmc range. Side-lobe levels are raised from those of a single reflector due to the spacing of the elements. This system would require individual feeds and a power divider network. The 4-individual-unit array would require a phase shifting network to compensate for the relative displacement among the various dishes.

For transportability, the multiple-reflector antenna system can be broken down into several smaller components more easily than a large single reflector, while still not affecting the reflector tolerances.

f. <u>Foldable-Fan Reflector</u>. The design concept shown in Figure 38 depicts a method of folding reflectors up to 20 feet in diameter. As shown, the reflector is sectionalized into fan-type panels with built-in stiffness such as sandwich construction. Each panel has a collar at the vertex, which fits

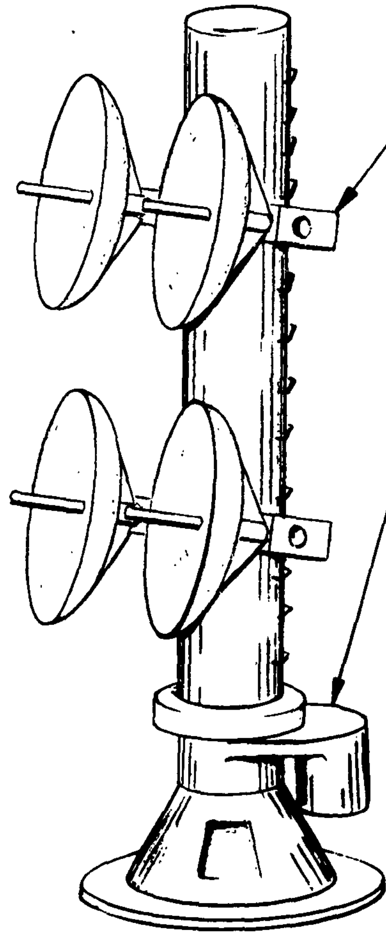

Figure 37. Multiple-Reflector Antenna
Synchronized Drive Units

over a central hub. The edges of the panels are flanged to provide surfaces for panel mounting. For shipping, spacers are installed between panels on the hub, and the panels are rotated individually to the down position, nested, and locked in place. The hub also serves as the feed-horn support mount.

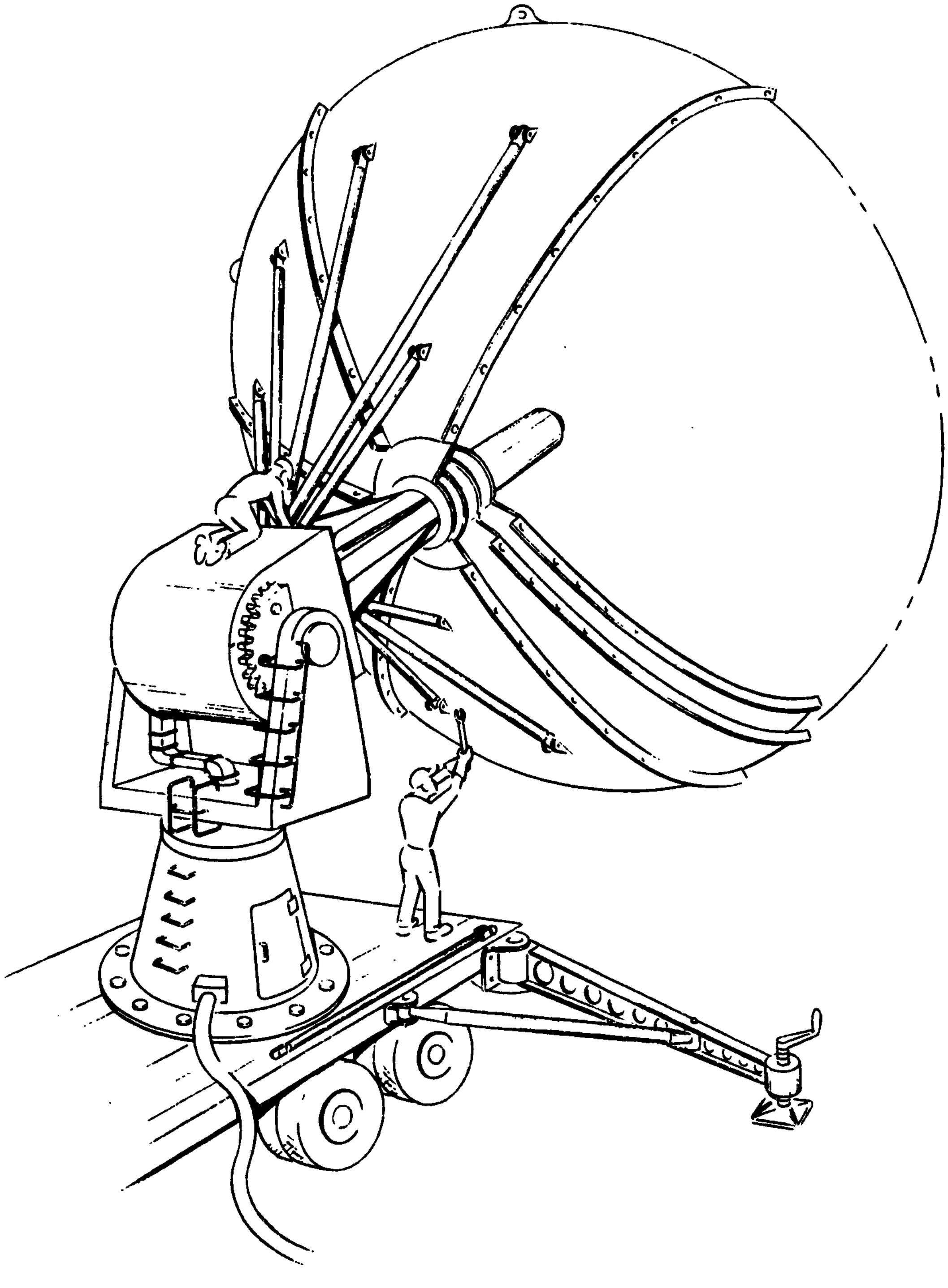

Figure 38. Foldable-Fan Antenna

The advantages of the foldable-fan antenna are mobility and quick erection for a rigid-type antenna.

The disadvantages presently appear to be predominant. The parabolic fan sections would have to be quite thick (depth of skin and backup structure) to provide adequate stiffness. This feature requires excessive axial displacement in order to nest the fan sections and involves considerable complexity at the hub. To provide foldability and the required stiffness, the entire structure would be complex, heavy, and expensive.

g. Rigid-Panel Swirlabola Antenna. This antenna, described in Section V, was developed initially for space vehicle applications. The basic concept can be adapted, with suitable modification, to ground-based applications. This folding petal reflector concept shows good potential for a transportable quick-erecting ground-based antenna that can be stowed and packaged for trailer or air transportation. An antenna of this type can be easily and quickly erected for operation and can be quickly retracted, stowed, and moved to another site. Structural integrity necessary to withstand high wind loadings and transportation loads would require special consideration for the supporting rib structure and hinge design; however, this does not appear to present a serious problem. The Swirlabola design provides a stowed diameter in the order of 40 to 50 percent of the extended diameter in the operating position. Permissible packaged size as required for transportation would dictate the maximum operational size. Fifteen tc 20 foot diameter operational size is considered reasonable.

h. Sandwich-Panel Antenna. Figure 39 shows an artist's concept of an antenna fabricated of individual sandwich panels that fasten together to form the antenna reflector. The panels have a honeycomb core with metalized fiberglass or metal skins that are preformed to contour in a mold at assembly. These

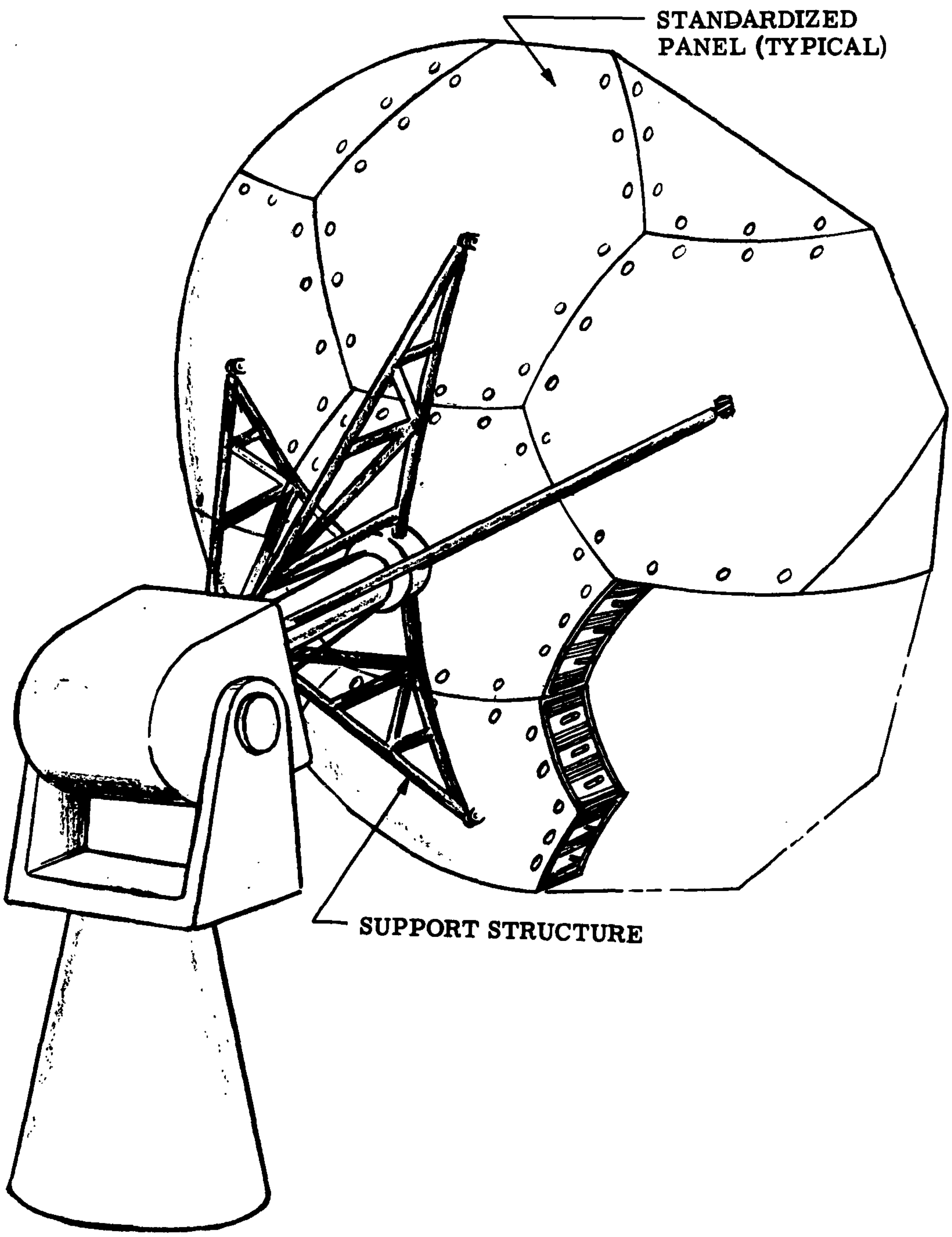

Figure 39. Sandwich-Panel Antenna

panels are bound at their edges by load-bearing channels that are aligned with pins in the factory to assume proper alignment when erected in the field.

This antenna reflector would be a very stiff structure. The greater weight would require sufficient stiffness in the reflector support structure, which would again add weight to the system. Tooling and fabrication costs would be high because of the close tolerances that would be required on joining the various surface contours.

3. Spherical Reflectors

Three different versions of spherical reflector surface antennas were considered on a cursory basis:

a. Spherical Curvature Reflector. A spherical surface can be made to have a gain which is equivalent to that of a paraboloid of the same diameter. This is accomplished by making the spherical surface variation within 1/16 of a wave length from the contour of a paraboloid with the same focal distance and same aperture size. This factor determines the minimum f/D ratio that can be used for a given size aperture. The upper frequency limitation is determined by the 1/16 of a wave length criterion. Long focal lengths are required in order for the spherical reflector to have a surface variation within $\lambda/16$ of the matching parabola, and therefore its use is limited by the minimum f/D ratio required for electrical performance.

For mechanically scanned reflectors in the size range considered in this program, the spherical contour reflector offers little if any advantage over the parabolic reflector from the standpoint of economy of manufacture. A parabolic surface can be produced as easily as a spherical surface with the manufacturing and tooling methods normally used in the manufacture of antennas in the 10 to 40 foot size range.

Basically, the spherical reflector has good potential for use as a stationary reflector for very large antennas that are too large to position practically by movement of the reflector itself. In this application, scanning is accomplished by movement of the feed, and only a portion of the spherical surface is illuminated at one time, while the feed scans at a constant focal distance from the reflector surface. In addition, the reflector size is large in comparison to the effective aperture size for large scan angles, and the geometry limits the extent of azimuth and elevation coverage obtainable with a single stationary metallic reflector.

b. Hemispherical Reflector. Another spherical surface configuration consists of a hemispherical reflector (see Reference 4) that is set on a pedestal containing the azimuth drive unit, while elevation scan and partial azimuth scan are accomplished by rotating the feed unit. This configuration is shown in Figure 40. The hemisphere is initially tilted to provide the desired elevation coverage. This reflector has a useful feed-scan angle of approximately 140 degrees, but the feed pattern should have at least -25 db side lobes in order to obtain a relative reflector side-lobe level of around -20 db. The specialized feed that is required to obtain the low-feed side-lobe levels makes this a narrow bandwidth device.

c. Inflatable Spherical Antenna. An inflatable spherical antenna that provides 360 degrees scanning in azimuth and limited elevation scanning is shown in Figure 41. Here only a portion of the spherical reflector surface is illuminated at one time. The radius of the sphere is sufficiently large so that the illuminated portion of the surface reasonably approaches a paraboloid. The feed is mechanically rotated in the azimuth and elevation planes such as to maintain a constant optimum focal distance from the surface. The feed is polarized at 45 degrees. A parallel grid of wires or conductive strips

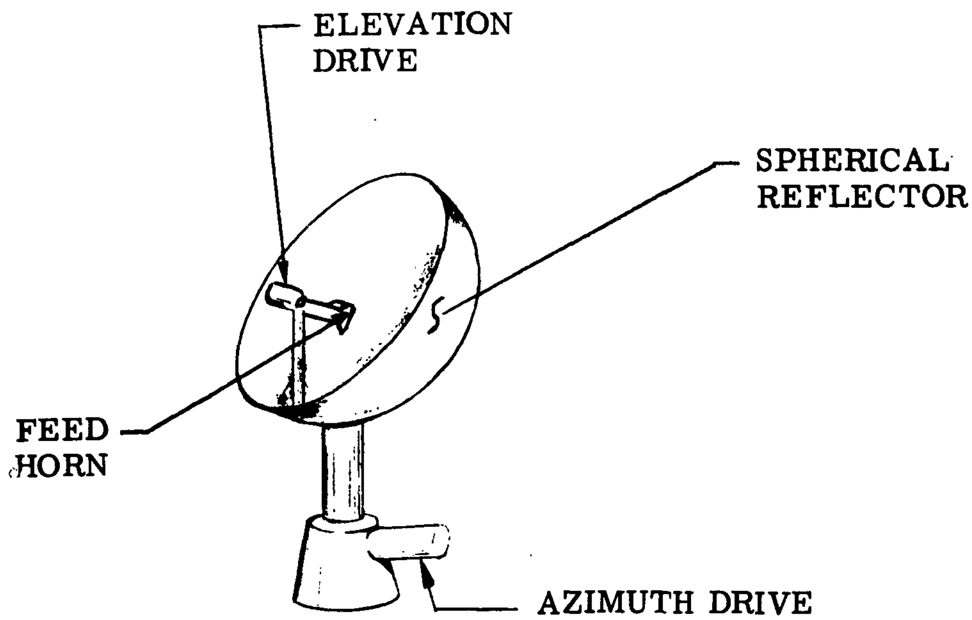

Figure 40. Spherical Antenna Dish

oriented at 45 degrees to the horizontal are attached to the surface of the inflatable sphere in a horizontal band around the central portion of the sphere. Thus, the conductors on one side of the sphere are perpendicular to those on the opposite side. The polarized radiation is reflected from the side of the grid facing the feed and passes through the opposite side, which appears transparent because of the opposite slope of the grid conductors. The lower portion of the sphere is coated with a reflective material since the r-f energy is not required to pass through this area, and therefore, a parallel grid is

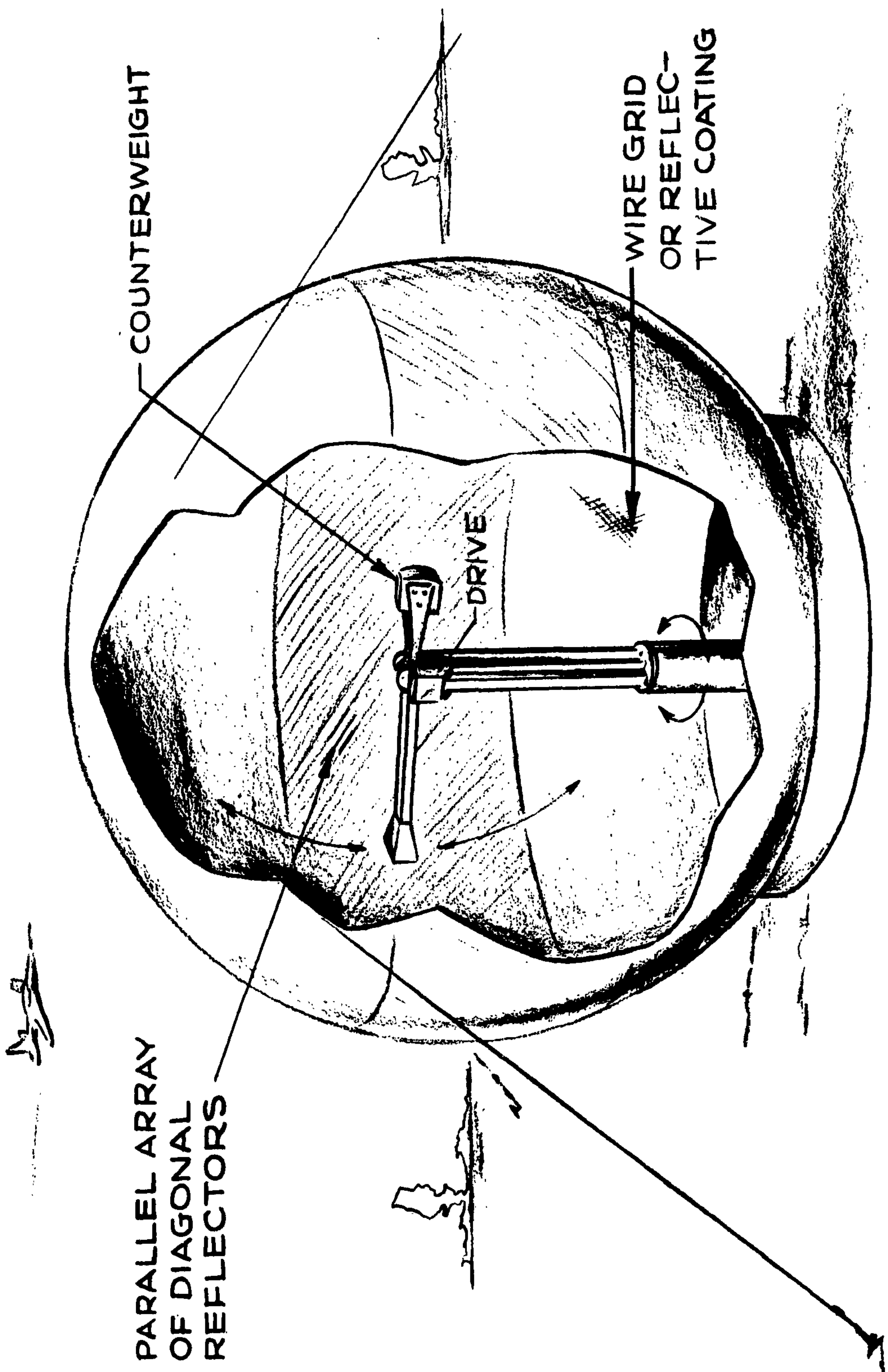

Figure 41. Inflatable Spherical Antenna

not required. The upper portion of the sphere requires no parallel grid or reflective coating, since this portion needs only to pass the energy reflected from the lower and central surfaces of the sphere.

d. Performance Considerations. The gain of a hemispherical reflector is 8 to 10 db below that of a paraboloid of the same diameter (see Figure 22). The half-power beamwidth is on the order of three times that for a typically illuminated paraboloid of the same size. For proper illumination, the feed pattern side lobes should be at least 25 db down. This restricts the bandwidth to approximately 1.4:1 in the 3 to 10 kmc range. Hemispheres have been designed to have side lobes 20 db down throughout a scan angle of 140 degrees. Although 180-degree scan angle is not possible for the hemispherical reflector using the feed rotation, the drive unit for elevation scan would be considerably smaller than in a conventional paraboloid system.

Of the three spherical reflectors, the inflatable concept appears to offer the best approach because of its low weight and packaging characteristic. In this case a rotating feed horn can be used to scan over any desired azimuth angle without moving the reflector. Also, limited elevation scanning can be accomplished by rotating the feed in the vertical plane; however, elevation coverage would be limited toward the zenith because of the feed and feed support blockage. An adaptation of this concept was studied and developed on Air Force Contract AF30(602)2753 (refer to Part I).

4. Fresnel Zone Plate Antenna

A Fresnel zone plate antenna, shown in Figure 42, would consist of a plane surface with alternate reflecting and transmitting rings that could be illuminated with a feed horn. The plane structure of the zone plate makes it easily adaptable to mechanical scanning in the azimuth and elevation planes. The edge diameter

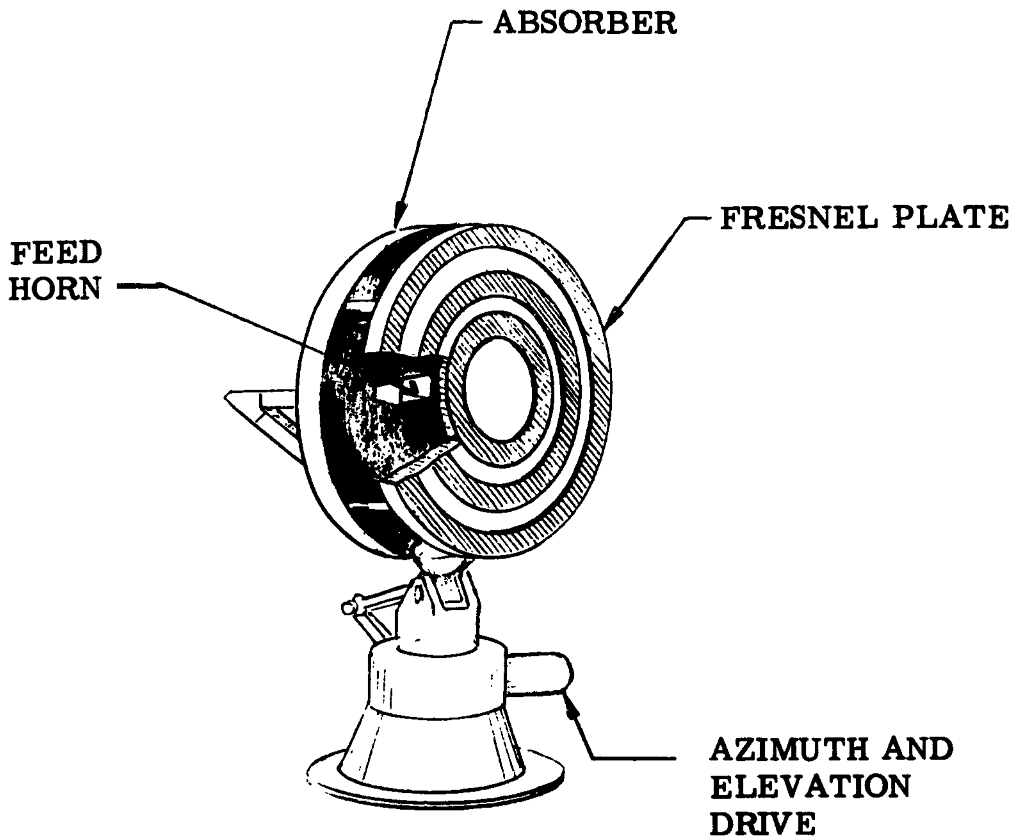

Figure 42. Fresnel Zone Plate Antenna

of the rings are determined so that the radiation from the feed to the edge has traveled half a wave length further or less than the radiation to the adjacent edge diameters. This results in a large aperture with a wavefront that is relatively in phase. Because of the zone spacing dependency on wave length, the antenna performance is very sensitive to frequency changes. But the antenna system can be tuned over a limited range by adjusting the position of the feed horn. The exact theoretical solution of the maximum gain that can be obtained from this type of antenna has not been derived; therefore, this antenna was not included on the comparative gain plots of Figure 22. The side lobe levels should be on the order of -10 db with respect to maximum gain.

The following versions of Fresnel zone plate configurations could be used:

(1) The feed mounted behind the zone plate with the radiation propagated through the transmitting zones. This type of configuration (see Reference 5) was found to give the lowest gain of the three versions.

(2) The feed mounted in front of the zone plate with the radiation reflected from the reflecting zones. The reflection of this type of configuration (see Reference 5) was found to be 1 db higher than the above transmission gain.

(3) The feed mounted in front of the zone plate with a reflecting plate mounted in back of the zone plate. This type of configuration (see Reference 5) was found to have a gain that was around 3 db higher than the transmission gain.

The Fresnel zone plate structure that should be most adaptable would use the energy transmitted through the zones. Although the gain would be about 2 db less than a structure utilizing both the transmitted and reflected energy (maximum possible), the side lobes are approximately 8 db lower using only the transmitted energy. Such a structure could be built in the 100 mcs to 10 kmc range. Due to the principle of operation, the antenna would be highly frequency-sensitive. However, the antenna could be tuned over a limited frequency range by adjusting the position of the feed horn. The maximum gain that is obtainable with this device would be less than that of a parabola of the same diameter. The zoned surface would be relatively simple to fabricate and to maneuver for mechanical scanning.

5. Leaky Wave Structure

A planar array of discrete elements such as dipole or leaky wave guide structures could be mounted and mechanically scanned by rotating the structure. The dipole array for lower frequencies would be proximity coupled dipoles (Figure 43),

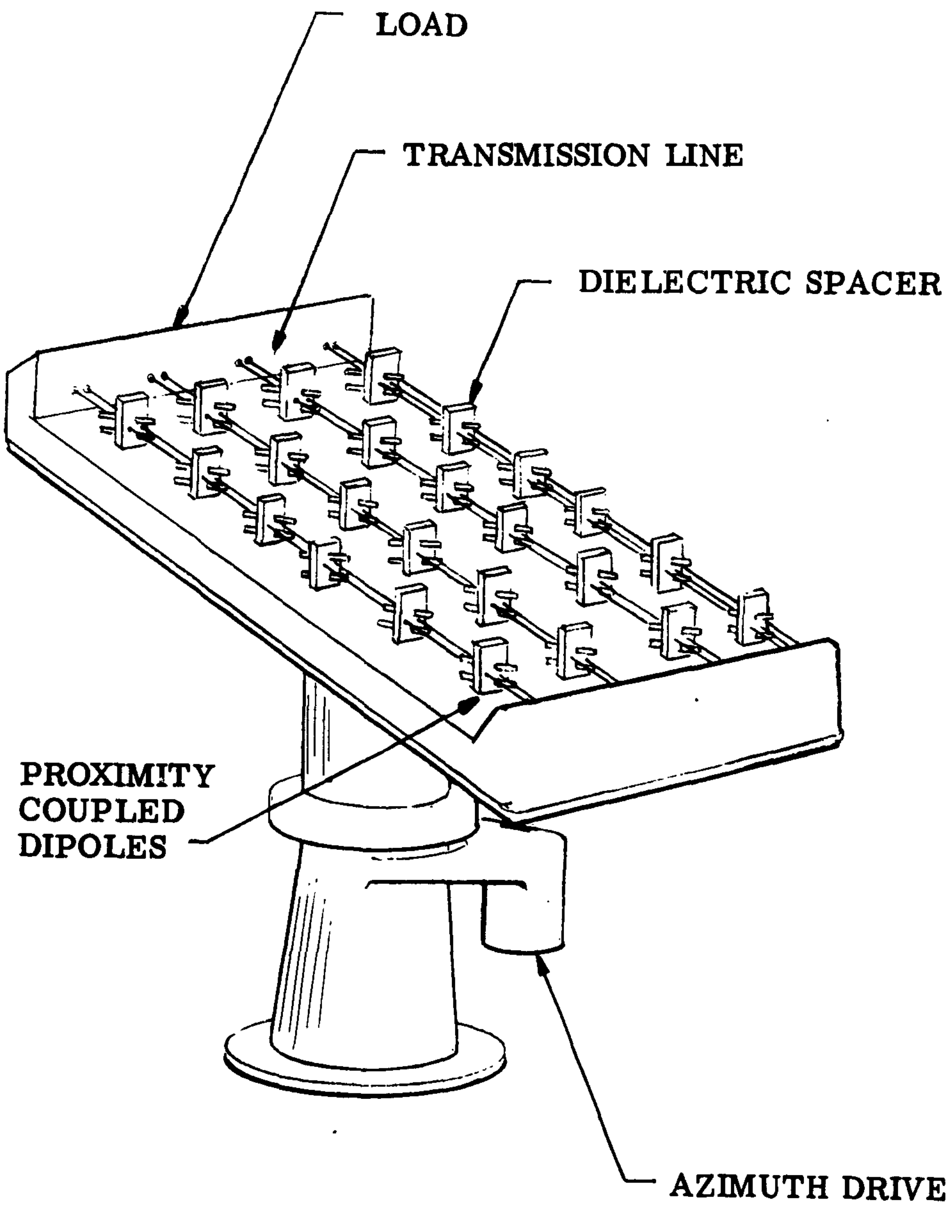

Figure 43. Leaky Wave Structure for Lower Frequencies

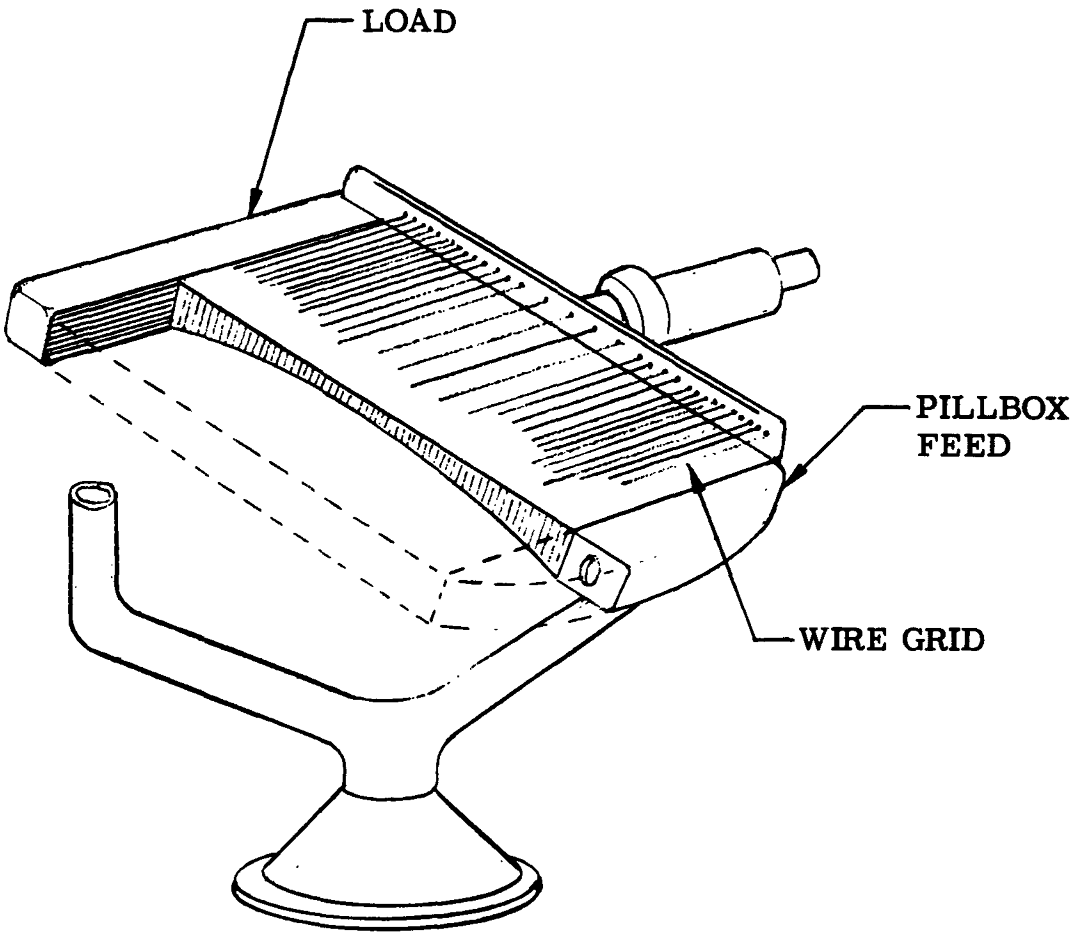

Figure 44. Leaky Wave Structure for Higher Frequencies

while for higher frequencies, a pillbox fed or log-horn fed inductive grid radiator would be used (Figure 44). Scanning could also be accomplished in the dipole structures by frequency changes, the scan being in the forward and backward quadrant. Frequency scan in the leaky guide structure occurs only in the forward direction (from the fed end). Mechanical scan in the forward direction in the leaky guide can be obtained by mechanically changing the phase velocity in the structure. For larger structures, an array of inductive grid structures could be used which would require power dividers and a feed network. Better than -25 db side lobes have been obtained with leaky wave structures by shaping the surface aperture distribution.

The discrete element structure of dipoles or inductive grid radiators could be controlled to give approximately the same gain, beamwidth, and side-lobe level performance of a paraboloid of the same physical area. The usable frequency range would be from 100 mcs to 10 kmc, the dipoles being used at the lower end of that frequency range. The proximity coupled dipoles require an open 2-wire transmission line which must be properly fed for the desired distribution across the structure. If an array of inductive grid radiators is used, a power divider and feed system are required. Although frequency scanning may be obtained with either structure, the leaky guide structure is limited to approximately 40 degrees in the forward direction.

6. Circular Hog-Horn Antennas

A circular array of hog-horn antennas, shown in Figure 45, could be used to eliminate spill-over losses and to minimize back lobes. Side lobes of this configuration should be better than -17 db, and back lobes are of the order of -70 db. A complex corporate feed structure results from this array. The frequency bandwidth is only limited by the bandwidth of the feed and is approximately 2 to 1. This configuration is mechanically scanned by rotation in the azimuth and elevation planes.

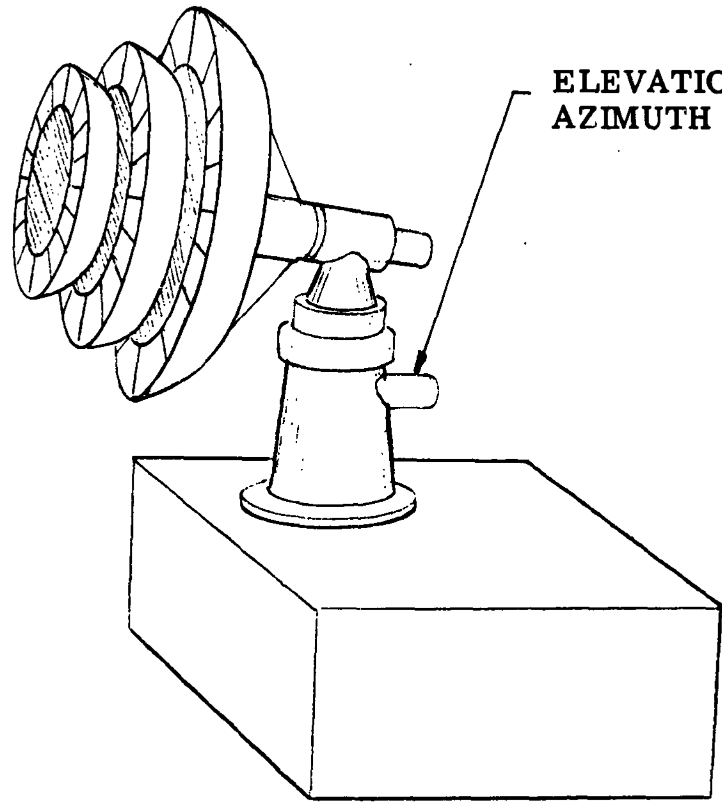

Figure 45. Circular Hog-Horn Antennas

A circular array of hog-horn antennas has the advantage of back lobes of the order of -70 db, thereby resulting in increased sensitivity by minimizing background noise. Although the aperture distribution can be partially controlled by using concentric arrays of these parabolic reflectors, a complex feed structure is necessary. The bandwidth is restricted to the bandwidth of the feed. The elongated shape perpendicular to the aperture results in large moments, making this configuration difficult to mechanically scan.

The basic problem with this type of antenna would be that it is considerably heavier and more expensive than most others.

C. RADOMES

1. Performance and Cost Comparison

Goodyear Aerospace has designed and manufactured many sizes and types of radomes. Since some of the ground-based tracking antenna concepts developed for this program will require radomes to reduce load conditions and provide protection from the elements, it was considered desirable to assess available data on various types of radomes and compile comparative information on transmission efficiency and cost. Accordingly, a comparison study was made for five distinct types of radomes on the basis of the individual radome's ability to perform over a 10 to 1 frequency band.

Certain arbitrary parameters were set as constants. The antenna's size was established at 30 feet in diameter with a 55-foot diameter, truncated spherical radome (see Figure 46). It was assumed that only a columnated single beam existed. It was also assumed that the tilting axis and rotational axis intersected through the spherical center of the radome. All radome configurations studied are adequate from a structural standpoint and are able to remain operational at 120-mph wind load.

The radome types considered were:

(1) The metal space frame with a thin skin (see Figure 47A)
(2) The honeycomb-sandwich with channel joints (see Figure 47B)
(3) The all-foam, bonded joint (see Figure 47C)
(4) The bolted-flange solid laminate (see Figure 47D)
(5) The inflatable (see Figure 47E)

Figures 48 through 52 show transmission efficiency versus frequency for these five radome types.

The all-foam, bonded joint configuration performance remained virtually flat

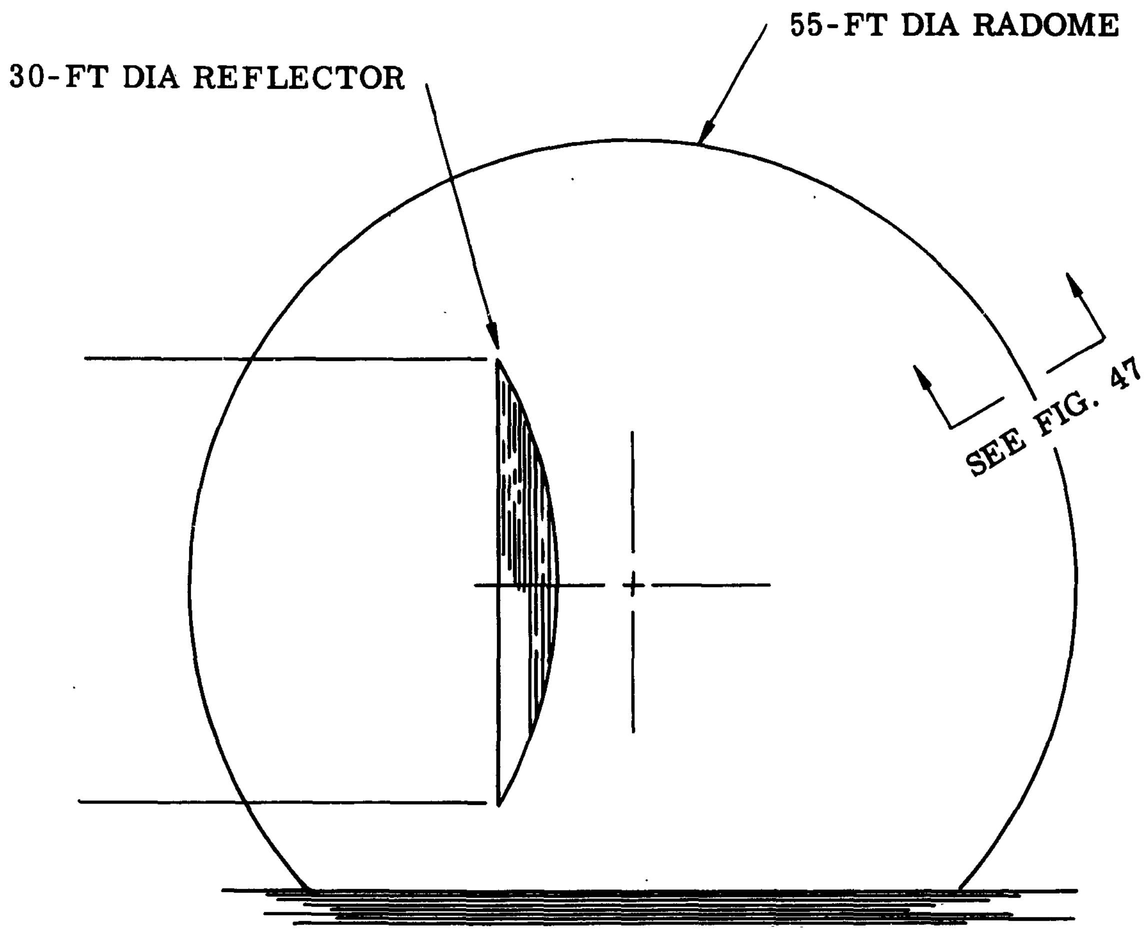

Figure 46. Radome and Antenna Relationship

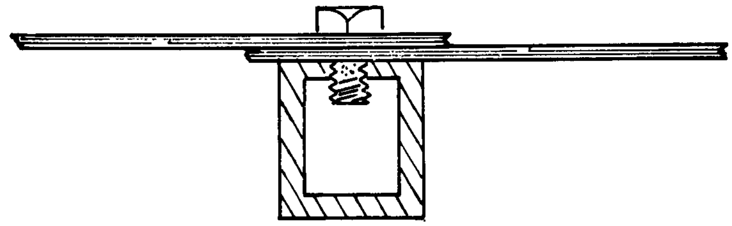

A. METAL SPACE FRAME

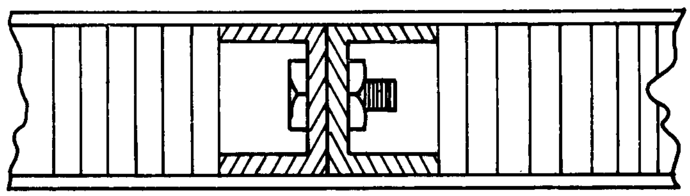

B. BOLTED JOINT HONEYCOMB SANDWICH

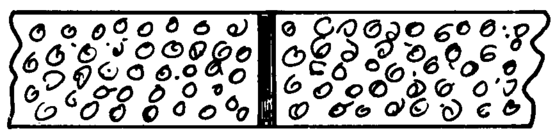

C. ALL FOAM, BONDED JOINT

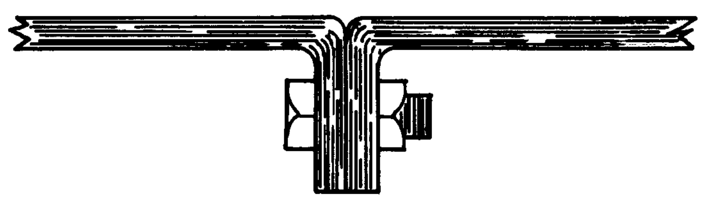

D. BOLTED FLANGE SOLID LAMINATE

E. TWO-PLY INFLATABLE

Figure 47. Radome Wall Configuration

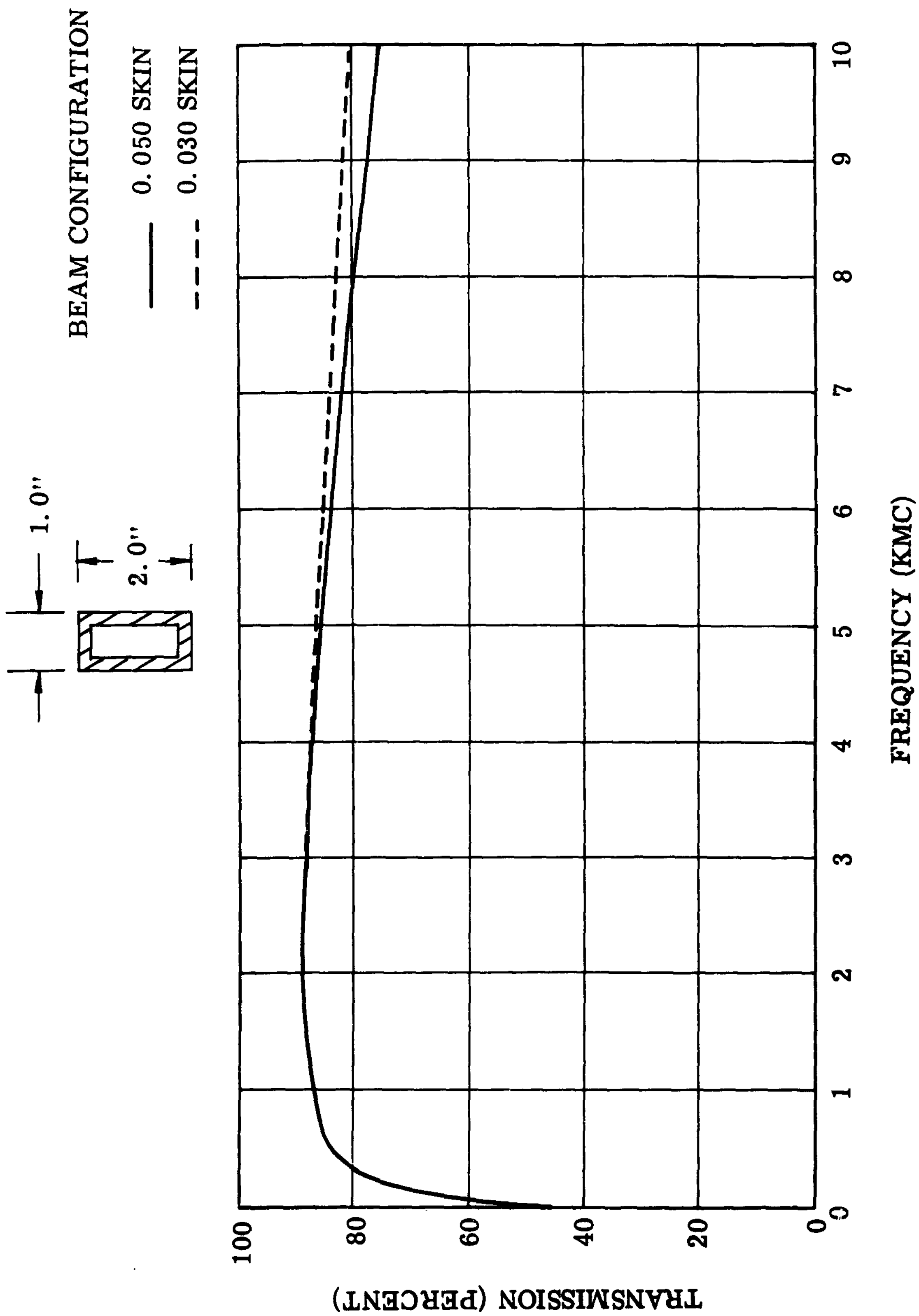

Figure 48. Transmission Efficiency versus Frequency for a 55-Foot Metal Space Frame Radome

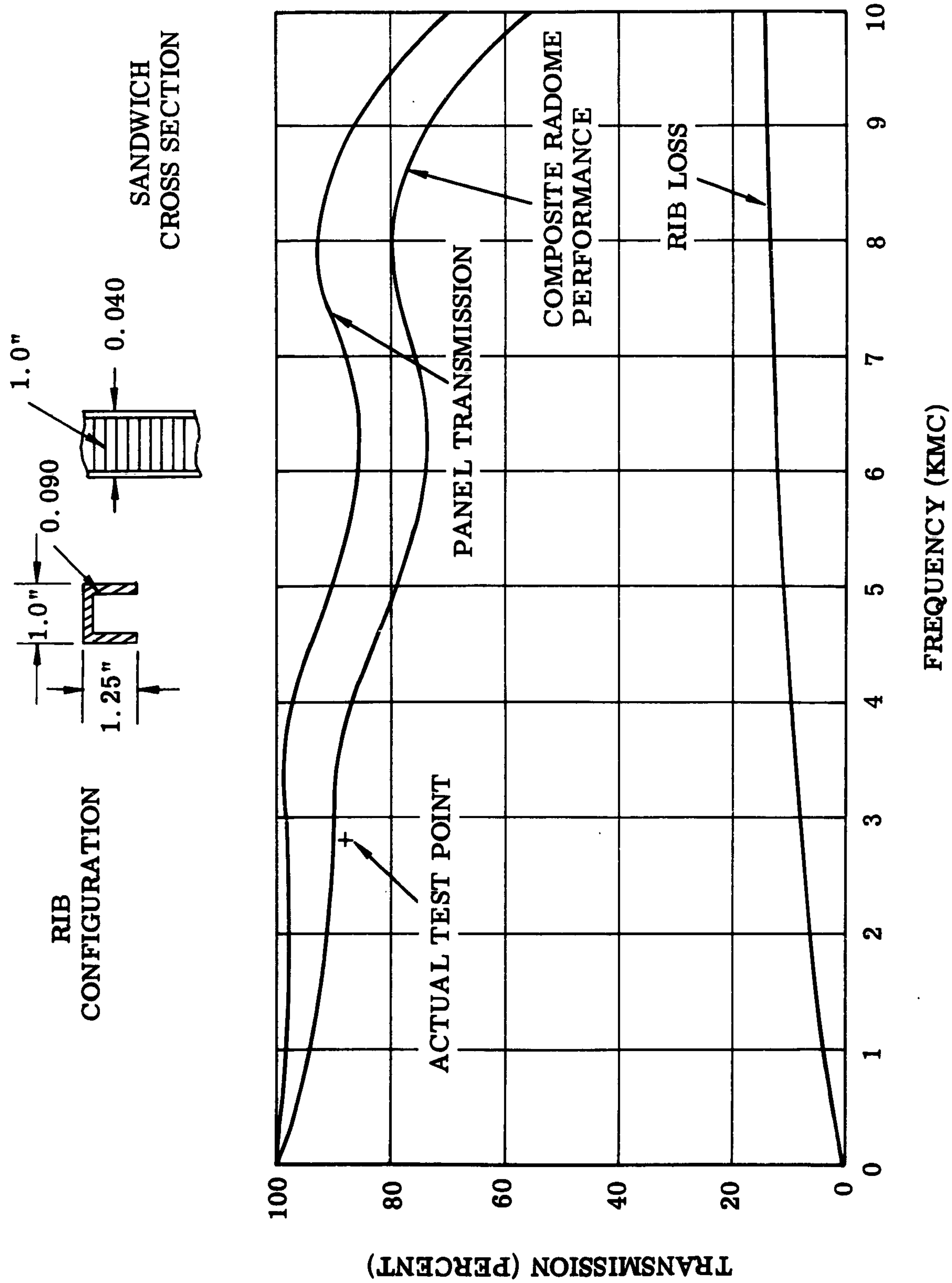

Figure 49. Transmission Efficiency versus Frequency for a 55-Foot Honeycomb Sandwich Radome

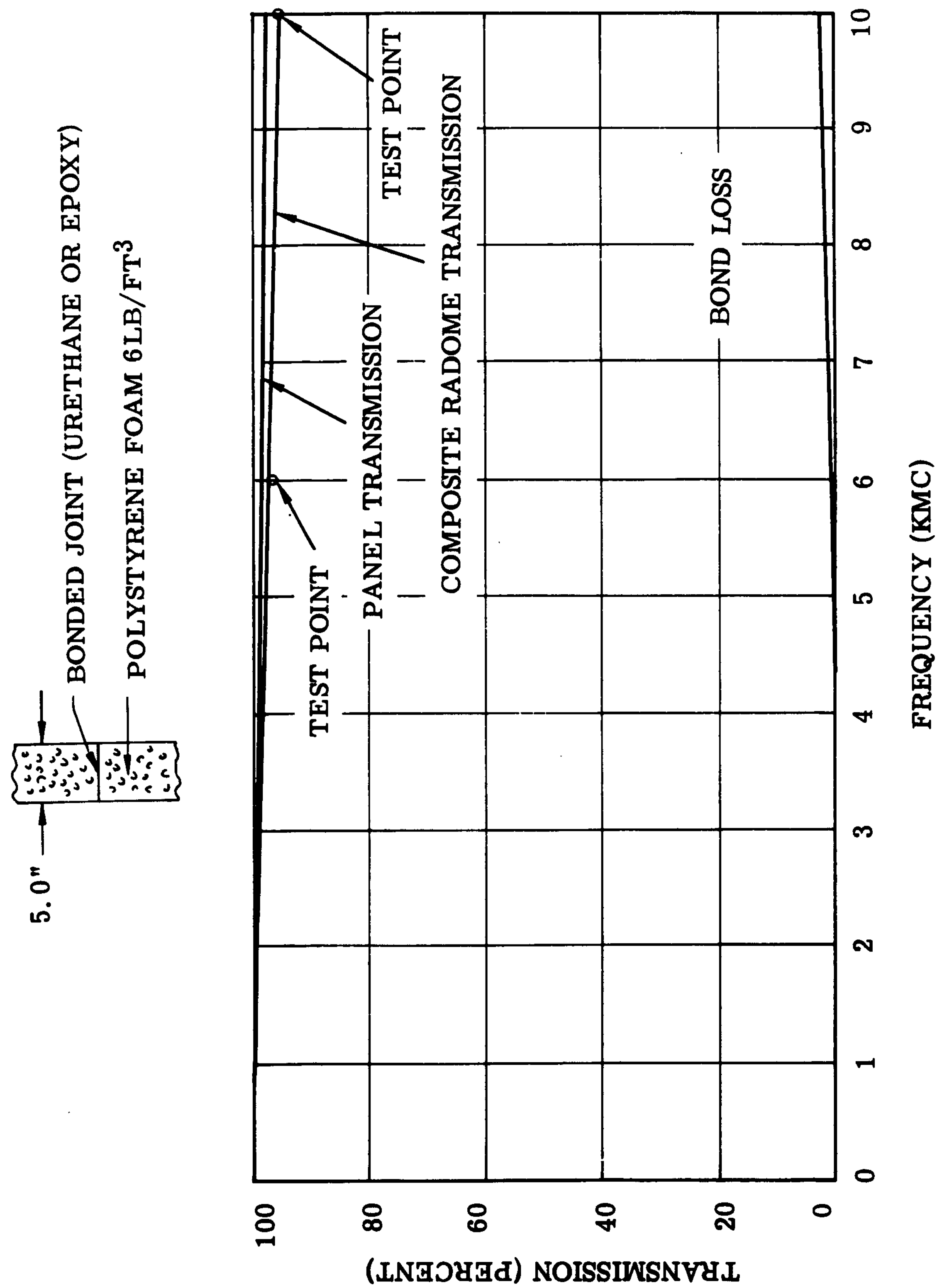

Figure 50. Transmission Efficiency versus Frequency for Bonded-Joint, 55-Foot Polystyrene Foam Radome

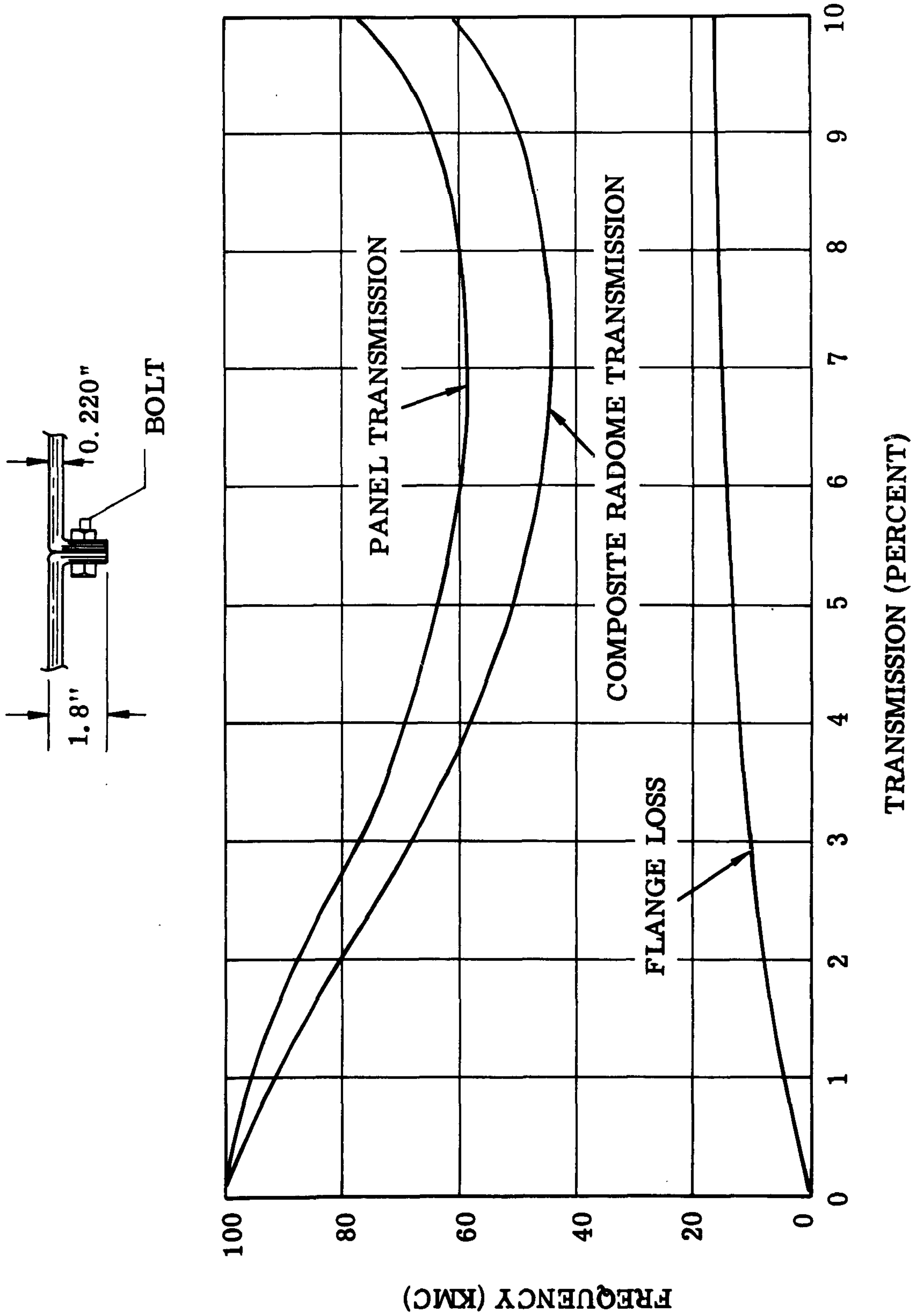

Figure 51. Transmission Efficiency versus Frequency for a Solid Laminate, Bolted Flange, 55-Foot Radome

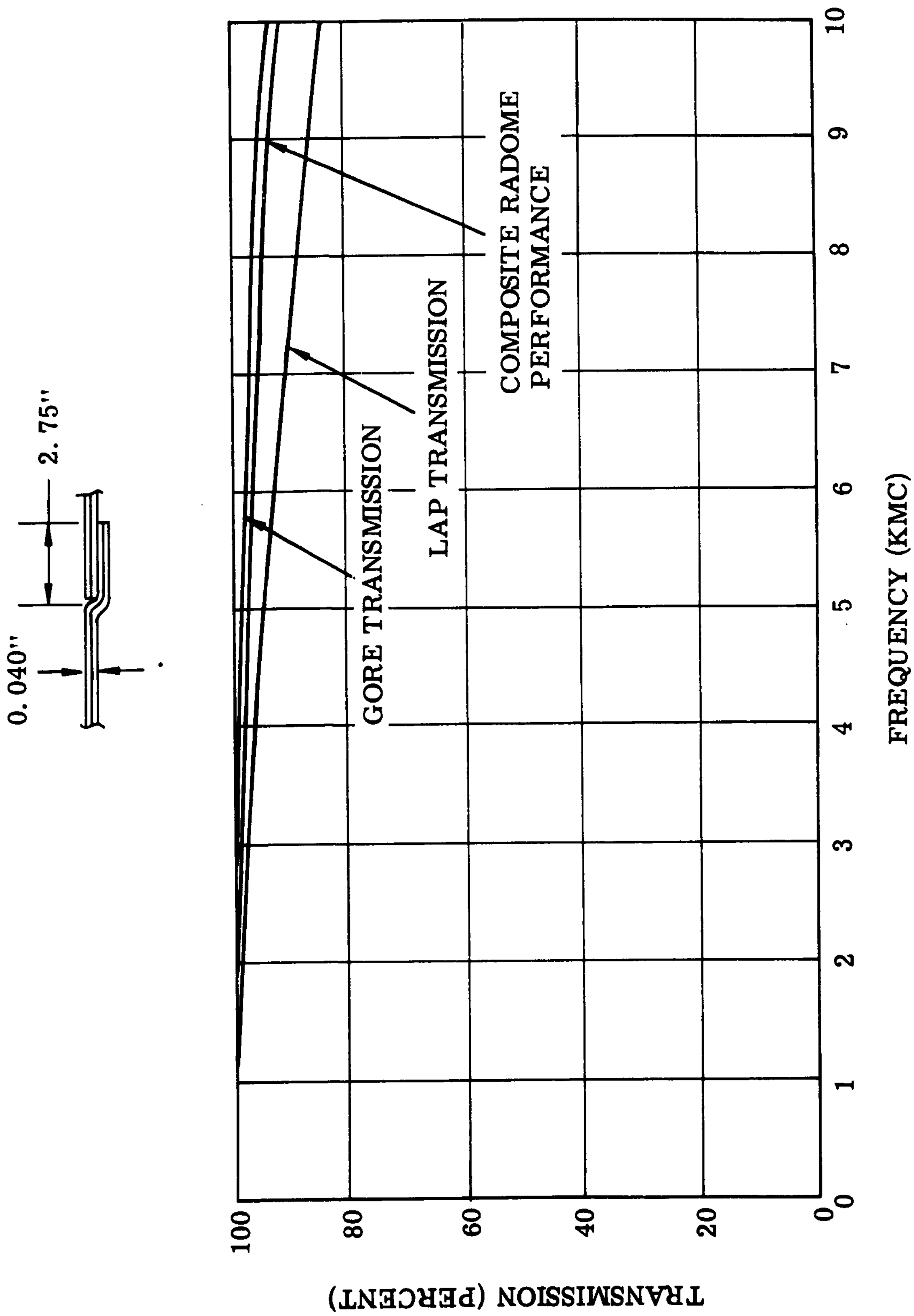

Figure 52. Transmission Efficiency versus Frequency for a Neoprene/Nylon Inflatable 55-Foot Radome

throughout the entire band as did the inflatable structure. The most significant loss, in both cases, was the joints in the case of the foam and the lap areas in the case of the inflatable. However, the dielectric constant and loss tangent of the foam material is less than that of the neoprene-nylon inflatable and, therefore, less sensitive to an increase in frequency (see Figures 50 and 52). Some corroborating test data for the foam radome was available and can be seen in Figure 50.

Unlike the foam and inflatable concepts, the honeycomb sandwich version showed the usual cyclic phenomena associated with sandwiches of high dielectric skins. However, in this case, the ribs, or channels which surround the individual panel sections, contribute a great deal to the overall loss, and especially at the higher frequencies (see Figure 49). At these higher frequencies the channel sections become more pure "shadow" area. At the lower frequencies, on the other hand, the channel section is electrically thin enough to allow some transmission of the impinging energy. The same sensitive cycling takes place in the solid-laminate dielectric every one-half wavelength (see Figure 51). The electrical disadvantage of a solid laminate over a wide band is evident, for the cycling becomes more pronounced with each one-half wave length or frequency doubling that takes place. A greater flange effect is also realized because more bearing surface is required for adequate support. At an average angle of incidence the flange area becomes quite large in terms of percentage "seen" by the antenna. As in the honeycomb sandwich channel sections, the flange is less sensitive to the signal at the lower frequencies and becomes more a pure "shadow" at the higher frequencies.

The metal space frame radome on the other hand is an entirely different entity in the radome art for it performs unlike other configurations. In the case of the metal space frame radome (Figure 48), the transmission efficiency rises very rapidly in the lower frequency region and levels out at perhaps 2 kmc. Notice that the cyclic phenomenon is not present as is apparent in the other radome configurations. As it is, the metal members of the structure act more or less as a reflector at the very low frequencies (i. e., the distance between members approach the free-space wave length) and is essentially shadow area. As the frequency increases, this resonant phenomenon disappears. At frequencies approximately 2 kmc for the beam spacing and beam length considered, the loss due to shadow area becomes asymptotic and a function now of aperture blocking only. The downward trend in the curve is caused by loss in the skins. (Note that the curve drops more rapidly for the 0.050 skins than for the 0.030 skins.)

Comparative transmission efficiency for the five types of radomes studied is shown in Figure 53. Five basic radome configurations have been studied. Various points of actual test data have aided in substantiating the theoretical analysis. However, it must be pointed out that this investigation is a generalized case. As in the instance of the foam, the solid laminate, and sandwich configuration, the particular antenna configuration and specific performance requirements would be taken into account in detailed radome designs. These structures can be optimized for specific frequencies and structural requirements. On the other hand, the space frame and the inflatable radomes are designed almost entirely from a structural standpoint and performance is estimated on this basis.

The cost comparison of the various radomes is very difficult to establish, because radomes built in the past have been built to different specifications and in different quantities. However, based on cost information that has been estimated for rather small quantities and for somewhat different requirements, a comparison chart for 55-foot-diameter radomes having 6750 feet^2 of surface area is given in Table II.

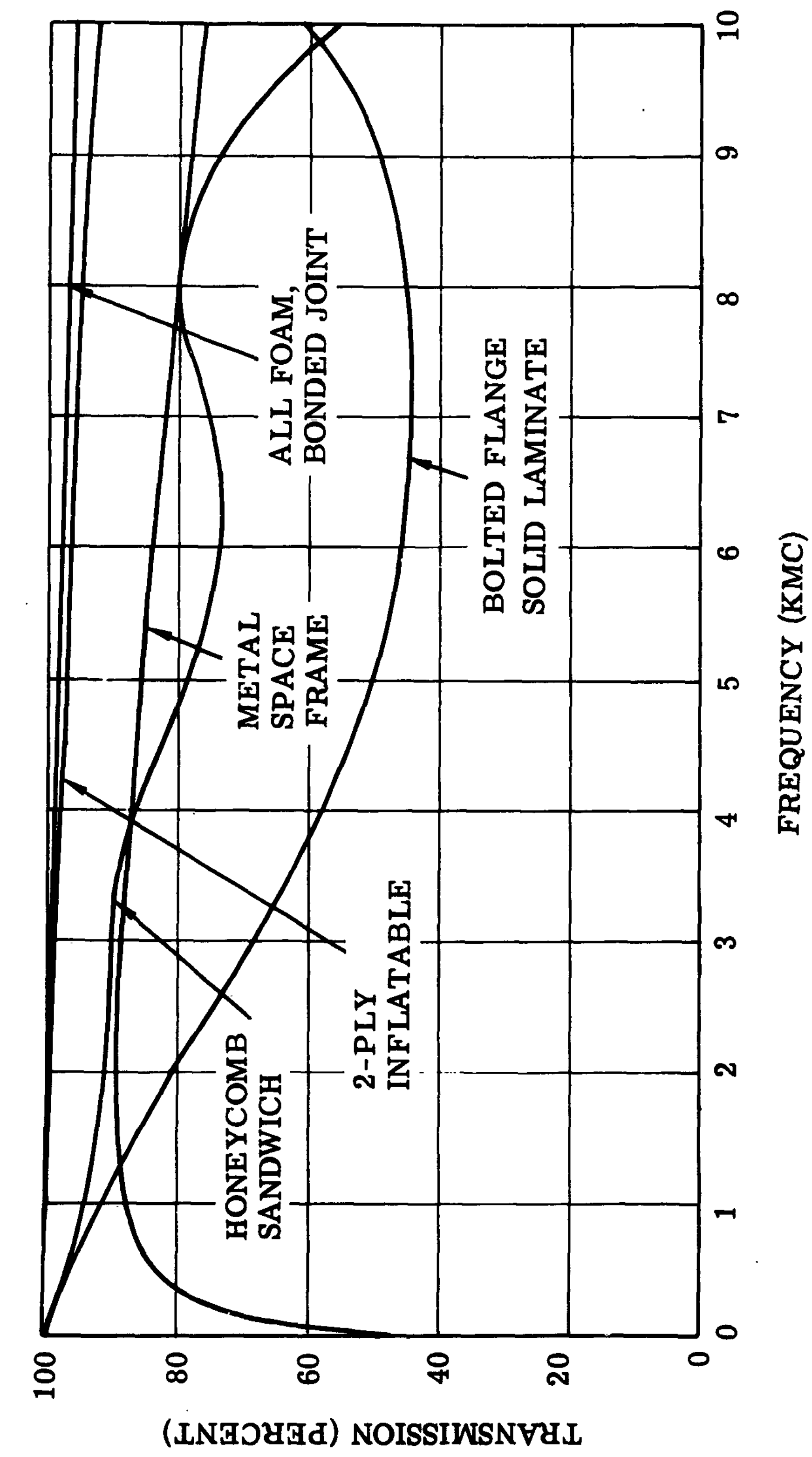

Figure 53. Transmission Efficiency versus Frequency for Various 55-Foot Radome Configurations

Table II. Comparison Chart for 55-Ft Diameter Radomes Having 6750-Ft^2 Surface Area

RADOME TYPE	RADOME COST	COST/FT^2 (Average)
Bolted Flange, Solid Laminate	$19,000	$2.80
Metal Space Frame	43,000	6.35
All Foam, Bonded Joint	34,000	5.05
Honeycomb-Sandwich	68,200	9.95
Inflatable	16,000	2.37

2. Monolithic Foam Radome Development

Goodyear Aerospace's most recent work in the radome field has included development and design of monolithic foam radomes. Figure 54 is a photograph of a 17-foot diameter rigid urethane foam radome that Goodyear Aerospace has designed, built, and installed for use with a high-resolution antenna in the FAA's major airport ground traffic control program. Designed to operate at K-band, the radome was erected at NAFEC, Atlantic City, N. J. (FAA test facility) on 1 November 1962. It has performed excellently to date. Transmission is 96 percent dry and 83 percent wet. Construction is 3-inch thick, 4 pound density foam. Panels were formed in a contoured closed mold, and edges were trimmed to size. The exterior surfaces were painted white and silicone-treated to enhance water shedding. Panels were bonded together in the field with epoxy. Clamps were used to hold them in place until the resin cured. Three unskilled men accomplished assembly in two days. Radome total weight including a 1/4-inch steel base shear plate was slightly under 1000 pounds.

Designed to last five years and to withstand 109-knot winds and 1/2 inch of ice or

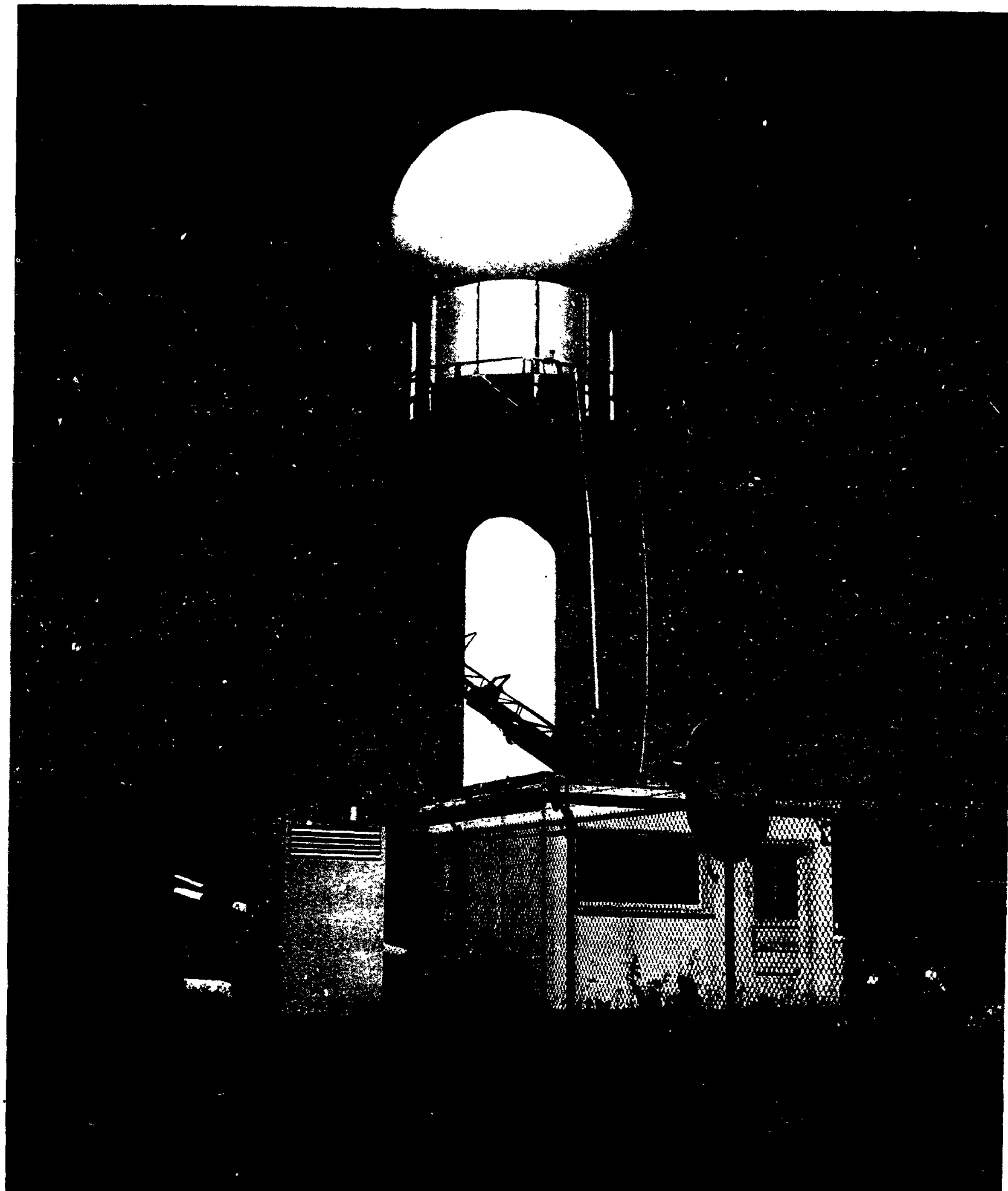

Figure 54. Seventeen-Foot-Diameter Monolithic Foam Radome Utilizing Bonded Joints

2 inches of ice with no wind, structural values were achieved as follows:

	Design	Experimental
Compression	28 psi	78 psi
Compression Modulus	1900 psi	3450 psi
Tensile	50 psi	70 psi
Tensile through Joint	50 psi	56 psi
Flexure	37 psi	47 psi

Goodyear Aerospace is continuing to do development work in larger monolithic foam radomes and sees no particular problem of producing them in sizes up to at least 55 feet in diameter.

PART 4. FACTUAL DATA

SECTION IX. GROUND-BASED ANTENNA CONCEPT EVALUATION AND SELECTION

A. GENERAL

The contract for this program requires that models shall be designed and constructed to demonstrate the feasibility of the three antennas that show the best potential for meeting the program objectives. It was determined that two ground-based and one space vehicle antenna would be selected for model demonstration. Selection of the space vehicle antenna is discussed in Section IV. This section discusses the evaluation, comparison, and selection of the two ground-based antennas.

During the various stages of the evaluation, 22 different ground-based antenna concepts were considered. These concepts are described in Section VIII. Eleven antenna concepts that showed the least promise after preliminary evaluation and comparison were discarded for any further detail study. Four other concepts, technically related to each other, were combined into two for purposes of evaluation, thus leaving a total of nine concepts to be compared for the final model selection.

Also, as part of the evaluation, the antenna concepts were considered on the basis of the antenna class in which they fit best. In some cases, modification of the basic design would be required to adapt a specific antenna concept to a class other than the one for which it was designed. Ground-based antennas were previously classified according to size and frequency to provide a family of antennas to fulfill the specified requirements. These classifications are reiterated as follows:

Class I: Size - 20 to 40 feet; frequency - 0.1 to 2 kmc

Class II: Size - 40 feet; frequency - 5 (±0.5) kmc

Class III: Size - 30 to 40 feet; frequency - 9.5 (±0.5) kmc

Each antenna that was eliminated from further consideration was studied only to an extent that indicated significant development problems. Therefore, a larger percentage of the design effort was placed on the antenna concepts that showed the best potential.

B. PRELIMINARY EVALUATION

1. General

It was necessary to simplify the evaluation procedure in the initial stages because of the large number of concepts (22) being considered in order to conserve the available funds for a more detail study and evaluation of the most promising concepts. Accordingly, the 22 concepts were compared preliminarily, and 11 of those showing the least potential were discarded. The antenna concepts and the reasons for retaining the concept or discarding it are given in the following paragraphs.

2. Foam-Rigidized Antennas

Foam-rigidized parabolic reflectors offer the potential of providing an antenna with good accuracy at a relatively low cost. Either the molded contour or swept contour method would yield comparable end products. The swept contour method would possibly provide increased accuracy; however, the molded process would probably show a cost advantage where large quantities are involved.

Both types of foam-rigidized reflectors appear to offer sufficient potential to be considered for further study and evaluation; however, because of the close similarity of the end products, the two concepts were combined as a single concept for the final evaluation.

3. Inflatable Parabolic Antennas

The inflatable parabolic antennas offer the potential of obtaining highly mobile, lightweight, quick-erecting antenna systems with operating efficiencies comparable to present conventional antennas. Because of these potential capabilities, the following four inflatable paraboloid antennas were retained for further study and evaluation.

(1) AIRMAT Paraboloid Antenna
(2) AIRMAT Vacuum-Supported Antenna
(3) Lenticular AIRMAT Antenna
(4) Torus-Supported Inflatable Antenna

The following two inflatable concepts were eliminated for further study and evaluation for the reasons stated:

(1) Inflatable-Horn Antenna. The inflatable-horn antenna utilizes long rigid members and represents a rather complex combination of inflatable and rigid structure that limits its packageability when compared to other inflatable concepts. Reflector tolerances are more critical, and it does not have the inherent low noise ratio characteristics of metal horns.

(2) Deep-Dish Inflatable Antenna. The deep-dish inflatable antenna has the basic difficulty that its long cantilevered configuration will present greater contour deflection than any other inflatable antenna type considered. Also, the large area of fabric presents severe difficulties in fabrication. The accumulation of small errors on each fabric section can produce excessive deviation from the required tolerances in

the completed structure. In addition, the large relative size of this antenna concept, for a particular reflector aperture, limits the practicality of using a radome to help reduce the environmental loading conditions. As an example, for a 40-foot antenna aperture, approximately a 110-foot radome would be required. In this case, the inflatable radome cost would be prohibitive, and the large radome size limits the number of available erection locations, which in turn severely hampers the tactical capability of the antenna system.

4. Foldable-Truss Antennas

Foldable-truss antenna support structures were considered to offer good potential, since they offer the advantages of rigid-type antennas, with the added feature of better packageability and transportability. This feature would be a trade-off item, since it results in increased complexity, added cost, and usually added weight. Light weight features would always be a design goal, but they are not usually a function of the foldability concept.

For the evaluation purposes, however, the two foldable-truss antennas are only modifications of the same basic concept. The basis of that concept is to find better methods of folding rigid-support structures to give the antenna better transportability features and to allow it to be erected and dismantled more easily. Therefore, since the rigid-antenna structure is the closest to state-of-the-art techniques, it was considered necessary to investigate this technique further. For the evaluation, though, the foldable-truss antenna support structures were considered as a single concept.

5. Multiple-Reflector Arrays

Multiple-reflector antennas offered the possibility of increased performance compared with a large single dish, since tolerances can be held closer on a smaller dish. It was recognized that some added complexity in electrical components will result; however, this concept was selected to be studied further to establish the amount of trade-off required in this area. Also, the study was limited to the four-element array.

6. Foldable-Fan Reflector

The foldable-fan concept was attractive from the standpoint of providing a rigid antenna with mobility and simple erection; however, the folding feature requires excessive axial displacement of the fan sections and involves considerable complexity at the hub. This configuration was complex and heavy and compared unfavorably on an economical basis with other folding truss concepts; therefore, it was eliminated for further study and evaluation.

7. Sandwich-Panel Antenna

Tooling and fabrication costs for the sandwich-panel antenna concept appeared to be high because of the close tolerance that would be required for forming the different contoured sections. This configuration also compared unfavorably with other rigid-structure concepts from a weight and cost standpoint and consequently was eliminated.

8. Spherical Reflectors

The spherical reflectors basically do not offer any advantage electrically, since the efficiency is reduced from that of a parabolic reflector.

The advantage that a spherical section or a hemisphere reflector offers is that the feed horn, instead of the reflector itself, can be rotated in azimuth or elevation. The increase in the size of the rigid-antenna structure to get comparable performance obviates the mechanical advantage of not having to rotate the reflector. On the other hand, an inflatable spherical concept offers the possibility of simplifying the fabrication of a large spherical structure and also utilizes the feature of rotating only the feed horn for complete 360-degree azimuth scanning and limited elevation scanning. Therefore, the inflatable spherical antenna was retained for further study and evaluation.

9. Fresnel Zone Plate Antenna

The Fresnel zone plate antenna concept did not appear to have any significant advantages from a structural or mechanical standpoint, and its electrical performance also did not compare favorably with parabolic antennas of the same diameter. This concept was eliminated.

10. Leaky Wave Structures

Leaky wave structures required costly structure without offering any significant advantage in electrical performance. This concept was not to be pursued further unless some additional advantages were recognized.

11. Circular Hog-Horn Antenna

This concept offers good electrical performance. However, the required structure appears to be prohibitively heavy and costly. Some additional study was considered desirable because of the performance potential, and therefore, this concept was retained for further evaluation.

C. DESIGN ANALYSIS AND STUDY FOR FINAL EVALUATION AND SELECTION

1. General

Before progressing into the final evaluation, additional technical information concerning the nine remaining concepts was required to form a firmer basis for the final evaluation and the selection of the two most promising concepts for further detail design study and model fabrication. An attempt here to definitely prove out the complete feasibility of the nine concepts by detail analysis or test would be beyond the scope of this program. The study at this point was directed toward turning up the more obvious problem areas by relying on past experience and know-how in parallel areas as well as the development effort on this program and other parallel development programs. Basic areas of investigation included structural considerations, fabrication techniques, mechanical performance, and electrical performance, as well as cost and reliability to a lesser degree. The investigations of the nine concepts are discussed in the following paragraphs. More detailed design studies and analyses for the concepts finally selected are covered in Section X.

2. Foam-Rigidized Antennas

a. General. A considerable amount of work was conducted on foam-rigidized antennas as a part of a separate Goodyear Aerospace supported development program. The significant results that are related to the objectives of this program are presented here. As stated previously, the two foam-rigidized antenna concepts are considered as a single concept for the final evaluation. Most of the development work completed at the time of this final report was in the area of the molded-foam technique.

b. Tooling for Producing Reflector Surface. A rigid metal tool with a contoured accuracy of ±0.007 inch was used as the basic tool over which 36-inch diameter test reflectors were foamed. Figure 55 shows this tool with a Mylar aluminum foil - Mylar laminated film stretched over the surface. The laminated film serves as the r-f reflective surface. A vacuum is utilized to form the laminated film closely over the metal tool. In this manner, a reflective surface is formed which very closely duplicates the surface and contour of the form on which it is made.

A variation of this process would be to spray a thin coat of metal spray or r-f reflective paint onto the foam surface after forming or onto the form prior to foaming instead of applying the laminated film. This would result in a considerable cost saving, particularly on large reflector panels, since it would

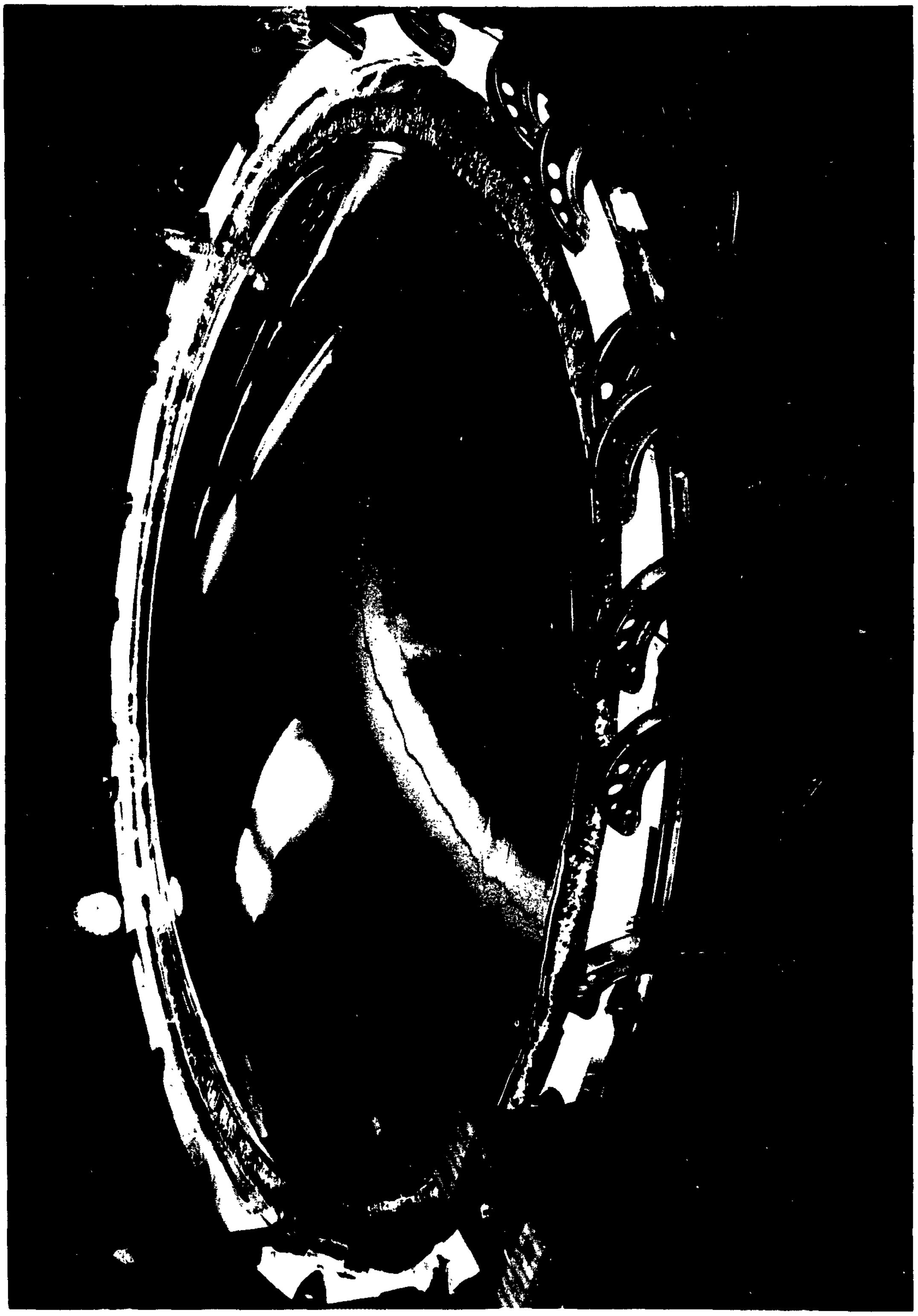

Figure 55. Foam-Rigidized Antenna Contour Tool (36-Inch Diameter)

eliminate the need for seaming the film as well as the need for vacuum-forming.

An inflated Mylar film technique has been developed for producing foam-rigidized solar collectors. In this process, an accurately patterned paraboloid of aluminized Mylar is air-inflated, and successive layers of polyurethane foam are poured over this envelope and integrated with the backup structure to form the rigid structure. However, as mentioned previously, in the field of microwave antennas, where extreme surface smoothness is not required, it appears that there are other methods of obtaining the reflective surface which may be cheaper and more adaptable to the use of precision tooling for producing reflector dish segments. However, it is mentioned here with the thought that, with the inflated Mylar process or perhaps a similar process using a fiberglass fabric envelope, it may become practicable, with further development, to accomplish on-site foaming of large antennas with the ultimate goal of developing an antenna sufficiently economical that it could be expendable.

c. <u>Antenna Backup Structure.</u> Two categories of backup structures have been considered: integral and non-integral.

The integral structure is generally lighter and more rigid than the non-integral structure. The non-integral structure may have some advantage in providing a more easily foldable structure but must be traded off basically against weight. The integral structure was used in the 36-inch foam-rigidized reflectors fabricated for test purposes. Other examples of integral structure included a 10-foot diameter swept plastic surface foam reflector and the 44-1/2 foot diameter solar collector. Figure 56 is a photograph of the structure for the 36-inch diameter reflector just before the final foaming operation. Figure 57 shows a rear view of the 36-inch diameter reflector

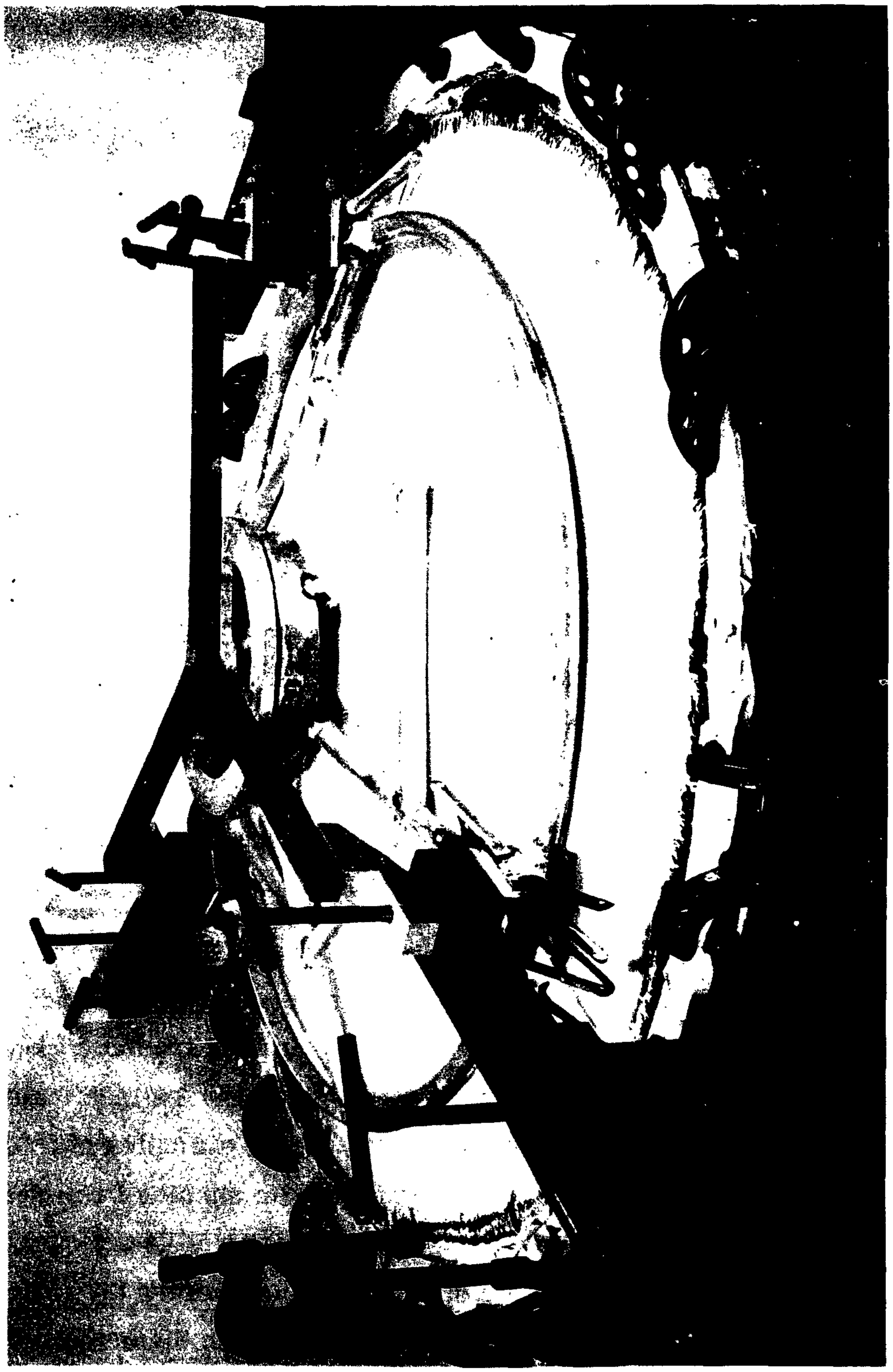

Figure 56. Thirty-Six Inch Diameter Foam-Rigidized Antenna Backup Structure

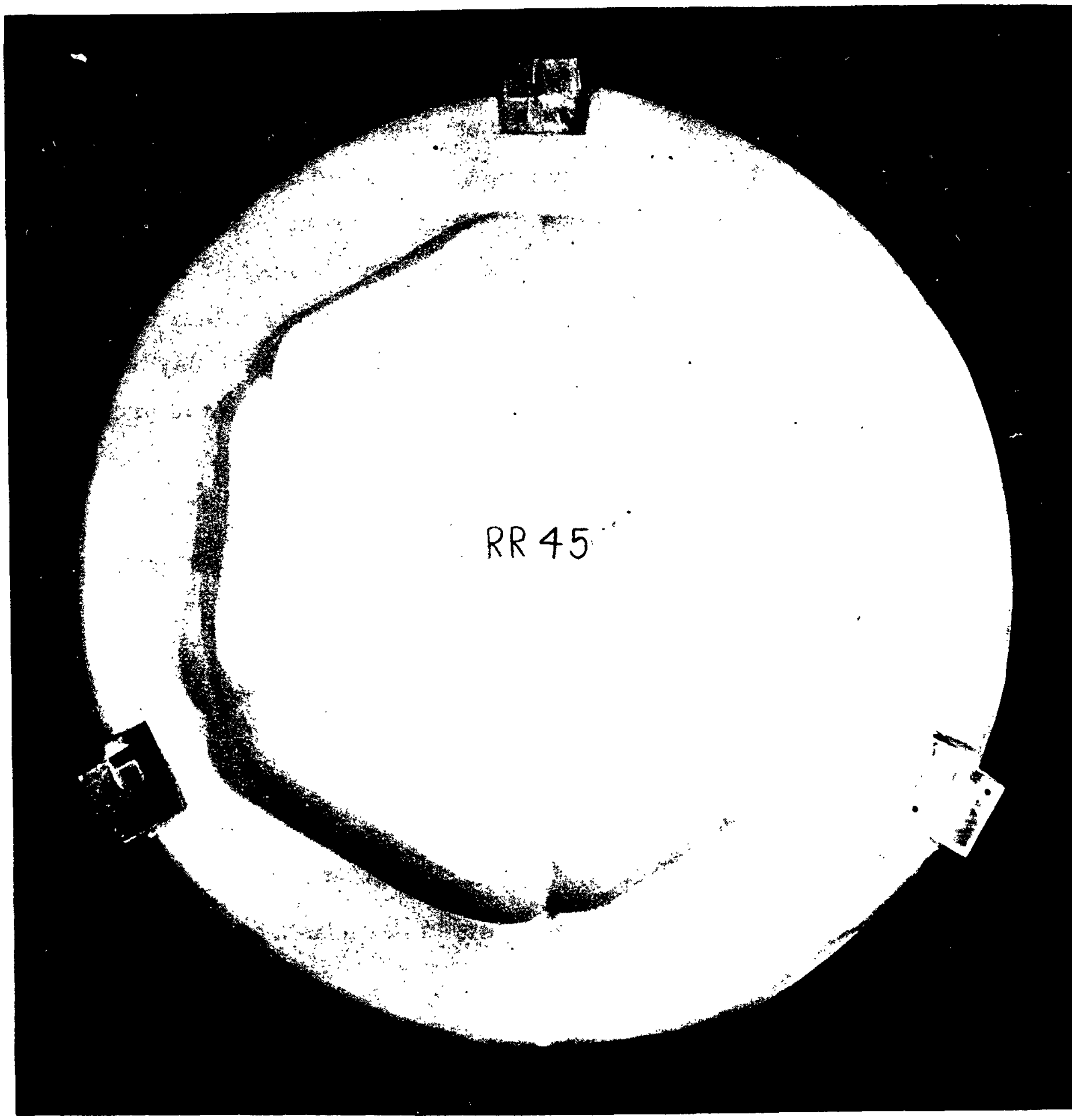

Figure 57. Thirty-Six Inch Diameter Antenna Backup Structure after Foaming

after the foaming operation. It has been determined then that not only is a good support structure required for a precision contour but also the degree of precision is based on the stiffness of support structure design.

The other category into which backup structures may be placed is the non-integral structure, where the foamed dish is attached by means other than direct encapsulating. There is a wide variety of possible configurations that may be considered in this category. The foam panels may be without integral reinforcement, or they may have a metal framework either partially or completely encapsulated within them. The backup structure may be bolted directly to the dish at close intervals, forming an integral structure, or it may be attached to the dish at fewer strong points to support it in the axial direction only.

d. Foam-Rigidized Antenna Fabrication. The foam-rigidized test reflectors were fabricated using the following technique:

(1) A laminate of Mylar-aluminum foil-Mylar was stretched over a male form representing the reflector surface and was held down with a vacuum.

(2) A high-density (10 - 15 pcf) 1/4-inch thick layer of polyurethane foam was poured over the film and allowed to cure.

(3) An aluminum support structure was suspended over the high-density foam.

(4) A low-density (2 - 3 pcf) 3-1/2 inch thick layer of polyurethane foam was poured over the support structure and allowed to cure.

Figure 58 shows a 36-inch diameter antenna test dish produced by this method. Figure 59 shows the contour check setup used to evaluate the results. The best contour control was obtained when the part was post-cured at a

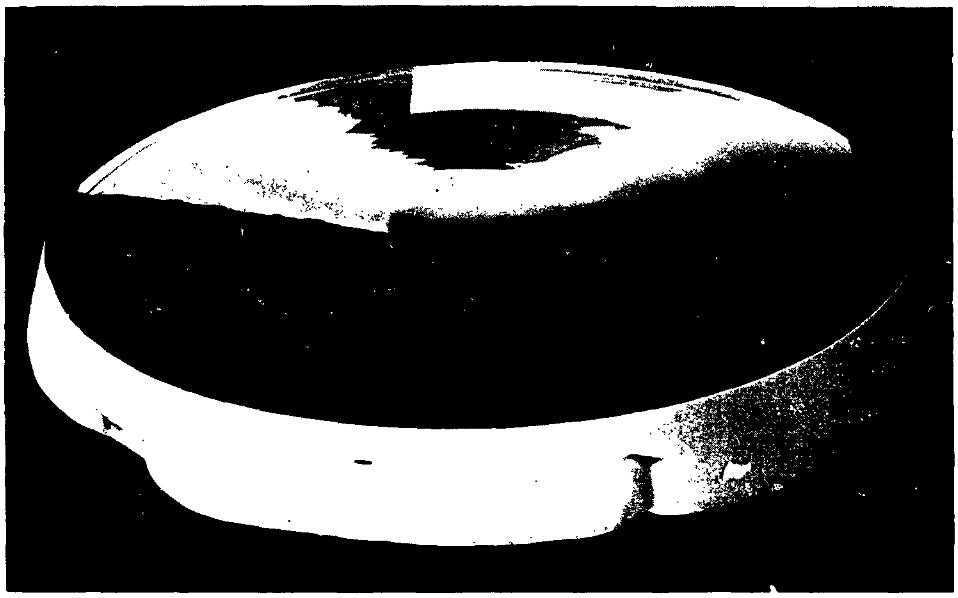

Figure 58. Thirty-Six Inch Diameter Foam-Rigidized Antenna Reflector

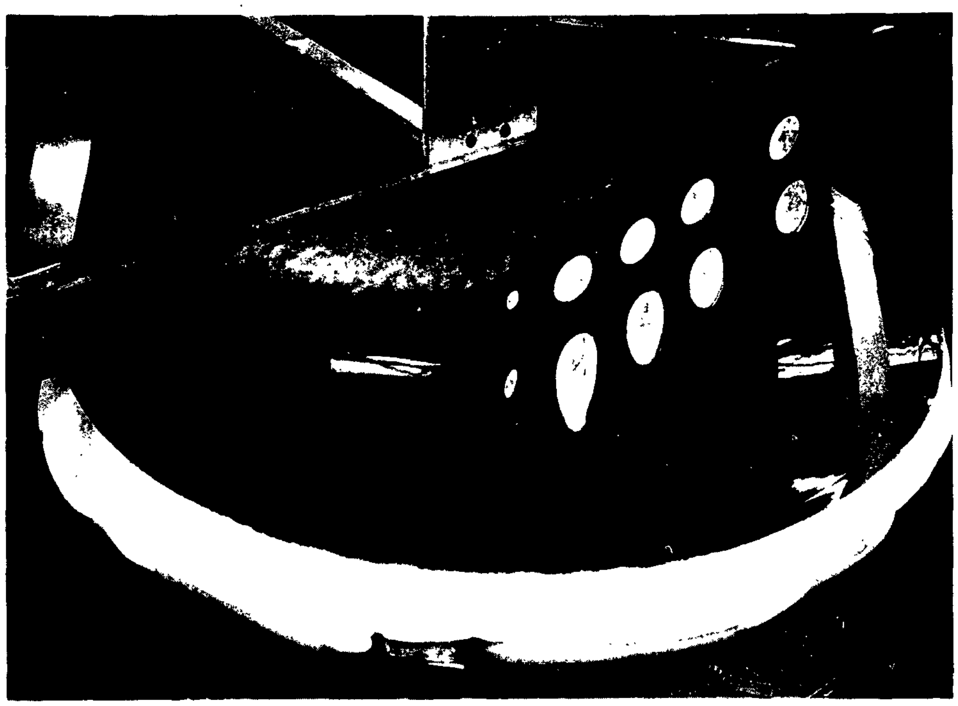

Figure 59. Foam-Rigidized Antenna Dish with Contour Test Setup

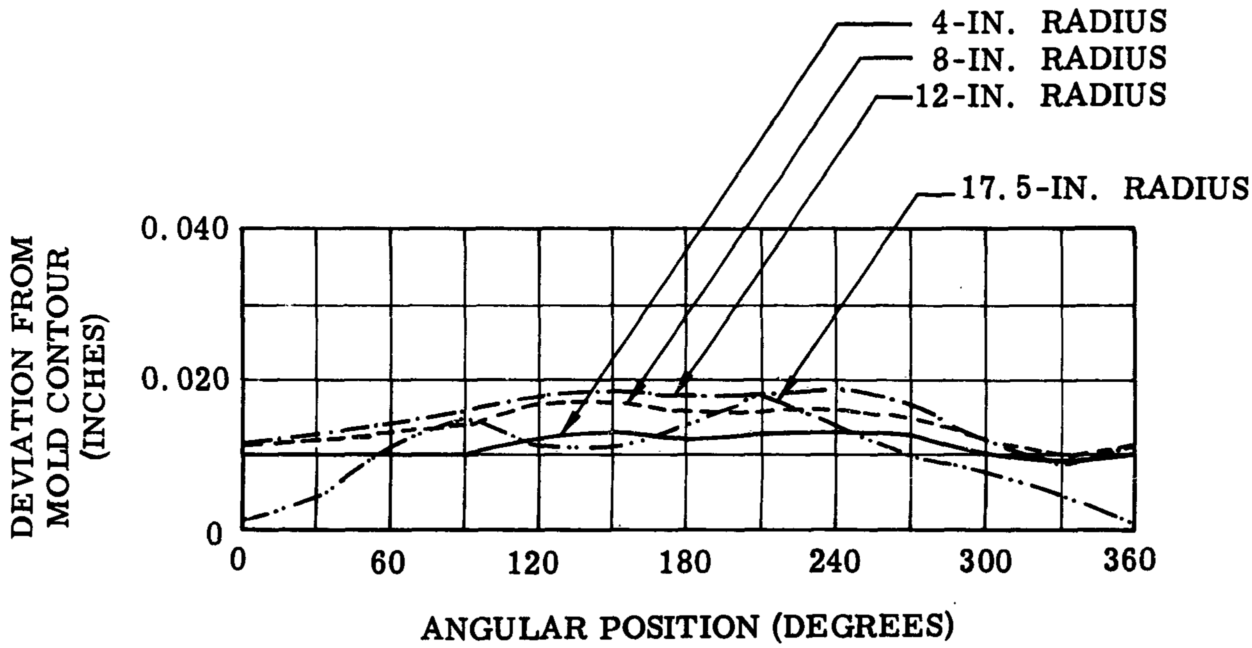

Figure 60. Surface Contour Deviation (Experimental Reflector No. RR 29)

higher than service temperature after the placement of each layer of foam. These post-cures required approximately eight hours.

Contour deviation measurements for a typical test panel are shown in Figure 60. For the test sample, the contour deviated only ±0.009 inch from an average theoretical contour.

e. Foam-Rigidized Antenna Testing. Using this molded-foam technique, reflective surfaces can be reproduced from the mold with satisfactory accuracy. A more difficult problem lies in producing a foam structure that will hold this contour within tolerable limits under the dynamic and environmental conditions to which it will be subjected in the operation of the antenna.

More knowledge of the structural behavior of foams was needed to perform the task of designing a foam-rigidized antenna with the assurance that its contour would stay within the required limits. As an adjunct to the problem of developing a fabrication technique and testing the resulting product, the foam used was tested for structural properties. These tests were used to accumulate more structural test data on polyurethane foams at various densities than is now available. Preliminary physical properties derived from these tests are shown in Figure 61. The data points obtained during the tests were very consistent, and the resulting curves are considerably higher than "catalog" data previously available. It is cautioned that this data applies specifically to the foam compounds that were processed for this program. Different foaming techniques and core depths may produce different results. Therefore, this data should not be taken as applying to all polyurethane foams in general.

To assess the reflector performance of both front-reflective and rear surface under the damaging effects of hail, rain, freeze, sand, and dust, sections of panels containing different coatings were environmentally tested under these conditions. No damage occurred to any of the test specimens, except those subjected to hail. Based on the tryout of a number of epoxy, acrylic, rubber, and other coatings, it was concluded that the front face could be protected adequately by using a double sandwich laminate (e.g., Mylar-aluminum foil-Mylar) over high-density foam with a subsequent elastic coating such as hypalon. The rear surface can be protected adequately by using a very elastic coating such as neoprene.

3. Inflatable Parabolic Antennas

a. General. As previously mentioned, the inflatable parabolic antennas basically offer the potential of obtaining lightweight, packageable antennas with the capability of achieving operating efficiencies comparable to conventional antennas.

The items that were pertinent in the preliminary evaluation will be considered

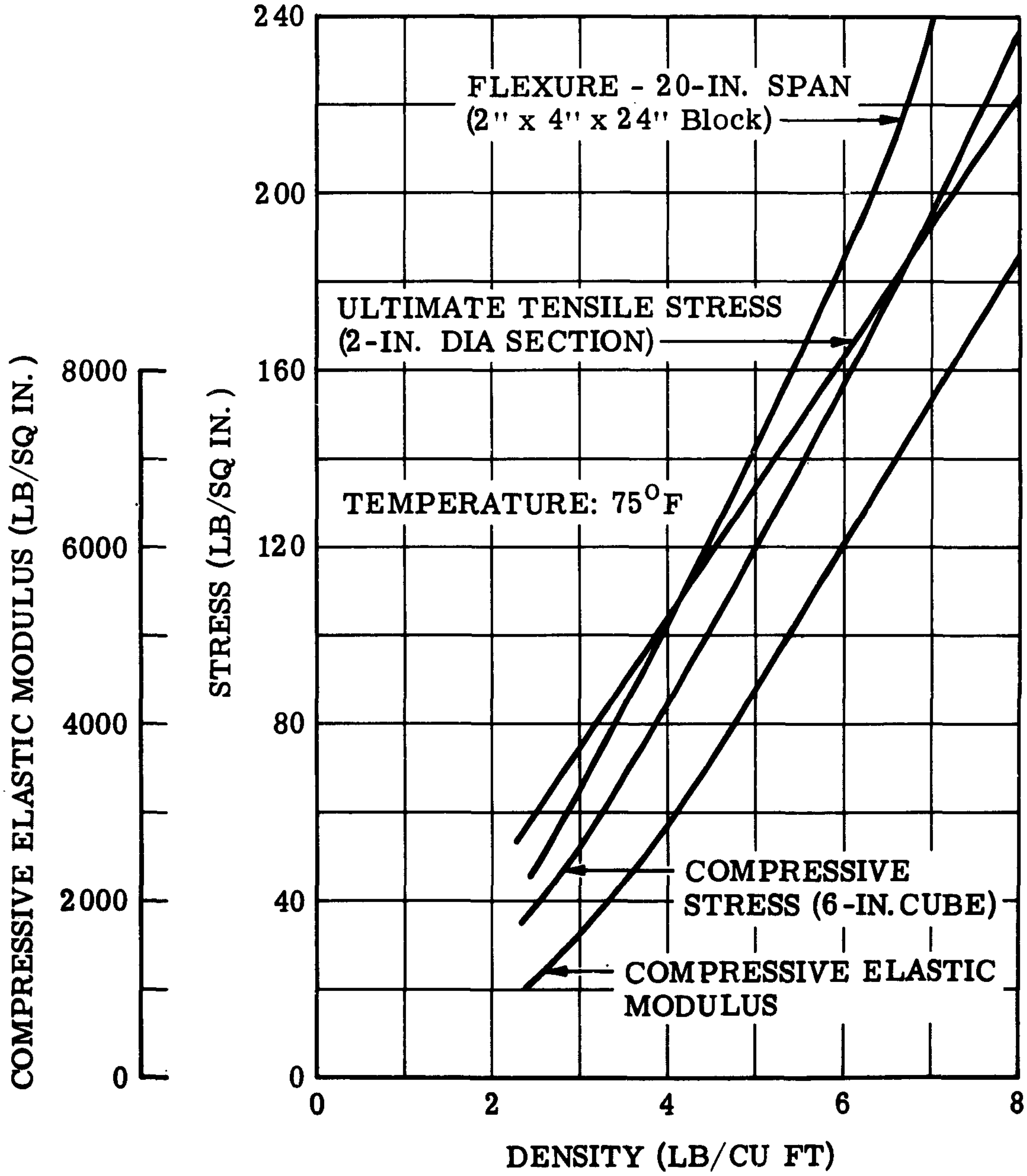

Figure 61. Preliminary Test Data - Polyurethane Foam

further to assist in the final evaluation. These items will include packageability, weight, antenna efficiency, fabrication techniques, and over-all system economy. The following four inflatable parabolic antennas remaining after the preliminary evaluation are discussed in the following paragraphs.

(1) AIRMAT Paraboloid Antenna
(2) Lenticular AIRMAT Antenna
(3) AIRMAT Vacuum Paraboloid
(4) Torus-Supported Inflatable Antenna

b. AIRMAT Paraboloid Antenna

(1) General. The AIRMAT paraboloid antenna was one of the four inflatable parabolic antennas selected for further study and evaluation during the final evaluation. To assist in comparing this antenna system to the other antenna concepts, it was necessary to establish the advantages and disadvantages between the inflatable concepts as well as between the other antenna concepts.

In some cases, it was necessary to simplify the work effort, and in other cases, it was necessary to conduct a rather detailed analysis and then extrapolate the results to fit other antennas. Basic areas of investigation included structural considerations, fabrication techniques, mechanical performance, and electrical performance, as well as costs and reliability to a lesser degree.

Based on the additional analysis of the AIRMAT paraboloid antenna, some design modifications were made on the original concept. As a result of some preliminary stress effort, it was found that shear deflections could cause some r-f pattern degradation during the acceleration and deceleration of the dish during tracking. Even though the periods of acceleration and deceleration for a tracking antenna are small, it appears that the problem of excessive shear deflection of the AIRMAT antenna can be greatly improved, if not eliminated. A new design concept utilizing slanted drop threads in the AIRMAT instead of vertical drop threads will cause the critical shear deflection to become almost negligible. With the realization of the great advantage in the utilization of slanted drop threads in holding the contour of the paraboloid structure to the critical tolerances required, the use of normal drop threads was not further considered in this study. The details substantiating this design modification are basically structural and are discussed in more detail in the following paragraphs.

Figure 62 illustrates the modified AIRMAT paraboloid concept, showing the use of diagonal drop threads arranged in a radial beam configuration.

The advantages of inflatable structures are quite evident, particularly the greater packageability and lighter weight. However, the biggest unknown in designing inflatable structures is their capability of functioning as required. In other words, can inflatable structures withstand the condition imposed upon them by wind loads, dynamic loads, static loads, and internal pressure loads, as well as the effects of packaging and erecting, and still perform satisfactorily as an antenna system? Preliminary structural calculations indicated that inflatable structures can be made capable of operating as rigid structures under similar conditions. Detailed substantiation of this capability will be discussed later.

(2) Design and Fabrication Techniques. Several design and fabrication techniques were considered, and even up to the point of the final evaluation of the concepts, the most practical and economical fabrication and structural concept had not evolved. Therefore, the best designs available

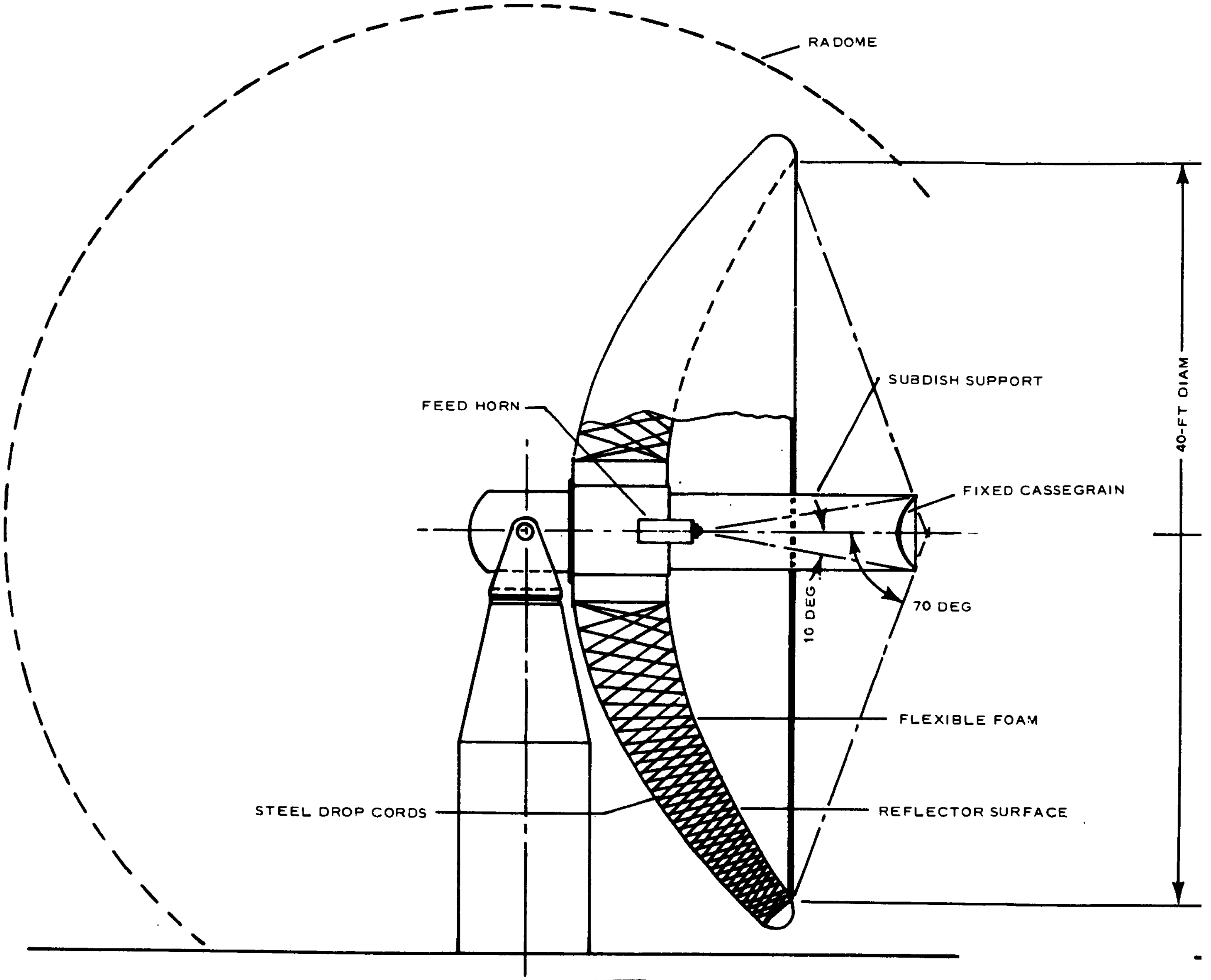
RADOME
SUBDISH SUPPORT
FEED HORN
FIXED CASSEGRAIN
40-FT DIAM
10 DEG
70 DEG
FLEXIBLE FOAM
STEEL DROP CORDS
REFLECTOR SURFACE

1

2

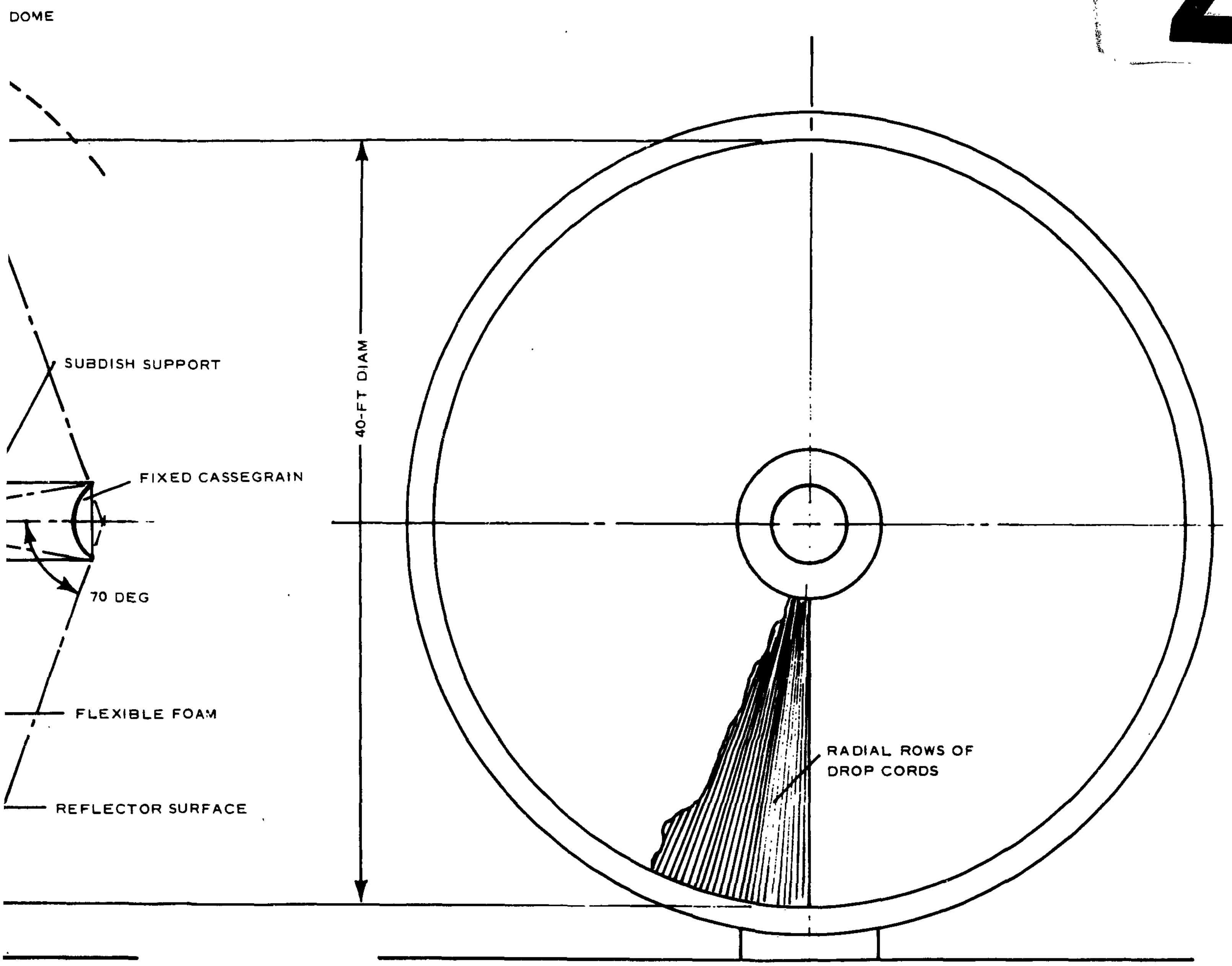

Figure 62. Profile of Inflatable Paraboloid Antenna

for the final evaluation are presented in chronological order.

An investigation of ways to utilize the slanted drop thread material in the fabrication of the circular paraboloid structure supported at the center soon indicated that the rows of drop threads should be radial rows instead of parallel rows. Several configurations utilizing parallel rows of slanted drop threads were considered and then eliminated as being less efficient and less practicable than radial rows. One of the configurations that was eliminated had a combination of canted drop yarn rows acting as radial beams supporting sector gores of normal drop yarn material (see Figure 63). This configuration, although it appears feasible, was eliminated as being less efficient than having all drop yarns canted and arranged in radial rows.

The radial row configuration utilizes the AIRMAT structure most efficiently in supporting shear and bending loads. Figure 62 shows a canted drop yarn arrangement that approximately achieves equal pressure loading on all drop yarns.

On a 40-foot diameter antenna, the spacing shown has one attachment point for approximately every 16 square inches of surface area. This somewhat coarse drop yarn spacing was selected to facilitate the fabrication of the antenna. Since the capability of weaving AIRMAT with drop yarns running in radial rows is not anticipated in the near future, a method for hand-lacing the drop yarns is shown, which is feasible and economical to perform. The structural analysis of an AIRMAT paraboloid is therefore based on a wide drop yarn spacing. Although the drop yarn spacing in the analysis is farther apart (fewer radial rows), the analysis is applicable to configurations such as that shown in Figure 62 for preliminary design purposes.

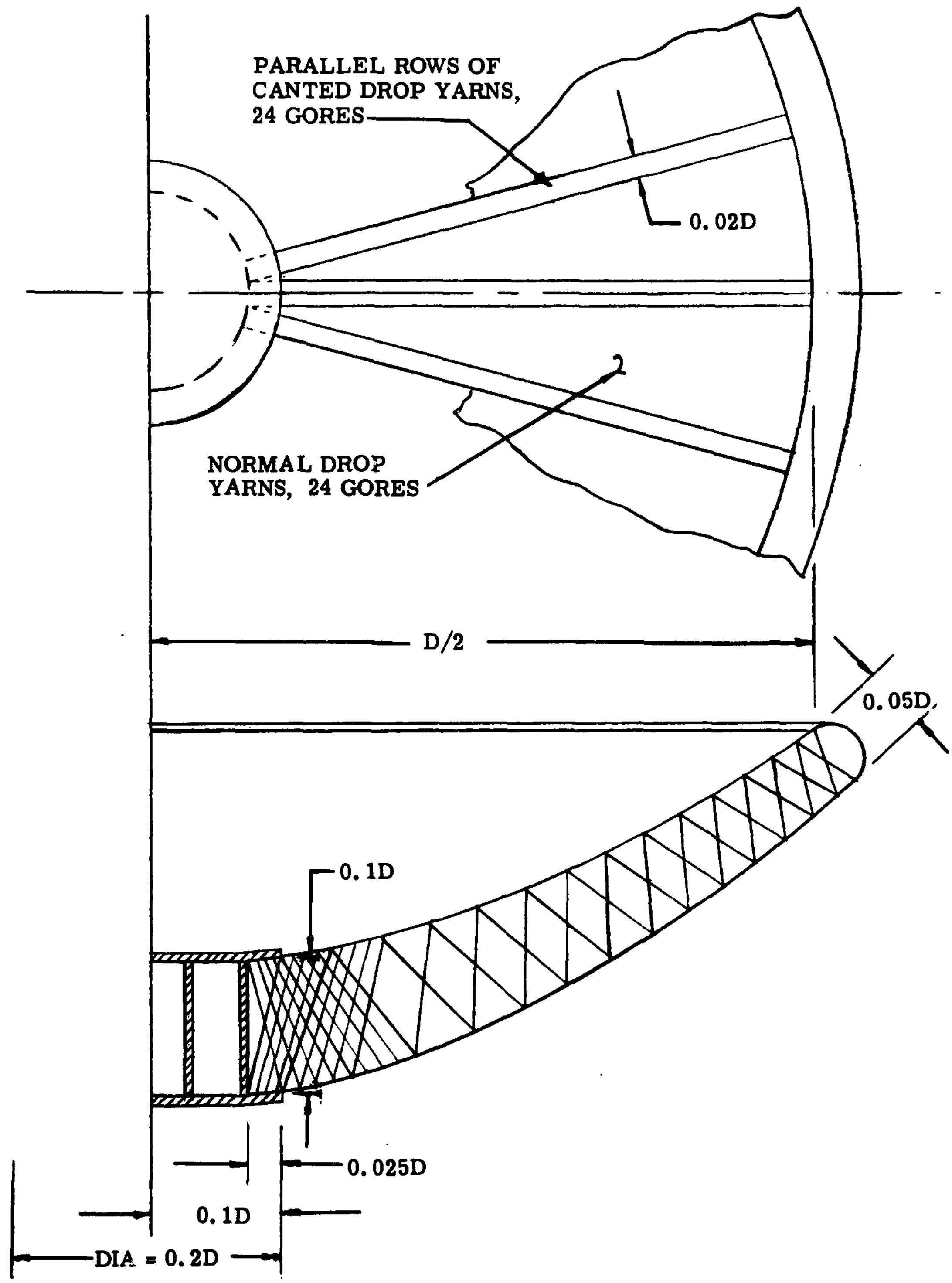

Figure 63. Radial AIRMAT Beam Concept

Two methods for fabricating the AIRMAT paraboloid shown in Figure 62 are suggested in the following paragraph. The number of radial rows and the spacing of the yarns in the rows were arbitrarily chosen and appear to be practicable for hand-lacing. The feasibility of hand-lacing this large number of yarns economically is predicated on the provision of some unique means of attaching the drop yarns to the cover fabric and to the radial cord structure quickly and easily.

Two methods were considered for attaching the drop threads to the cover fabric. These methods are characterized by the following:

(1) Bonding drop thread fittings between the two cloths of each cover ply. During the AIRMAT fabrication, the drop threads are attached to the cover plies merely by quickly connecting the drop thread to the fittings.

(2) Sewing the drop threads into the first fabric cover ply and allowing the sewn length of the drop thread to be fixed in position by cementing the second cover ply to the first cover ply after the drop threads have been sewn into it.

Using the first suggested method, the fabric surfaces are laid up in the required ply arrangement over a sector mold used as a tool to form the AIRMAT cover plies. The radial cords are incorporated into the lay-up, as are the provisions for drop yarn attachment, whatever they may be. The assembly is then bonded together on the form by either an air-dry cement process or by a heat and pressure cure process. The finished assembly, then, has the drop yarn attachment fittings on the inner surface at correct locations and is an airtight fabric surface.

A contour template is made to the correct contour of the inner cross-section of the AIRMAT paraboloid or the contour of the row of drop yarns. The thickness of the template is less than the minimum space between rows at the hub. On this template, the pattern of the drop yarns is accurately scribed. There are two separate ways to use the template in lacing the drop threads. One is to put the fabric directly onto the template in correct position and then attach the yarns, using the template to accurately gage the length of each yarn. After a row is completed, the template is relocated for the next row. The other method is to make up each row of drop yarns on the template as a separate assembly, apart from the fabric. Then each row assembly of drop yarns is attached to the fabric without the use of any special tooling.

After the AIRMAT sectors are thus laced, they are seamed together to form the paraboloid dish. The sectors could be oriented properly for seaming by placing them on the lay-up tools mentioned previously.

The second method of fabricating the AIRMAT paraboloid utilizes the concept of sewing the drop threads directly into the first cover ply and fixing the drop threads in position by cementing the second cover ply onto the AIRMAT, thus sandwiching the attachment length of drop thread between the two plies. Utilizing this concept, the sewing of the drop threads would eliminate the need for fittings and although it may consume somewhat more time in the sewing operation, it would eliminate some steps in the fabrication.

Another method that may have possibilities would make use of the heat preforming characteristics of synthetic fabrics. This method is based on the concept of fabricating a dish from sectional gores of AIRMAT that have been preformed to a double contour by a heat-setting process. The advantage in making the antenna dish with gore panels having double curvature over making it with flat gore panels curved in only one direction is evident. The resulting contoured dish would require a much thinner layer of flexible foam to obtain the final contour accuracy, not only saving a large amount of weight but also improving packageability and relieving possible creasing problems.

It must be recognized that the concept presented here does not necessarily represent the optimum method of fabrication but is presented here only as an alternate method that could possibly be developed with further study. Also, this method can be used only with synthetic fabrics. It is not anticipated that this fabrication technique will be pursued further during this program. The concept of preforming the flat AIRMAT into double-curvature gore panels is explained in the following paragraphs.

The flat AIRMAT material is woven using "un-heat-treated" Dacron yarns in the base cloths. The drop yarns used in this weaving are of heat-treated Dacron stock that has been preshrunk at 350°F or higher.

The AIRMAT material is then coated, and the cover plies are added. The neoprene coating is left in the uncured state, or it is only partially cured. The AIRMAT is then heat-shrunk to contour and cured in a female mold. This is accomplished by clamping the material in such a manner that the final dimensions of the outer surface are greater than that of the inner surface.

After cure, the material is removed from the mold, and each surface is trimmed to its respective correct shape. The outer and inner surfaces of the resulting gore panels have been formed to their desired surface contour, and the drop yarns are oriented approximately normal to the surface. The slight error incurred in making both surfaces to the same radius of curvature is considered negligible.

Regardless of which fabrication technique is used, the completed AIRMAT paraboloid is then attached to the hub and inflated. The fabric surface will have dimples due to the wide drop thread spacing, and other small contour errors are anticipated. To correct the reflecting surface contour, a layer of flexible foam is put on the AIRMAT surface. The foam is molded in place on the fabric surface. It is anticipated that a full-size parabolic tool will be used to achieve the best accuracies, but the use of a sector mold would also be considered. It is estimated that the required thickness of the foam layer to bring a 40-foot diameter dish into contour would probably vary from a minimum of 0.06 inch to a maximum of approximately 0.50 inch.

R-f reflective paint (powdered silver in a flexible paint vehicle) is then applied to the foam to provide the reflective surface. The obvious objective of this technique is to provide a flexible foam-paint combination on the fabric surface. Preliminary investigation indicates that no severe problems with recovery of contour after folding should occur as long as the optimum flexible foam composition, adequately cured on the mold, is used.

c. Lenticular AIRMAT Antenna

(1) General. The lenticular AIRMAT antenna has several of the same features as the AIRMAT paraboloid antenna, with a few basic exceptions that show up in some cases as advantages and in other cases as disadvantages. Figure 64 shows the latest concept of the lenticular AIRMAT antenna. Several similarities are evident. One similarity is that AIRMAT structure is being used with diagonal drop threads to provide

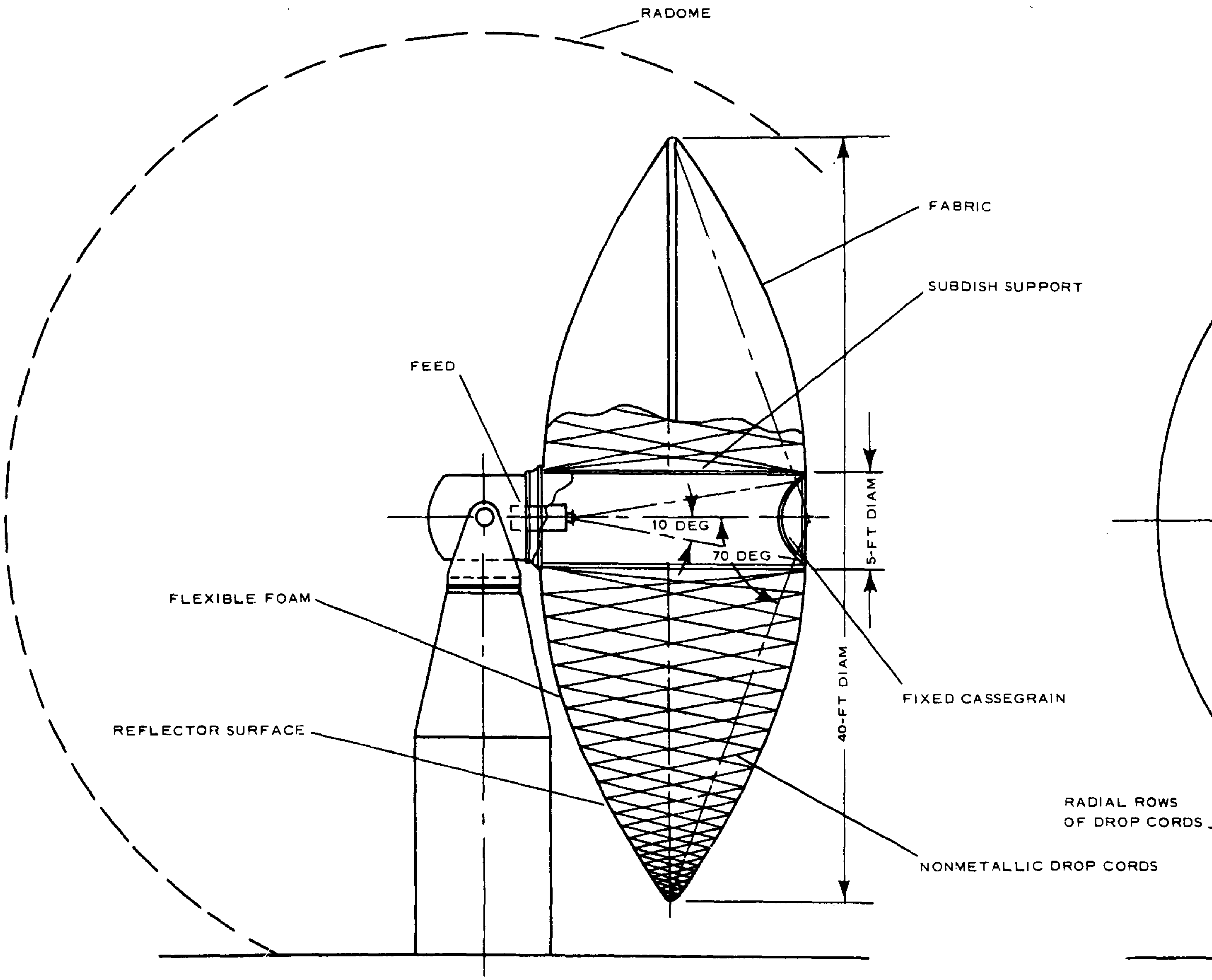

Figure 64. Profile of Inflatable Lenticular Antenna

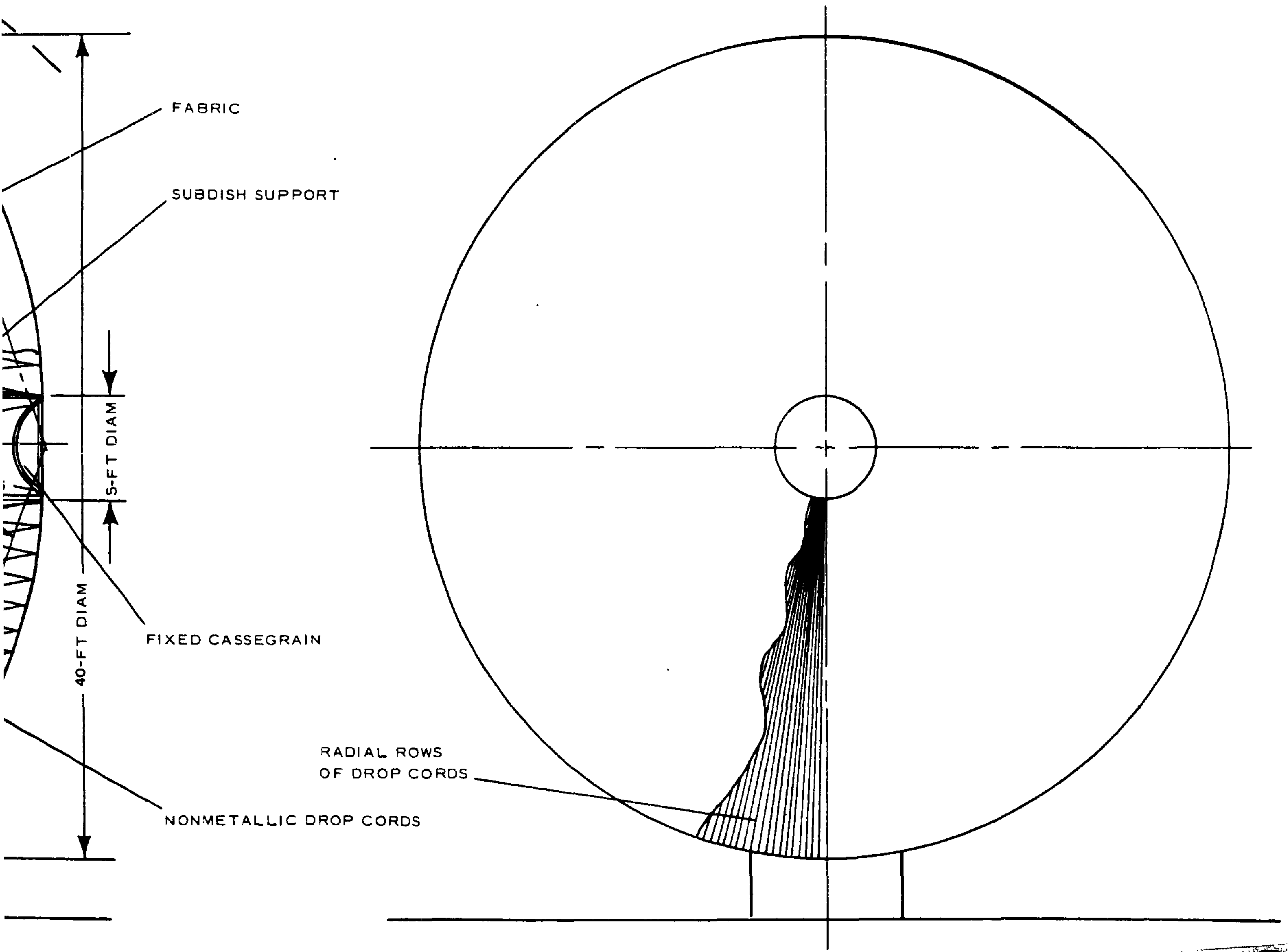
FABRIC
SUBDISH SUPPORT
5-FT DIAM
40-FT DIAM
FIXED CASSEGRAIN
RADIAL ROWS
OF DROP CORDS
NONMETALLIC DROP CORDS

additional shear stiffness. The method of producing an accurate reflector is also the same, i.e., foaming the AIRMAT surface against a parabolic tool to make up for the deviations and inaccurate fabrication of the AIRMAT structure. The reflective r-f surface is also the same, i.e., r-f reflective paint is used.

The lenticular concept has some advantages and disadvantages when compared to the paraboloid concept. As can be seen when comparing Figure 62 to Figure 64, for an aperture of the same size, a smaller radome is required for the lenticular concept. Also, the center of gravity of the dish is closer to the support tower. Even though the inflatable structure is heavier, the cg location assists in minimizing the counterbalance weights and the over-all weight of the systems. The greater thickness of the AIRMAT section is also an advantage in providing greater resistance to bending deflections.

The disadvantages of lenticular AIRMAT when compared to the AIRMAT paraboloid are also evident. The r-f energy must be reflected through the drop threads, both AIRMAT skins, and through the flexible foam that supports the reflective surface. In this process, some energy will be attenuated, some absorbed, some reflected, and some refracted, causing some loss of efficiency in the system. The amount of loss caused by this feature will be discussed later. Also, because the r-f energy must pass through the AIRMAT structure, this structure must be a material that is essentially transparent to the microwave energy. Therefore, the selection of material is immediately limited to fabrics such as Type 51 Dacron, which has a ratio of modulus of elasticity to ultimate strength equal to 4.8, and fiberglass, which has a ratio of 66.7. This compares unfavorably with steel fabrics $(E/F_{tu}) = 530$, which can be used in the AIRMAT paraboloid concept. In addition, fiberglass fabric has a self-destruction characteristic that can cause failure in the fabric at the crease after being folded a number of times.

(2) Fabrication Techniques. The fabrication techniques considered for the lenticular antenna are the same as for the AIRMAT paraboloid. As in the case of the AIRMAT paraboloid, the slanted drop yarns of the lenticular AIRMAT antenna must be arranged in radial rows, and a similar hand-lacing method is suggested for fabricating the lenticular as was suggested for the AIRMAT paraboloid. The fabrication procedure is essentially the same for both types of antennas, except for differences in tool dimensions. The attachment of the drop yarns by a simple nonmetallic means appears to present a problem in fabricating the lens, but it is believed that a simple and economical means of attachment can be devised, making the concept practicable to build.

d. AIRMAT Vacuum Paraboloid. The AIRMAT vacuum paraboloid antenna is similar to the AIRMAT paraboloid antenna in that it utilizes the same type of inflatable backup structure. The difference between the two is that the reflecting surface of the AIRMAT paraboloid antenna is foamed by a molded flexible foam surface, whereas the AIRMAT vacuum paraboloid antenna surface is formed by a secondary fabric surface supported around the edge of the AIRMAT structure. The parabolic shape of the surface is achieved by pulling a vacuum between the secondary fabric surface and the AIRMAT, thus causing the ambient atmospheric pressure to form the reflector surface.

This concept utilizes the same method that, prior to this program, has been the only one used for producing an inflatable antenna reflector. That is, namely, a contoured diaphragm formed by air pressure and supported by a structural ring. This concept, however, offers some basic improvements over so-called standard inflatable antennas. The ring used to support the reflective surface in this case is an AIRMAT dish that should represent a significant structural improvement over a torus-supported diaphragm as well as a significantly more packageable ring than the metal truss supported rings that have been used in some systems. This system will have mobility and light weight advantages that are similar to the other inflatable antennas.

One disadvantage of this antenna compared to the AIRMAT paraboloid is that the secondary fabric surface cannot be formed as accurately as the foamed surface of the AIRMAT paraboloid. In addition, the added complexity of providing a vacuum system is a disadvantage.

e. Torus-Supported Inflatable Antenna. The torus-supported inflatable antenna has been considered a Cassegrain-type antenna. Figure 30 shows the preliminary profile sketch of a 40-foot dish.

This antenna concept is essentially based on the well-known concept of using an inflatable torus to support two identically contoured parabolic skins, one of which, when inflated, is used as the desired reflector surface. This concept, however, should represent an improvement over previous concepts, since the torus is supported off a center hub by means of a series of straps arranged in a bicycle-spoke configuration around the hub to the torus. Also, as compared to other similar previously developed inflatable antenna configurations, it will require less rigid support structure, and it will present an improved support, since it is supported from the center of the reflector instead of from one side of the dish, thus reducing the length of cantilevered antenna structure.

Some of the same problems that are evident in other similar inflatable antennas will present some problems here. By the fact that the fabric material used in this concept must be transparent to r-f energy, the design is normally limited to the use of fiberglass, Dacron, and possibly Fortisan as candidate materials. This limitation, by not permitting the use of metallic fabrics, which have superior stiffness characteristics, will present additional fabric growth problems in comparison to the inflatable antenna configurations in which metallic fabrics can be used. One possibility that was investigated, however, was the use of metallic fabric for all of the antenna structure except for the parabolic surface through which the r-f energy must pass. Further investigation would be needed to resolve the problem completely; however, some deflection and deviation in the reflective surface can be expected, since the loading pattern on the torus will change as the elongation of the fabric having the lower modulus of elasticity begins to change the direction of the loading where it is attached to the torus.

In general, inflatable structures will grow in size over a period of time. This growth is due to crimp in the fabric, twist in the yarn, and creep and temperature elongation in the basic material. These growth characteristics can be reduced by optimizing the design and selecting a fabric having a minimum of crimp woven in the fabric and a minimum of twist in the yarns. Also, some investigation is being conducted presently with monodirected cloth and yarns in an attempt to eliminate the inherent crimp and yarn twist in woven fabrics. To date, it appears that monodirectional cloth can reduce the amount of crimp and yarn twist but the creep will exist in any material under load. However, the creep becomes significantly reduced after about two weeks under load. Therefore, it is planned that any inflatable antenna will be pressurized and held at its operating pressure for at least a period of two weeks before finalization of its contoured reflective surface. This action will also reduce the value of monodirectional cloth, since the crimp and twist in the fabric would normally come out of the fabric during the same period.

Fabrication methods are also usually set up in an attempt to allow for the amount of expected crimp elongation in an inflatable antenna. This allowance, however, is difficult to predict accurately at first; therefore, final fabrication adjustment to reduce the crimp growth and fabrication errors as much as possible is planned.

On the other hand, no allowance can be made for material creep or temperature elongation over a range of temperatures, because the characteristic is a function of the basic material itself. Material creep occurs in all materials and is a function of the load versus time. Temperature elongation also varies from one type of material to another and is a function of load and temperature. The only way to minimize the creep and temperature elongation for a particular application is by the selection of material.

Inorganic fabrics such as Dacron, nylon, and rayon have relatively low moduli of elasticity when compared to glass and are very low when compared to steel. In addition, their creep characteristics are high compared to these two materials. Glass fabrics, however, are not as good as metallic fabrics, relative to elongation properties, and the glass has a self-destruction characteristic that causes serious degradation to the fabric strength to the point of failure after repeated flexure. However, significant improvements in this flexure or abrasive damage characteristic have been achieved by various new methods of coating the glass fibers or yarns with a protective material; therefore this characteristic is not as important as before.

All the mentioned fabric materials except steel fabrics are relatively transparent to r-f energy. Therefore, if the antenna design configuration is such that it must pass r-f energy through its structure, metallic fabrics with their inherently superior structural properties cannot be used for that particular antenna. A trade-off between the better folding capabilities of Dacron, nylon, and rayon to the better elongation characteristics of glass fabric must then be made for that particular antenna system. Such is the case for the torus-supported inflatable antenna. However, the amount of folding encountered in this application may not be a critical factor.

4. Foldable-Truss Support Structure

Some additional effort was put on the foldable-truss support structure, since the concept here is to attempt to define better methods of folding rigid structure and improve its transportability features. As mentioned previously, the two types of folding trusses were combined for purposes of evaluation since they represented essentially a single concept.

The additional work effort was devoted mainly to the axial folding, or umbrella-type folding, truss backup structure.

The configuration shown in Figure 34 is considered to be geometrically and structurally feasible. In this configuration, the feed support and the antenna dish are removed from the truss structure before folding. The dish is assumed to be in segmented panels similar to the Syncom dish.

It is intended that the backup structure be placed in the horizontal facing attitude before folding, as shown in Figure 34. Thus, the individual trusses can be mechanically tied together to synchronize their actions and minimize the actuation power that would be required. In general, the foldable-truss antenna does not appear to show much merit in terms of outstanding features. The amount of folding that is provided would save some time in erection and dismantling; however, the segmented reflector dish must still be attached segment by segment. The best estimate of time saving that the foldable-truss concept would provide over Syncom is approximately a 12-hour elapsed-time savings out of a 48-hour erection schedule. Also, for this partial folding capability, a trade-off must be made against the complexity of the backup structure, which increases cost and probably the weight. It is also difficult to provide on-the-site adjustment for the folding structure, which would leave the alternatives of a numbering system for factory-adjusted panels or some inaccuracy between the reflector dish segments after erection.

5. Multiple-Reflector Array

A multiple-reflector antenna system was briefly explained in Section VIII. A similar array of parabolas has been investigated by Radiation Incorporated, and in evaluating the information they presented, together with that generated by Goodyear Aerospace, it was believed that the multiple-reflector concept would have merit as a monopulse antenna system. Figure 65 shows various arrangements of parabolic reflectors in a multiple reflector array.

The electrical problems connected with this antenna system, however, could be numerous. One such problem is in attempting to predict the principal pattern based on the feed separation, which is the distance between separate parabola feeds. The feed separation design is a trade-off between gain and side lobe effects. If the side lobe level is not very critical, a design can be made to provide maximum gain. However, if low side lobes are required, then the gain must be sacrificed. By studying the effect of spacing on the array factor, the design can be determined for different trade-off combinations of gain and side lobe levels. The optimum design to achieve a good side lobe level with a minimum reduction in gain results in a -20 db and a -16 db side lobe level for a four-element array and a seven-element array respectively, if the beamwidth is set equal to that of a large single reflector. Another trade-off would be to choose a spacing between feeds which produces maximum gain but a poor side lobe level. Intuitively, the blockage could be greater than that of a single dish. In the investigation conducted by Radiation Incorporated, experimental data substantiates the analytical analysis,

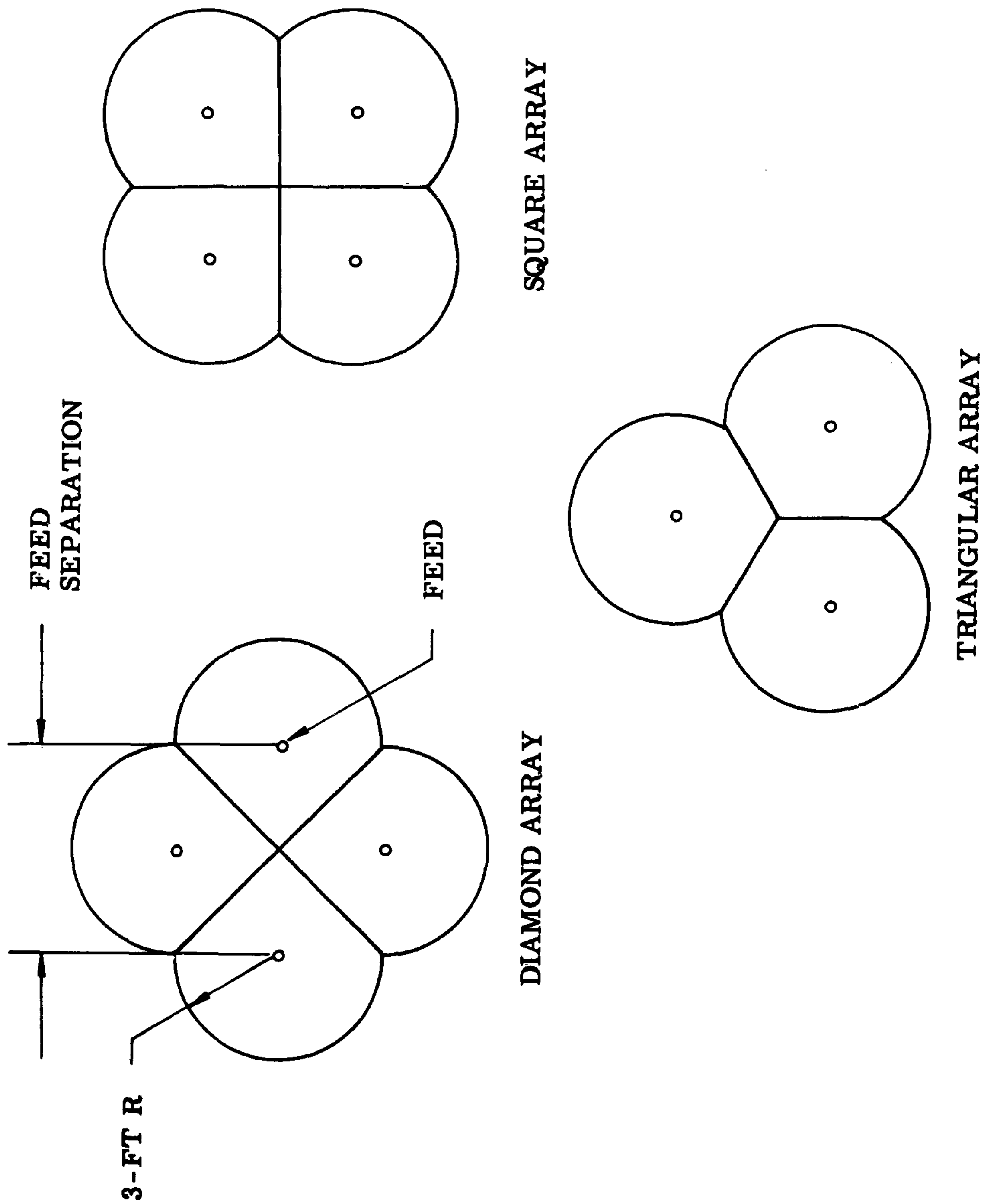

Figure 65. Types of Multiple-Reflector Arrays

which indicates the problem of poor side lobe levels when maximum gain is desired.

If four parabolas are joined with their circumference meeting in a single point at the center as shown in Figure 65, the loss in area would be approximately 18 percent compared to a single parabola of the same diameter. This corresponds to a gain loss of less than 1 db.

Structurally, the feed assemblies of the array would not protrude as far as that of a single-dish feed. The smaller dishes can be fabricated with more accurate surface tolerances than a single larger dish; however, the multiple-dish array would require a phase shifting network to compensate for the relative displacement between the various dishes if close displacement tolerances are not held between the dishes.

6. Inflatable Spherical Antenna

The inflatable spherical antenna is designed as an inflatable antenna that provides 360-degree azimuth scanning and limited elevation scanning by rotation of the feed horn rather than the reflector structure. Elevation scanning is limited toward the zenith position due to the blockage of the feed and feed support.

The basic advantages of this antenna system are as follows:

(1) One basic structure serves as both the radome and reflector, and therefore a separate radome is not required.
(2) Only the feed rotates, affording a considerable saving in driving power and the size and weight of the rotating mechanism.
(3) The inflatable thin wall construction offers very good packageability and transportability.

In general, this type of antenna system would have poorer performance than any of the other antenna systems considered here for the higher frequency applications.

This antenna would be best utilized as a Class I antenna system. The performance is reduced for several reasons. These reasons include:

(1) In order to achieve azimuth and elevation scanning, a spherical reflector is required, and even though the area illuminated at one time approaches a paraboloid, the efficiency is reduced somewhat from a true paraboloid.

(2) Operation is limited to a single linear polarization.

(3) The parallel conductor grid introduces both reflective and transmission losses. Tests have shown that for a typical configuration the combined reflectivity and transmissivity losses due to the grid are approximately 1 db.

(4) The over-all size of the sphere is large in comparison to the effective surface that is illuminated at one time. Also, for this reason, the size of the antenna is large in comparison to the other inflatable concepts for the same aperture size. Therefore, elongation effects inherent in woven fabrics, such as material crimp, yarn twist, temperature elongation, and material creep, will be greater for this antenna in proportion to its larger size. Greater elongation results in more deviation from the desired contour and thus additional loss in efficiency.

(5) Because the r-f energy must pass through the one side of the spherical antenna wall, for the reasons mentioned in the discussion on the torus-supported inflatable antenna, the antenna structure is limited to the materials with greater elongation characteristics by the nature of its configuration. Metallic fabric cannot be used because of the r-f transparency requirements.

This antenna, as mentioned previously, cannot provide full elevation scanning and therefore does not completely meet the objective established for tracking antennas. This type of antenna could be utilized more advantageously for other applications where full elevation scanning is not required, such as search radar, troposcatter, and microwave communication links.

7. Circular Hog-Horn Antenna

The circular hog-horn antenna was retained until the latter part of the program evaluation, because there were some areas of interest relative to its r-f considerations. However, its mechanical problems by far overwhelm any electrical advantage it may have.

The basic feature of this concept would be its advantage of low back lobes which result in increased sensitivity by minimizing background noise.

D. FINAL ANTENNA SYSTEM EVALUATION

1. General

An evaluation procedure was established wherein the various ground-based antenna types selected for further review could be evaluated and compared with the Syncom antenna system and with each other. The Syncom antenna was selected as a norm or standard, so that each antenna type being considered could be compared with an existing high performance system of known characteristics. Five major categories of comparison were established for consideration in determining the relative value of each antenna type as compared to the Syncom antenna system. These major categories were in turn broken down into various sub-item factors that have bearing on the major evaluation categories. The Syncom system was given a standard rating for each major category and sub-item.

Table III shows the items of comparison and the standard or norm rating established for Syncom. The ratings shown in Table III are not weighted relative to the different major evaluation categories. Therefore, it is not intended that the ratings can be added to give a total value for an antenna type for comparison with

Table III. Evaluation Categories for Ground-Based Antennas

ITEM OF COMPARISON	SYNCOM RATING
I. Cost	100
A. Development	30
B. Production	70
II. Tactical Capability	
A. Transportability	100
1. Packageability	30
2. Weight	20
3. Mobility	50
B. Simplicity of Erection	50
1. Time Required	30
2. Erection Crew	20
III. Performance	
A. Electrical	100
1. Gain-Beamwidth	50
2. Side Lobes	50
B. Mechanical	100
1. Life	30
2. Maintainability (Logistics)	30
3. Versatility	40
IV. Reliability	100
V. Growth Potential	100
A. Physical Size	40
B. Development Potential	60

Syncom or with other types. Each category must be compared separately between the different antenna systems. In this manner, when a particular type of antenna is evaluated, it can be graded on the basis of its specific advantages and not given an over-all high or low rating because it has a high or low rating in one or two other less important categroies.

The nine antenna systems were compared mainly as a Class III type. It was recognized that, if the antenna concept would function as a Class III antenna, it could also meet the specifications for a Class II or Class I type. However, some consideration was given to an antenna concept if it met the Class II or Class I requirements, even if it could not be used as a Class III antenna. On this basis, only one of the nine antenna concepts did not meet the Class III electrical requirements, as will be explained later. The inflatable spherical antenna concept would function efficiently only as a Class I antenna system due to its inherent structural characteristics. In evaluating this antenna, it was rated very low in electrical performance since the chart was basically set up for a Class III comparison. However, it received a modest rating in growth potential, since it was considered here that the antenna concept could have some merit as a Class I antenna.

To discuss the evaluation of the various antenna systems, an explanation of the evaluation categories is presented first. After this discussion, a general explanation of the ratings for each antenna system is included together with a discussion of their comparison to the Syncom antenna and to the other antennas being evaluated.

2. Evaluation Category Explanation

To explain evaluation categories, a brief description of the important considerations is presented in the following paragraphs.

a. Cost. The cost evaluation category was divided into two separate items:

(1) Development Costs
(2) Production Costs

The development costs are compared on a relative basis and include the cost of design, development, tooling, and fabrication and testing of one prototype unit.

The production costs are also relative and are considered as the cost of producing subsequent antennas in quantities of 10 to 25 units.

b. Tactical Capability. Tactical capability consists of two major items of comparison, namely transportability and simplicity of erection. Transportability is an appraisal of the comparative ease of transporting the antenna packaged components from point of manufacture to operational site and from one site to another. Here packageable size and weight of components are considered for initial shipment as well as for relocation from site to site. The packageability considers the over-all system size as well as the size of individual packages. It also considers the foldability of the various subsystems and assemblies. The mobility aspect considers, in addition to size and weights, how readily the antenna system lends itself to a mobile configuration. Some of the items considered here include:

(1) Can the antenna system be mounted to mobile unit such as a truck or trailer?
(2) If so, the size of the mounting configuration is considered together with the number of mobile units required for each system.
(3) Is the configuration such that it must be stored in groups of individual packages that must all be assembled on the erection site?

Simplicity of erection includes consideration of the elapsed time required to assemble and set up the antenna system in operating condition. Also, the size of the erection crew required is considered.

c. Performance. Electrical and mechanical performance are considered as separate items affecting the over-all performance.

(1) Electrical Performance. In comparing the various antenna systems, the electrical performance forms a significant factor. The approach taken for the evaluation and comparison of the performance for the various antenna concepts is discussed below. The electrical performance can be measured in terms of gain, side lobes, beamwidth, bandwidth, bore-sight, patterns nulls, impedance match, noise temperature, etc. However, to minimize the number of parameters and their evaluation in this study, the Syncom antenna has been selected as the norm. That is, for the X-band type, a size of 30 feet is selected, reducing the critical parameters to gain, bandwidth, and side lobes.

The following is a summary of these performance norms, based on an operating frequency of 7369 mc in the X-band range:

Side lobes - lower than 25 db

Gain - 52.4 (±1) db

Bandwidth - ±350 mc

Surface tolerance (static) - 0.010 inch rms

Feed and support - 18.6 square feet

A detailed analysis of surface tolerance and blockage was conducted on the Syncom program. However, for the evaluation here, approximate computations will suffice. Of particular importance on the Syncom program was the finding that feed blockage is the major factor. While the surface tolerance was necessary to achieve the performance, a further reduction of these deviations would not appreciably affect either gain or side lobes. This may be seen in the following discussion.

The blockage effects on antenna gain and side lobes may be approximately determined by assuming that the blocked power is radiated with a 180-degree phase reversal to the main beam (computed assuming no blockage), by an aperture that is of the shape and size of the blocking apparatus. This would be completely valid if the blocked power were completely absorbed by the blocking structure. While this is not the case, energy striking the blocking structure is generally scattered in such a way that the energy forms little contribution to the space near the main beam. This concept has been definitized and utilized at Goodyear Aerospace with good results.

In a similar manner, random distortions of the reflector may be considered to give rise to a set of scatters which will cause the amplitude of the ideal side lobes to be modified. The effect on each side lobe will be random, in general, but will follow a Gaussian distribution about a mean line when considering a large number of antennas and a large number of side lobes.

This effect of surface tolerance has been theorized by Ruze for circular parabolic antennas. While the validity of all of the assumptions has not been established for the various types of antennas considered here, the approximate expressions for side lobe effects and gain effect are useful in a preliminary evaluation.

The pattern "P" of an antenna with tolerance effects may be computed from the ideal antenna pattern P_0 by

$$P \approx P_0 + \frac{4C^2 \pi^2 \ \bar{\delta}^2}{\lambda^2 G_0} \ (e) - \frac{\pi C^2 \sin^2 \theta}{\lambda^2} \tag{3}$$

where

C = correlation interval or distance over which the errors tend to be unrelated,

$\bar{\delta}^2$ = rms of deviation magnitude,

λ = wave length,

G_0 = ideal gain,

and

θ = angle from peak of beam.

The gain for large correlation intervals is given by

$$G = G_0 \cdot e^{-\bar{\delta}^2} \tag{4}$$

Since blockage also produces an effect on both the gain and side lobe level, the next effect is a combination of both blockage and surface tolerance effects. Hence, for the normal case of significant blockage, once the surface deviation effect becomes small compared to the blockage effect, no further advantage is gained by refining the surface.

The correlation interval and surface tolerance will be different in the systems considered. As is evident, some trade-off in these two parameters is possible. However, the approach employed is to estimate these factors approximately for each of the systems. The rms surface accuracy is determined by the material to be used for the surface, the static deflection of the surface, and the number of support elements.

Figure 22 shows a comparison of maximum gain for various antenna types including the Cassegrain type.

An analysis was made to show the effects of surface tolerance on gain and side lobe level. Due to the fact that, except for the inflatable spherical antenna, all the antennas being considered have parabolic reflectors, and many utilize Cassegrainian feeds, the analysis was based on a 30-foot parabolic reflector with a Cassegrainian feed system designed for minimum blockage under the following conditions:

Parabolic reflector diameter = 30 feet

f/D ratio = 0.424

Frequency = 9.5 gcs

Side lobe level = approximately 22 db down

Parabolic surface errors, (3-σ tolerance): 0.015 inch, 0.030 inch, 0.050 inch, and 0.100 inch

Correlation interval, distance where errors are approximately unrelated = 15 feet

The following performance was found. The gain of the ideal antenna would be 56.6 db. The resulting gain due to blockage and surface errors (with corresponding blockage and error voltages) is presented in Table IV.

Table IV. Gain due to Blockage and Surface Errors

SURFACE ERROR (Inches)	ERROR VOLTAGE (Volts)	BLOCKAGE VOLTAGE (Volts)	GAIN (DB)
0.015	0.6	3.4	56.5
0.030	3.4	3.4	56.5
0.050	9.5	3.4	56.4
0.100	36.5	3.4	56.1

References 6 through 11 were used in calculating the data presented in Table IV. The calculated data is based on a Cassegrain feed with minimum blockage as noted. Blockage is the antenna reflector aperture area blocked by the feed and feed support structure. The blockage of a Cassegrain feed system would be similar in magnitude to the blockage encountered by the Syncom feed system. As blockage increases, surface tolerances have less effect on side lobe levels.

Electrical performance is evaluated by making a comparison of gain and side lobe levels based on estimated surface accuracy deviations due to manufacturing tolerances and deflection for each antenna type being considered.

(2) Mechanical Performance. Mechanical performance evaluation is based on an appraisal of expected operational life of the antenna system under normal tactical operating conditions and with normal maintenance and repair. Also, maintainability is considered in regard to the extent of maintenance expected and the ease with which it can be accomplished based on the relative complexity of the antenna systems being considered. Further, versatility is considered in terms of how well the antenna system can perform the mission for which it is designed.

d. Reliability. First, the reliability objectives were established in accordance with the original program requirements. Then, conducting some reliability effort concurrent with the design of each antenna concept, an effort was made to maintain inherent reliability in subsequent design levels.

As part of the evaluation, the over-all system reliability was preliminarily estimated for each antenna concept. This estimate was based mainly on applying past experience to the basic antenna configuration as well as to the subsystems that make up the over-all system.

e. Growth Potential. Two basic items were considered in evaluating the growth potential of the remaining nine antenna concepts.

First, each antenna system was considered for limitations in physical size. It was recognized that some antenna types have more potential in achieving larger antenna apertures than others; therefore, the antennas were rated here according to their practical ultimate size limitations.

Second, the antennas were rated according to their development potential. The development potential category is based on the possible design improvements that may simplify an antenna concept or may improve it in any of the previous categories. It also considers the potential use the antenna concept has for various applications other than a tracking antenna system.

3. Evaluation

a. General. The evaluation ratings are summarized in Table V. To explain these ratings, a brief discussion is given of each comparison category in which the antennas are compared to the Syncom and to the other antennas being considered.

The higher the score in Table V, for a particular antenna, the higher the the rating for that antenna. For example, the higher the score in the transportability category, the more transportable the antenna would be. Moreover, the higher the score in the cost category, the lower the cost of the antenna.

The individual items within each category are additive to give a total score for each category. However, to reiterate, the major categories are not weighed relative to each other and are not additive to give a total score that will indicate the best system. The evaluation chart can only compare antennas within individual categories.

Table V. Ground-Based Antenna Evaluati

Item of Comparison	SYNCOM Rating	Foam-Rigidized Antenna	AIRMAT Paraboloid Antenna	AIRMAT Vacuum Paraboloid	Lenticular AIRMAT Antenna	Su In A
I. Cost	100	150	95	85	95	
A. Development	30	20	10	10	10	
B. Production	70	100	75	85	80	
II. Tactical Capability						
A. Transportability	100	70	270	270	265	
1. Packageability	30	20	90	90	85	
2. Weight	20	20	30	30	30	
3. Mobility	50	30	150	150	150	
B. Simplicity of Erection	50	55	130	120	125	
1. Time Required	30	35	90	80	85	
2. Erection Crew	20	20	40	40	40	
III. Performance						
A. Electrical	100	100	100	100	100	
1. Gain-Beamwidth	50	50	50	50	50	
2. Side Lobes	50	50	50	50	50	
B. Mechanical	100	100	75	70	75	
1. Life	30	30	15	15	15	
2. Maintainability (Logistics)	30	30	20	15	20	
3. Versatility	40	40	40	40	40	
IV. Reliability	100	100	75	65	75	
V. Growth Potential	100	150	180	160	150	
A. Physical Size	40	50	60	60	50	
B. Development Potential	60	100	120	100	100	

Table V. Ground-Based Antenna Evaluation Chart

AIRMAT Paraboloid Antenna	AIRMAT Vacuum Paraboloid	Lenticular AIRMAT Antenna	Torus Supported Inflatable Antenna	Foldable-Truss Antenna	Multiple-Reflector Array	Inflatable Spherical Antenna	Hog-Horn Antenna
95	85	95	110	80	60	120	35
10	10	10	20	25	20	30	15
75	85	80	90	55	40	90	20
270	270	265	270	135	80	225	25
90	90	85	90	45	25	90	10
30	30	30	30	15	15	35	5
150	150	150	150	75	40	100	10
130	120	125	125	60	40	80	35
90	80	85	85	40	20	60	15
40	40	40	40	20	20	20	20
100	100	100	100	100	100	30	100
50	50	50	50	50	50	15	50
50	50	50	50	50	50	15	50
75	70	75	70	95	95	60	95
15	15	15	15	30	30	15	30
20	15	20	15	25	25	15	25
40	40	40	40	40	40	30	40
75	65	75	65	100	90	80	80
180	160	150	150	110	95	40	20
60	60	50	50	40	45	20	10
120	100	100	100	70	50	20	10

2

For this reason, Table V can be used to select different antenna systems to fit different sets of requirements and specifications. The selection can then be based on whatever categories best fit the particular application.

b. Cost. The antenna system costs are discussed as separate items of development and production costs.

(1) Development Costs. The foam-rigidized antenna development cost would be somewhat higher than for the Syncom antennas because of the considerable amount of development of new fabrication and design techniques involved with the foam application.

The three concepts utilizing AIRMAT would require much more development cost than the Syncom system because of the many new design problems and fabrication techniques involved. However, there would be little difference in cost between the three, since the problems and techniques are similar.

The development costs for the inflatable torus-supported antenna would be somewhat more than for Syncom but less than the AIRMAT concepts. This concept involves techniques that are not as conventional as Syncom but are, however, less complex than the AIRMAT techniques.

The development costs for the foldable-truss antenna would be only slightly higher than Syncom mainly because of the added complexity of the folding joints. The reflector panels would be comparable to Syncom.

The multiple-reflector array would require considerable complexity in the multiple feed and associated r-f circuitry. Structural design would require consideration for maintaining the positioning accuracy between the multiple reflectors. The development costs would be somewhat higher than for Syncom.

The inflatable spherical antenna development costs would be comparable to Syncom. The configuration is quite similar to inflatable radomes for which there is considerable experience. The principal problem area would be control of contour accuracy.

The circular hog-horn antenna development costs would be somewhat higher than for Syncom due to the severe complexity involved with the many feeds. Also the structural design would be complex due to the problems involved with tolerances and the support of the large number of separate horn structures.

(2) Production Costs. The production costs for the foam-rididized antenna would be lower than Syncom because the manufacturing techniques involved would be quite simple, permitting effective utilization of mass production methods.

For the AIRMAT concepts it is expected that production costs would be somewhat less than for Syncom. The manufacturing techniques would be fairly complex, but this would be offset to a large degree by the fact that there are relatively few parts involved. The AIRMAT paraboloid antenna production cost would be expected to be slightly higher than the lenticular AIRMAT antenna because of the more complex shape of the AIRMAT structure. It would probably also be slightly higher in cost than the AIRMAT vacuum antenna because of the closer tolerance required in fabricating the AIRMAT surface and because of the foaming application required. In the case of the vacuum-formed reflector, the contour accuracy is more simply obtained by tailoring the reflector diaphragm to the proper shape.

The inflatable torus-supported antenna and the inflatable spherical antenna production costs would be comparable to each other and would be expected to be somewhat cheaper than Syncom, primarily due to the high cost of the BONDOLITE* panels used for the Syncom reflector.

For the foldable truss, the production cost would be somewhat higher than the Syncom, due primarily to the added complexity of the folding trusses.

The multiple-reflector array would have considerably higher production cost than Syncom, primarily due to the complex nature of the feed and r-f system and to some extent the more difficult nature of holding the position accuracy between the multiple reflectors.

The circular hog-horn antenna would be much more expensive than Syncom in production, due to complex feed and the greater quantity and weight of parts involved.

c. Tactical Capability

(1) Transportability. The transportability will be discussed on an over-all basis, taking into account the packageability, weight, and mobility aspects.

The foam-rigidized antenna would be somewhat less transportable than Syncom. Greater packaging volume would be required because of the more bulky nature of the foamed panels. The weight would be comparable. The mobility would not be as good because of the bulk.

*TM, Goodyear Aerospace Corporation, Akron, Ohio.

The AIRMAT concepts, the inflatable torus-supported antenna, and the inflatable spherical antenna would have a great advantage over Syncom from the transportability standpoint. All are inflatable and can therefore be folded and packaged in a relatively small volume. All are quite light in weight and are adaptable to good mobility techniques.

The foldable-truss antenna would offer some improvement over Syncom because of the folding feature of the truss structure. The reflector panels would be quite similar and would therefore offer no particular advantage. Weight would be slightly greater than Syncom but would be offset by the improved packageability.

The multiple-reflector array would be somewhat less transportable than Syncom, due primarily to the larger packaging volume required for the individual reflectors and multiple r-f feed components. The weight would be slightly greater than Syncom. The mobility would be adversely affected by the greater weight and packaging volume.

The circular hog-horn antenna would be very poor from a transportability standpoint because of the great number of large and heavy components.

(2) Simplicity of Erection. The foam-rigidized antenna would be only slightly better than Syncom from an erection standpoint. There should be some small improvement in erection time, since there would be fewer separate structural parts. The size of the erection crew required would be about the same as for Syncom.

The AIRMAT antenna concepts and the inflatable torus-supported antenna would be considerably better than the Syncom antenna from a simplicity of erection standpoint. The inflatable feature of these concepts provides for simple erection techniques that improve the time required and reduce the size of the crew.

The foldable-truss antenna would show some improvement over Syncom from an erection standpoint. The folding truss feature should decrease the erection time somewhat; however, the size of the erection crew would remain about the same as for Syncom.

The multiple-reflector array would have a slight disadvantage as compared to Syncom from an erection standpoint, due to the more complex feed system and more difficult alignment adjustments required for the multiple reflectors. The size of erection crew would be about the same as for Syncom.

The inflatable spherical antenna would offer some advantage over Syncom from an erection standpoint, due to the fact that it can be rather simply inflated; however, due to its large size and the requirement for ground tie-down and guy cable adjustment, it would not be as advantageous as the other inflatable concepts. The size of the erection crew would be about the same as for Syncom.

The circular hog-horn antenna would be somewhat less simple to erect than Syncom, due to the larger number and size of structure and r-f components involved. The size of erection crew, however, would be about the same as for Syncom.

d. Performance. The antenna performance is discussed in separate items of electrical performance and mechanical performance.

(1) Electrical Performance. Electrically, all the best design techniques resulted in parabolas of various physical configurations. It was

determined that an evaluation of these similar concepts would be based on surface tolerance effect on gain and side lobe level. The tolerances were considered random. It was determined that systematic errors would probably have a greater effect on electrical performance. Systematic errors would be dependent upon the detail structural configuration of the various concepts being considered. Because of the number of different configurations involved and the preliminary nature of the structural design, a detail study of the random errors and an analysis of their effects on the performance were considered beyond the scope of this program.

As mentioned previously, the evaluation is based on a Cassegrainian feed with minimum blockage. The blockage of a Cassegrainian feed system for the antennas being evaluated would be of similar magnitude to the blockage of the Syncom feed system. The surface error voltage is masked by the blockage error voltage. Thus, as blockage increases, surface tolerances have less effect on side lobes. All the parabolas listed in the evaluation chart will be equivalent to the Syncom antenna if the tolerances predicted can be achieved.

Electrical evaluation of Class I and II antennas is extrapolated from the Class III evaluation. For Class II the evaluation would indicate no appreciable changes in gain and side lobes from Class III antennas, as the frequency and size are not significantly different.

A noticeable decrease in the gain would be recorded for Class I antennas. This would be a result of the lower frequency and the decrease in antenna aperture size. In Class I the inflatable spherical antenna may compete with others in its class size, since as the frequency is reduced, the effects of tolerances on gain and side lobes are reduced.

As a prelude to evaluating each antenna system electrically, it was necessary to estimate the over-all and surface deviations that could be expected in each antenna concept. The surface deviations were separated into fabrication tolerances and environmental deflections, and a value was estimated for each. The estimates were based on past experience with inflatable structures and on some preliminary stress and deflection efforts. A summary of the estimated tolerances is given in Table VI.

Table VI. Estimated Surface Tolerances

ANTENNA CONCEPT	3-σ TOLERANCES	
	FABRICATION	ENVIRONMENTAL
Foam-Rigidized Antenna	0.010	0.035
AIRMAT Paraboloid Antenna	0.020	0.050
AIRMAT Vacuum Antenna	0.060	0.060
Lenticular AIRMAT Antenna	0.020	0.050
Torus-Supported Antenna	0.060	0.070
Foldable-Truss Antenna	0.015	0.035
Multiple-Reflector Antenna	0.010	0.020
Inflatable Spherical Antenna	0.30	0.30
Hog-Horn Antenna	0.015	0.035

Based on the above estimated manufacturing tolerances and environmental deflections and the previously mentioned study of random surface errors, all the antennas were rated the same, except the inflatable spherical antenna concept. As previously mentioned, that antenna was rated low here, because it could not meet the Class III or the Class II tolerance requirements.

(2) Mechanical Performance. As previously explained, the mechanical performance was divided into three categories: life, maintainability, and versatility. The expected operational life would be the same as Syncom on all the rigid-type antenna systems. On the other hand, all the inflatable antenna concepts were rated as having about half the operational lifetime of the rigid-type antenna systems. The inflatable antennas were expected to have a lifetime of about five years.

The maintainability of the antennas was rated somewhat different from Syncom, with only the foam-rigidized antenna being as high as Syncom. The foldable-truss antenna, multiple-reflector array, and the hog-horn antenna were rated the same as each other, but somewhat lower than Syncom and the foam antenna because of the increased mechanical and electrical complexity. The inflatable antennas, as shown in Table V, were rated lower than the rigid antennas, with the AIRMAT paraboloid and the lenticular antenna being rated somewhat better than the others. These two were given their rating basically because they had a simpler inflation system and because their structure should be inherently sturdier than the others.

The versatility of the antennas was all rated the same except for the inflatable spherical antenna. The ratings were given on the basis that the antennas would be designed for a particular mechanical function and, if at all possible, would be designed to meet those requirements even though it may mean lower ratings in other categories. Only the inflatable spherical antenna could not completely meet those requirements, because in the zenith position, the mechanical blockage of the feed horn support would severely degrade the performance in this position.

e. Reliability. The foam-rigidized antenna, the foldable-truss concept, and the Syncom antenna were considered to have about the same reliability and were rated higher than any of the others. The hog-horn antenna and the multiple-reflector array were rated here less than the other rigid types because of their added system complexity. The inflatable concepts were again rated below the rigid types mainly because of the added pressurization subsystems that would reduce the over-all reliability. The rating differences between the inflatable antennas were basically differences in the pressurization subsystem complexity.

f. Growth Potential. The growth potential category showed some rather large differences between the different antennas.

(1) Physical Size. In physical size, it was considered that the inflatable concepts had an edge over the rigid types because of their lower weight characteristics.

The multiple-reflector array is rated here only slightly better than Syncom on the basis that several smaller dishes can be held within a closer surface tolerance because of their smaller sizes. For this reason, this type of system may be utilized by grouping together a sufficient number of dishes to give a larger equivalent dish aperture than that for a single-reflector dish. It must be recognized, however, that the electrical problems would be numerous, as mentioned in the previous discussion on the multiple-reflector array.

The inflatable spherical antenna was given some rating here, because even though it cannot be used efficiently as a Class III or a Class II antenna, it shows potential as a Class I. The antenna tolerances cannot be held as accurately because of the large amount of fabric surface area. The contour deviation caused by fabrication, temperature elongation under load, fabric crimp, and fabric creep are generally proportional to the fabric dimensions. Therefore, larger sizes mean larger deviations from the desired contour.

The inflatable spherical antenna has other characteristics that limit its performance relative to the other antennas, as mentioned in the discussion on this antenna, all of which tend to reduce the rating of this antenna concept. Therefore, the limitations of physical size are significant with possible use only as a Class I antenna.

The circular hog-horn antenna has also received a poor rating, since its major structural problems preclude its practical use as a tracking antenna system. The system does not show any particularly significant advantages except for good back lobes, which are in the order of -70 db. From the physical size basis, the structural problem gives this antenna a low rating.

(2) Development Potential. From the standpoint of development potential, inflatable antenna concepts are rated considerably higher than the Syncom and other rigid structural concepts. The inflatable designs presented here are anticipated to be only preliminary in nature and with additional development will improve considerably, especially in the categories of mechanical performance and reliability. Also, inflatable antenna structures offer great improvement basically in the categories of transportability and simplicity of erection.

All the inflatable concepts are rated the same except for the AIRMAT paraboloid antenna, which was rated higher, and inflatable spherical antenna, which was lower.

The AIRMAT paraboloid was rated the highest, since it has some inherent design advantages that can offer some significant advances in the state-of-the-art. The design advantages over other inflatable antennas include the following:

(1) Its structural design allows the use of metallic fabrics with their superior strength and elongation properties.
(2) The reflector surface is supported along its entire surface at accuracies comparable to those of rigid-type antennas.
(3) The AIRMAT paraboloid uses less structure than most concepts, allowing it to be packaged in somewhat less space than other types.
(4) Problems that are inherent with inflatable structures, such as crimp, creep, and temperature elongation, can be controlled considerably better, since the concept allows the foam surface to take out the surface deviations after they have occurred. (The same is true for the lenticular AIRMAT antenna.)
(5) The AIRMAT paraboloid configuration is such that there is no need for r-f energy to be reflected through any part of the antenna reflector structure.

The inflatable spherical antenna was rated rather low here for the same reasons as those mentioned in the previous paragraph in regard to this concept and because this antenna can only be used as a Class I type antenna.

The growth potential of the foam-rigidized antenna concept was rated a considerable amount above Syncom and even comparable to some of the inflatable concepts. With further development, this concept offers the potential of providing expendable foamed-on-site antenna structures that offer the accuracy and the performance characteristics of rigid antennas and transportability characteristics nearly as good as inflatable antennas. The potential use of an inflatable reflector contour tool and an antenna reflector that is so economical that it can be considered expendable will greatly enhance the transportability of the foam-rigidized antenna concept. However, somewhat greater erection time will probably prevent the foam antennas from being as transportable as the inflatable concepts.

The development potential of the multiple-reflector array is rated less than the Syncom antenna system, because in the tracking mode, the auxiliary equipment required to support this antenna system is much greater than the Syncom.

The foldable-truss concept was rated slightly better than the Syncom, since it offered some possibility of improvement with the concept of providing an antenna utilizing foldable rigid structure.

The development potential of the hog-horn antenna is rated low here for the same reasons as previously mentioned. The system has very little potential, since the required heavy structure appears to obviate its use in any antenna class.

4. Evaluation Results and Concept Selection

A review of the preceding evaluation ratings shows that the foam-rigidized antenna offers the potential of achieving improved contour accuracy and ultimately lower cost as compared to the Syncom antenna. However, this antenna offers no advantage from the standpoints of transportability and simplicity of erection. The inflatable AIRMAT paraboloid antenna and the lenticular AIRMAT antenna have very good transportability and erection capabilities with the prospect of reasonable accuracy. Other inflatable types are about equal to the two AIRMAT reflector types from the standpoints of transportability and erection but do not have as good a surface accuracy potential.

The AIRMAT paraboloid antenna and the lenticular AIRMAT antenna offer the best over-all potential for providing large aperture tracking antennas of minimum weight, low cost, and simple and economical assembly and erection on site. These two antenna types were, therefore, selected for further detail design study and model fabrication.

PART 4. FACTUAL DATA

SECTION X. DETAIL STUDY AND ANALYSIS OF GROUND-BASED TRACKING ANTENNAS

A. GENERAL

The general approach during this phase of the program was to further investigate the AIRMAT paraboloid antenna and the lenticular AIRMAT antenna. The purpose of this investigation was to technically develop the concepts to determine what problem areas exist, if any, and to establish the advantages of each concept.

In addition to design studies on the antenna concepts, design of the scale models was initiated in February 1963, even though it was not scheduled to begin until 1 March 1963. As reported in the third quarterly report (Reference 12), it was found that perhaps more time would be needed to fabricate the models than initially planned and that the model work would also contribute to the full-scale antenna study and analysis.

B. AIRMAT PARABOLOID ANTENNA DESIGN

1. General

Three basic areas of investigation were considered in the design of the AIRMAT paraboloid antenna. These areas are the electrical design, the structural analysis, and the mechanical design.

The electrical design attempted to establish a design for a maximum gain antenna configuration as well as an optimum design based on mechanical and electrical considerations. Further consideration was also given to the phase delay angles and the phase variation across the dish aperture. No serious electrical problems are anticipated in this concept.

The structural analysis conducted indicated that the application of diagonal drop threads to an AIRMAT structure offers additional substantiation that an AIRMAT paraboloid antenna can be built to operate as a Class III antenna system.

The mechanical design did not turn up any significant problem areas, and indications are that there are possibly several methods of fabrication that can be utilized. These methods are very practical from an economic standpoint and a technical viewpoint. So far, the problems involved appear to be minor.

2. Electrical Design Considerations

The electrical design for the AIRMAT paraboloid was based on a 40-foot diameter Class III Cassegrain antenna.

An attempt was made to establish a maximum gain antenna configuration as well as an optimum design based on mechanical and electrical considerations. With an f/D (ratio of focal distance to aperture size) of 0.35, a hyperbolic subreflector 1.6 feet in diameter was selected for the maximum gain configuration. This subreflector size was established in conjunction with the minimum blockage design requirement and a realistic feed horn design.

For the maximum gain antenna configuration, it appears difficult to keep the location of the single-frequency feed horn within the antenna hub and behind the surface of the paraboloid. The feed horn in this case would be eight feet long, which is excessively long. Therefore, a seven-foot focal length was used, yielding a more practical feed horn length of 3.55 feet.

Assuming a 55 percent efficiency, the AIRMAT paraboloid antenna will have a gain of 59.5 db, not considering blockage effects. The addition of blockage effects would then result in a new gain of 59.47 db.

The secondary dish support structure has not been included as part of the above blockage consideration; however, several types of support methods are presently under consideration. Some of the types being considered include a rigid multi-strut support, an inflatable cylinder support utilizing stabilizing cables, and an inflatable cone support also with stabilizing cables. The rigid fiberglass cylinder support, as shown in Figure 31 of the second quarterly report (Reference 13), was eliminated because of the r-f transmission problems it would create.

In addition to blockage and the r-f transmission problems, the secondary dish support is also being considered in terms of the phase delay angles and the phase variation across the aperture. However, a detailed study of phase shift variation is beyond the scope of this program.

3. Structural Approach

In an attempt to resolve some of the structural unknowns, an investigation was conducted to consider some basic structural problems as well as problems of design and fabrication on the AIRMAT paraboloid. Even though the AIRMAT paraboloid was selected for the major part of the structural study, the information acquired can also be extrapolated somewhat for limited use in other AIRMAT antenna concepts.

The first and most basic structural problem considered was that of shear deflections in the AIRMAT antenna structure. Unlike most metal structures where shear deflections are negligible when compared to bending deflections, shear deflections are significant in AIRMAT structures, and in fact, were anticipated to be larger than the bending deflections in these AIRMAT antennas.

$$Y_{sr} = \frac{w}{2Gh} \left\{ \left[a^2 \ln (a/b) \right] - \left[\frac{a^2 - b^2}{2} \right] \right\} \quad (5)$$

and

$$Y_b = \left(\frac{k_1}{6}\right)\left(\frac{wa^4}{Eh^2}\right) \quad , \qquad (6)$$

where

Y_{sr}, Y_b = shear and bending deflections respectively (in.),

w = uniformly distributed load (lb/in.^{2}),

a, b = radius to the rim and hub respectively (in.),

h = thickness of the plate or depth of the AIRMAT (in.),

E = modulus of elasticity of the skins of the AIRMAT (lb/in.),

G = transverse shear modulus of the AIRMAT (psi),

and

k_1 = a constant given in Reference 14, page 114.

From Equation 5, it is seen that Y_{sr} decreases as b increases. It is then desirable to use the largest possible hub. The limitations of the maximum hub diameter must yet be specified.

It appears from Equations 5 and 6 that, as h increases, the deflections decrease. It must be remembered, however, that the dead weight also increases because of longer drop threads and because of heavier AIRMAT skins required to carry the increased pressure stress (σ = (ph)/2). The deflections may actually increase with increasing AIRMAT depth. In fact, this is known to be true if just enough pressure, p, is used to prevent buckling of the compressive skin.

The best solution seems to result by increasing G and E in Equations 5 and 6. However, for AIRMAT structures with drop threads normal to the surface, the shear modulus may be considered equal to the internal pressure (Reference 15).

Then Equation 5 becomes

$$Y_{sr} = \frac{w}{2ph}\left\{\left[a^2 \ln (a/b)\right] - \left[\frac{a^2 - b^2}{2}\right]\right\}. \tag{7}$$

It is immediately seen that increasing p has nearly the same effect as increasing h; in this case, however, the weight increases since the skins of the AIRMAT must be heavier to carry the higher pressure stress. The only solution is the possibility of using a material of sufficiently high strength-to-weight ratio to withstand the pressure required to meet the deflector criteria. In addition to the high strength-to-weight ratio requirement, the AIRMAT material must have low creep characteristics to meet the reasonable operating life requirement. Nylon may be discarded since Dacron offers over-all better physical characteristics including minimum creep. The new metal fabrics such as René 41 and the stainless steels are attractive and will also be considered.

Also, even if an adequate design can be developed by choice of the best material and optimum values of the parameters b, h, and p of Equations 6 and 7, the conflicting requirements of a high pressure for low shear deflection and a low pressure for minimum creep still exists. However, it was noted that this situation could be eliminated if the shearing modulus were independent of the inflation pressure (as is the modulus of elasticity).

The AIRMAT flexible-foam antenna was considered first for the Class III ground-based tracking application, which is the most difficult of the three classes. A diameter of 40 feet was considered, with a maximum allowable rim deflection of ±0. 05 inch. Following conventional design practice, 40 percent of the total allowable deflection was allowed for manufacturing tolerances. The allowable structural deflection is then ±0. 03 inch. Of this deflection, ±0. 02 inch was arbitrarily used as an allowable shear deflection for a preliminary design of the AIRMAT, and bending deflection was then checked.

A preliminary analysis had previously shown that high wind loadings present a difficult problem with inflatable antennas; therefore, a radome was used to reduce the deflection problem. The live loads on the AIRMAT structure are the weight of the flexible foam, the weight of the r-f reflective surface, and a small aerodynamic pressure due to the inertia of the air mass inside the radome when the antenna is accelerated at the specified rate of 6 degrees/second^2. Since the dead weight of the AIRMAT is the greater part of the total load, an iteration process was required to determine the deflections.

The analysis considered the AIRMAT structure as a flat circular plate of uniform thickness. The resulting bending deflections are somewhat conservative, but the shear deflections are probably about the same for the paraboloid as for the flat plate.

The symmetrical loading condition was the first case considered. In this case, the antenna is oriented at zenith (see Figure 66). The shear and bending deflections at the rim (radius = a) for such a plate are given in Equations 5 and 6 respectively.

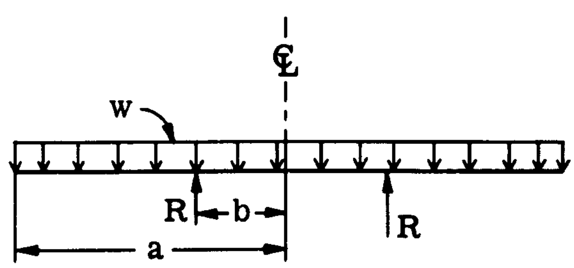

Figure 66. Flat Circular Plate Symmetrical Load Condition

A new fabrication technique that involves slanting the drop threads with respect to the middle plane of the AIRMAT not only makes G essentially independent of p but yields a much higher shear stiffness than ph as used in Equation 7. For the slanted drop thread construction, the shear stiffness $\left(\frac{dQ}{d\gamma}\right)$ is given by Equation 3 of Reference 15 as

$$\frac{dQ}{d\gamma} = ph + 2mnh\, A_d E_d \sin^2 \theta \cos \theta \tag{8}$$

where

$2n$ = the total number of drop threads per unit length in the direction that the drop threads are slanted,

m = number of rows of slanted drop threads per unit width,

A_d = cross-sectional area of one drop thread (in.^{2}),

E_d = modulus of elasticity of the drop thread material (psi),

and

θ = angle between the slanted drop thread and the normal to the AIRMAT surface.

It can be seen that the pressure term of Equation 8 can easily be made negligible compared to the second term by using metal drop threads which will also yield a high shearing stiffness.

An examination of load conditions and deflection criteria indicates that the deflection resulting from symmetrical loading conditions is less critical than the deflection due to antisymmetrical loads. A preliminary deflection analysis has been made for the antisymmetrical loading condition by considering a pie-shaped segment of the paraboloid as a flat plate of uniform depth. The results here are somewhat conservative, since the analysis neglects hoop stiffness; however, they should be quite adequate for the preliminary design studies for which they are intended.

The AIRMAT structure analyzed was made up of wire cover plies and slanted wire drop threads to provide maximum bending and shearing stiffnesses. The required wire diameters along with their respective minimum bend radii (and indication of foldability) were determined for various allowable rim deflections for both 40-foot diameter and 20-foot diameter reflectors.

The required wire diameter, as determined in this study, is based on the necessary cross-sectional area of the 96 pairs of radial warp wires in the 40- and 20-foot diameter dishes. For design purposes, since it is a cross-sectional area of wire that is required structurally, it is possible to vary the size of the wire relative to the number of radial wires as long as the cross-sectional area is held constant. The details covering the AIRMAT paraboloid structural approach are given in Appendix I.

4. Mechanical Design

The mechanical design has attempted to integrate the efforts of the electrical design and the structural analysis. Figure 67 shows an engineering layout for a 40-foot diameter maximum gain AIRMAT paraboloid antenna configuration. In this maximum gain configuration, the secondary hyperbolic reflector is supported by an inflatable cylinder and a series of 12 guy cables. The inflated cylinder functions to provide an axial pressure force on the secondary dish assembly, which is reacted by the 12 guy cables anchored to the outer edge of the rigid hub structure. Thus, the cylinder provides only an axial force, and the guy cables serve to orient the dish in focal distance, lateral position, and angular position. Additional cables are also provided and attached to the outer rim of the inflated dish to provide additional support to the secondary dish.

A rough adjustment of the Cassegrain reflector position is made by adjustment of the cable lengths, and a fine adjustment is then made by a separate Cassegrain adjustment as shown in Figure 67.

The feed horn is supported on an adjustable tripod arrangement inside the inflatable cylinder.

The AIRMAT reflector design uses hand woven radial rows of diagonal drop threads and is basically the same as described in Section IX, except for some improvement in the drop cord pattern. Figure 67, however, defines further the hub configuration and the related dish and feed horn support and secondary dish attachments.

The drop cord fitting is attached to the skin at the intersections of the concentric straps and the radial straps. The fitting is a swage attachment having a grommet that is bonded to the skin and the straps. The drop cord loop is pushed up through the fitting. A small pin is inserted through the loop to prevent any slippage, and the cable is then swaged to the fitting. A drop cord layout fixture is used to layout the exact length of the cords for a complete radial member.

A second paraboloid antenna configuration, which features a more packageable subdish and feed horn configuration and utilizes a larger secondary reflector with somewhat greater blockage effects, was also studied. The results of this study were used basically to define the paraboloid antenna model design.

C. LENTICULAR AIRMAT ANTENNA DESIGN

1. General

The lenticular AIRMAT antenna design was also considered in three basic areas of investigation: electrical design, structural design, and mechanical design.

The electrical design has considered the effects of phase angle variation and

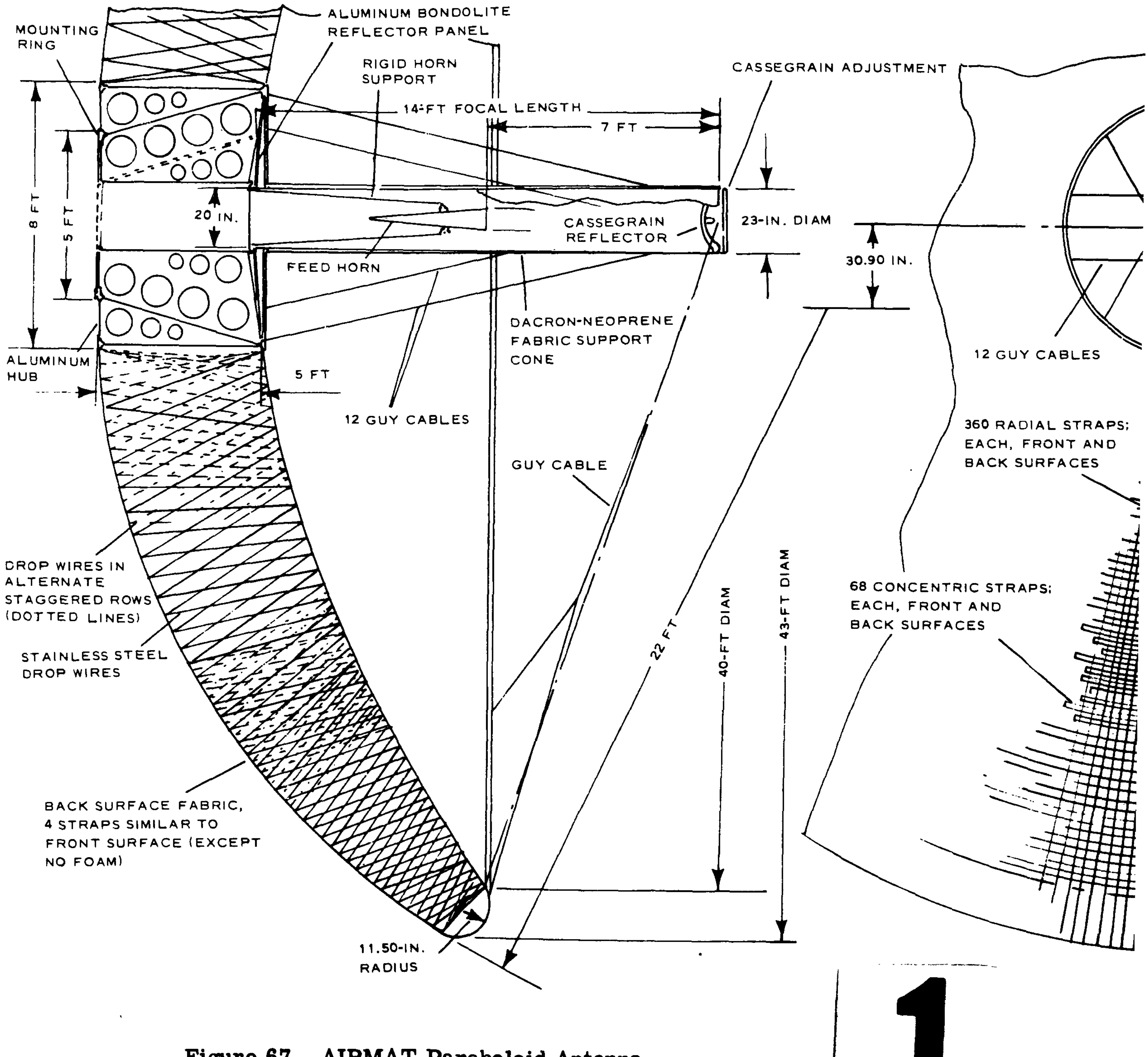

1

Figure 67. AIRMAT Paraboloid Antenna

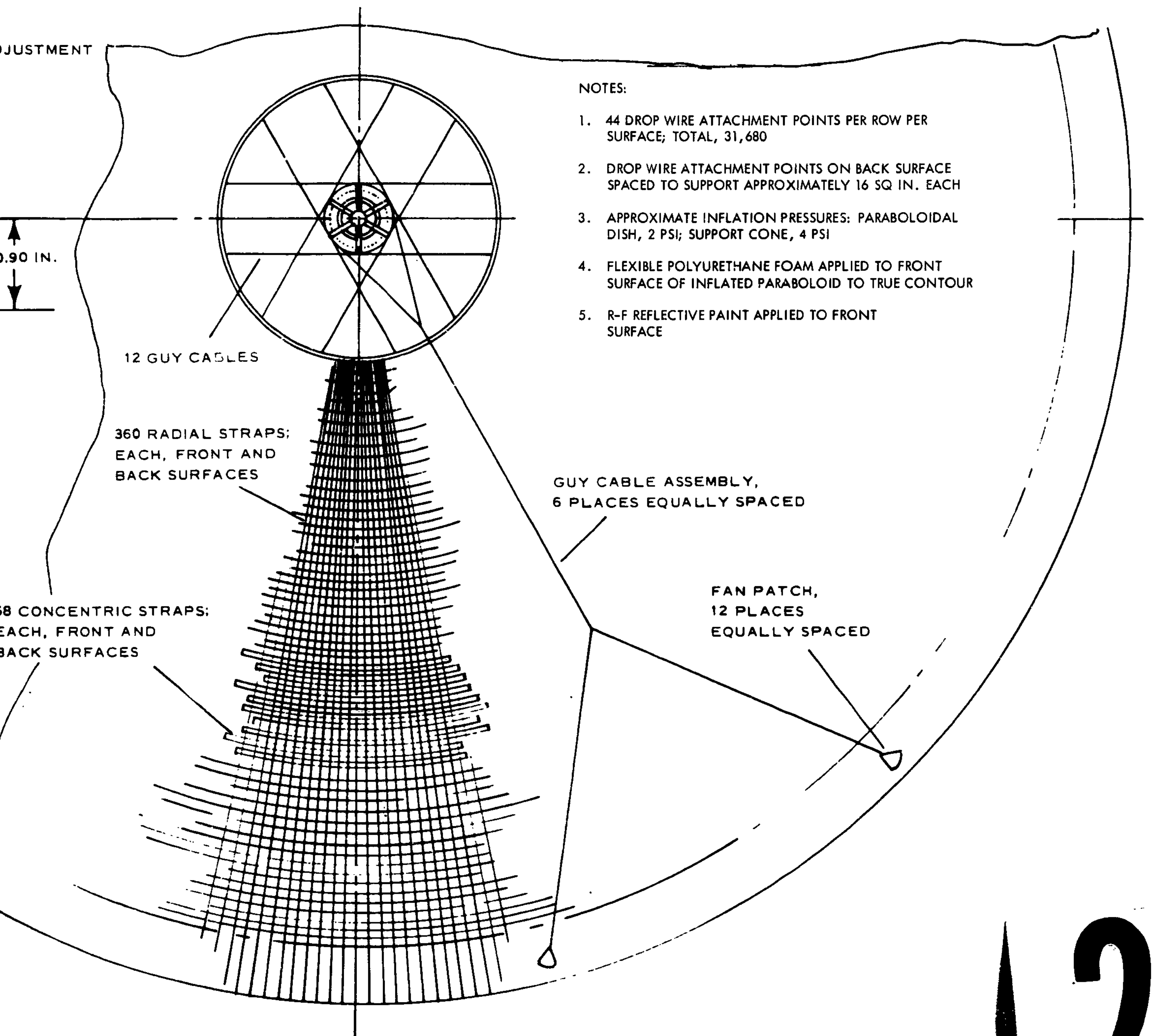

JUSTMENT
.90 IN.
12 GUY CABLES
360 RADIAL STRAPS; EACH, FRONT AND BACK SURFACES
8 CONCENTRIC STRAPS; EACH, FRONT AND BACK SURFACES
GUY CABLE ASSEMBLY, 6 PLACES EQUALLY SPACED
FAN PATCH, 12 PLACES EQUALLY SPACED
NOTES:
1. 44 DROP WIRE ATTACHMENT POINTS PER ROW PER SURFACE; TOTAL, 31,680
2. DROP WIRE ATTACHMENT POINTS ON BACK SURFACE SPACED TO SUPPORT APPROXIMATELY 16 SQ IN. EACH
3. APPROXIMATE INFLATION PRESSURES: PARABOLOIDAL DISH, 2 PSI; SUPPORT CONE, 4 PSI
4. FLEXIBLE POLYURETHANE FOAM APPLIED TO FRONT SURFACE OF INFLATED PARABOLOID TO TRUE CONTOUR
5. R-F REFLECTIVE PAINT APPLIED TO FRONT SURFACE

12

reduction of gain due to the drop threads and outer structure. Based on the initial assumptions and the resulting calculations, it appears that the use of this antenna may be limited to frequencies below 5000 mc. On the other hand, based on the latest structural design improvements, this frequency limitation appears to be less critical than indicated by the original assumptions.

The mechanical design also has not indicated any severe problem areas.

2. Electrical Design Considerations

The electrical design for the AIRMAT lenticular antenna was based on a 40-foot diameter Class III Cassegrain antenna.

An f/D (ratio of focal length to aperture size) of 0.35 was selected for the antenna design. With this f/D ratio (assuming that the antenna envelope is a symmetrical double-paraboloid lenticular shape), the focal point is thereby located very near the forward surface that is opposite the reflective surface of the antenna. This f/D selection eliminates the need of additional support structure for the secondary reflector which can then be supported by the opposite side of the lenticular structure.

The secondary reflector dish that was chosen for this design is 39.6 inches (3.3 feet) in diameter. This is greater than the 1.6-foot diameter required for the maximum gain configuration, as was used in the design of the AIRMAT paraboloid antenna.

The electrical characteristics for the AIRMAT paraboloid antenna, with 55 percent aperture efficiency, will have a gain of 59.5 db. Due to blockage, the gain of the lenticular AIRMAT antenna will be 59.38 db instead of the 59.5 without blockage. The degradation in side lobe level resulting from this increase in blockage might be considered negligible as compared to the benefit derived from the increased diameter of the secondary dish, for it permits the location of the feed horn within the hub, rather than in an extended position toward the secondary dish as was done in the case of the AIRMAT paraboloid (see Figure 67). This simplifies the feed horn support and provides better packageability.

The lenticular AIRMAT antenna electrical analysis has been conducted with the following assumptions:

(1) The dielectric constant of the drop threads is 6.1.

(2) The drop threads are uniformly distributed in the lenticular AIRMAT antenna volume.

(3) The volume ratio of drop threads to enclosed air volume in the antenna is 0.000965.

(4) The opaque surface will have a negligible effect on the electrical parameters.

In evaluating the antenna concept in support of continued mechanical development, the aperture phase distribution appears to be the most critical problem area thus far encountered.

The dielectric constant of the drop threads is 6.1, and the drop threads are considered uniformly distributed throughout the enclosed antenna volume. This allows the use of the following formula to determine a fictitious composite dielectric constant:

$$\begin{aligned}\epsilon_c &= 1 + \frac{\text{volume of dielectric}}{\text{total volume}} (\epsilon_0 - 1) \\ &= 1 + 0.00097\,(6.1 - 1) \\ &= 1.0049.\end{aligned}$$

This new dielectric constant can be used to determine the velocity of the energy propagating through the drop threads. The collimated wave that leaves the main reflector surface must pass through the drop cord structure before entering the free space (air) medium. If all other effects are neglected (reflections etc), the predominant effect will be to change the wave's phase from that of a homogeneous plane wave. This phase error will vary radially across the aperture. The maximum permissible variation should be less than 1/16 wave length to ensure negligible effects on the antenna's electrical characteristics.

As shown in Figure 68, a ray of energy travels along paths from the subdish toward the reflector, where they are reflected back parallel to the axis of the feed. From elementary geometry, the phase of this energy in a plane perpendicular to the direction of propagation will be constant. The rays of energy in the lenticular AIRMAT antenna will travel the same path, but due to the more dense dielectric, the velocity of propagation will be reduced. However, each ray has been reduced in velocity by the same amount. After these rays leave the "plane wave front" in Figure 68, their velocities change as soon as the rays pass through the front surface of the antenna. Their phases are modified depending on the length of travel in the drop-cord medium.

To determine the maximum phase deviation between this phase front and a plane wave, phase difference between a ray at the center of the reflector and a ray at the edge of the reflector is determined.

Since the propagation velocity in any lossless medium is

$$\frac{\text{velocity of light}}{(\text{dielectric constant})^{1/2}},$$

and the wave length at 10 gcs in free space

$$\lambda_0 = \frac{984}{f(\text{mc/sec})} = \frac{984}{10000}\ \text{ft} = 0.0984\ \text{ft},$$

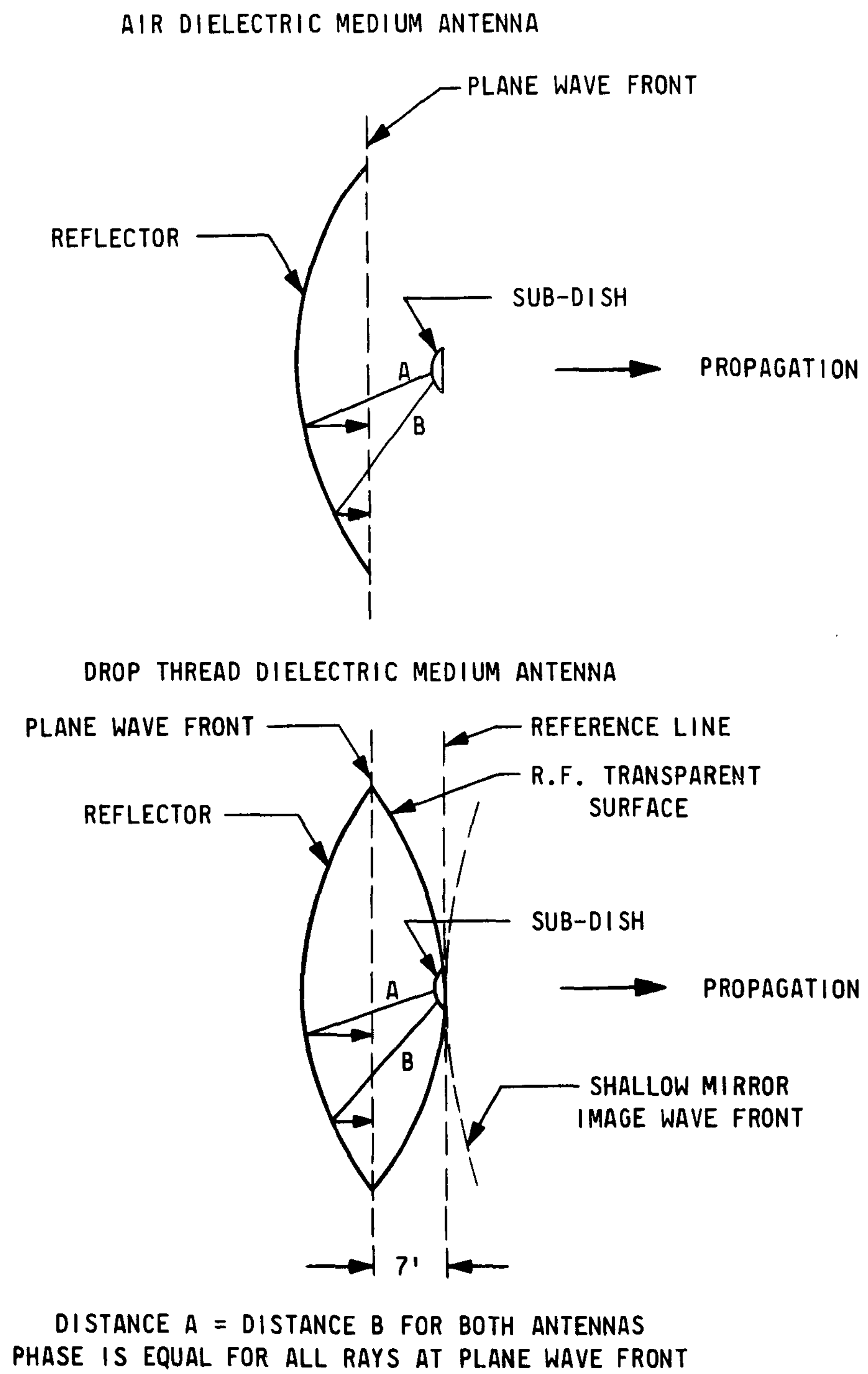

Figure 68. Schematic Wave Front Comparison between Air and Drop-Thread Dielectric Medium

then the wave length in the dielectric is

$$\lambda_{\theta} = \frac{0.0984 \text{ ft}}{\sqrt{\epsilon_c}}$$

$$= \frac{0.0984 \text{ ft}}{\sqrt{1.0049}}$$

$$= \frac{0.0984}{1.00245} \text{ ft} .$$

The differential phase, $\Delta\phi$, occurs over a distance of 7 feet:

$$\Delta\phi = \frac{7 \text{ ft}}{\left(\frac{0.0984}{1.00245}\right) \text{ ft}} - \frac{7 \text{ ft}}{0.0984 \text{ ft}} = 0.174 \text{ wave length.}$$

Thus, as previously stated, the phase variation should be less than 1/16 wavelength. This value would cause appreciable degradation of the side lobe level with slight degradation of gain for a frequency of 10,000 mc. At a frequency lower than 5000 mc the phase variation will be less than 1/16 wave length and amount to only slight degradation.

The amount of degradation depends upon the magnitude of the gain and side lobes. If the side lobe level had been -26 db, the new side lobe level would be approximately -23 db, a 3-db increase in side lobe level. This example is a result of interpolating the information from a normalized antenna radiation pattern and may contain some inaccuracies. Had the ideal side lobe level been lower, the resultant side lobe level with this phase error would remain at approximately -23 db. The gain would be slightly decreased, but in all cases would be less than 1 db.

Moreover, based on the radial beam concept of slanted drop cords, the reflected microwave energy travels parallel to the radial beams rather than through a homogeneous dielectric medium. In this case, the phase shift variation is not as much of a problem, since only a small percentage of the energy will be affected by the drop cords. This fact may again allow an increase in the frequency range, although r-f testing will be the best indication of the true performance of this antenna concept.

3. Structural Considerations

As in the case of the AIRMAT paraboloid antenna, several simplifying assumptions have been made to reduce the over-all effort and for use in expediting the design of this concept. On the other hand, the design criteria has been established to meet the more severe deflection requirements of the 40-foot diameter, Class III antenna. Also, the assumptions made for the analysis in most cases are conservative so that any problem areas can be readily established.

The structural analysis is based on a circular flat plate of constant thickness with the pattern drop threads being constant in either direction. In the actual antenna where the slant drop threads are in radial rows terminated at the hub, the equivalent of this condition can be closely approximated by proper spacing and staggering of the drop thread attachment points to create equal pressure areas.

Only the symmetrical loading condition was investigated. In this case, the applied forces are from the static weight of the antenna with the antenna in the zenith attitude. For this condition, it has been shown that the deflections are well within the required limits. With this analysis and with the additional information that can be extrapolated from the AIRMAT paraboloid analysis, it has been adequate for the additional preliminary design studies.

4. Mechanical Design

The mechanical design of the full-scale Lenticular antenna, shown in preliminary form in Figure 69, has attempted to integrate the electrical design considerations and the structural analysis. Neoprene-coated fiberglass fabric and fiberglass drop cords were selected for the structure to obtain maximum stability and rigidity.

The configuration is essentially the same as previously described, with the exception of the secondary dish support. The rigid fiberglass cylinder secondary dish support has been eliminated because of the r-f transmission problems it would create. The dish is supported in an adjustable manner from a rigid circular BONDOLITE plate mounted directly to and supported by the envelope fabric. The drop cords, which support the circular plate to the outer rim of the rigid hub structure, are arranged to give rigidity to the secondary dish support in the axial and lateral directions and in angular position.

The feed horn is mounted within the hub with its aperture at the apex of the paraboloid. A flexible pressure seal is provided between the horn aperture and the hub structure to allow for horn adjustment. The hub structure shown is a tubular-space frame-type structure with a 5-foot diameter mounting ring for mounting to the pedestal. Inflation pressure is retained at the hub by the rigid reflector panel in the outer portion and by an aluminum bulkhead attached to the feed horn support tube.

Figure 69 shows the arrangement of the drop cords, which are arranged in radial rows, each row terminating at the hub area. The drop cord attachment points are carefully spaced in the rows and staggered from row to row to achieve approximately equal pressure loading on all cords and to achieve approximately the same slant angle on all cords. The attachment of the drop cords to the fabric envelope is made by lacing the cords into a fabric "T" section which forms a part of the seam between gores. A fabric "T" is installed for each row of drop cords. The exact length of each drop cord is predetermined by use of a layout fixture onto which each radial row of cords is laced before assembly into the envelope.

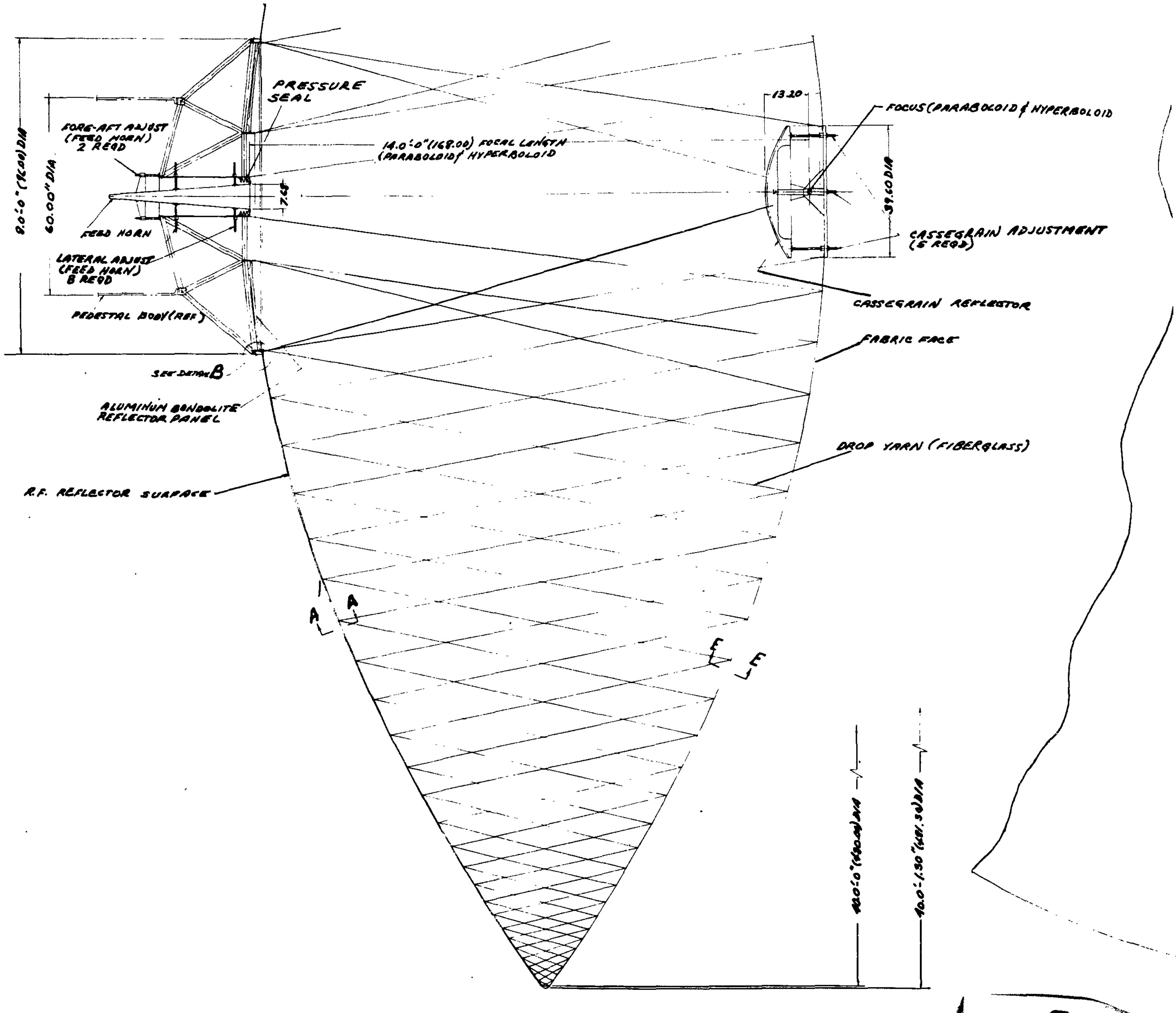

Figure 69. Lenticular AIRMAT Antenna (Sheet 1)

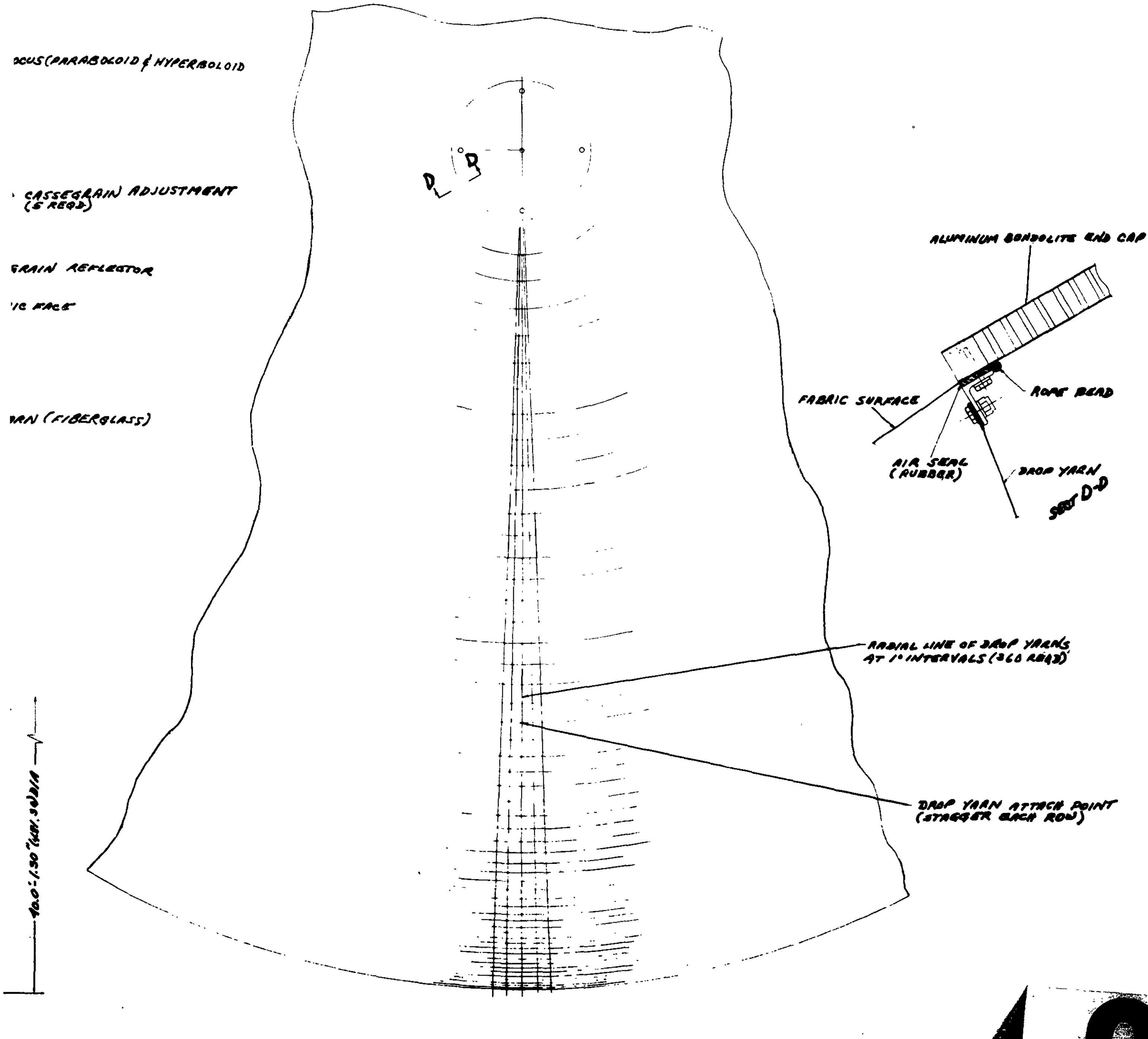
OCUS (PARABOLOID & HYPERBOLOID
CASSEGRAIN ADJUSTMENT (5 REQD)
GRAIN REFLECTOR
IC FACE
ARN (FIBERGLASS)
ALUMINUM BONDOLITE END CAP
ROPE BEAD
FABRIC SURFACE
AIR SEAL (RUBBER)
DROP YARN
SECT D-D
RADIAL LINE OF DROP YARNS AT 1° INTERVALS (360 REQD)
DROP YARN ATTACH POINT (STAGGER EACH ROW)

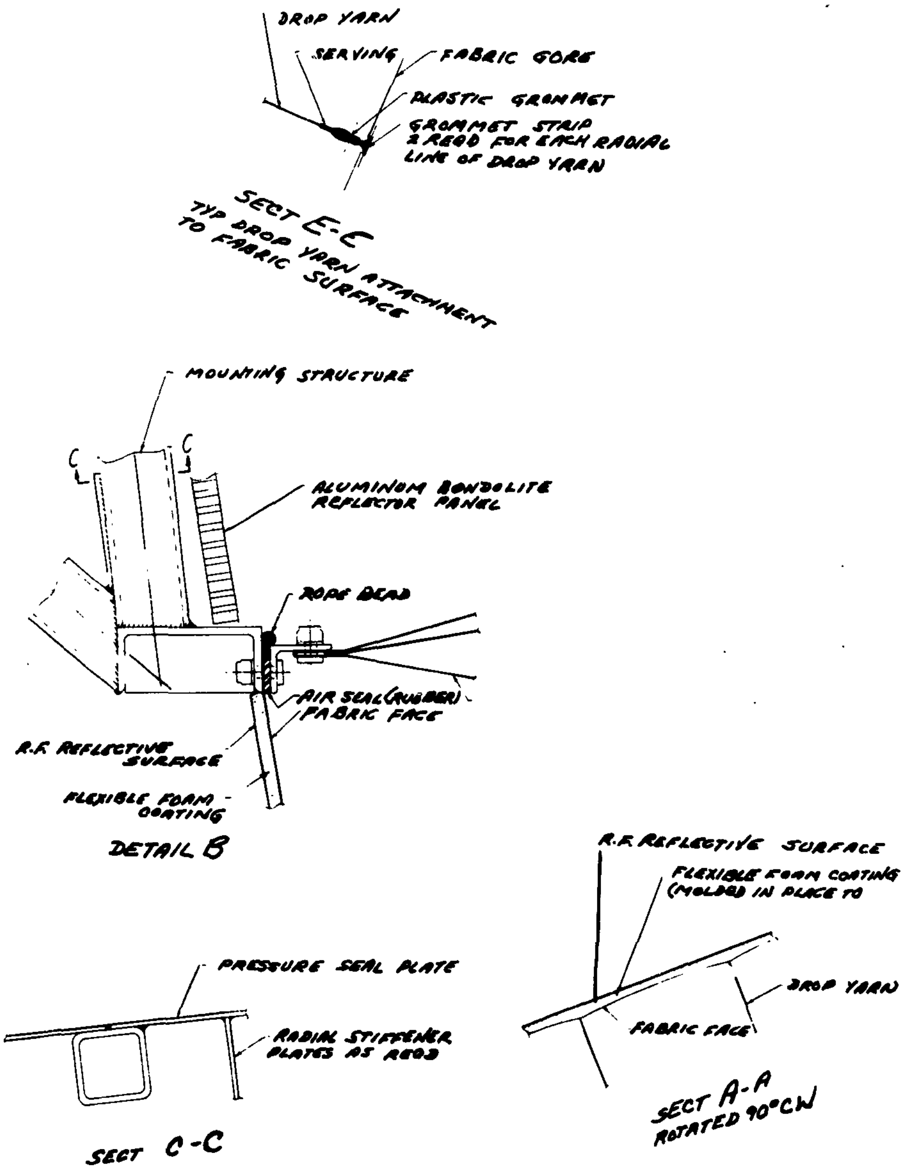

Figure 69. Lenticular AIRMAT Antenna (Sheet 2)

D. ADVANCED INFLATABLE STRUCTURE DESIGN APPROACH

In previous reports of this study, methods and techniques of fabricating the AIRMAT antennas have been discussed. The evolution of the concept has progressed from constant thickness normal drop-thread AIRMAT to slanted drop-cord AIRMAT parabolic dishes having single-contour sections with a tapered cross-sectional thickness. However, although each design feature represents a logical advance in the state-of-the-art in loom-weaving of AIRMAT, each of these features would represent development of new loom-weaving techniques. For this reason, most of the suggested fabrication techniques have been based on hand-weaving the slanted drop-thread antenna dishes. These slanted drop-thread arrangements provide a satisfactory means of achieving an AIRMAT structure which, as determined by the preliminary analysis, will maintain the antenna contour within the desired limits. The fabrication of these structures can be accomplished without an excessive amount of tooling cost, and the over-all fabrication cost of the antennas does not appear to be excessive. However, in the interest of improving the design still further, and with the possibility of making a reduction in fabrication costs with comparable weight and packaging bulk, the following new structural concept evolved as a possible improvement over the previous designs.

The improvement suggested for the antenna designs is to replace the rows of relatively widely spaced slanted drop threads with continuous shear webs having threads spaced closely together. This new inflatable structure concept appeared to offer such good possibilities that it was used for the construction of the models that will be discussed in Section XI. The main difference between the prototype antennas and the models is that the fabrics required for the prototype antennas would be a stiffer material to provide better rigidity and dimensional control.

The concept features radial contoured webs that would be fabricated such that the webs would function in the same manner as the radial rows of slanted drop threads.

Thus, the web becomes a two-directional cloth with the direction of the two sets of threads arranged at an optimum angle with respect to each other.

Attachment of the webs to the surface fabric is accomplished by use of a woven fabric "Y" member which, in effect, makes a "foot" on the web to attach to the surface fabric (see Figure 70). Heavy cords are integrated with "Y" member at its intersection to become the radial tension member (or cap) of the radial beam structure. This member takes the place of the radial straps in the previous designs.

Some basic features of the continuous-web concept are as follows:

(1) It appears to function in all respects as well as any previous concept.

(2) The continuous attachment of the web to the surface fabric eliminates the stress concentrations that occur in the previous design at the drop cord attachment points. In addition, the concentric straps are no longer required to transfer the drop cord load to the fabric.

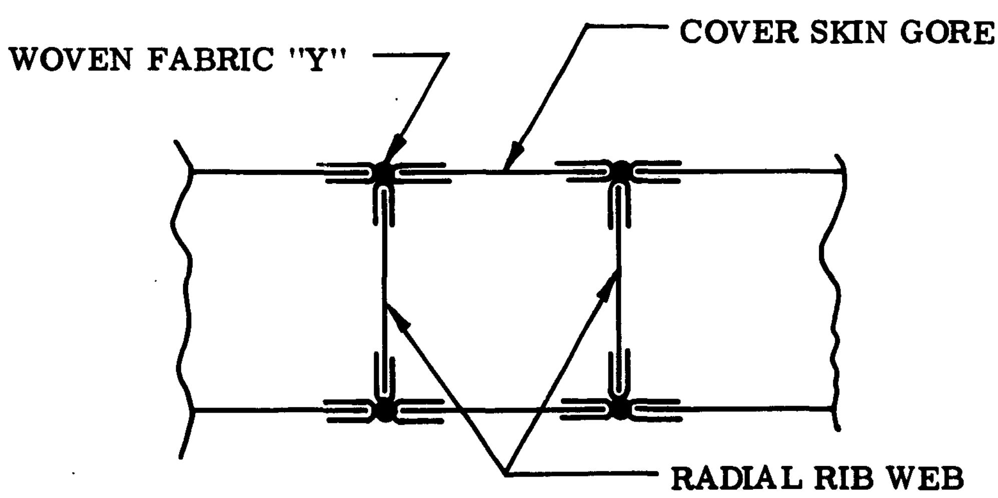

Figure 70. Schematic of Inflatable Web Structure

(3) Fabrication is simplified for several reasons. They include:
   (a) The concept uses a web patterned from fabric instead of hand-weaving the slanted drop cords.
   (b) Continuous bonding of web instead of individual point attachments.
   (c) No need to handle large portions of surface envelope as in previous concepts, since the narrow surface gores are progressively attached to the webs, requiring a minimum of tooling and fabric handling.

(4) Because of the elimination of the concentric straps, the weight would likely be decreased and the package bulk may also be improved.

In Section XI, which covers the antenna models, this concept will be discussed further. For the purpose of the models, the fabric-web concept offered not only structural benefits over previous AIRMAT concept but also an economic advantage. In addition, the structural and deflection analysis on the slanted drop cord AIRMAT is still valid for the fabric-web concept, except for the fact that it is now somewhat conservative.

Before attempting to design and build the two scale models, a simpler model was designed and built to determine the most economical model fabrication techniques and to develop the technique for use in the 5-foot diameter model. This model, shown in Figures 71 and 72, simulates a panel of the AIRMAT paraboloid. The only differences are that it has a single-curvature surface and the fabric webs, which are used instead of diagonal drop threads, are arranged in parallel rows, rather than radiating from a central hub. The most important function that this model served was the development of a means of simulating the radial rows of slanted drop threads in a way that would be most economical to build and yet be satisfactory in performing the other functions of the model. Methods of slanted drop thread installation similar to the full-scale design were investigated, and

Figure 71. Inflatable Shear Web Structure (Edge View)

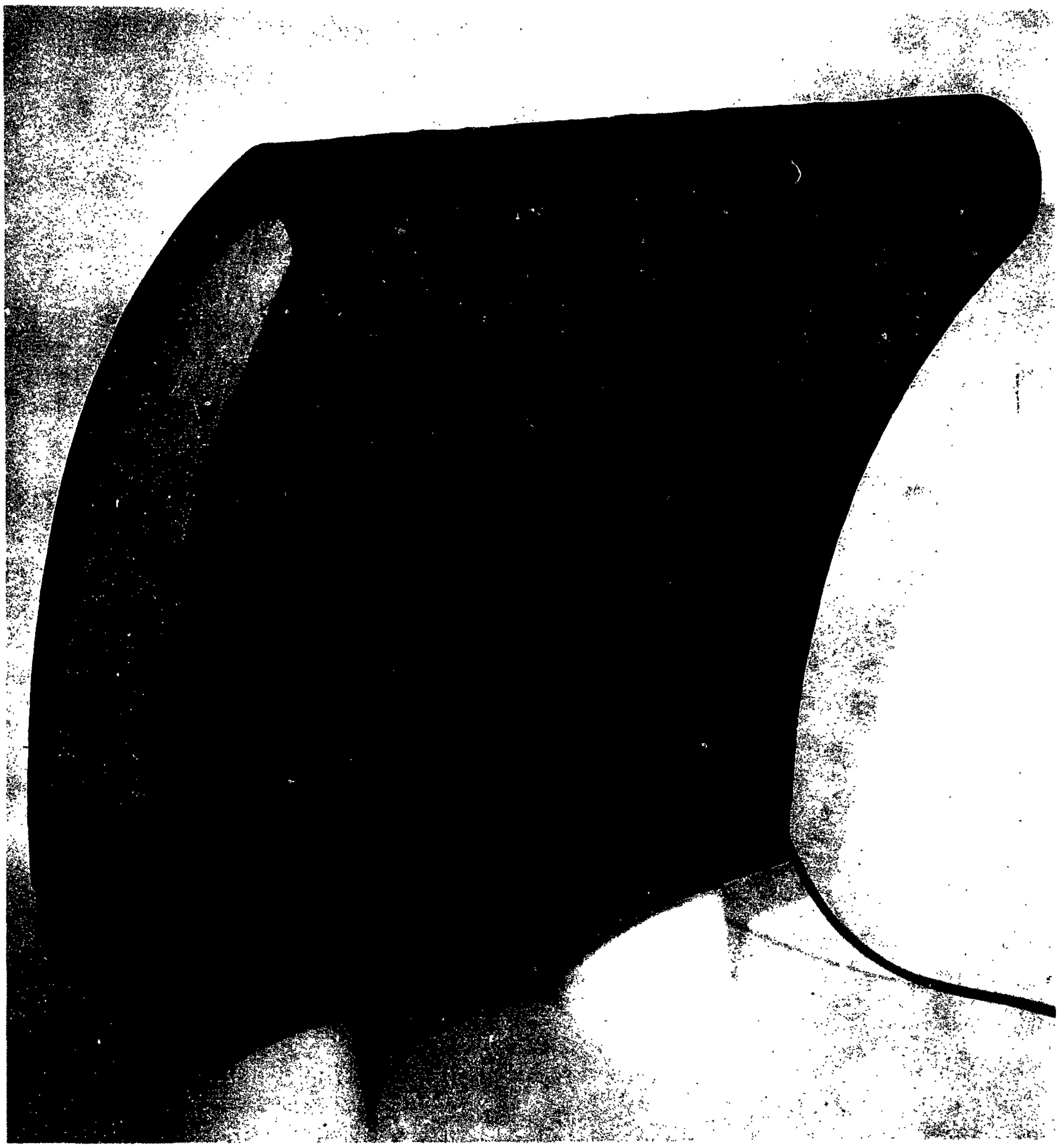

Figure 72. Inflatable Shear Web Structure (3/4 Front View)

workable techniques were conceived. However, because of the small size of the model, it was decided that the fabric web panel construction would be easier and more economical to build than the slant drop-thread arrangement. Good similitude of the full-scale item is difficult to achieve in any scale model of a fabric structure, and it was recognized that the fabric-web construction would create a greater penalty in weight and bulk, but these penalties were considered to be outweighed by the economy of construction.

Figures 73 and 74 show different views of the model during fabrication. The success of this model was quite evident after completion. The surface contour of the model was held very close to the planned contour, and no noticeable contour deviations showed up when the internal pressure was varied.

E. REFLECTOR CONTOUR DEVELOPMENT

1. General

The reflective contour development consisted mainly of investigating various flexible foams and foaming techniques as well as development of an r-f reflective surface. Goodyear Aerospace development funds were used for a large percentage of this investigation, which will also be applicable to other studies.

This portion of the program extended through the third and fourth quarters and resulted in the successful application of foam surfaces and reflective surfaces to the five-foot inflatable antenna models.

2. Foam Contour Development

The first foam tests were relatively simple and were made on small flat AIRMAT samples, 18 x 18 inches square and 1-inch thick, for the purpose of observing the physical characteristics of both latex and polyurethane foams during the foaming process and to examine different foaming techniques. The tests were also intended to determine foam adherance to AIRMAT and its resistance to permanent creasing when folded.

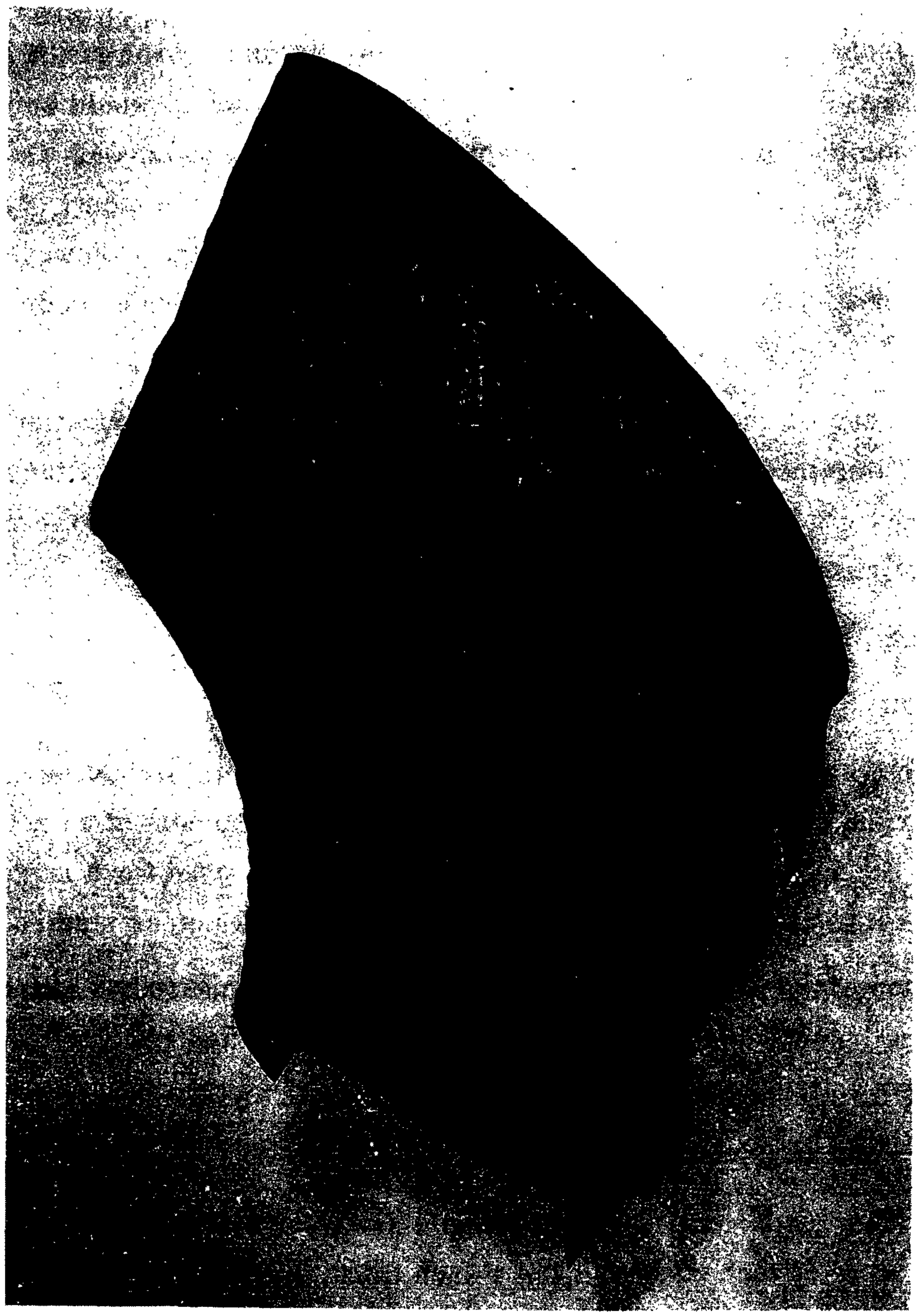

Figure 73. View of Model Hub End Showing Fabric Webs (before Hub Was Attached)

Figure 74. Reverse Side of Model during Fabrication (with Contour Forms in Place)

In the latex tests, the foam was swept over the panels in depths varying from 1/8 to 1/2 inch. On some panels, an adhesive was used to check the difference in adhesion. The foam was allowed to gel for several minutes, a glass plate was placed on the foam surface, and a load was applied to compress the uncured foam. The test panel was then cured at 212^{o}F. Figure 75 is a photo of some of the samples.

These samples exhibited the following characteristics:

(1) Excellent crease resistance after repeated folding.
(2) Good adherence to the AIRMAT panel.
(3) Surface porosity and open-celled foam structure.
(4) Tendency of surface to form meniscus during gel.

The polyurethane samples were made by pouring the liquid mixture onto the mold surface covered by a polyethylene sheet used as a separator. The AIRMAT and mold surface were then held in position to resist the pressure caused by the foam as it expanded. The polyurethane had the following characteristics:

(1) Good adherence to the AIRMAT.
(2) It generates a significant pressure while expanding.
(3) There was a surface skin; however, some gas bubbles were formed and damaged the surface locally.

In comparing the two types of foams, the following physical characteristics were noted:

(1) The latex foams exhibit better crease resistance. It is anticipated that the difference will be more pronounced at lower temperatures.

(2) Polyurethane foam has a closed surface equal in finish to the surface of the mold. However, it has the tendency to form gas bubbles, which cause local damage.

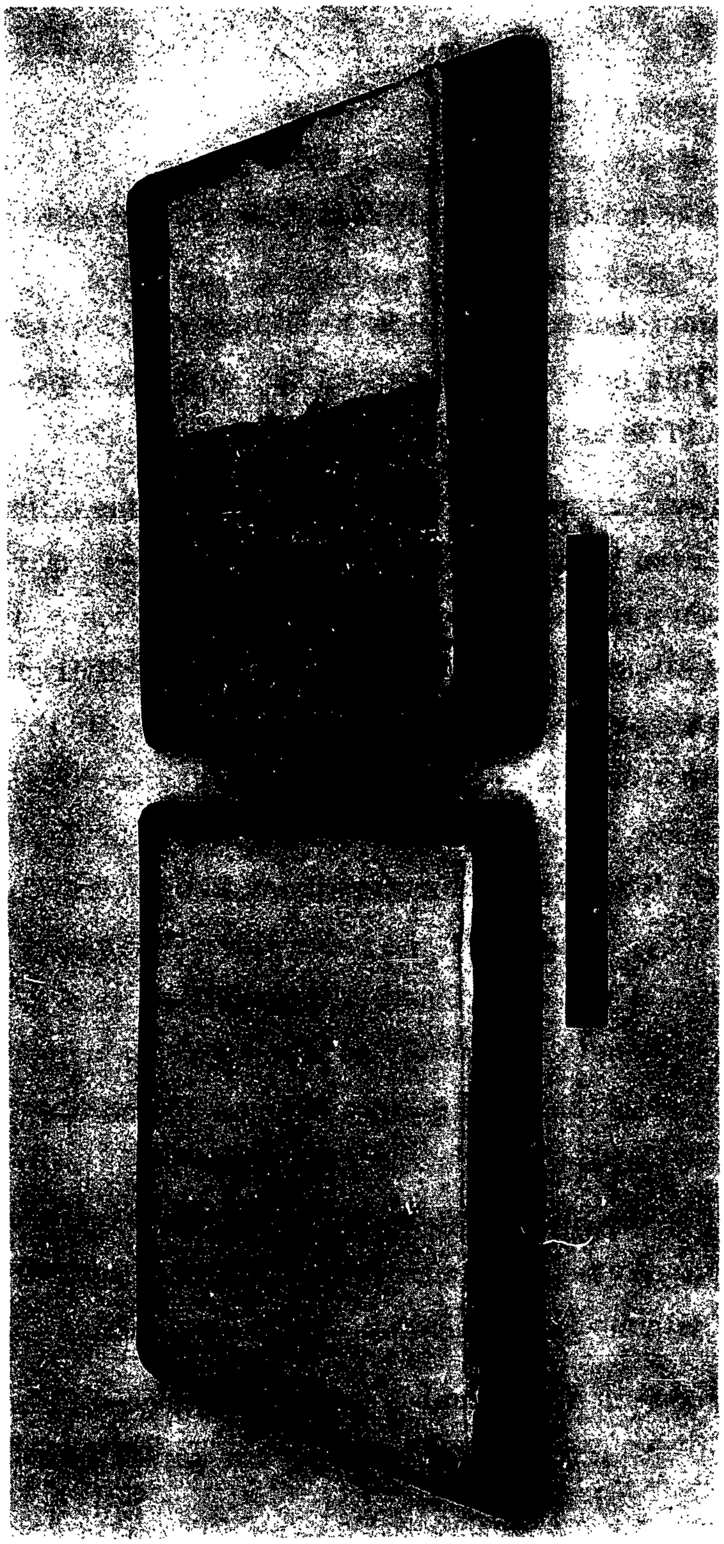

Figure 75. Flat AIRMAT Samples for Foamed Surface Development

(3) Both foams can be cured at ambient temperatures or in an oven. In either case, the polyurethane cures in a much shorter time, not allowing as much flexibility in the foaming operation.

(4) The cured weight of polyurethane foam is about 1/6 that of latex. This fact may not be too significant when compared to the over-all weight of the antenna.

(5) Polyurethane foam tends to blow itself out when forced to enter small cavities. This may be a consideration, since the optimum foam cross section would be as thin as possible.

One discrepancy was evident in some of the samples. Some of the surface contours were irregular even though molded against flat plates. This was obviously due to the fact that, when the mold is pressed against the foam, the AIRMAT panels were deflected slightly. Then, after the mold is withdrawn, the panel returns to its natural shape, forming the irregular surface in the thin foam surface. To preclude this situation, two methods were devised to eliminate the warpage in the thin panels. One method is the use of a granular backup material in a shallow container. The granular material would be agitated such that it would conform to the irregularities on the underside of the panel and thus be able to support it uniformly. A second method is the application of a rigid polyurethane foam to the backs of the panels, which would also serve to support it uniformly when pressure is applied by the mold plate. Figures 76 and 77 show sample surfaces formed by each of these methods and the improvement over the preliminary samples. It should be noted that these measures are necessary only when using the thin test panels and may be eliminated with thicker structural panels such as those of the five-foot demonstration models, which have ample inherent stiffness.

At this stage of the program, the samples were becoming sufficiently flat to require a sensitive, accurate method of measuring the surface for comparison with

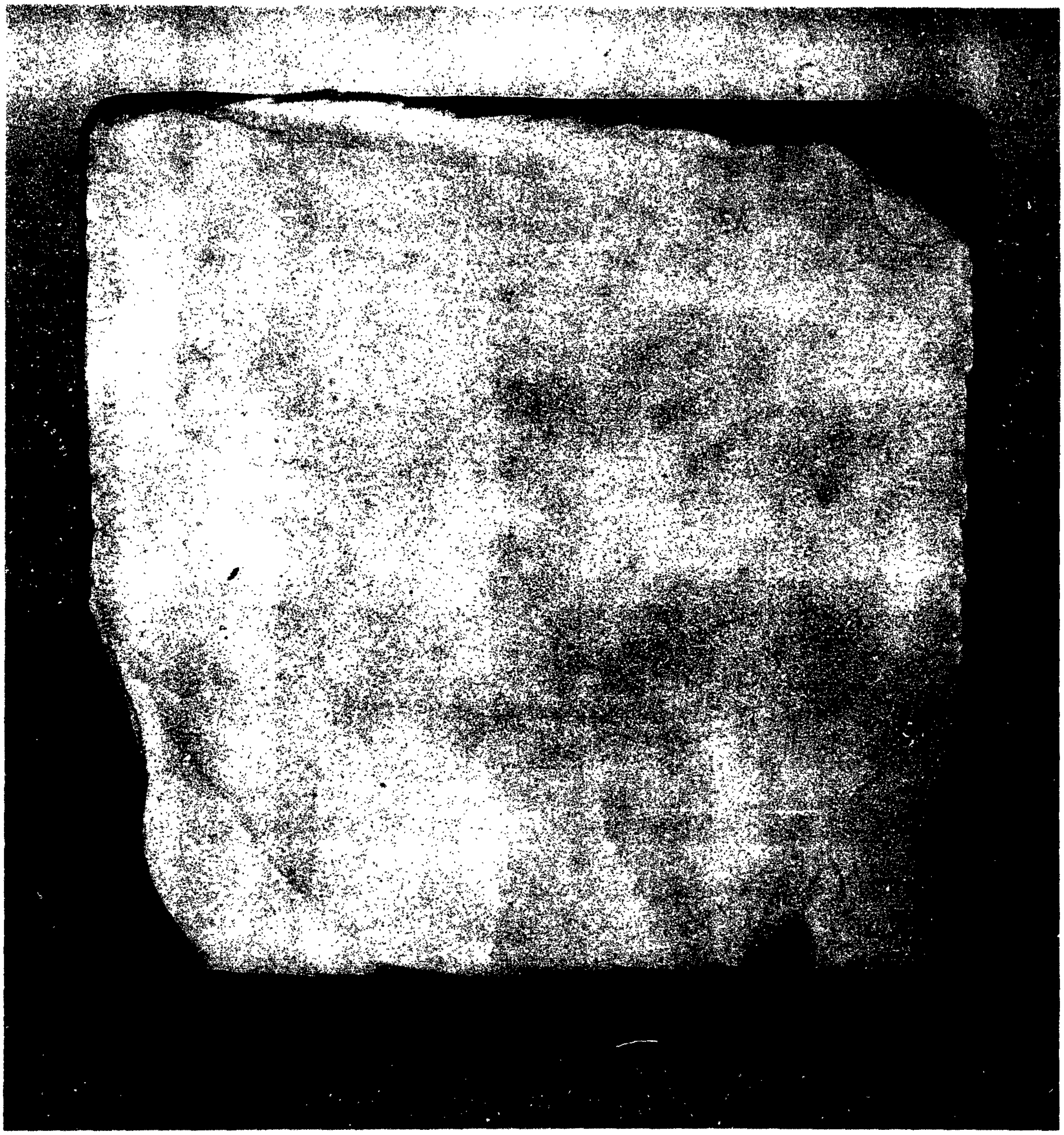

Figure 76. Foamed Surface of AIRMAT Panel (Granulated Backup Support)

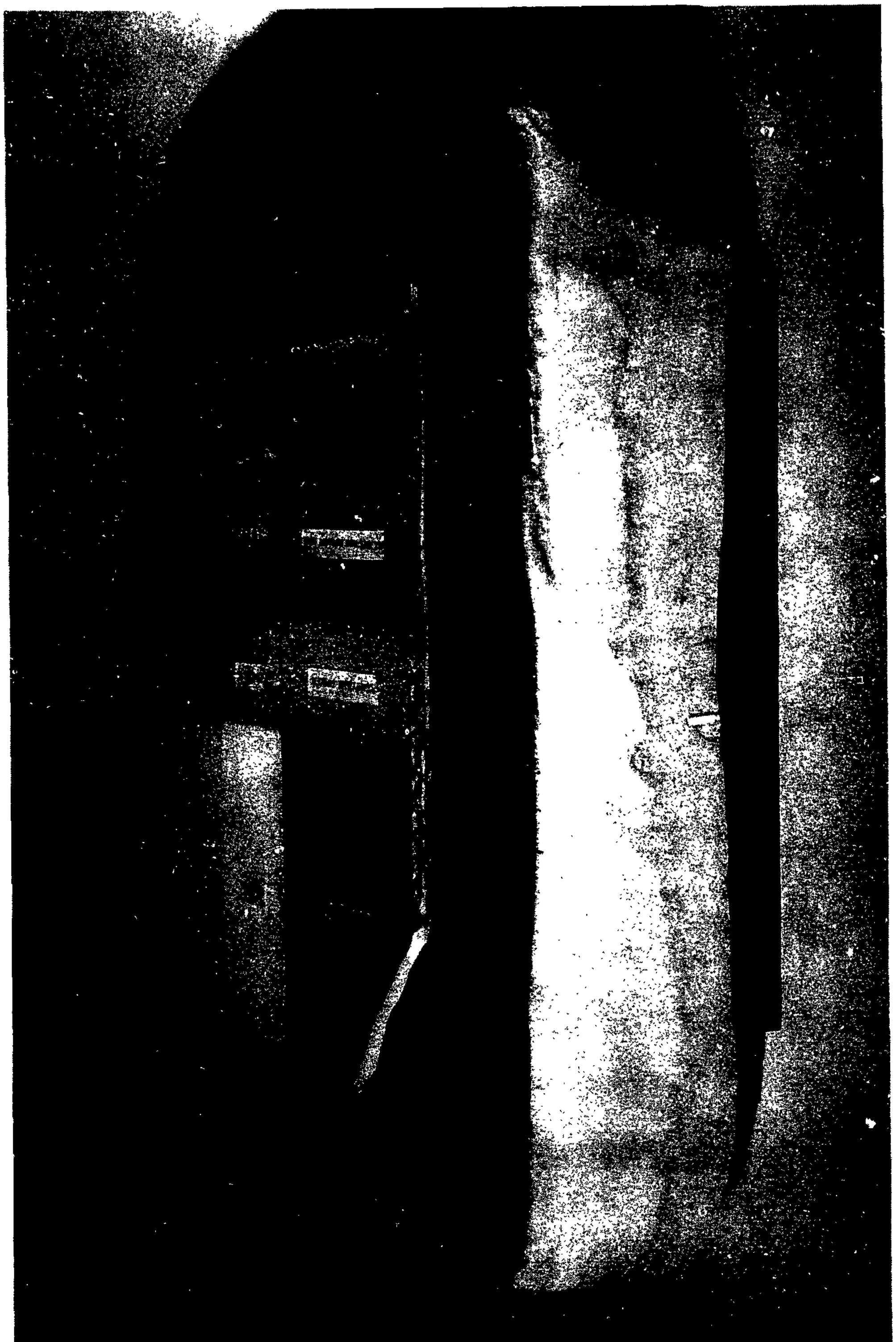

Figure 77. Foamed Surface of AIRMAT Panel (Rigid Polyurethane Foam Backup Support)

the mold. Since the sample surfaces were flat, it was decided to use a dial indicator having a 1.25-inch diameter disc over the end of the probe to distribute the load. With this method, the mold is indexed at various points with a grease pencil so that the foam will be indexed at the same points when it picks up the grease. Both the mold and the foam surface are then measured, providing the necessary information to determine how accurately the mold surface was duplicated. Figure 78 shows a foam surface sample indexed as described. The numbers, however, indicate actual dial indicator readings and not contour accuracy as compared to the same points on the mold. The contour accuracy in this case is ±0.0017 in.

In considering contour accuracy, it can be seen that the total amount of error would result from discrepancies in the foam layer itself plus any deformation in the AIRMAT panels that could not be eliminated by the methods mentioned. To study the relative proportion attributed to each cause, several tests were made with natural and synthetic latex foams and polyurethane foam while substituting a rigid metal plate for the AIRMAT panel. This approach was used because it permits isolation of the deformation that occurs in the foam layer cross section. The most successful attempts were made with two samples of natural latex foam. One was applied directly against the mold; the other was applied against a mold plate covered with a prestretched polyethylene film. These samples conformed to the mold contour to within 0.0017 inch maximum, and both displayed excellent surface characteristics free from flaws. This proves to be an advantage because it indicates that surface accuracy requirements will not limit the choice of reflective surface application with respect to whether a film is used or not. Two samples of synthetic latex foam have also been made using a similar technique and show a maximum variation from the mold surface of 0.0055 inch. Surface characteristics of this sample were excellent and free from flaws.

Several samples of flexible polyurethane film were also made. Their surfaces

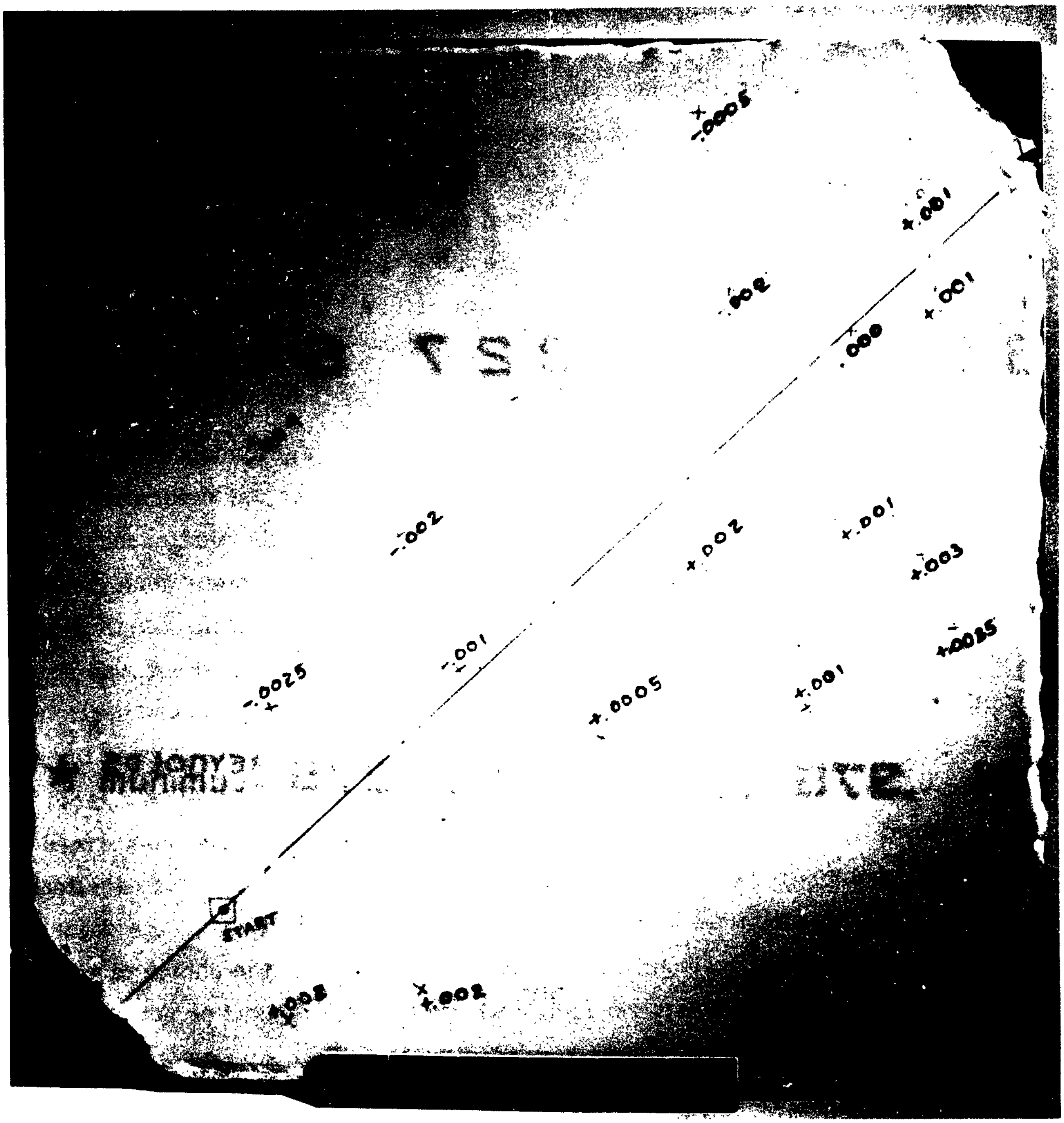

Figure 78. Flat Surface of Flexible Foam Measured to ±0.0005 Inch

displayed a wider variation of surface characteristics and dial indicator readings than the latex samples, although all the polyurethane samples were made under the same conditions. The dial indicator readings gave values that ranged between 0.0024-inch TIR for the one best sample to 0.0040-inch TIR for the one having obvious surface irregularities.

The following summarizes the results of this series of tests of foam-covered rigid plates to determine ability to duplicate the mold contour. The values are in inches and represent the amount of discrepancy from this contour. Obviously, the smaller the value, the better the sample conforms to the mold contour.

Natural latex foam	±0.0017
Synthetic latex foam	±0.0055
Polyurethane foam	±0.0024 to ±0.040*

* The polyurethane samples displayed a wider variation of surface characteristics and dial indicator readings than the latex samples, although all the polyurethane samples were made under the same conditions.

An additional sample was made with the synthetic foam applied to a thin flat AIRMAT panel that had previously been rigidized with a rigid polyurethane foam backup as previously described. The purpose of this test was to provide dial indicator readings on an actual foam-covered AIRMAT sample. In this case, the readings showed a maximum variation from the mold surface of only 0.0067 inch, which is comparable to the contour duplication of the foamed metal plates.

F. R-F REFLECTIVE COATING

Development of the r-f reflective coating, as in the case of the surface contour, was performed mainly in the third and fourth quarters. During the first two quarters, many approaches to the application of the coating were generated and evaluated. One of these included the use of a fine 5-mil wire mesh screen molded into the flexible surface or the use of a metal film laminate preset to the proper contour to be picked up by the foam during molding. Several methods for using an r-f reflective paint were also considered. One of these was to spray the paint directly on the mold after an application of separator and then foam on this surface. The intent in this case is that the foam will then adhere and pick up this coating when it is removed from the mold. A second paint method, which is by far the simplest method, is to spray the coating on the contour surface after molding. Combinations of these methods were also considered, such as spraying an r-f reflective paint on a film before or after molding process or spraying the surface contour and then applying the film.

Some of the above concepts were eliminated just from studying the various advantages and disadvantages related to them. Others were eliminated by preliminary testing, and since funds were limited on this program, others were passed over in lieu of the simpler more straightforward approaches.

It was found in some initial testing that available r-f reflective paints on the market were not flexible and did not adhere to some films. Also, several films, of which Mylar is a good example, had inherent stresses that had to be eliminated by heating before the foaming operation to preclude any warping of the surface during the foam cure.

One simple approach that appeared to have good merit was to spray paint the antenna surface with an r-f reflective paint. Since one very flexible vinyl-based paint was available on the commercial market, this product was tried. This paint had very good reflective characteristics, but tests showed that the latex foam on which the vinyl-based paint was applied removed the plasticizer from the paint. Consequently, the paint became brittle after drying, cracked when the foam samples were flexed, and the r-f reflectivity of the painted samples was significantly reduced.

In an effort to eliminate this difficulty, several combinations of flexible polyurethane and VITEL* film sprays were used as an undercoating to prevent the loss of plasticizer from the reflective paint. Also, the merits of polyurethane and Vitel spray films as an environmental protective overcoating were investigated. The film overcoat and undercoat also provide additional tensile strength to the r-f paint, which in turn assists in preventing cracking or permanent deformation that may be encountered in tight folds during packaging. Figure 79 shows a typical coating test sample. The coatings labeled in each section of the photgraph are listed in the order of their application.

The combination that gave the best results was the one using the polyurethane spray for both the undercoat and overcoat. After deforming the surfaces of all the samples, this particular combination returned to its original condition in the shortest time with no permanent deformation apparent.

Another approach that was tested was the development of an r-f reflective paint that would be compatible with the latex foam surface of the inflatable antenna models. One possible solution to this problem would be to use a latex vehicle rather than a vinyl-based vehicle.

In this case, obviously, the latex foam will not draw the plasticizer from the reflective paint, since the latex paint and the latex foam are more compatible. Consequently, the latex-based reflective paint should remain flexible when the antenna is folded and packaged.

Many latex samples were made in varying combinations of vehicle formulation and proportions of silver powder. Each successive set of test samples showed further improvement, until the later test samples began to demonstrate the required flexibility and strength. These samples were then given an actual r-f reflective test at 3.0 and 9.0 kmc. Figure 80 is a schematic of the test setup.

*TM, Goodyear Tire and Rubber Co., Akron, Ohio

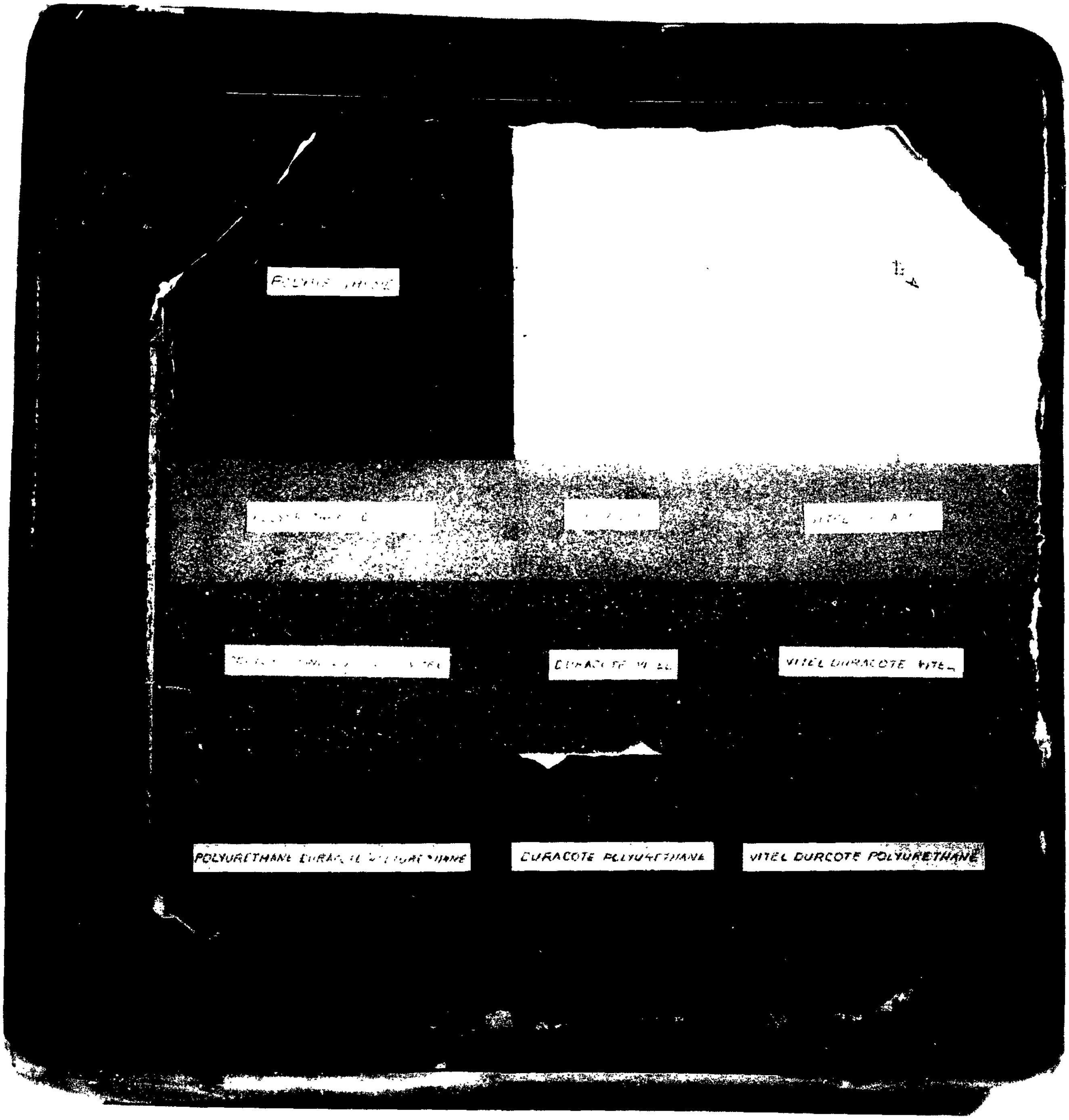

Figure 79. Samples of Film Spray and Reflective Coating Combinations

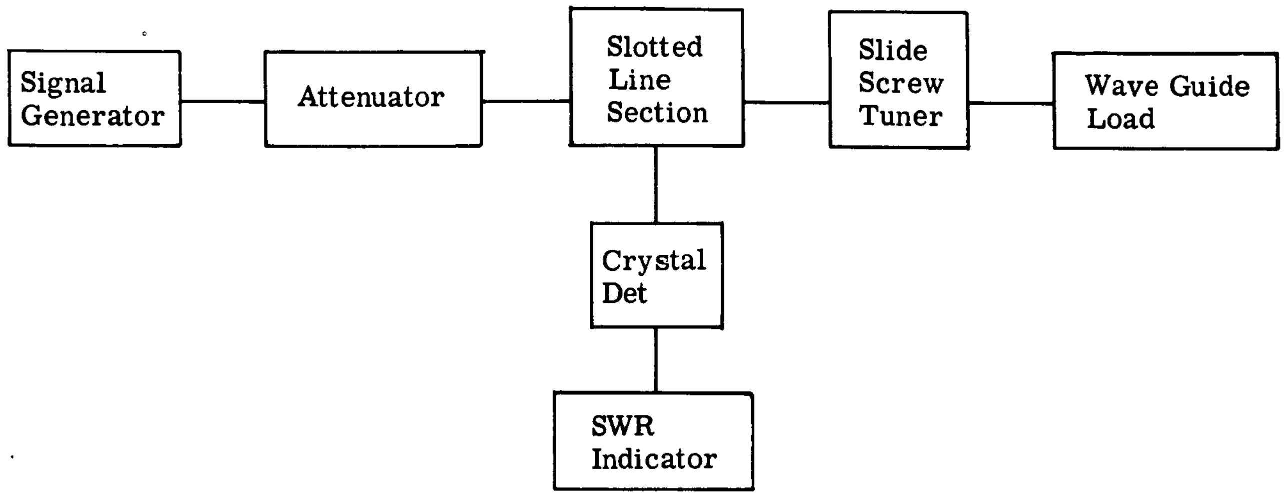

Figure 80. R-F Reflective Test Setup Schematic

The complete system was tuned with the slide screw tuner for minimum reflected power at the two test frequencies (VSWR 1.01:1). The waveguide system was then unbolted and the sample placed (painted surface toward the signal generator) between the slotted section and the slide screw tuner. The reflected power of the sample was then measured in decibels.

The most satisfactory of the samples indicated an r-f reflectivity of better than 98 percent in the 3-kmc range and 96 percent in the 9-kmc range after, as well as before, heavy folding, crushing, and rolling of the samples by hand. This sample, which then was shown to have excellent flexibility and strength as well as r-f reflective characteristics, was then chosen for application in the two demonstration models.

Subsequent to the painting of these models, another paint developed with a vinyl base also showed equally good characteristics in the same areas, thus supplying a second solution to the r-f reflective coating problem.

G. GOODYEAR AEROSPACE RIGID-FOAM ANTENNA DEVELOPMENT

An internally funded development program on foam-rigidized antenna dishes was being conducted concurrently with this advanced antenna study program. For this reason, it was also considered that a brief report of its results would enhance this report, since Section IX included foam-rigidized antennas through the final evaluation. The foam antennas were previously eliminated in lieu of the transportable advantages of the two inflatable parabolic antennas.

As noted in Section IX, rigid-foam antenna dishes were thought to have offered the potential of producing highly accurate dishes that are relatively economical. The additional information does not entirely negate the previous opinions; however, these opinions will have to be tempered at this time relative to the testing information that will be explained below. It appears that the resolution of the problems relating to temperature shock and accelerated aging are not evident at this time.

A number of 36-inch diameter test panels were made by the molded-foam method for environmental testing. Some utilized integral metal frame structure as described previously. Several others had no internal metal structure, but utilized fiberglass skins for structural rigidity. Temperature shock and accelerated aging tests were performed on separate test panels. Temperature shock tests consisted of three cycles of alternate 4-hour periods at +170°F and -40°F. Accelerated aging tests consisted of 10 repeated cycles of (1) 24 hours at 100°F temperature and 100 percent relative humidity, (2) four hours at -70°F, (3) 12 hours at +160°F with ambient humidity, and (4) 8 hours of ultraviolet light exposure. Contour measurements, subsequent to the temperature shock tests, showed contour variations in the range of ±0.019 to ±0.034 for the integral metal structure panels and ±0.009 to 0.014 for the panels with fiberglass skins. Subsequent to the accelerated aging tests, considerable warpage of the surface was evident, and contour changes were beyond the range of measurement of the dial indicators used in the contour test setup. Some cracks in the foam structure were evident after both tests; however, they were more pronounced in the panels subjected to the accelerated aging tests.

Various factors probably contribute to the dimensional changes and cracking. These include, but are not limited to, the following:

(1) Different coefficients of thermal expansion for the different density of foams, and the metallic structure or fiberglass.
(2) Non-uniform cellular structure of the foam.
(3) The effects of moisture on the various properties of the foam.
(4) Temperature lag due to the insulating properties of the foam.
(5) Stress concentration due to heat sinks during the foaming operation.

The solution to the problems of poor dimensional and structural stability under varying environmental conditions are not apparent at this time. Improved sealing against moisture, changes to the metallic structure configuration, improved fabrication techniques, and optimization of the basic foam formulation probably could effect significant improvements; however, extensive further development and testing would be required to assure success.

Similar problems would be expected with the concept utilizing the swept-plastic process for applying the final contoured surface, since this concept also uses the molded-foam process to fabricate the rough contoured reflector.

A different approach in utilizing the swept-plastic technique for achieving a very accurate reflector surface economically is under development and appears promising at this time. In this approach, a conventional metallic segmented reflector structure is used with a perforated metal skin fabricated to rough contour. A thin layer of foam is used as a foundation or buffer layer on which the final swept-plastic contoured surface is applied. Here the foam is not used as a basic structural material.

PART 4. FACTUAL DATA

SECTION XI. GROUND-BASED TRACKING ANTENNA MODELS

A. GENERAL

As previously mentioned, one of the program objectives was to fabricate a model to demonstrate the principle of the two selected ground-based tracking antenna models, the AIRMAT paraboloid antenna and the lenticular AIRMAT antenna.

Due to the funding limitations of the program, it was recognized that all the technical problems could not be resolved with these models, so it was planned to demonstrate the following features:

(1) Feasibility of an inflatable structure to form the required contour.
(2) Technique of developing the structural integrity of the antenna by using the new shear web technique to develop shear stiffness.
(3) Fabrication techniques.
(4) Surface-foaming techniques.
(5) Development of a preliminary r-f reflective surface.
(6) Preliminary packaging of the inflatable antennas.

The size and contour selected for both antenna models were based on an existing paraboloidal male tool, which was used to form the final reflector surface contour. This tool is a five-foot diameter paraboloid with an f/D ratio (focal length to aperture size) of 0.30. The five-foot diameter is a convenient size, and the f/D ratio is satisfactory for the purposes of the models, even though it makes a somewhat deeper paraboloid than the f/D ratio of 0.35 used for the full-scale antennas. The tool was used for spreading a thin layer of flexible foam onto the inflated paraboloidal dish to fill in the inherent contour deviations and to furnish a highly accurate surface for the r-f reflective paint covering the surface contour. A female tool was used to form a similar contour for the lenticular antenna model.

To reduce the model costs while still maintaining the structural integrity, both models used the contoured fabric webs that radiate from the central hub. The only tooling required to fabricate the inflatable portion of the model consisted of several wooden templates cut to the contour of the webs and a metal template of the gore pattern. The weight and packaging of the antenna models were not optimized, but these disadvantages were outweighed by the economy of construction and were considered to be adequate for the purposes of the demonstration models. Also, substituting textile fabric (Dacron) for steel or glass fabric is a permissible deviation even though the stiffness of Dacron is only about 1/30 and 1/6 of steel and glass fabrics respectively.

At this time, since the models were no longer to be of AIRMAT construction, and since the fabric web design concept offered an improvement for the full-scale antenna as well, the two selected ground-based tracking antennas will be called the inflatable paraboloid antenna and the inflatable lenticular antenna. Figure 81 is a photograph of the two ground-based antenna models.

B. INFLATABLE PARABOLOID ANTENNA MODEL

1. General

Figure 82 shows the completed inflatable paraboloid antenna model mounted on a stand made for two models. Figure 83(A) shows the inflatable paraboloid antenna model with a vacuum package of the inflatable lenticular antenna at the base of the antenna stand. Since both antenna models package into similar size packages, Figure 83(A) simulates the relative packaged and inflated size of the inflatable paraboloid model. Figure 83(B) illustrates the relative package sizes of

Figure 81. Ground-Based Tracking Antennas

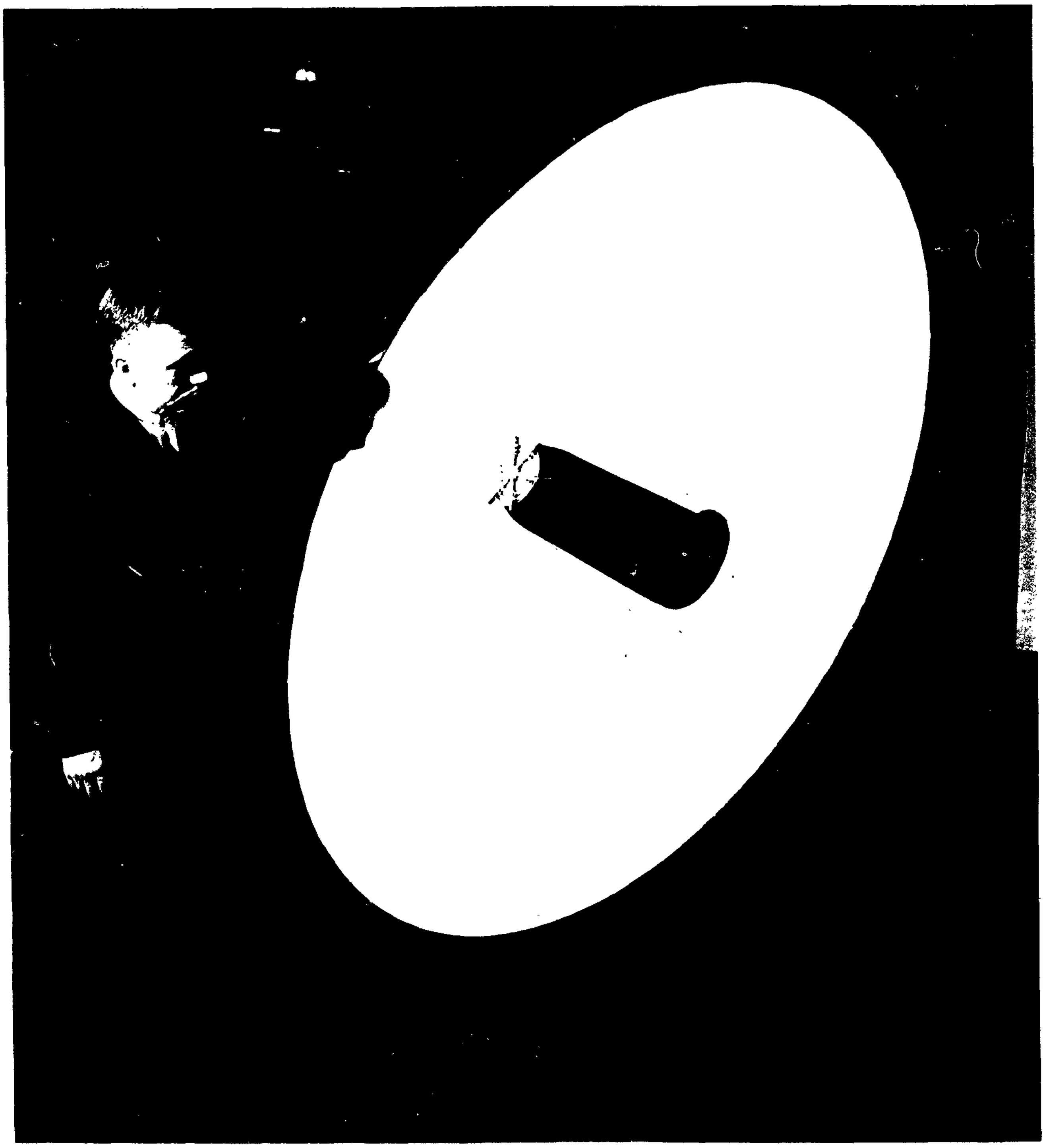

Figure 82. Five-Foot Diameter Inflatable Paraboloid Antenna Model

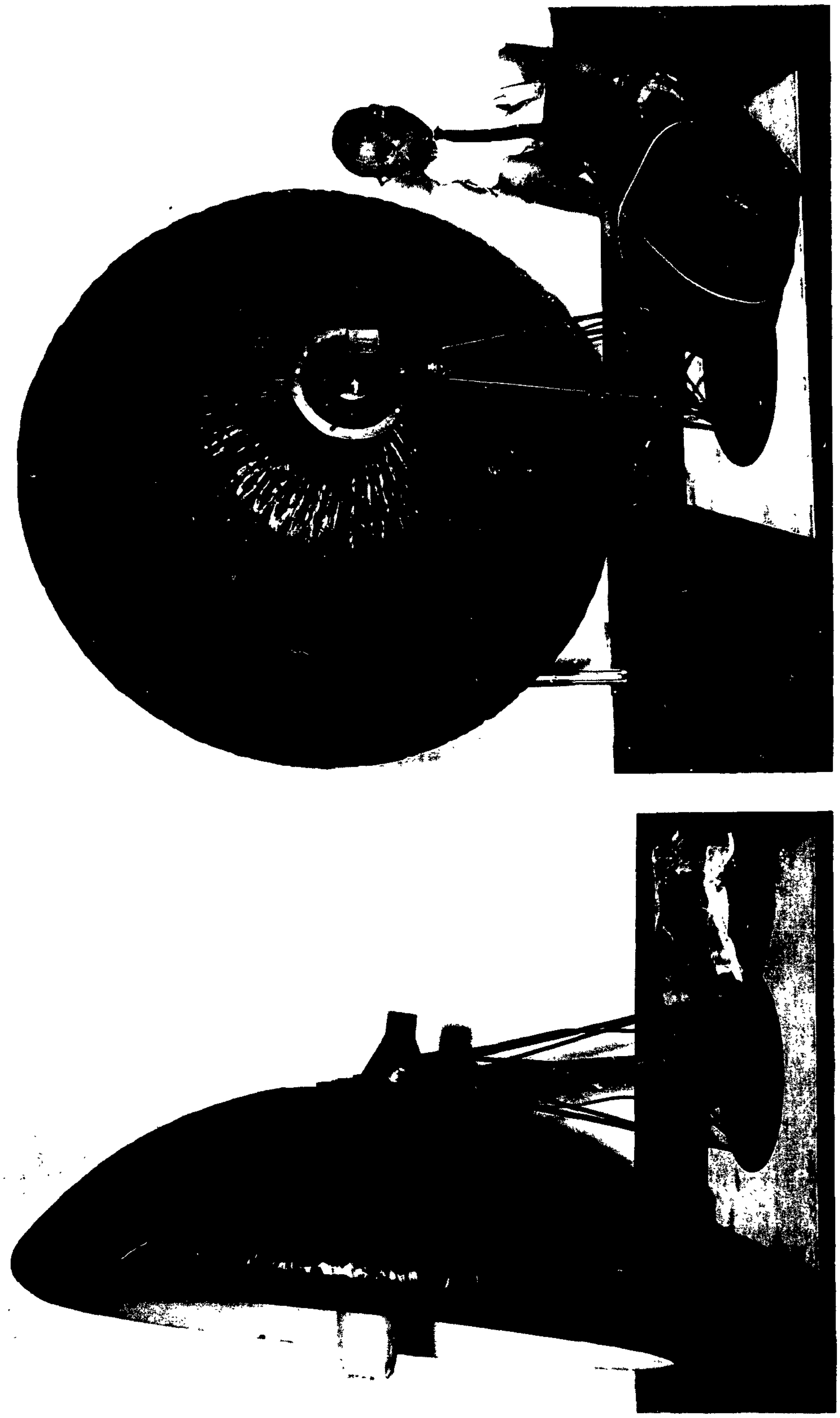

B. Inflated Model with Packaged Lenticular Model

A. Inflated Model with Vacuum Packaged Lenticular Model

Figure 83. Inflated Paraboloid Antenna Models with Packaged Lenticular Antenna Models

the packaged and inflated paraboloid model where the package is not a vacuum package.

The following paragraphs describe the design, fabrication, and the limited evaluation efforts made on the paraboloid model.

2. Design Configuration

The inflatable paraboloid antenna model design can best be explained by reference to the drawings. Figures 84 and 85 show the antenna model, and Figure 86 shows the interchangeable pedestal model that can be used with both antenna reflector models.

As previously reported, the models were not expected to represent the optimum weight and package configuration, since the materials cannot be practically and economically scaled down from the full-scale tracking antennas to the 1/8 scale that is utilized for the models. In addition, other structural and mechanical unknowns in a program of this size must be circumvented for expediency. This circumventing obviously must be compensated for by beefing the design. However, the antenna models very definitely demonstrate the six objectives listed in paragraph A.

3. Structural Considerations

The demonstration models were not structurally designed to be used as r-f test models; however, a preliminary deflection analysis of the models was made to indicate what can be expected in terms of deflection and rigidity. Several simplifying assumptions were made, and are discussed in the following paragraphs.

The reflector has been analyzed as though it were constructed of 45 individual identical beams, each acting independently of the others. Each beam consists of one concave gore, one convex gore, one long web, one-half of each of two short webs, and the inflation gas contained within these boundaries.

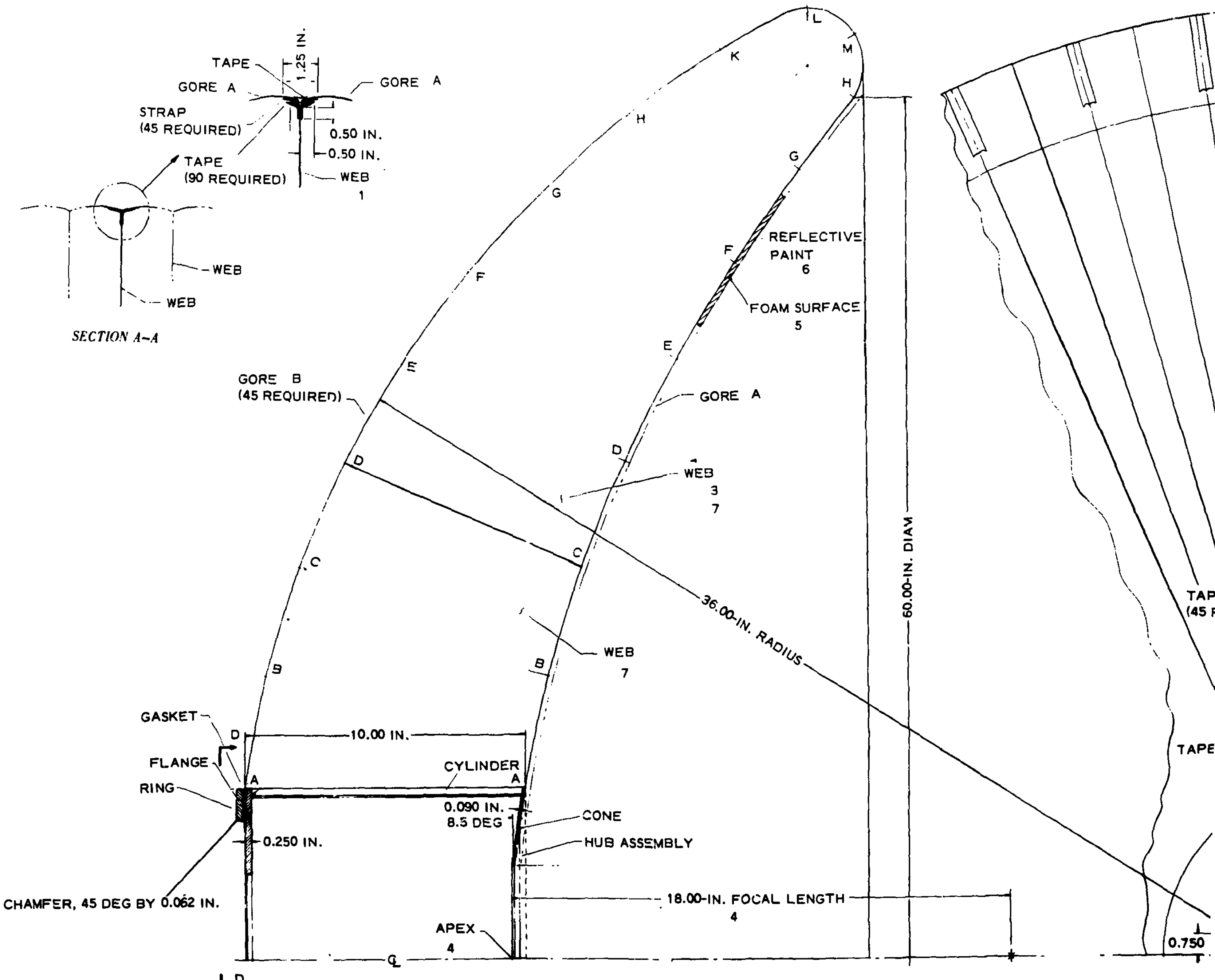
TAPE
1.25 IN.
GORE A
GORE A
STRAP
(45 REQUIRED)
0.50 IN.
0.50 IN.
TAPE
(90 REQUIRED)
WEB
1
WEB
WEB
SECTION A–A
L
M
K
H
H
G
G
REFLECTIVE PAINT
6
F
F
FOAM SURFACE
5
E
E
GORE B
(45 REQUIRED)
GORE A
D
D
WEB
3
7
C
C
60.00-IN. DIAM
36.00-IN. RADIUS
B
B
WEB
7
GASKET
D
10.00 IN.
FLANGE
A
CYLINDER
A
RING
0.090 IN.
8.5 DEG
CONE
0.250 IN.
HUB ASSEMBLY
CHAMFER, 45 DEG BY 0.062 IN.
18.00-IN. FOCAL LENGTH
4
APEX
4
D
TAP
(45 F
TAPE
0.750

1

2

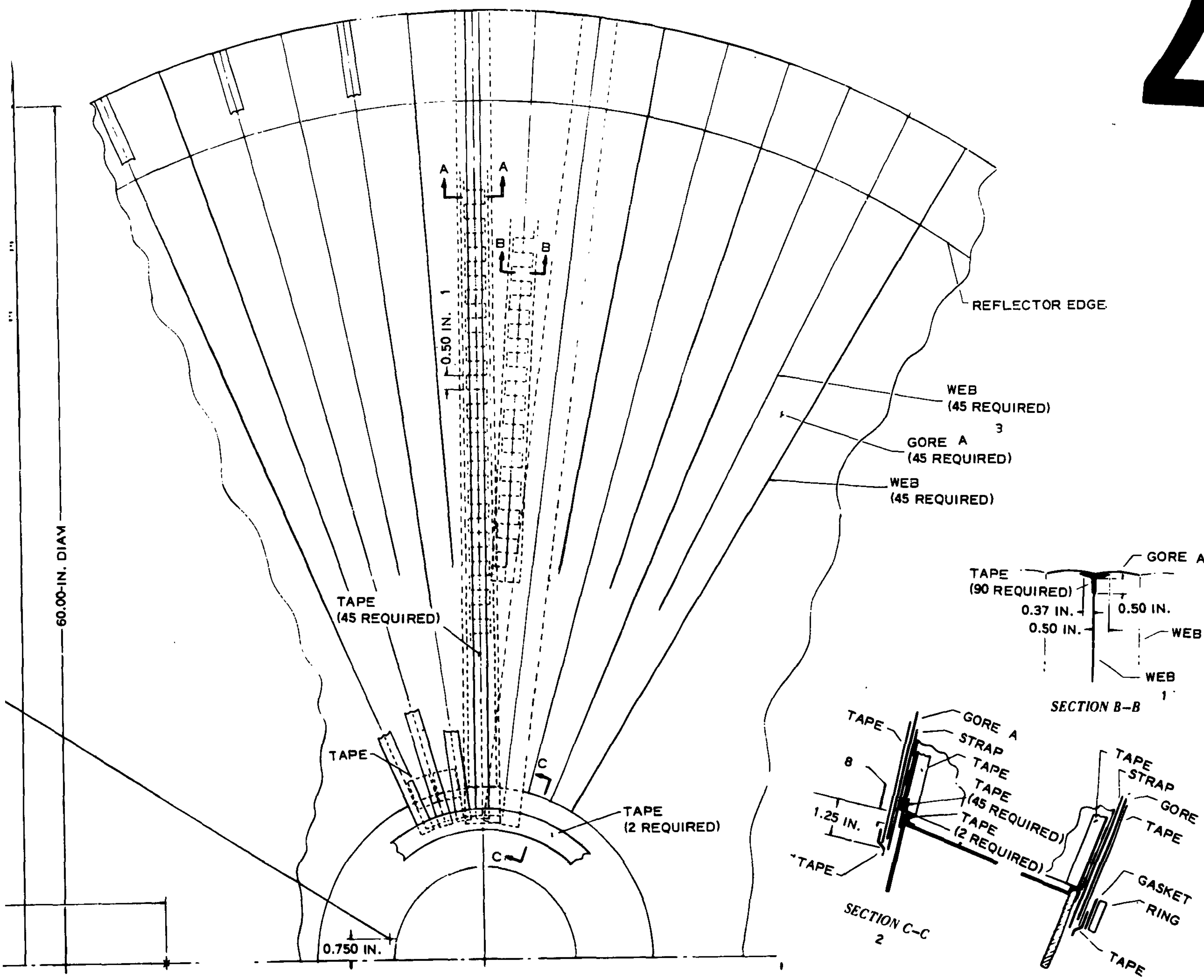

Figure 84. Detailed Engineering Model Design of Inflatable Paraboloid Antenna (Sheet 1)

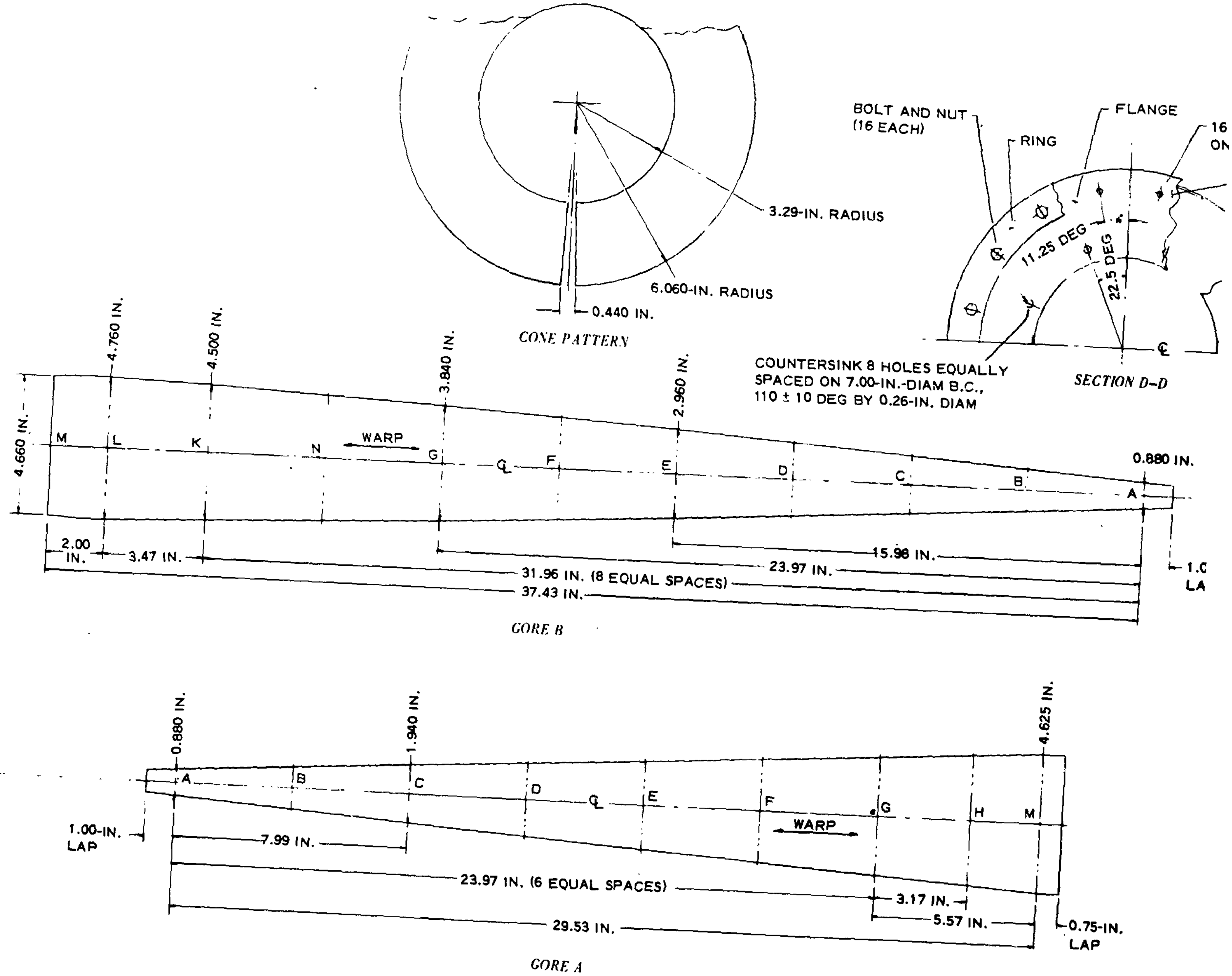

Figure 84. Detailed Engineering Model Design of Inflatable Paraboloid Antenna (Sheet 2)

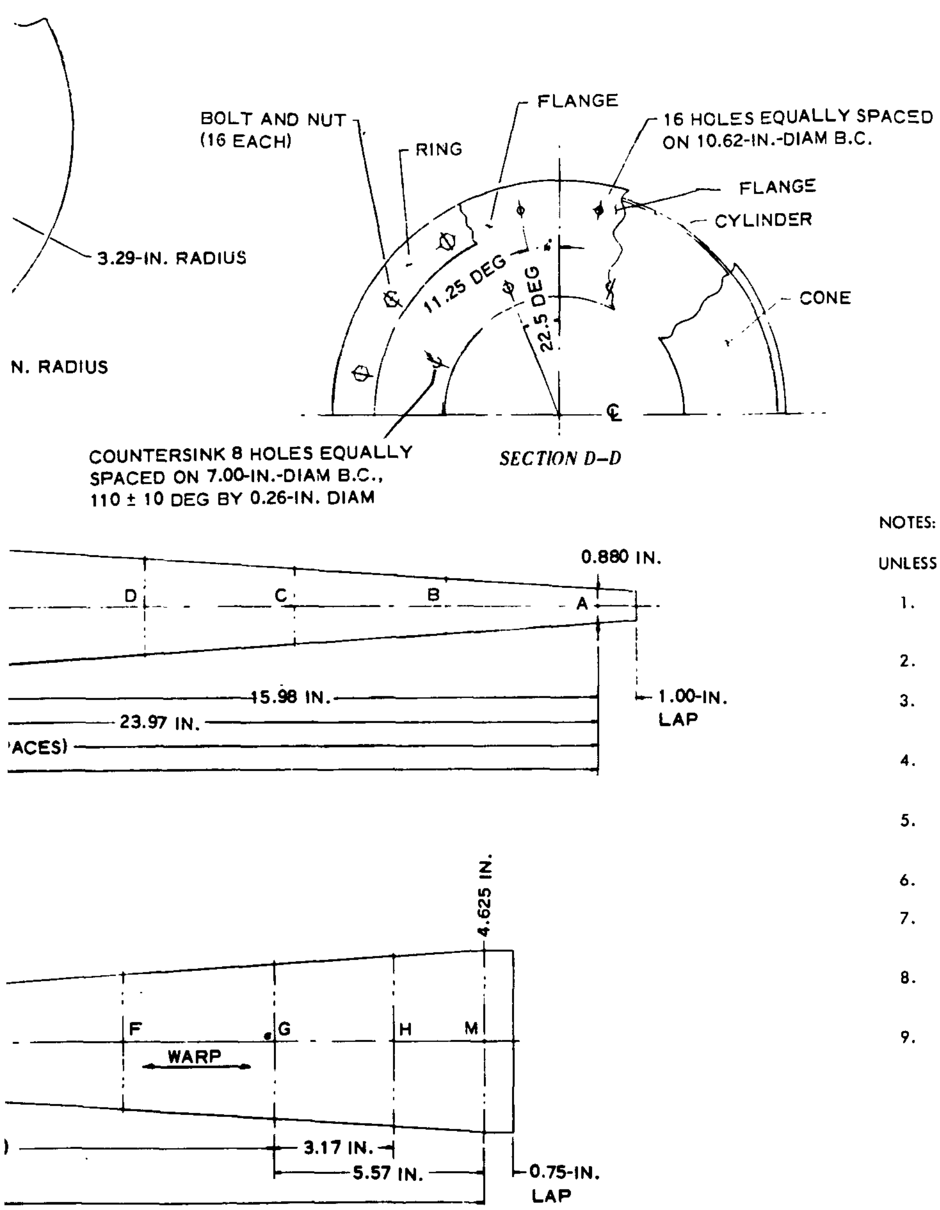

NOTES:

UNLESS OTHERWISE SPECIFIED

1. SLIT EDGE OF WEBS AT 0.50-IN. SPACING TO FORM ALTERNATING FINGERS AS SHOWN
2. GOODYEAR TIRE AND RUBBER CO., AKRON, OHIO, FABRIC CODE
3. WEB TO TERMINATE AT STATION ON GORE A AND STATION D ON GORE B
4. APEX AND FOCAL POINT SHOWN ARE WITH RESPECT TO CONTOUR OF WEBS
5. FLEXIBLE FOAM SURFACE (LATEX FOAM) TO BE APPLIED BY USE OF TOOL NO. 216 NS-2-5-LM
6. R-F REFLECTIVE PAINT
7. USE OZALID PRINTS OF DRAWING FOR DIRECT DETERMINATION OF CONTOUR FOR WEB TEMPLATES
8. EXTEND BASE OF TAPE 0.50 IN. BEYOND WEB AND TRIM LEG OF TAPE FLUSH WITH WEB AS SHOWN
9. BREAK EDGES OF HUB AND RING 0.16-IN. RADIUS

n of Inflatable

12

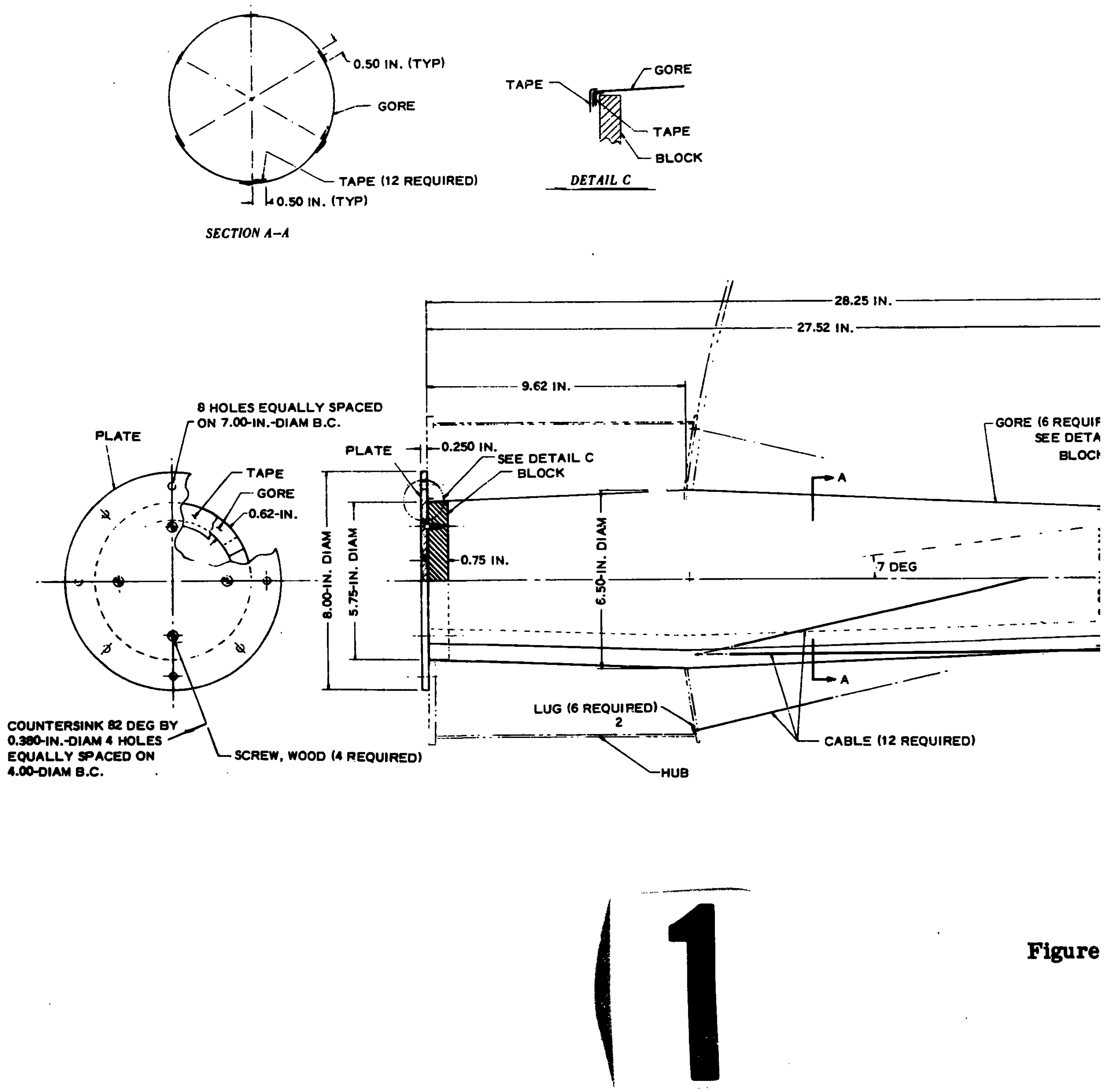
0.50 IN. (TYP)
GORE
TAPE (12 REQUIRED)
0.50 IN. (TYP)
SECTION A–A
TAPE
GORE
TAPE
BLOCK
DETAIL C
28.25 IN.
27.52 IN.
9.62 IN.
8 HOLES EQUALLY SPACED ON 7.00-IN.-DIAM B.C.
PLATE
PLATE
0.250 IN.
SEE DETAIL C
BLOCK
TAPE
GORE
0.62-IN.
GORE (6 REQUIR
SEE DETA
BLOCK
A
8.00-IN. DIAM
5.75-IN. DIAM
0.75 IN.
6.50-IN. DIAM
7 DEG
A
LUG (6 REQUIRED)
2
CABLE (12 REQUIRED)
COUNTERSINK 82 DEG BY 0.380-IN.-DIAM 4 HOLES EQUALLY SPACED ON 4.00-DIAM B.C.
SCREW, WOOD (4 REQUIRED)
HUB
1

Figure

2

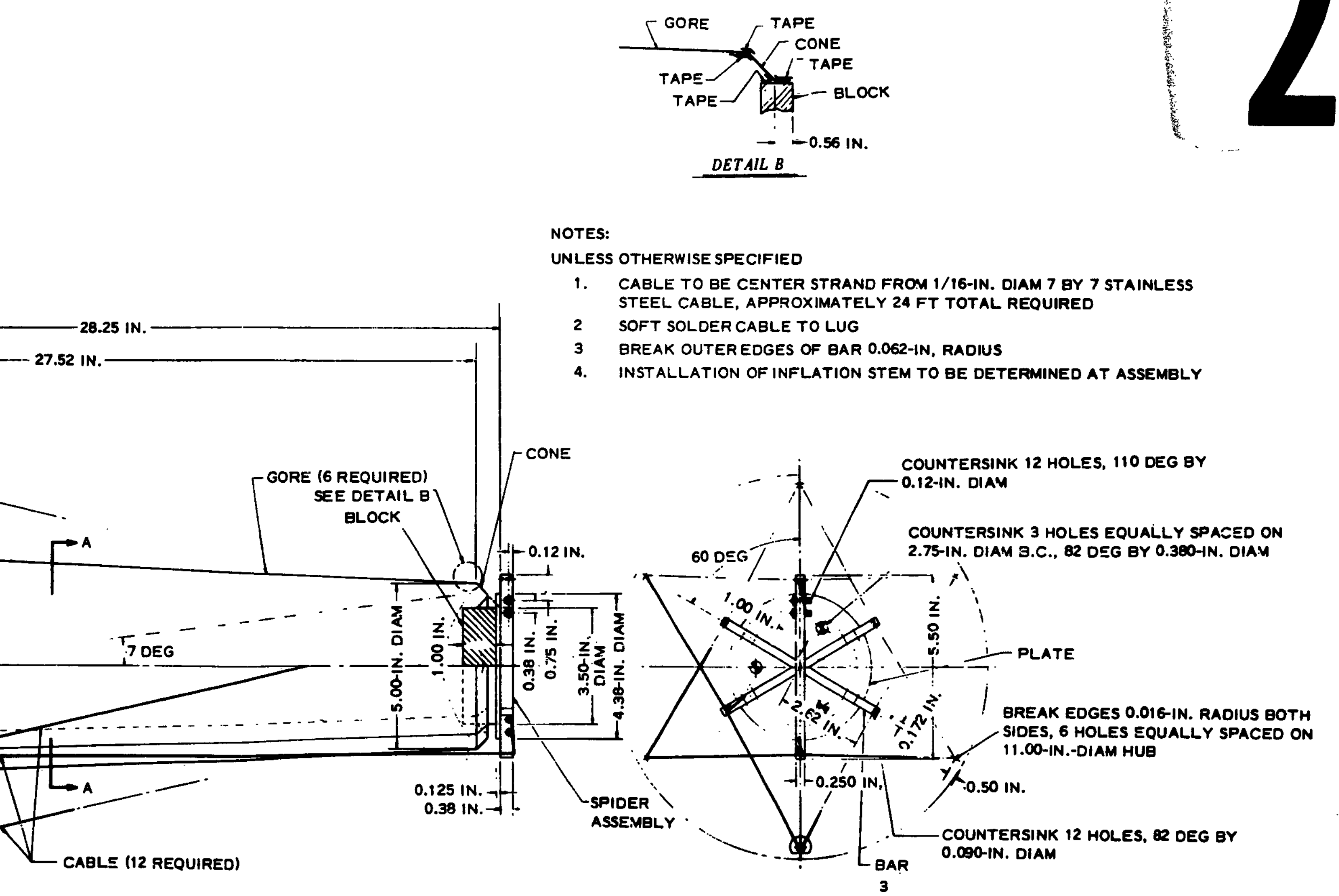

Figure 85. Inflated Cassegrain Support for Inflatable Paraboloid Model

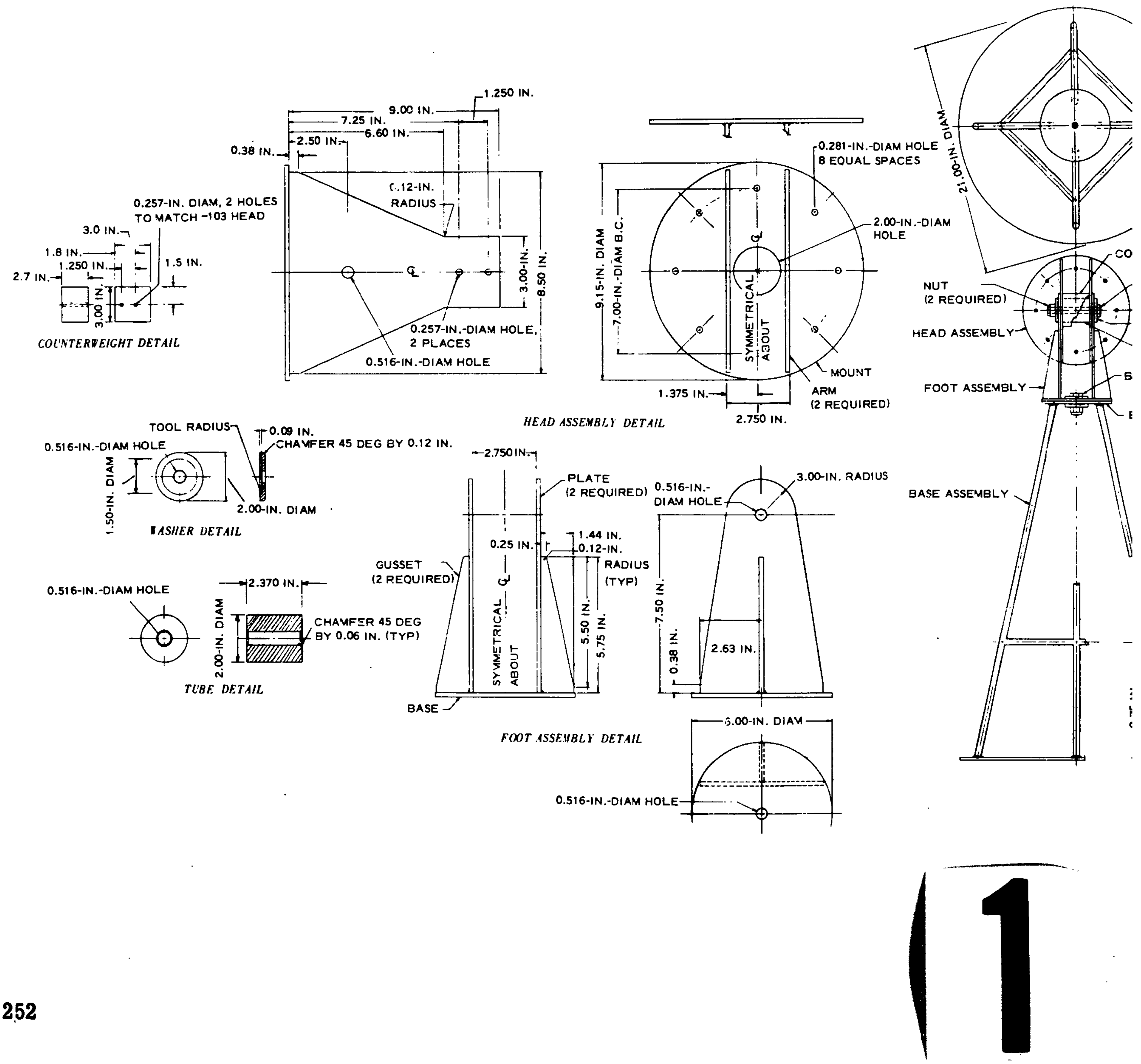
1.250 IN.
9.00 IN.
7.25 IN.
6.60 IN.
2.50 IN.
0.38 IN.
0.12-IN.
RADIUS
3.00-IN.
8.50 IN.
0.257-IN.-DIAM HOLE,
2 PLACES
0.516-IN.-DIAM HOLE
0.257-IN. DIAM, 2 HOLES
TO MATCH -103 HEAD
3.0 IN.
1.8 IN.
1.250 IN.
1.5 IN.
2.7 IN.
3.00 IN.
COUNTERWEIGHT DETAIL
0.281-IN.-DIAM HOLE
8 EQUAL SPACES
2.00-IN.-DIAM
HOLE
9.15-IN. DIAM
7.00-IN.-DIAM B.C.
SYMMETRICAL
ABOUT
MOUNT
ARM
(2 REQUIRED)
1.375 IN.
2.750 IN.
HEAD ASSEMBLY DETAIL
21.00-IN. DIAM
NUT
(2 REQUIRED)
HEAD ASSEMBLY
FOOT ASSEMBLY
BASE ASSEMBLY
TOOL RADIUS
0.09 IN.
CHAMFER 45 DEG BY 0.12 IN.
0.516-IN.-DIAM HOLE
1.50-IN. DIAM
2.00-IN. DIAM
WASHER DETAIL
2.750 IN.
PLATE
(2 REQUIRED)
0.25 IN.
1.44 IN.
0.12-IN.
RADIUS
(TYP)
GUSSET
(2 REQUIRED)
SYMMETRICAL
ABOUT
5.50 IN.
5.75 IN.
BASE
0.516-IN.-
DIAM HOLE
3.00-IN. RADIUS
7.50 IN.
0.38 IN.
2.63 IN.
FOOT ASSEMBLY DETAIL
3.00-IN. DIAM
0.516-IN.-DIAM HOLE
0.516-IN.-DIAM HOLE
2.370 IN.
2.00-IN. DIAM
CHAMFER 45 DEG
BY 0.06 IN. (TYP)
TUBE DETAIL
1

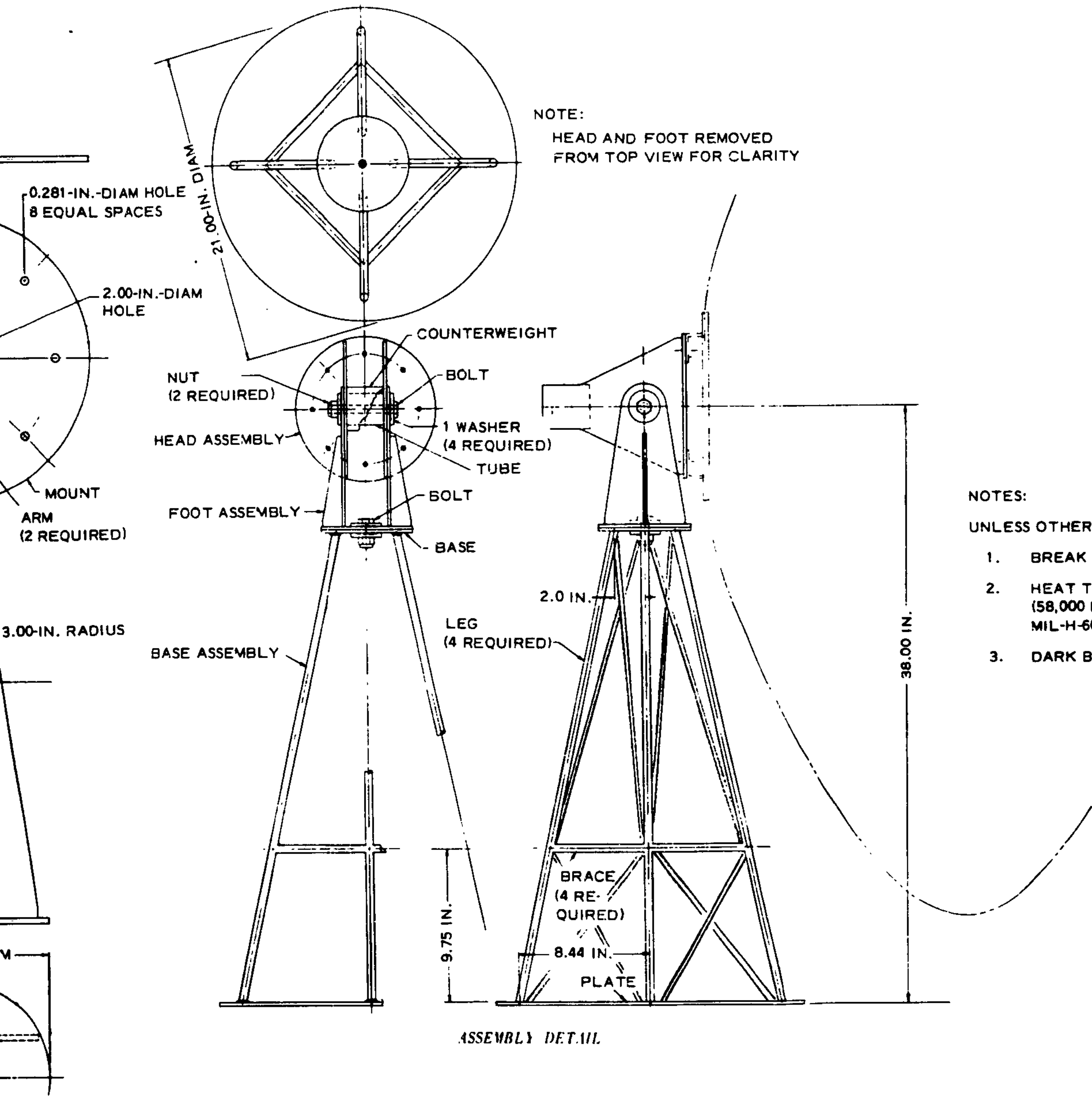

NOTES:

UNLESS OTHERWISE SPECIFIED

1. BREAK ALL SHARP CORNERS AND EDGES
2. HEAT TREAT AFTER WELDING TO T4 TEMPER (58,000 PSI MIN TS) IN ACCORDANCE WITH MIL-H-6088 (GAC PROCESS SPEC. HT-1.00)
3. DARK BLUE ENAMEL SPRAY FINISH

Figure 86. Antenna Model Base

The beam is broken into 16 equal increments of length along the beam center line, and the weight and section properties of each increment are determined. The gore fabric weighs 6.35 oz/yd^2; the web fabric weighs 15.5 oz/yd^2.

Using a stiffness-to-weight ratio of 1.8×10^6 inch for Dacron-Neoprene fabric, the stiffness of the gore fabric, E_g, is 550 lb/in., and the stiffness of the web fabric, E_w, is 1350 lb/in. The shear stiffness of the web fabric, G_w, is assumed to be $0.4E_w$ or 540 lb/in. Curvature is considered only for determining the normal and tangential load components of the weight load for each increment. Otherwise, the beam is treated as a straight member, varying in both depth and width.

The beam shear and beam bending moments are determined, and the tangential load components are assumed to be axial loads. The normal tip deflection due to bending, δ_B, is determined by the moment area method and is 0.0037 inch. To determine the normal tip deflection due to shear, the part of the beam shear load resisted by the fabric webs and the part resisted by the inflation pressure must be calculated. The total shear deflection is determined by adding the separate deflections caused by the two parts of the load. The normal tip deflection due to shear is then calculated by using the part of the beam shear load resisted by the fabric webs in conjunction with conventional deflection formulas. This deflection, δ_S, is 0.007 inch, and since the total normal tip deflection is the sum of the bending deflection and the shear deflection, $\delta_N = \delta_B + \delta_S = 0.0044$ inch. The axial tip deflection, δ_A, is determined from conventional formulas, using the section properties and the assumed axial loads, and is 0.0014 inch.

With the reflector axis in a horizontal position and the reflector loaded by only its own weight, the reflector deflection causes the upper part to tend to increase the concavity. The maximum deflection at the rim is 0.0044 inch normal to the reflector surface. The rim also tends to deflect in the plane of the reflector.

The maximum deflection in this direction is 0.0014 inch, contraction at the upper rim and extension at the lower.

These deflections were considered well within the limits for the purpose of the models.

4. Inflatable Structure Fabrication

Fabrication of the inflatable structure for the model is a matter of accurate tailoring and fitting of various fabric parts. Figure 87 shows the two different fabric subassemblies that make up the entire inflatable structure. These subassemblies include the radial shear webs and the gore patterns already cemented together. The inflatable structure is made up of 45 of each of these two subassemblies. Figure 88 shows a partially completed inflatable structure assembly. Figure 89 shows the completed inflatable structure assembly with the center hub installed. As shown, the structure forms the basic paraboloid contour and is ready for the application of the flexible-foam surface.

5. Paraboloid Foaming Operation

In view of the accuracies achieved with the samples, as a result of the Goodyear Aerospace funded foam development program, sufficient information was available to begin the work of applying the foam surfaces to the five-foot demonstration models. As mentioned before, because of the apparent stiffness of the inflatable paraboloid structures, it was decided to make a preliminary trial of applying the flexible foam surface without using a rigid-foam backup structure.

In order to determine the accuracy of a surface formed by this more expeditious method, the mold surface was measured. These points were marked on the mold with a grease pencil after the application of separator, so that the marks would transfer to the foam surface, permitting measured comparison of identical locations. A guide was fabricated and attached to the mold for use in centering the inflatable structure over the mold.

Figure 87. Fabric Structure Subassemblies of Inflatable Paraboloid Antenna

Figure 88. Partially Completed Fabric Structure of Inflatable Paraboloid Antenna

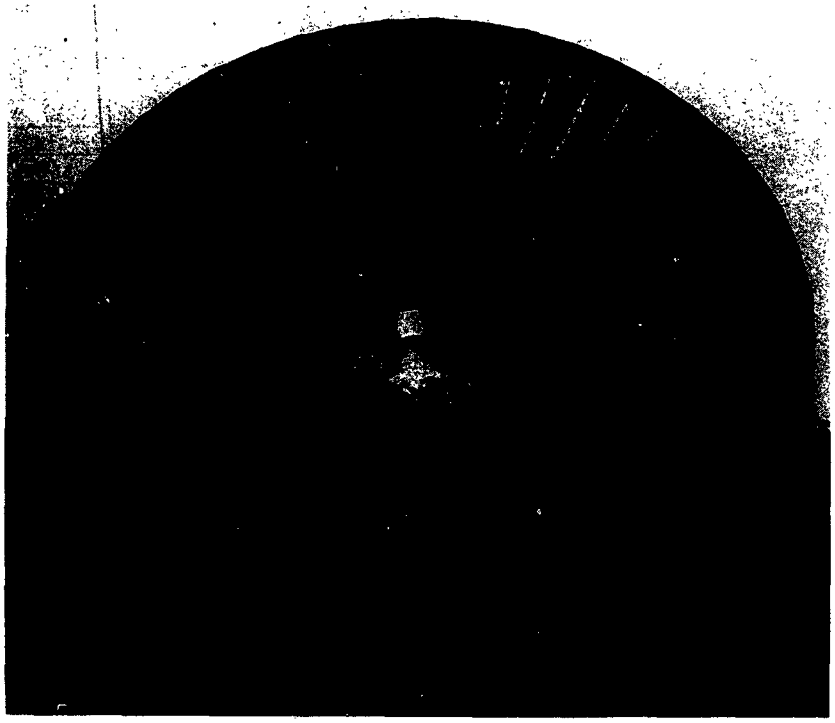

Figure 89. Completed Inflatable Paraboloid Subassembly before Application of Foamed Surface

For this sample, foam was taken from a continuous process production source and flowed directly over the mold. The inflatable structure, while under operating pressure, was then inverted and lowered directly over the mold. This condition is shown in Figure 90. Heat lamps were then applied to facilitate the gel process and to achieve as much curing as possible before moving the mold and antenna model to the cure oven.

After curing the latex-foam surface, the antenna was released from the mold and inspected. Inspection of the resulting surface revealed that a very smooth surface had been formed and that the surface had not only picked up the grease pencil marks but also reproduced the circumferential marks used in measuring the tool. In addition, however, there was a void of considerable area formed between the foam and the inflatable structure. It was determined that this void was caused by the fact that the mold was oriented convex face upward. As a result, the relatively steep contour allowed the foam to drain downward more rapidly than originally anticipated and with insufficient thickness remaining. A problem also existed from the fact that the inflatable structure was placed over the male mold, providing the possibility of trapping an air pocket.

Both the rapid drain-off of the liquid foam and the trapped air conditions were eliminated at one time by merely inverting the positions of the mold and inflatable structure as shown in Figure 91. In this case, the foam was poured into the inverted parabolic antenna dish, and the male mold was eased downward forcing the excess foam out around the circumference. Figure 92 shows the resulting contour.

Contour accuracy as well as the surface finish on this first foaming run with the inverted mold appeared to be fairly good except for a few small areas, which represent a small percentage of the surface. One area in the right side of the photo was a conventional problem in latex foams termed an "air check". The

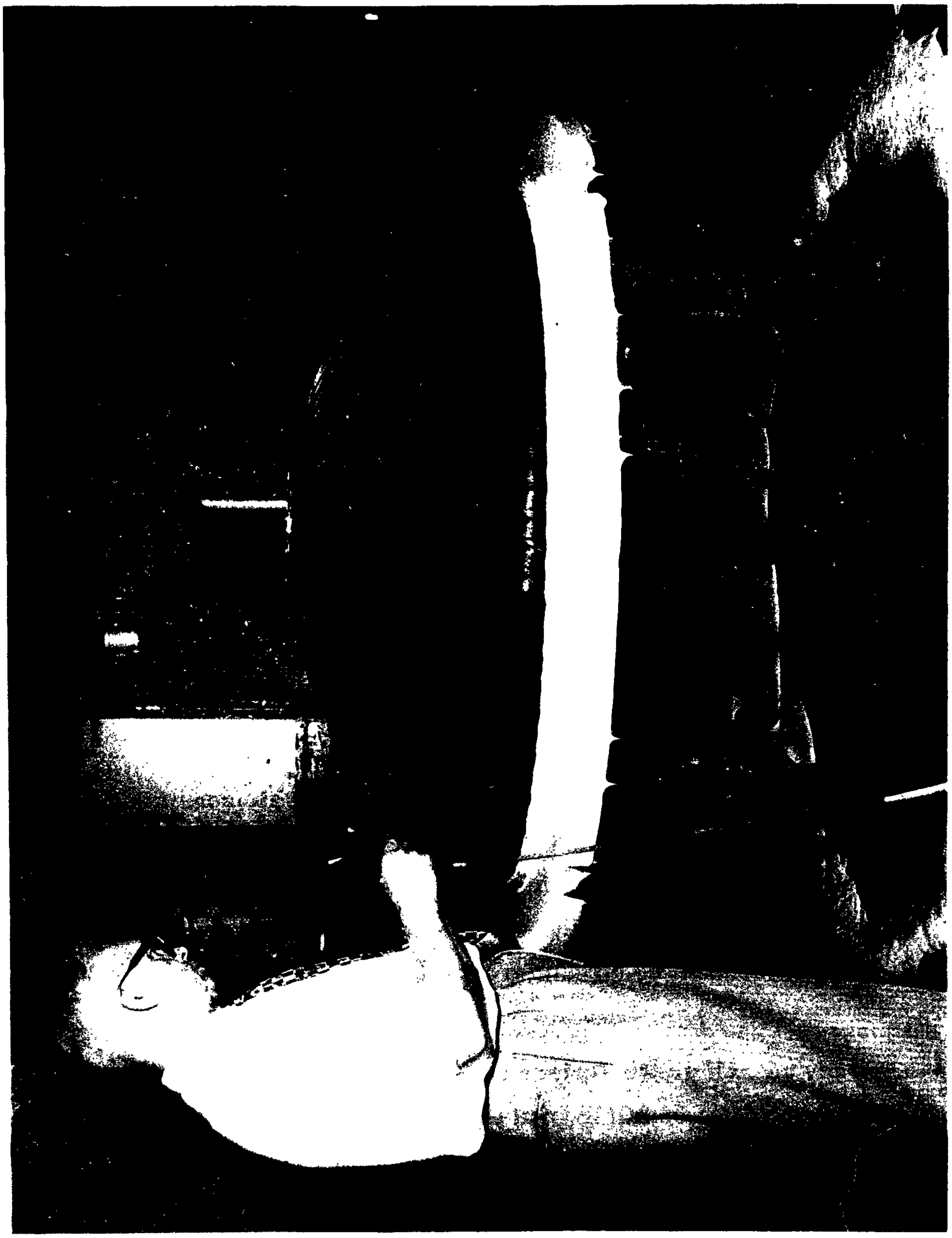

Figure 90. Paraboloid Antenna Surface Foaming Operation with Upright Mold Position

Figure 91. Paraboloid Antenna Surface Foaming Operation with Inverted Mold Position

Figure 92. Inflatable Paraboloid Antenna Model after First Foaming Run (Inverted Mold)

"air check" results from the foam shrinking away from the mold instead of adhering to the mold. Usually this "air check" is initiated by some defect, and this particular problem resulted from a slight misalignment of the inflatable dish with the male mold. A second surface area problem was caused by trapping an air pocket in the foam puddle during the pouring operation. These flexible foam surface defects can also be seen in Figure 92. In any case, the resulting foam surface was considered unsatisfactory; therefore, a second pass at the foaming operation was made to eliminate these discrepancies.

In the second attempt with the inverter mold, the existing foam was not removed and only a very thin additional skin was applied; the results are shown in Figure 93. In general, the surface contour and the surface finish appeared to be very good. Measurements taken later proved the model surface to be a very accurate duplication of the mold. One problem that did occur in this final foaming pass was a few small air bubbles in the surface. However, these air bubbles are also a matter of control during the latex foaming operation. It was found later that the bubbles were a result of not allowing sufficient time for the mix to smooth out after the change in foam density. The foam density used for the antenna was higher than the density being run for the production run. The local imperfections caused by these bubbles are still in the model. However, since they can be logically explained, it was not considered worth the expense to eliminate them.

In each of these three surface foaming operations, production equipment was used, since the laboratory mixing apparatus was not large enough for the antennas. Therefore, some side problems evolved that would not have occurred if the production run had been set up specifically for the antennas. For example, the foam that was used was whatever happened to be in production at the time. Consequently, the flexible foam on the models is a cheaper commerical grade than would be

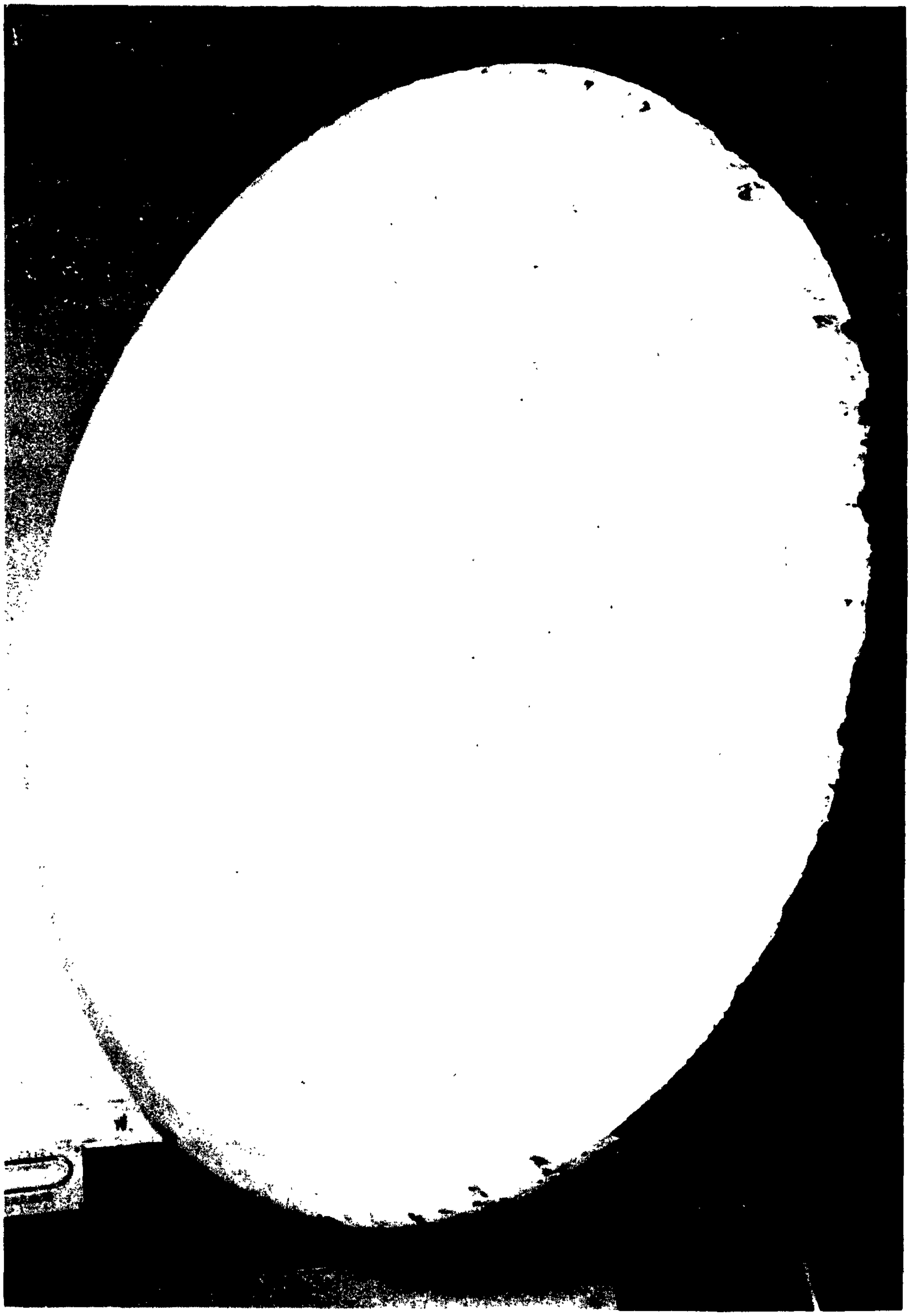

Figure 93. Inflatable Paraboloid Antenna Model after Second Foaming Run (Inverted Mold)

wanted on any prototype models. Moreover, the cheaper commercial grade will show some permanent creases and wrinkles after packaging.

For any future antenna models, a special latex foaming machine will be used. This machine will then permit optimization of the latex-foam formulation to meet the particular antenna requirements such as packaging, environment, strength, weight, etc.

6. Inflatable Paraboloid Antenna Model Surface Contour Measurements

Measurements of the surface formed on the antenna were made using a pair of theodolites on the same points previously measured on the mold as indicated by the grease marks. This optical method was chosen over other possible systems because it required no extra tooling, all the instruments were immediately available, and the tolerances involved were comparable to the other systems (±0.005 inch). To ensure the highest degree of accuracy for these measurements, a special room was set aside to prevent any disturbances for the duration of the testing. Further, the utmost care was taken in the initial alignment of the instrument setup to ensure the accuracy of each of the succeeding readings. A diagram of the setup is shown in Figure 94.

Briefly, the theodolites were erected at a distance of less than six feet from each other, but greater than antenna diameter. A plumb line was suspended from each theodolite with the plumb bob immersed in liquid for damping. Theodolite No. 1 was sighted on the plumb of theodolite No. 2 and its plate reading and micrometer were set to zero. Theodolite No. 1 was rotated 90 degrees, and a reading was taken on the six-foot scales. The same procedure was followed for theodolite No. 2, thus permitting calculation of the exact distance between the theodolites. Theodolite No. 1 was then rotated to point at the center of the antenna contour, and theodolite No. 2 was rotated through an equal angle. The position of the antenna was moved along the line of sight of theodolite No. 1 to a position where

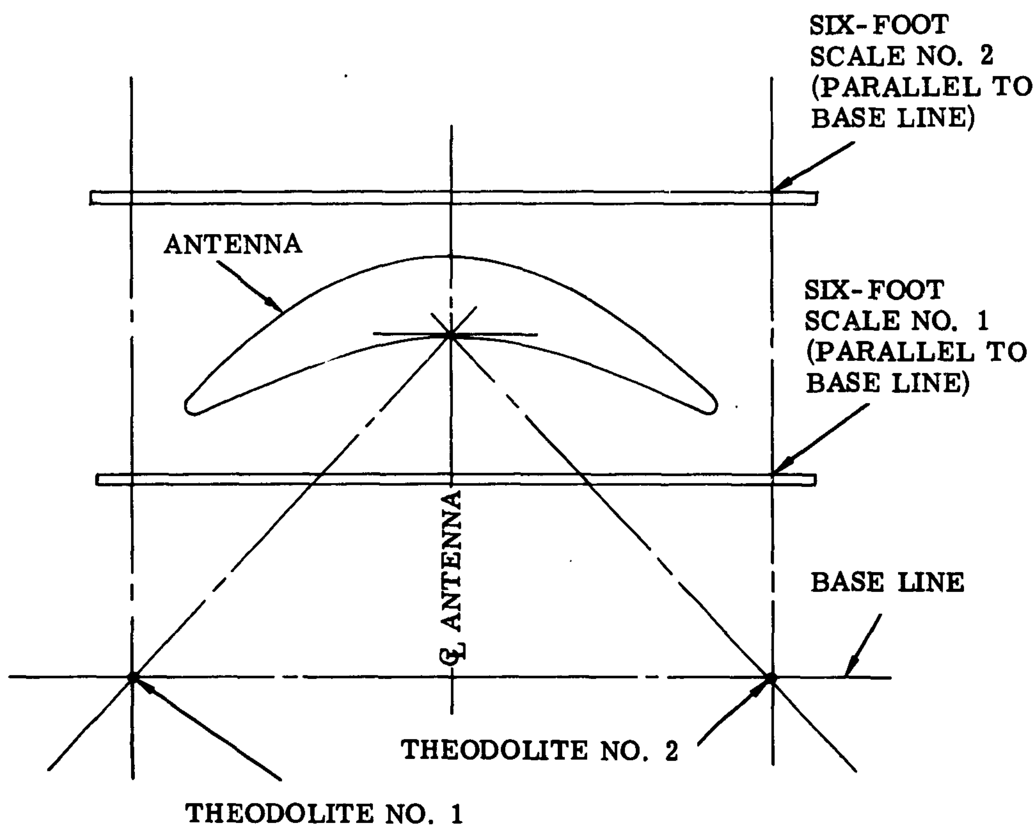

Figure 94. Instrument Setup for Contour Measurement

the line of sight of theodolite No. 2 also intersects the center of the antenna contour. The antenna was rotated about its vertical and horizontal axis until the plane of the outermost radius of index markings was both vertical and parallel to the base line.

Readings were taken on each of the points in the antenna contour and by calculation were compared with the measurements taken at corresponding points in the mold surface. The first set of readings were taken while the antenna was inflated to normal operating pressure (4 psi). The results indicated that the antenna conformed to the mold to within ±0.015 inch in this condition. The antenna pressure was then doubled, and a second set of measurements were taken. In this instance, the error was ±0.030 inch deviation from the mold contour. It should be noted here that in the first instance the antenna formed a paraboloid that was more "closed" than the mold, and in the second instance it was more open. This indicated the possibility that, at some pressure in between, the antenna contour may have been closer to the mold from which it was made. This presents the possibility that, if the ultimate in reflector contour accuracy is desired, an effort can be made as part of the quality control operation in the manufacture of this type of antenna. At that time the pressure that gives the most accurate surface can be determined, and the pressure regulator can be set to continually provide this pressure.

C. INFLATABLE LENTICULAR ANTENNA MODEL

1. General

The inflatable lenticular antenna model was the second antenna model to be fabricated and had the advantage of some fabrication experience. Figure 95 shows the lenticular model inflated and mounted on the antenna stand.

The packaged lenticular model was shown previously in Figure 83, and reference to size can be easily made since the antenna stand is the same one used in all the photos.

The design and fabrication of this model are described in the following paragraphs.

2. Design Configuration

The inflatable lenticular antenna model is fabricated in a fashion similar to the paraboloid model. Figure 96 shows a detailed engineering drawing for the inflatable lenticular antenna model.

This lenticular configuration uses considerably more fabric than the paraboloid model; however, this model packages in a slightly smaller size, since it does not utilize a rigid hub attachment for both fabric skins.

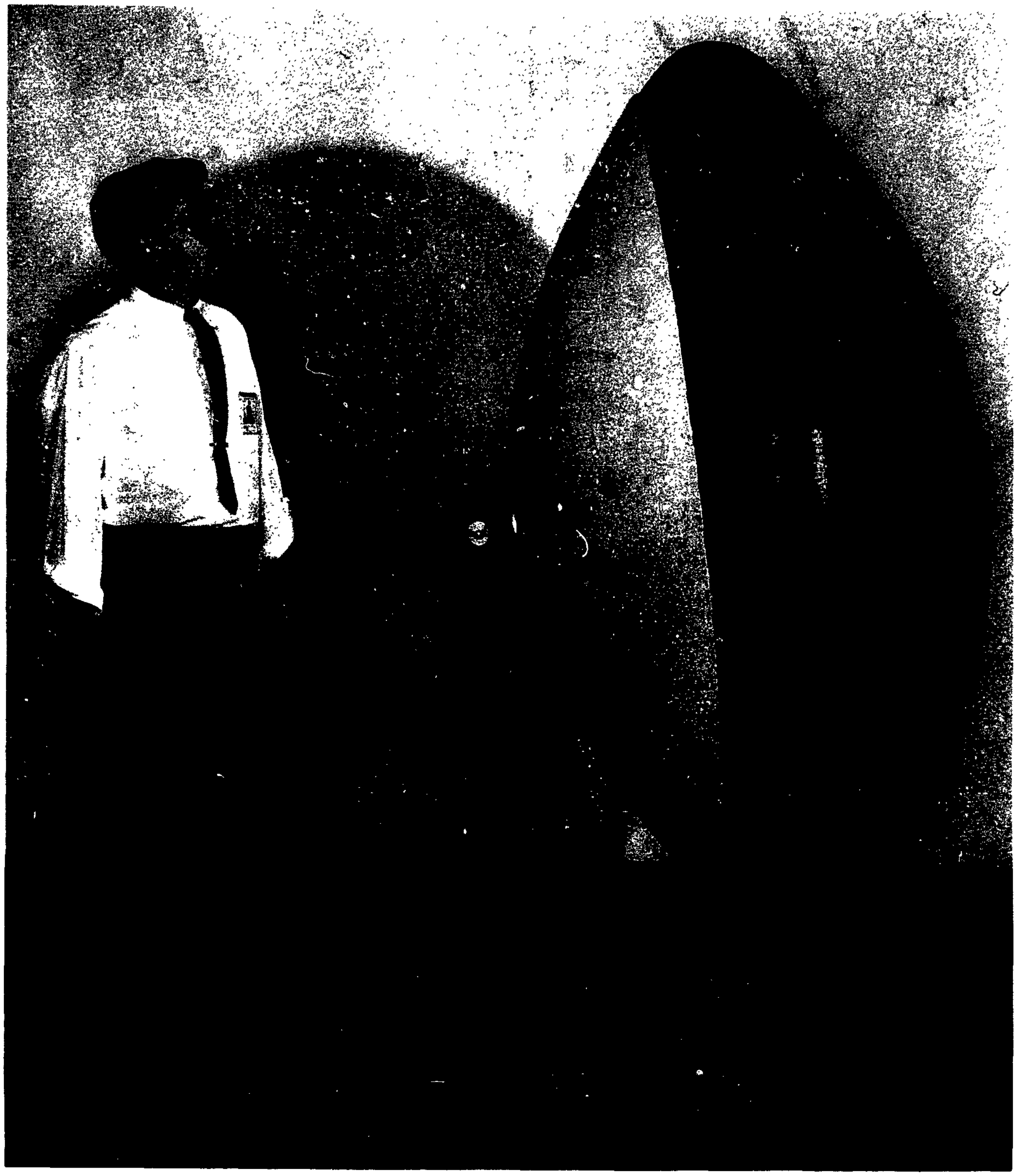

Figure 95. Inflatable Lenticular Antenna Model

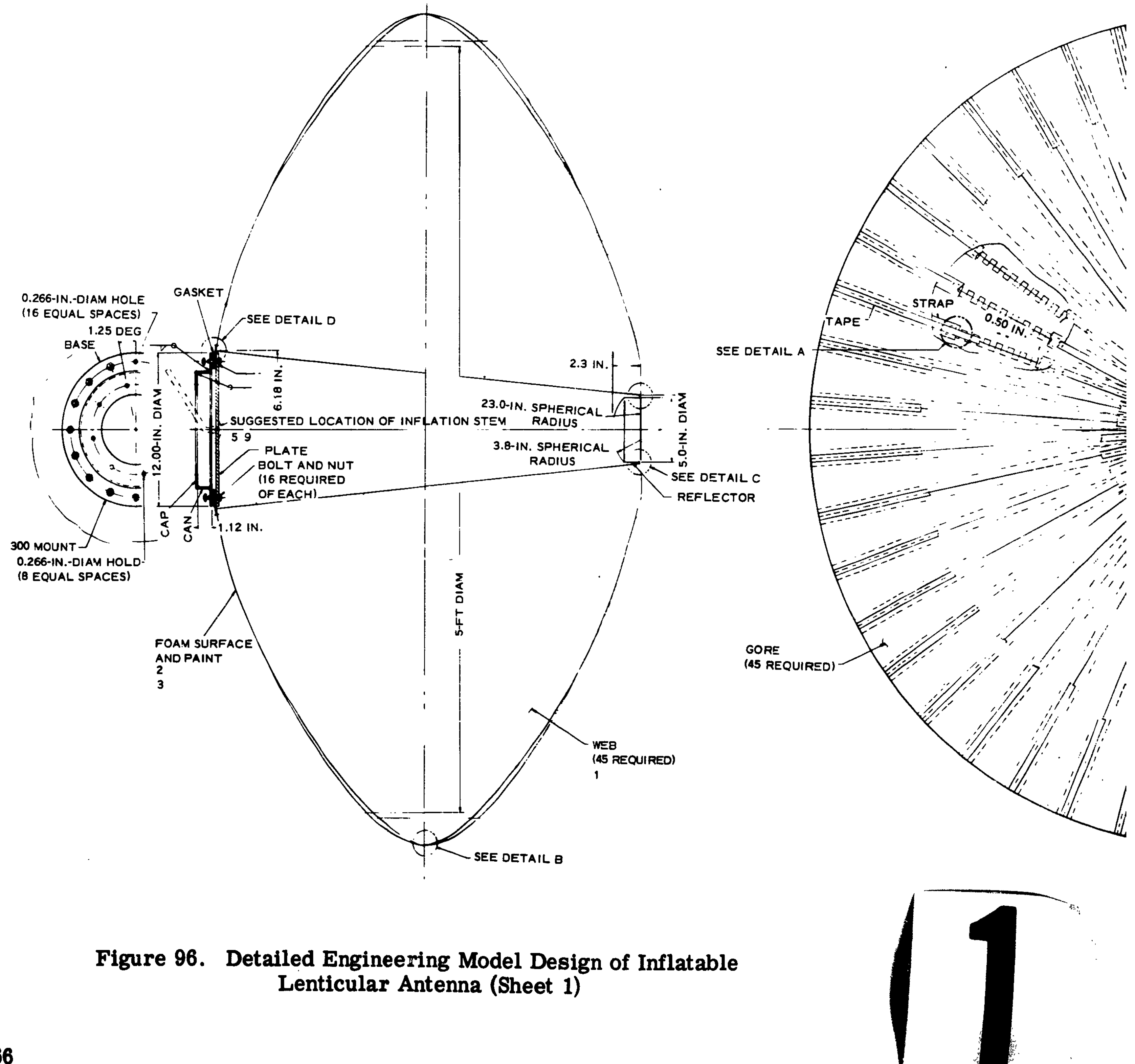

Figure 96. Detailed Engineering Model Design of Inflatable Lenticular Antenna (Sheet 1)

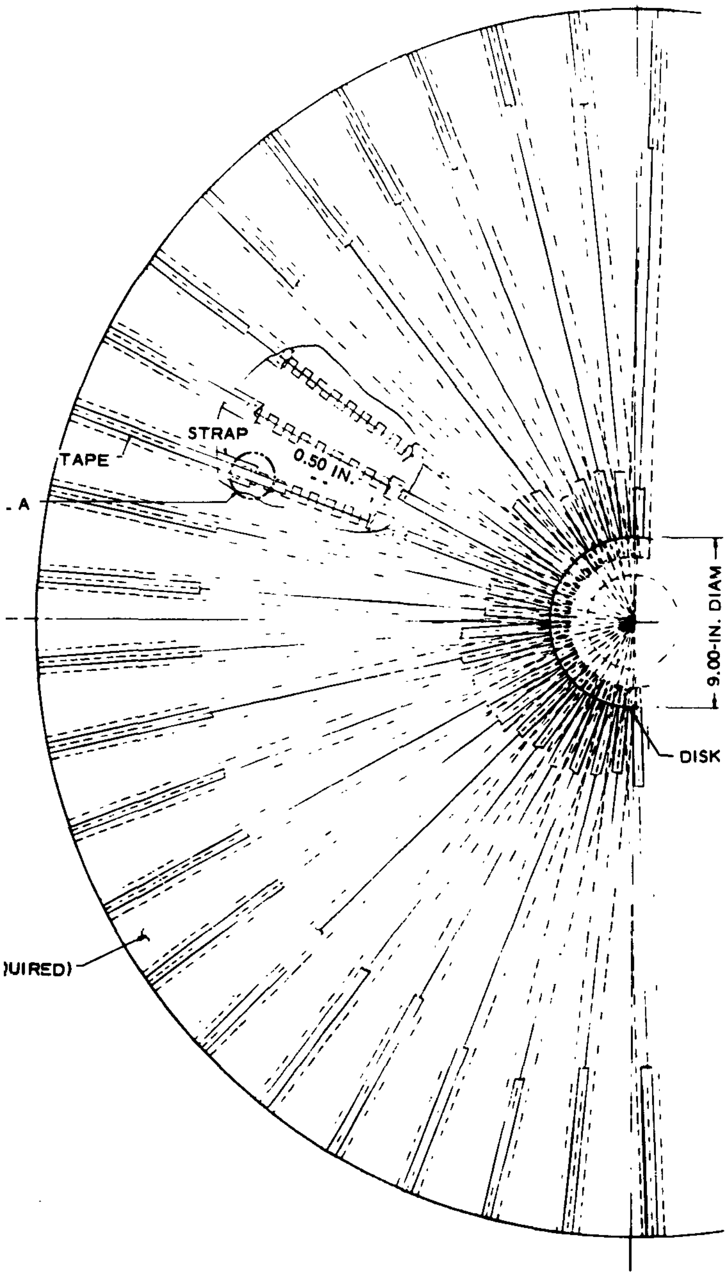

NOTES:

UNLESS OTHERWISE SPECIFIED

1. SLIT EDGE OF WEB AT 0.50-IN. SPACING TO FORM ALTERNATING FINGERS AS SHOWN
2. FLEXIBLE FOAM SURFACE (LATEX) WILL BE APPLIED ON BACK SURFACE OF ASSEMBLY
3. R-F REFLECTIVE PAINT
4. BREAK ALL SHARP EDGES OF METAL PARTS APPROXIMATELY 0.016-IN. RADIUS
5. INSTALLATION OF INFLATION STEM TO BE DETERMINED AT ASSEMBLY
6. CEMENT FABRIC TO FABRIC IN ACCORDANCE WITH GAC PROCESS SPEC. C-100 TYPE 45
7. CUT GORE PATTERN ON 45-DEG BIAS ALTERNATE WARP DIRECTION FROM GORE TO GORE
8. CUT WEB PATTERN ON 45-DEG BIAS ALTERNATE WARP DIRECTION FROM WEB TO WEB
9. "SCHRADER" CATALOG NO. TR-179 OR EQUAL

12

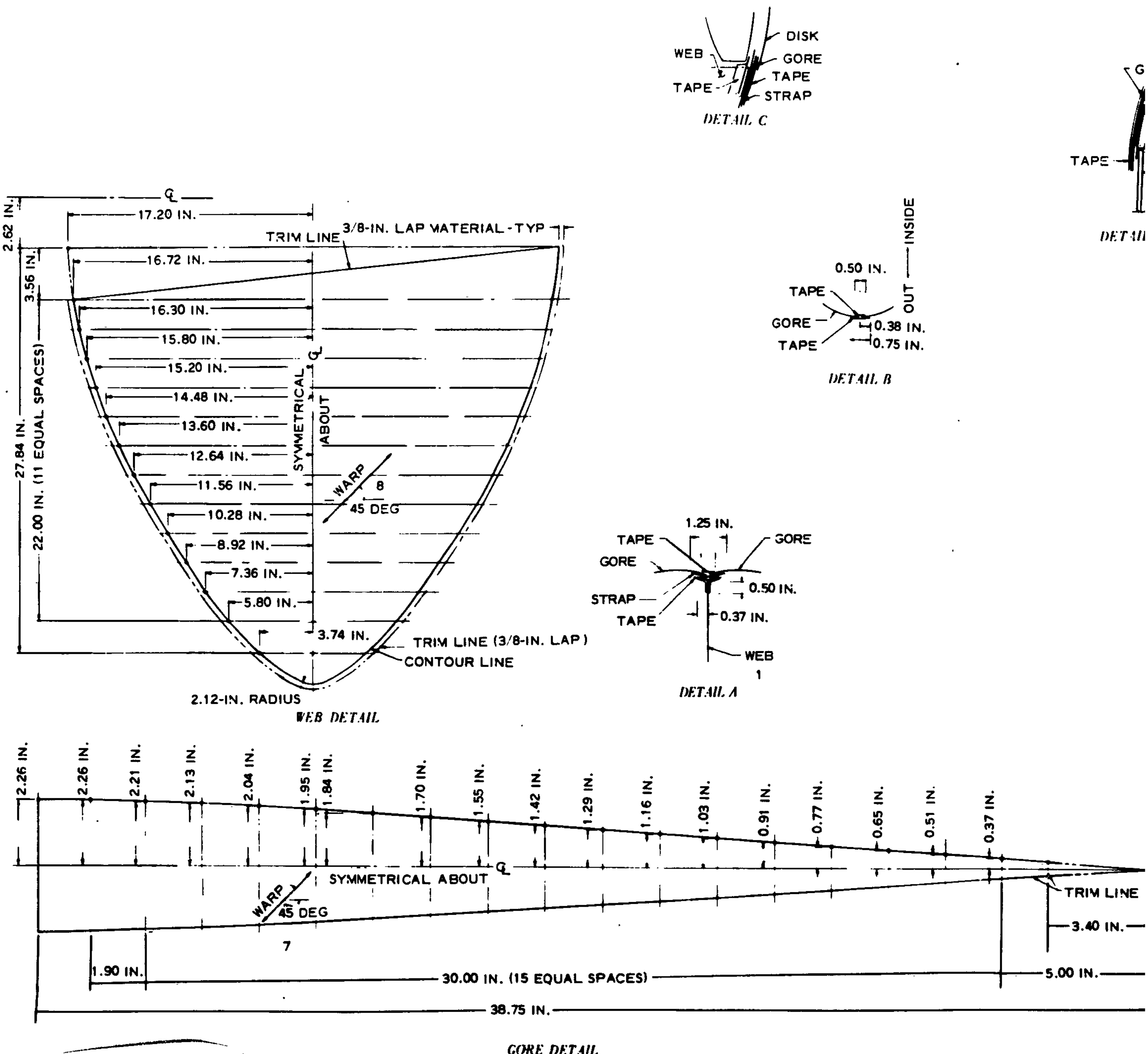

1

Figure 96. Detailed Engineering Model Design of Inflata Lenticular Antenna (Sheet 2)

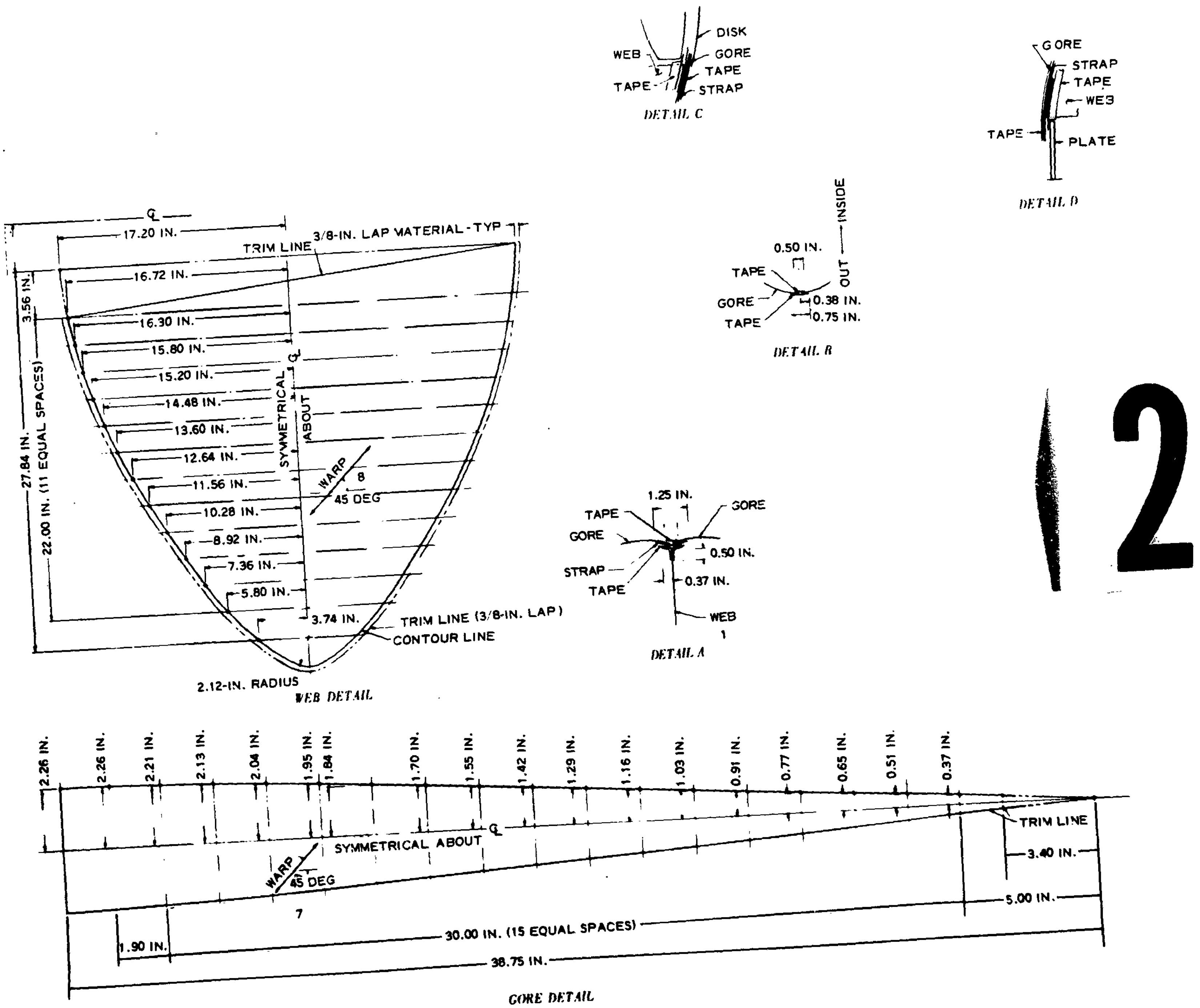

Figure 96. Detailed Engineering Model Design of Inflatable Lenticular Antenna (Sheet 2)

The rigidity at the hub attachment in this model must be attained either by having the webs physically attached to the hub and the sub-reflector or by a set of guy wires attached to the hub and sub-reflector. The lenticular model does not have either provision, since it was not originally designed for any r-f testing; consequently, this model will not demonstrate a very rigid attachment to the antenna mounting ring. On the other hand, very good rigidity of the inflatable structure is demonstrated outside the mounting ring attachment.

The inflatable structure for the lenticular model has the characteristic of having smaller lobing between the web attachment locations than the paraboloid model. This characteristic occurs because the lobing is a function of the inflatable structure thickness. The thicker the structure, the less the lobing.

3. Inflatable Structure Fabrication

The lenticular model inflatable structure was fabricated in a manner similar to the paraboloid model utilizing the radial fabric shear webs. The webs form the basic contour and resist deflection due to shear, which is the most critical with inflatable structures. Figure 97 shows the inflatable structure for the lenticular model approximately half completed.

One problem that occurred on the paraboloid model was eliminated on the lenticular model. This problem was the peeling failure of the web seams during the heat of the curing operation. The problem was not severe enough with the paraboloid to affect the final surface contour, since the foaming operation smoothed out any deviations in the inflatable structure surface. However, a design and fabrication change was made to preclude any failure on the lenticular model. Instead of having the T section of the web bonded to the inside of the gores edges, as shown in Figure 98 (A), the T section of the web was bonded to the outside of the gores. This design and fabrication change should eliminate any tendency of peel failures due to possible overloading of the cemented joints.

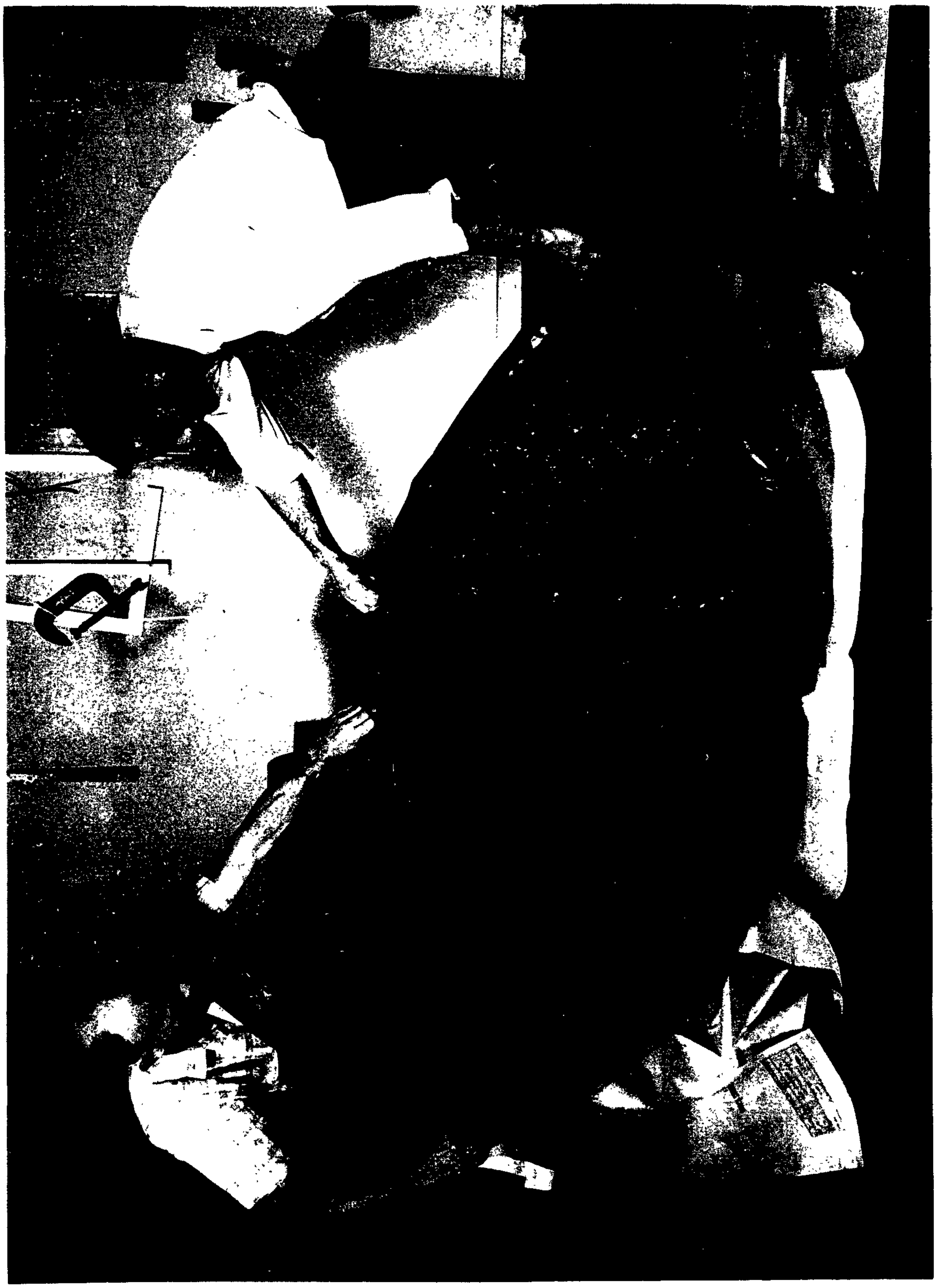

Figure 97. Partially Completed Inflatable Structure for the Inflatable Lenticular Antenna Model

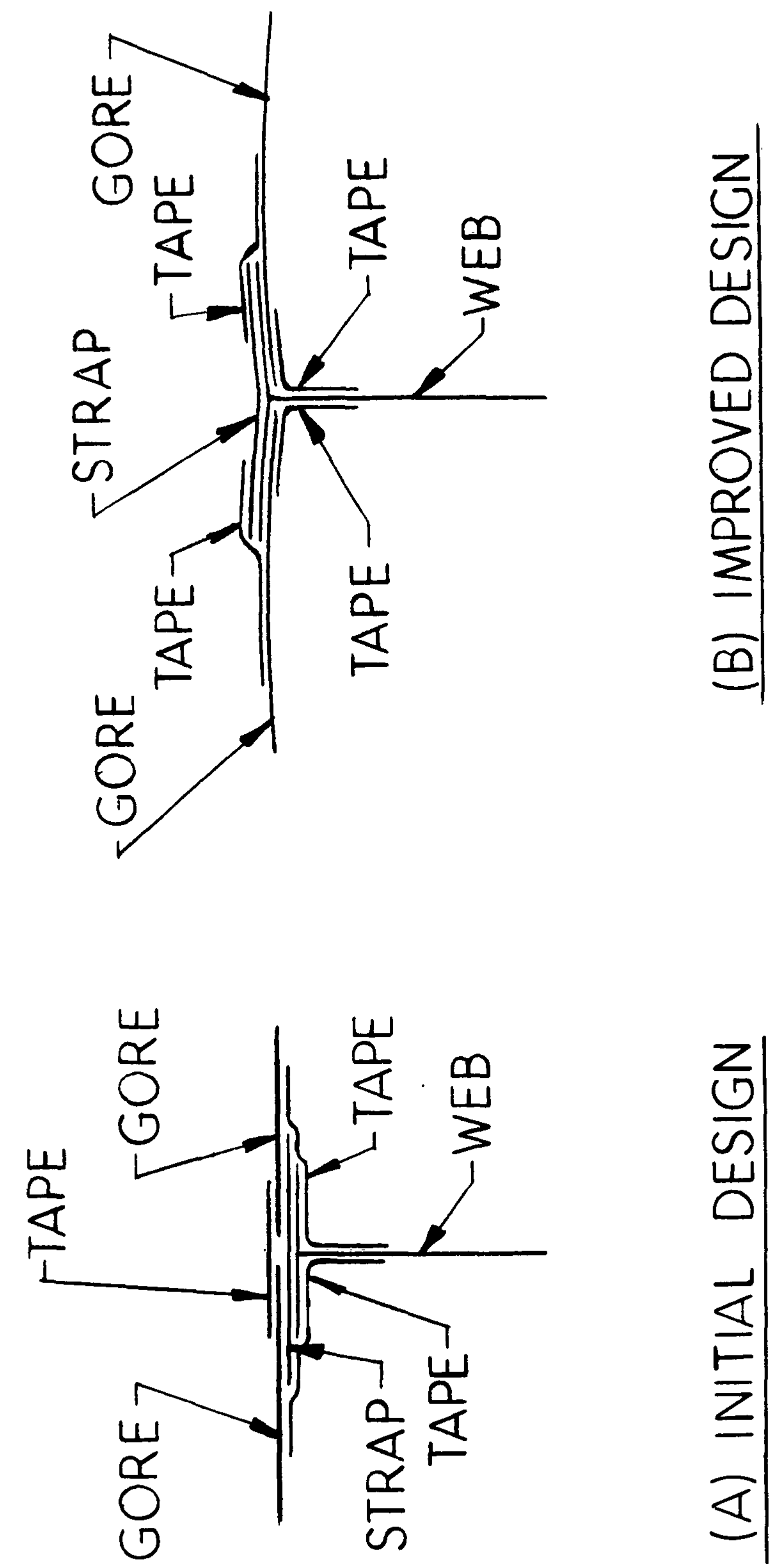

Figure 98. Web-Gore Attachment Designs

Another item that was actually a design change but occurred during the fabrication was the change in the outer ends of the webs. It was noted that the web did not have a function at the outer rim of the antenna and only added stiffness to the antenna during packaging. For this reason, the web was trimmed off at the tangency point with the outer rim. Elimination of this material reduced the weight, resulted in a smoother antenna rim without wrinkling, and allowed the model to be more packageable because of this reduced stiffness where it is not needed.

Figure 99 shows the completed inflatable structure for the lenticular model ready for the foam surface application.

4. Lenticular Model Foaming Operation

Before the surface could be applied to the lenticular model, a female mold had to be made. This was accomplished by making a three-layered "splash" of rigid polyurethane foam on the mold used for the paraboloid model. Again, a grease pencil was used to transfer index points in the event that future comparison of these points might be of some advantage.

In the previous instance of the paraboloid antenna, the foam was poured into the inverted antenna and the weight of the heavy mold was sufficient to sink it to a depth controlled by spacers giving the desired foam thickness. In the case of the lenticular model, the reverse situation existed: the foam was poured into a female mold, and the antenna structure was lowered into the foam. It was anticipated, however, that due to the light weight of the inflatable structure, weights would have to be used to force the light antenna into the foam and that these weights would cause deformation. For this reason, a similar rigid polyurethane "splash" was formed on the back of the inflatable structure to evenly distribute the load of these weights. Figure 100 shows the female mold used to form the surface contour for the lenticular model.

77.10 (5-63) REF: ENGINEERING PROCEDURE S 017

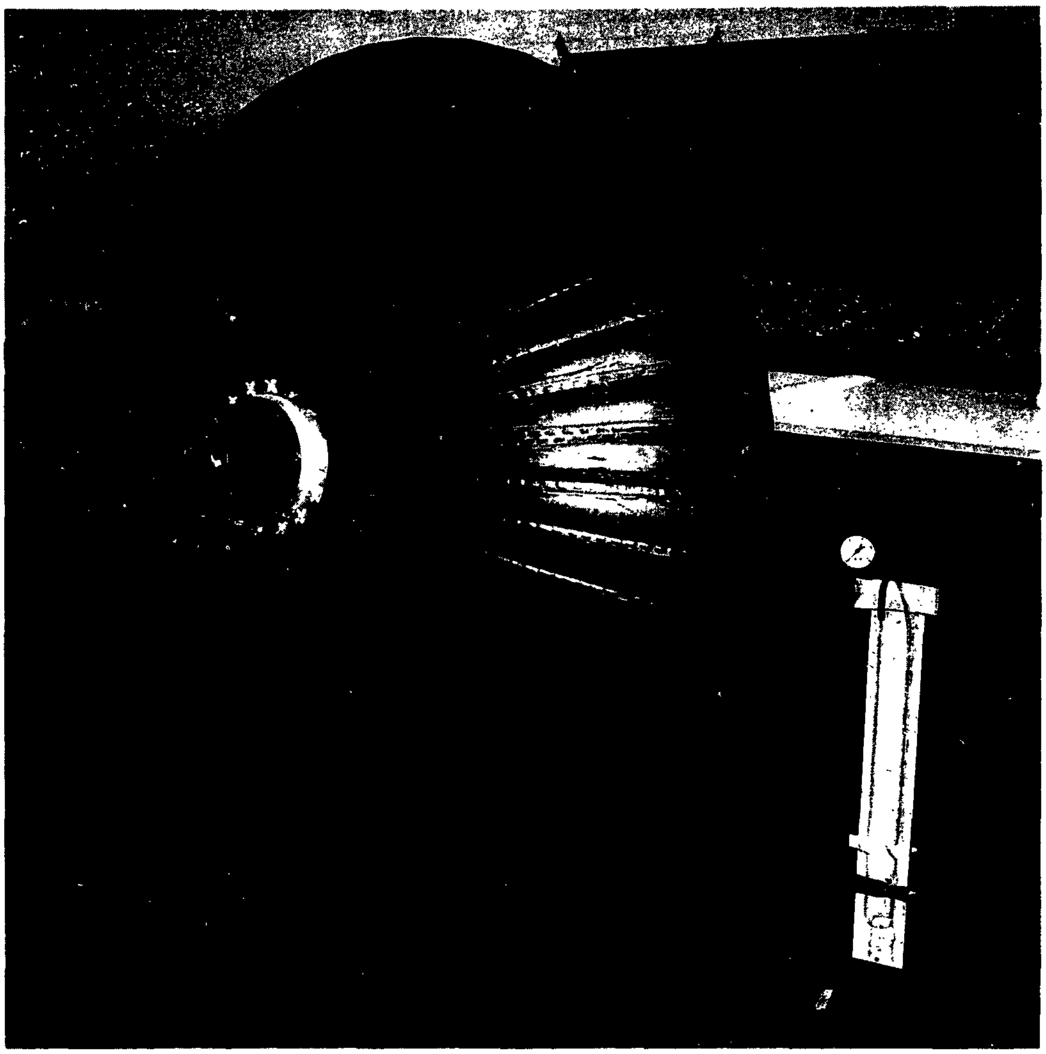

Figure 99. Completed Inflatable Structure for
Inflatable Lenticular Antenna Model

Two attempts were made to attain a satisfactory contour for this model. The first was unsuccessful because of a leak in a tube used to align the inflatable structure with the mold. Although more than enough liquid foam is supplied in the process, the leak was great enough to prevent obtaining sufficient thickness. In the second attempt, the leak was eliminated and a very good surface attained without further incident. Figure 101 shows the foamed surface of the lenticular model just after

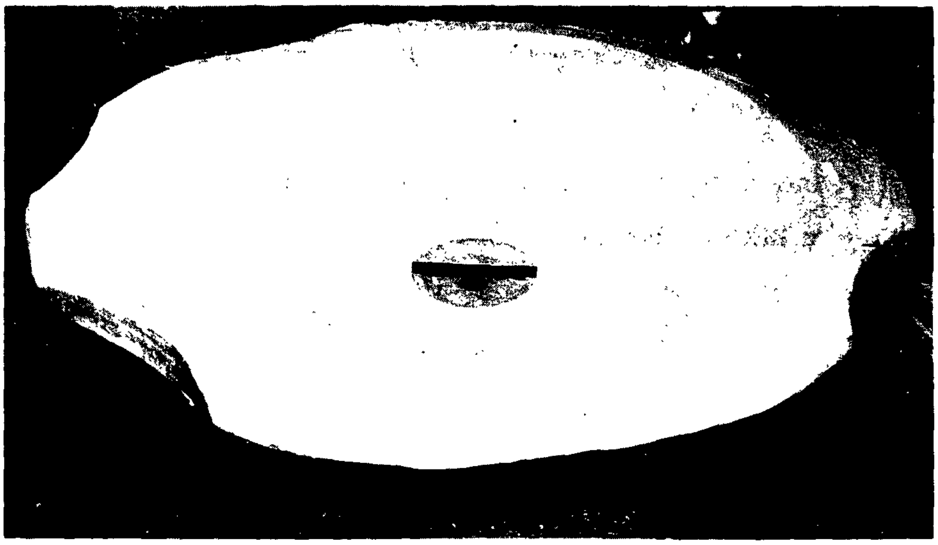

Figure 100. Female Mold Used to Form Inflatable Lenticular Antenna Model Surface

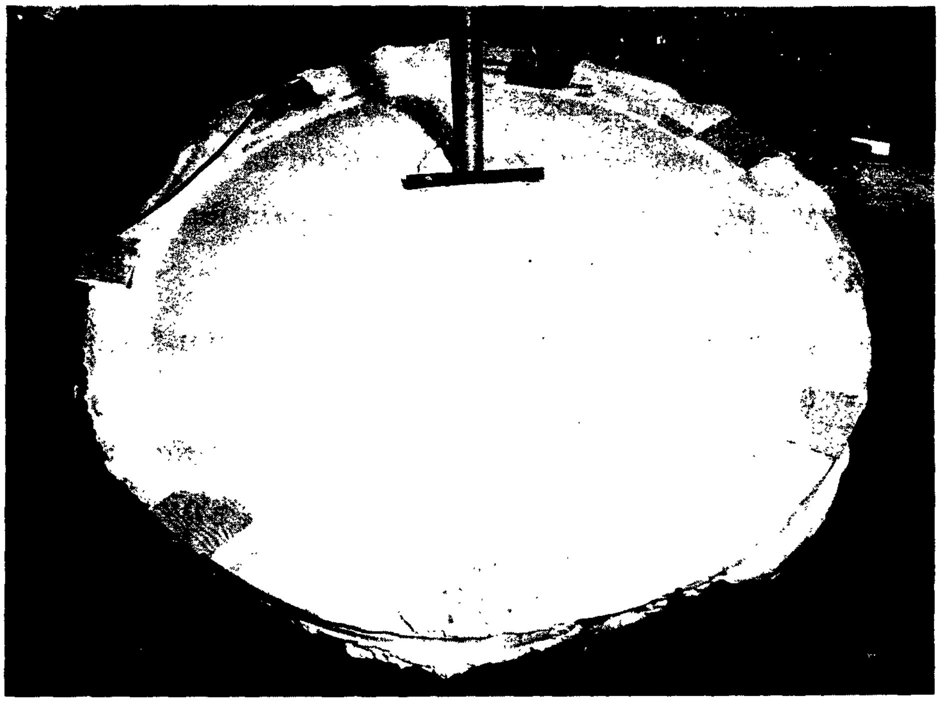

Figure 101. Lenticular Antenna Model Immediately after Removal from Mold

being removed from the mold. The edge of the foam backup structure can also be seen around the outer rim of the reflector surface.

The grease pencil index marks were also used on the lenticular model, but no measurements were taken. Because both models utilized the same foam formulation and similar application techniques, it was not believed that sufficient new information would be gained to warrant the expenditure.

D. ANTENNA MODELS REFLECTIVE SURFACE APPLICATION

The application of the r-f reflective surface to the inflatable antenna models was a simple spray painting of the two reflectors. The paint used on the lenticular model consisted of a silver powder suspended in an acrylate vehicle which was developed by a combined Goodyear Tire and Rubber Company and Goodyear Aerospace Corporation effort supported with company development funds.

This acrylate paint formulation was basically the same as that which showed such good results in the development program previously described. However, it appears that the painted antenna surface is not as good as the original test samples, probably due to some slight change in the paint formulation or variation in the flexible foam itself.

As a result of continued investigation of r-f reflective paint formulations, the Duracote Company of Ravenna, Ohio, supplied a reflective paint that also showed very good characteristics when applied to flexible foam samples. This paint utilized powdered silver in a vinyl-based vehicle. The paraboloid model was given a final application of this vinyl-based vehicle reflective paint, thus providing an opportunity for comparison with the lenticular model that was painted with the acrylate vehicle formulation. In addition, two flexible foam samples painted with the two different reflective paints were delivered with the models for examination by the Signal Corps.

E. ANTENNA MODEL PACKAGING TESTS

Preliminary packaging tests were conducted on the antenna models. As previously reported, it was known that the packaging configuration had not been optimized; however, some preliminary tests will be helpful in predicting problem areas.

Packaging testing has considered package size and shape, packaging effort required, relation of time and permanent creasing of flexible foam, and effects of creasing on r-f reflective surface.

The package size and shape have been determined for both the vacuum packages and non-vacuum packages. As shown in Figure 83(A), the vacuum packaged lenticular model is about 18" x 24" x 8". The non-vacuum package, Figure 83(B), is about 18" x 24" x 11". The vacuum packaged paraboloid model, Figure 102, is about 20" x 24" x 14" with the aluminum center hub making up a large part of the volume. Note the 12-inch scale in Figure 102. Figure 103 shows the paraboloid model packaged without the use of a vacuum bag.

The models were packaged as follows: The antenna was deflated into a flat dish. The fabric was folded twice toward the center of the dish from two opposite sides into a long slender package. Then, the long slender package was folded twice from each end toward the center. The package was then tied.

The packaging effort to fold the models into a long slender package is rather minor, but the final folds into the square package takes a little more effort. Some improvement in the models could be effected with an enlargement of the pressure inlet tube. This larger tube would allow for a reduced pressurization and deflation time, which would be desirable.

Even though a relatively lower grade of commercial latex foam was the only foam available in the desired quantities, it was still considered necessary to examine the antenna for any permanent creasing that could occur during packaging. The amount of permanent creasing is a function of time. The longer the antenna is

Figure 102. Vacuum Package of Inflatable Paraboloid Antenna Model

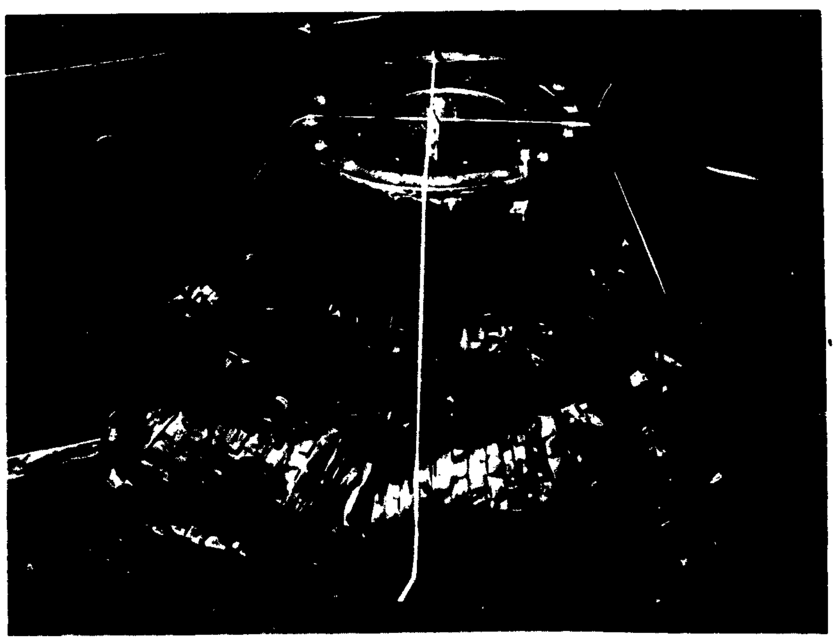

Figure 103. Packaged Inflatable Paraboloid Antenna Model

packaged, the more evident the permanent creasing will be. In addition, nearly all of this permanent creasing can be eliminated by optimization of the flexible-foam formulation. The models were folded and packaged in several different configurations before selecting one for long-term stowage.

To show the effects of time, the lenticular model was packaged for periods up to one week in duration. The effects of these tests showed no degradation in the r-f reflectivity as determined from surface resistivity measurements, but some permanent creasing in the flexible foam did occur. Some cracking of the acrylate formulation r-f reflective paint on the lenticular model was evident, which at some later date, would eventually result in loss of reflectivity. As mentioned before, this characteristic was definitely inferior to the final r-f reflective paint developed for this purpose. A slight change in the paint formulation must have occurred in the paint mixed for the antenna models.

To check the above characteristic, additional acrylate formulation paint samples were made up and applied to additional foam samples to see if a problem would result in duplicating the originally developed r-f paint. These additional samples turned out to have excellent flexibility when subjected to severe wrinkling, crumpling, and creasing, without showing any degradation in r-f reflectivity.

As mentioned previously, a vinyl vehicle r-f reflective paint was applied to the paraboloid antenna model. This particular formulation did not become available until late in the program, and time did not permit extensive packaging tests; however, packaging tests with small samples and very limited packaging of the paraboloid model indicated that this paint had excellent flexibility and resistance to cracking when folded. However, the flexibility of this new paint will not be demonstrated by the paraboloid model, since the acrylate paint is also on the surface and some permanent creasing after packaging will occur with the combination of the two reflective paints. Both types of reflective paint may be suitable after further development and final selection of an r-f reflective paint for operational antennas would be dependent on additional evaluation and testing with the final flexible foam formulation.

F. EVALUATION OF INFLATABLE ANTENNA MODELS

The completed 5-foot diameter inflatable antenna models were quite successful from the standpoint of fulfilling their design objectives.

The feasibility of forming an inflatable structure into an open dish paraboloid and into a lenticular configuration is now obviously demonstrated by the models.

Although a physical test program is beyond the scope of this program, the technique of developing shear stiffness with the use of fabric shear webs can be easily shown. This capability is demonstrated mainly by observing the stiffness and rigidity of the models and by examination of the structural analysis.

Fabrication techniques have been demonstrated by the very existence of the models.

The application of the flexible-foam surface has been demonstrated by the models and by the surface contour measurements, which show the paraboloid model to deviate about ±0.015 inch from the contour of the mold as explained in Section X.

An r-f reflective surface has been shown by the model and by a Goodyear Aerospace development program to be compatible with the flexible-foam surface, as requred for the inflatable antenna concepts.

Preliminary packaging of the antenna models has been accomplished. Although the models are bulkier than a prototype unit would be, they have definitely demonstrated their packaging capability.

PART 5. CONCLUSIONS

As a result of this design program, three antenna concepts have evolved that can fulfill the growing need for large erectable space antennas and transportable, lightweight, ground-tracking antennas.

From the standpoint of the space antennas, the Swirlabola space antenna studies have indicated the concept to be a high-gain antenna that is mechanically feasible, practical to manufacture, and quite applicable to a space vehicle with its related thermal, dynamic, and structural requirements. In addition, although a single space antenna model was fabricated, the two inflatable antennas developed as part of the ground-based antenna study also offer good potential as space antennas.

Goodyear Aerospace has evaluated 22 ground-based tracking antenna concepts of various sizes up to 40 feet in diameter. The evaluation has compared cost, packageability, weight, mobility, simplicity of erection, accuracy, reliability, mechanical performance, electrical performance, and growth potential. The two ground-based antenna systems having the best over-all potential are the inflatable paraboloid antenna and the inflatable lenticular antenna. These systems will meet best the current program objectives of low-cost, lightweight, easily packageable antennas that can be erected simply and economically on site.

In addition, several specific conclusions have evolved as a result of this program:

(1) Five-foot diameter scale models of the inflatable paraboloid antenna and the inflatable lenticular antenna have been fabricated which demonstrate the mechanical and structural feasibility and indicate potential packaging and erection capability and potential contour accuracies by closely duplicating the antenna contour tooling.

(2) The inflatable paraboloid antenna concept, in particular, offers excellent potential for use as a quickly erectable, lightweight, packageable mobile antenna system.

(3) The utilization of the fabric web structural concept provides a practical, economical, and structually sound design for the inflatable antennas.

(4) It appears that highly accurate paraboloid surface tolerances can be held with the utilization of the molded flexible-foam concept.

(5) Flexible r-f reflective paints have been developed. These paints, which can be applied to a flexible-foam surface, will maintain their flexibility and r-f reflectivity even after severe folding, wrinkling, and rolling.

PART 6. RECOMMENDATIONS

Many research and development programs result in an interesting review of the state-of-the-art or in a new approach to an old problem and are necessary to normal evolution. Goodyear Aerospace, however, under Contract DA-36-039-SC-90746, has generated two completely new antenna concepts that use pressurized fabric as the structural material: the inflatable paraboloid antenna and the inflatable lenticular antenna. Both concepts show considerable potential as lightweight mobile antennas suitable for a wide range of applications, including use as a highly mobile radio-relay, troposcatter, or tracking antenna system.

To investigate this potential, Goodyear Aerospace recommends that further investigation be made to include a test program that will establish the detail r-f characteristics of the two antenna concepts and determine their operational capability under anticipated environmental conditions.

Specifically, Goodyear Aerospace recommends that a follow-on investigation should include the fabrication of a 10-foot diameter inflatable paraboloid antenna prototype model to be used for r-f testing. The r-f testing should determine pattern characteristics (gain, side lobes, and beam width), the type and effect of mechanical tolerances, packaging and erection capabilities throughout the expected environmental temperature range, and the effect of packaging and erection on electrical performance.

In addition, it is also recommended that a future program also be implemented to fabricate a prototype Swirlabola antenna for testing the erection and operation under simulated space conditions, and to determine the electrical performance by range pattern tests.

PART 7. IDENTIFICATION OF PERSONNEL

A. PROGRAM MANHOUR BREAKDOWN

Table VII lists the manhour totals used by key personnel during the course of the program.

Table VII. Manhour Breakdown for the Program

PERSONNEL		MANHOURS
Name	Title	
Collins, D. D.	Project Engineer	1104
Bell, J. C., Jr.	Assistant Project Engineer, R & D Coordination	896
Benner, W.	Space Systems Engineering	165
Roth, J.	Space System Engineering	218
Ahart, A. P.	Stress Analysis	96
Houmard, J. E.	Stress Analysis	257
Huber, J.	Microwave Engineering	207
Koller, W. B.	Microwave Engineering	238
Godwin, D. L.	Microwave Engineering	78
Fretz, G.	Plastics Engineer	120
	Total	3379*

*Total represents only those hours used by key personnel and does not include all hours expended on the program.

B. PERSONNEL RÉSUMÉS

Name: Collins, D. D.

Education: B. S. in mechanical engineering, 1936, Tri-State College, Angola, Indiana; courses in aircraft electrical and radio engineering, 1940 to 1943, Johns Hopkins University, Baltimore, Maryland; courses in aircraft stress analysis, 1945 to 1947, University of Maryland, Baltimore, Maryland.

Experience: Mr. Collins has over 24 years of experience in aircraft engineering and design and in electrical and electronics systems. Recently, he has been project engineer for research and development antenna contracts and Goodyear Aerospace funded investigations of new antenna systems.

As group engineer and design section head, Mr. Collins was responsible for complete electrical and electronic systems for large military attack ASW and AEW aircraft in the HTA, LTA, and missile (SUBROC) fields. These systems included communications, navigation, ecm radar, and antennas. He has served as manager of LTA project engineering, a job that involved (1) technical coordination with specialized design and analytical groups and with military technical branches and (2) engineering administration and management on an over-all project basis.

Name: Bell, J. C., Jr.

Education: Mathematics and physics, 1953, California State College, California, Pennsylvania; B. S. in engineering science, mathematics major, 1957, Fenn College, Cleveland, Ohio.

Experience: Mr. Bell has six years of experience in the Goodyear Aerospace Aero-Mechanical Research and Development Department. Presently, he is assistant project engineer on the antenna study program for the Signal Corps and coordinates the research and development for that program. In addition, he has recently coordinated a Goodyear Aerospace funded inflatable antenna systems development program.

Mr. Bell's work has included development engineering and technical proposal efforts on inflatable telescoping antennas, whip antennas, communications repeater systems, and hardened antenna systems. He has coordinated all engineering on such projects and has made numerous contributions to the design and development of various types of antenna systems.

Mr. Bell also has had development and project engineering experience in escape capsule systems for high-performance aircraft, re-entry vehicle drag decelerator systems, and space station and re-entry vehicle research. This work involved the coordination of parametric studies on various systems and included investigation of launch vehicles, orbital mechanics, orbital control and stabilization, subsystems and their environments, high-resolution photography, human factors studies, and radar cross-section studies relative to absorption, reflection, and attenuation of microwave radiation.

Name: Benner, W.

Education: B. S. in chemical engineering, 1947, B. S. in electrical engineering, 1949, Washington University, St. Louis, Missouri; M. S. in electrical engineering, 1957, University of Michigan, Ann Arbor, Michigan.

Experience: Mr. Benner directed the development of space microwave structures and antennas in the Goodyear Aerospace Astronautics Systems Department. Before joing Goodyear Aerospace, he participated in design, planning, and proposing of electronics for space projects and gained knowledge of antenna design and integration problems for space work. Previous experience includes research coordination of tri-service research and development funding on battle-field surveillance. He has also conducted Project Michigan Radar Research Review, high-resolution radar studies and circuit design, technical write-up and systems design of an air defense integrated system, and circuitry development of air defense radars. A registered professional engineer, Mr. Benner is a senior member of the Institute of Electrical Engineers, and a member of American Rocket Society, American Radio Relay League, and the American Meteorological Society.

Name: Roth, J.

Education: B. S. E. E., 1959, University of Toledo; courses toward advanced degree, 1960, University of Akron.

Experience: At the present, Mr. Roth is a member of the space microwave structures and antennas group of the Astronautic Systems Department. He is responsible for company-advanced R & D efforts in the area of lightweight deployable space antennas. In this regard, he is also directing efforts on the theoretical and experimental determination of the reflectivity of electromagnetic energy by lightweight wire-grid bodies, particularly spheres. In the past, he has been concerned with antenna and communication system problems, in connection with AEW airships, the development of the Goodyear Space Station, and with similar problems under Air Force Contract on recoverable booster system studies and strategic orbital system studies.

Name: Houmard, J. E.

Education: B. S. in civil engineering, 1957, Purdue University, West Lafayette, Indiana; M. S. in civil engineering, 1958, Purdue University, West Lafayette, Indiana.

Experience: As a member of the research and development group in the Goodyear Aerospace Stress Analysis Department, Mr. Houmard has actively participated in the development of theoretical methods for stress analyses of inflatable structures such as AIRMAT and has conducted experimental work for the verification of these theories. He has conducted structural analyses for development programs such as for expandable re-entry vehicles, space stations, and flexible helicopter rotor blades. Recently, he has been responsible for the structural analyses of foam-rigidized solar concentrators and has done the stress and deflection studies for 10-foot diameter and 44.5-foot diameter concentrators.

Name: Koller, W. B.

Education: B. S. in Mathematics, 1957, Florida State College.

Experience: Mr. Koller is a Senior Development Engineer in the Goodyear Aerospace Microwave Laboratory. He has for the past five years worked in the microwave communications systems field. Presently he is studying various antenna and antenna range accuracies and is directing a range accuracy analysis of all Goodyear Aerospace antenna ranges. He has worked on the following projects: Defense Communication Control System, Caribbean Keying Link, Criticomm, Aircom, and Siskyow Telephone Company Microwave System. He was a lead engineer on the Siskyow System where he designed and installed the complete r-f microwave system.

Name: Huber, J.

Education: B. S. in electrical engineering, 1957, M. S. in electrical engineering, 1957, Massachusetts Institute of Technology, Cambridge, Massachusetts.

Experience: Mr. Huber is an antenna engineer assigned to the Radiation Systems Group. He has developed shaped-beam antenna systems for airborne use and has conducted investigations on periodic antennas for space applications. He has worked with artificial dielectric material for approximately two years. He has been associated with the radar detection study program and is familiar with its technical and administrative aspects.

Name: Ahart, A. P.

Education: B. S. in civil engineering, 1950, Ohio University, Athens, Ohio; additional work in vibration analysis, University of Akron, Akron, Ohio.

Experience: As a stress analyst with Goodyear Aerospace, Mr. Ahart has acquired extensive experience in the stress analysis of all types of structures and materials. He has had the responsibility for detail structural analysis for component structures for numerous radar antennas including 6B, AN/SPG-47, AN/SPQ-5, FPS-3, and FPS-6. He has also had the responsibility for detail analysis of F-101 empennage components and wrote the analysis of the B-52G nose radome. He has worked on the development of methods of analysis for airship suspension systems. He was responsible for the development of the blast loads on the Nike-Zeus LAR transmitter and receiver antennas and the dynamic response of these antennas to the blast loads.

Name: Godwin, D. L.

Education: B. S. in mechanical engineering, 1958, G. M. Institute, Flint, Michigan; B. S. in electrical engineering, 1961, Masters in Electrical Engineering, 1962, Texas A and M, College Station, Texas.

Experience: Mr. Godwin is a development engineer at Goodyear Aerospace Corporation. His work has included study of tolerance effects on radiation patterns of apertures and establishment of a cross-section range. His work in school included two unpublished papers on a feed for paraboloids and a study of rhombic antenna admittances. His research assistanceship was in antennas and microwaves. He is a member of Eta Kapp Nu, Institute of Radio Engineers, and the I. R. E. professional group on antennas and propogation.

Name: Fretz, G.

Education: B. S. in mechanical engineering, 1940, University of Akron, Akron, Ohio.

Experience: For the past five years, Mr. Fretz has concentrated on large ground radomes, radar reflectors, and large reinforced-plastic structures.

Mr. Fretz has extensive experience in plant layout, organization, and production, as well as in the design and development of both military and commercial products. He has organized and administered such production units as the P-38 tail assembly department, the F6F wing section department, a steel kitchen cabinet production line, and an aircraft container welding department. Some of these operations have included as many as 400 employees. He was one of the engineers involved in the development of BONDOLITE and its applications to numerous aircraft and antenna products. As manager of BONDOLITE engineering, he was responsible for all engineering efforts in bonded assembly, quality control, scheduling, production, and sales.

Mr. Fretz is the author of several symposium papers and published technical articles. He is a registered professional engineer and a member of Sigma Tau National Engineering Honorary Society.

PART 8. REFERENCES

1. Jasik, Antenna Engineering Handbook, McGraw-Hill, N. Y., 1961.
2. Gray, C. L., "Estimating the Effect of Feed Support Member Blocking on Antenna Gain and Side-Lobe Level", soon to appear in Microwave Journal.
3. Jacobsen and Ayre, Engineering Vibrations, McGraw-Hill, N. Y., 1958, p 163.
4. Tinge Li, A Study of Spherical Reflectors as Wide Angle, Scanning Antennas, IRE Professional Group on Antennas and Propagation, AP-7, July 1959, p 223 - 226.
5. Van Buskirk, L. F., and Hendrix, C. F., The Zone Plate as a Radio Frequency Focusing Element, IRE Professional Group on Antennas and Propagation, AP-9, May 1961.
6. Hannan, P.W., PGAP, Volume AP-9, March 1961, pp 140 - 153.
7. Silver, S., "Microwave Antenna Theory and Design", MIT Radiation Lab Series, Volume 12, p 364.
8. Doundoulakis and Gethin, "Far Field Patterns of Circular Paraboloidal Reflectors", I. R. E. National Convention Record, 1959, pp 155 - 173.
9. Boardmann, W. J., Feed and Secondary Radiation Patterns Associated with Parabolic Reflector Type Antennas, 6 September 1962, GAC AP 106320.
10. Ruze, J., Physical Limitations on Antennas, MIT Technical Report No. 248, 30 October 1952.
11. Jasic, H., Antenna Engineering Handbook, McGraw-Hill, 1961, pp 2 - 9.
12. Collins, D. D., and Bell, J. C., Jr., Third Quarterly Progress Report on Advanced Antenna Design Techniques, GER 11045, Goodyear Aircraft Corporation*, Akron, Ohio, 28 March 1963.
13. Collins, D. D., and Bell, J. C., Jr., Second Quarterly Progress Report on Advanced Antenna Design Techniques, GER 10979, Goodyear Aircraft Corporation* Akron, Ohio, 29 January 1963.

*Now Goodyear Aerospace Corporation.

14. Timoshenko, S., Strength of Materials, Part II, Third Edition, D. Van Nostrand Company, New York, March 1956.

15. Topping, A.D., Analysis of Prismatic AIRMAT Structural Members, GER-9875, Goodyear Aircraft Corporation*.

16. McComb, H.G. Jr., and Leonard, R.W., "Slanted Drop Cords in Inflatable Airmat Beams", Journal of the Aerospace Sciences, Volume 29, April 1962, p 476.

*Now Goodyear Aerospace Corporation.

APPENDIX I. AIRMAT PARABOLOID STRUCTURAL ANALYSIS

A. GENERAL

The AIRMAT paraboloid deflection analysis was made to assist in establishing the structural configuration and the type of material required to limit the antenna deflections within the specified limits for a Class III antenna.

Since the AIRMAT paraboloid antenna will be the first application of diagonal drop threads in AIRMAT structure, a very extensive stress and deflection analysis could be made on this antenna configuration. To minimize expenditures and to reduce the amount of effort required for this analysis, several simplifying assumptions were made. However, the assumptions made are mostly conservative in nature; therefore, they do not affect the results adversely, since we are attempting to determine the feasibility of the concept. The first assumption is that this deflection analysis is based on a circular flat plate instead of a paraboloid. This flat plate assumption is conservative since a paraboloid dish is inherently a better structure than a circular flat plate. The second assumption is that a constant AIRMAT thickness is assumed. This assumption is not critical since the AIRMAT thickness can be any thickness that is desired. However, in the actual design, the thickness would probably be tapered, since the same thickness at the edge of the dish would not be required to resist bending and shear deflection as is required near the antenna hub. Another assumption is that 96 pairs of radial warp wires and their drop wires are considered as cantilevered from the center hub. In this case, actually more than 96 radial wires would be utilized; some additional support would be provided by the adjacent radial members, and some hoop tension would be carried in the AIRMAT skins.

Two antenna sizes were analyzed here: a 40-foot diameter antenna and a 20-foot diameter antenna. These antennas are discussed in the following paragraphs.

B. FORTY-FOOT DIAMETER REFLECTOR

1. General

The primary structure is a metal AIRMAT composed of stainless steel warp and fill wires of equal diameter, d_c, and slanted stainless steel drop threads of diameter d_d. The warp wires of the cover plies are oriented along radial lines, and the fill wires form a series of circular hoops to provide hoop tension and compression carrying ability. Ninety-six pairs of radial warp wires and their rows of drop wires are considered as cantilevered from an 8-foot diameter hub as shown in Figures 1-1 and 1-2. The AIRMAT depth is taken as 5 feet, so that there are essentially 96 radial trusses 16 feet long and 5 feet deep.

The 4-inch spacing of the hoop wires is compatible with the spacing of the drop wires and has been chosen as a realistic minimum spacing from a fabrication viewpoint. The resulting hoop stiffness should be more than adequate for deflections due to symmetrical loadings. This analysis for the antisymmetrical part of the loading is then conservative, since the spacing of the hoop wires may probably be increased and/or their diameters decreased. On the other hand, the excess weight of the hoop wires may very possibly be compensated for by the weight of bias plies required for shear stiffness under shear and torsional loadings, which are not considered in this preliminary analysis.

The slanted drop threads (or diagonals of the radial trusses) provide shear stiffness and hold the cover plies the prescribed distance apart. The angle, θ, between the drop thread and the normal to the surface is taken as 33.7 degrees, which results from an interval of every 10 of the 4-inch spaces as shown in Figure 1-2. This arrangement requires the attachment of 10 pairs of drop wires

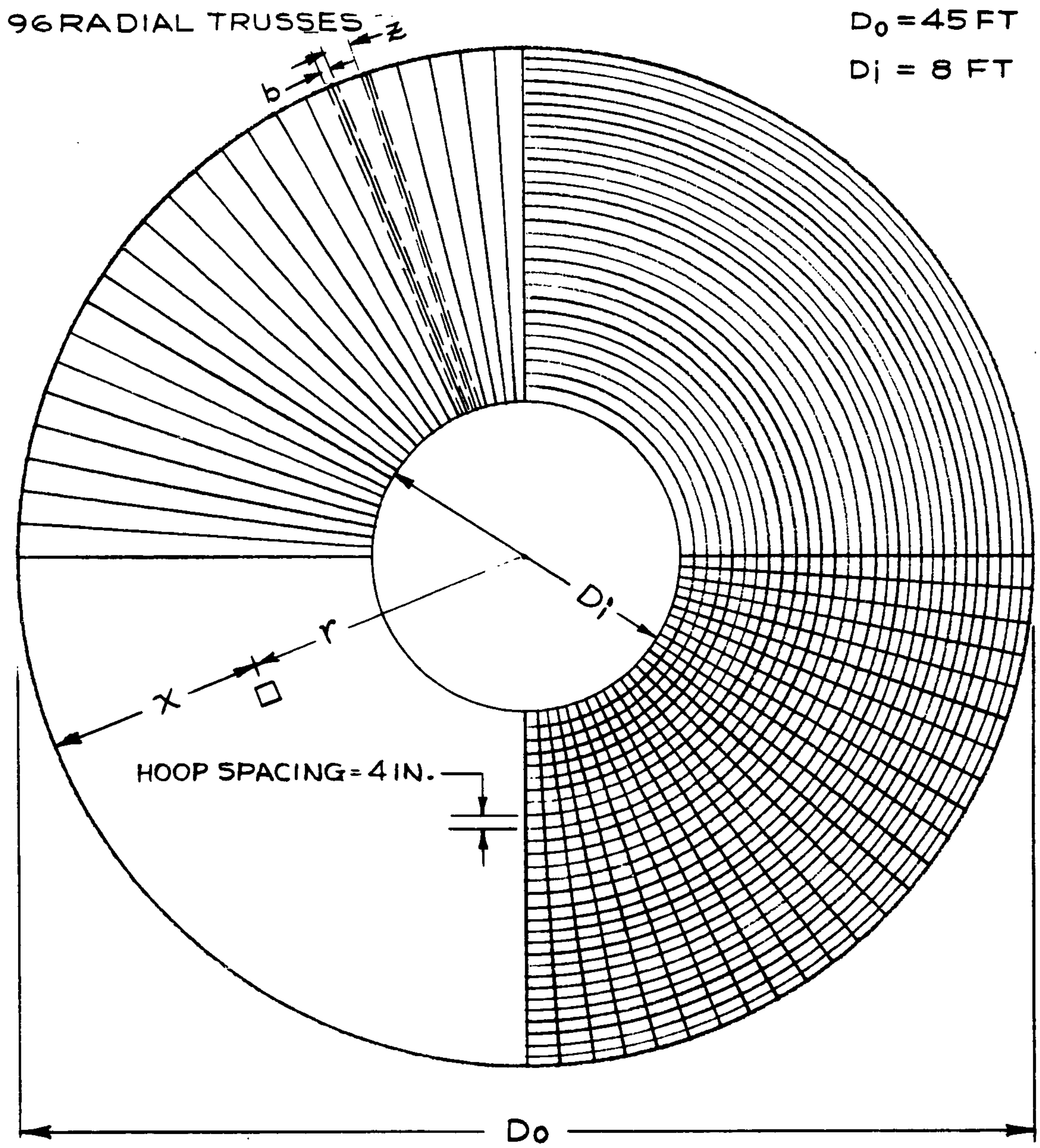

Figure 1-1. Primary Structure Configuration

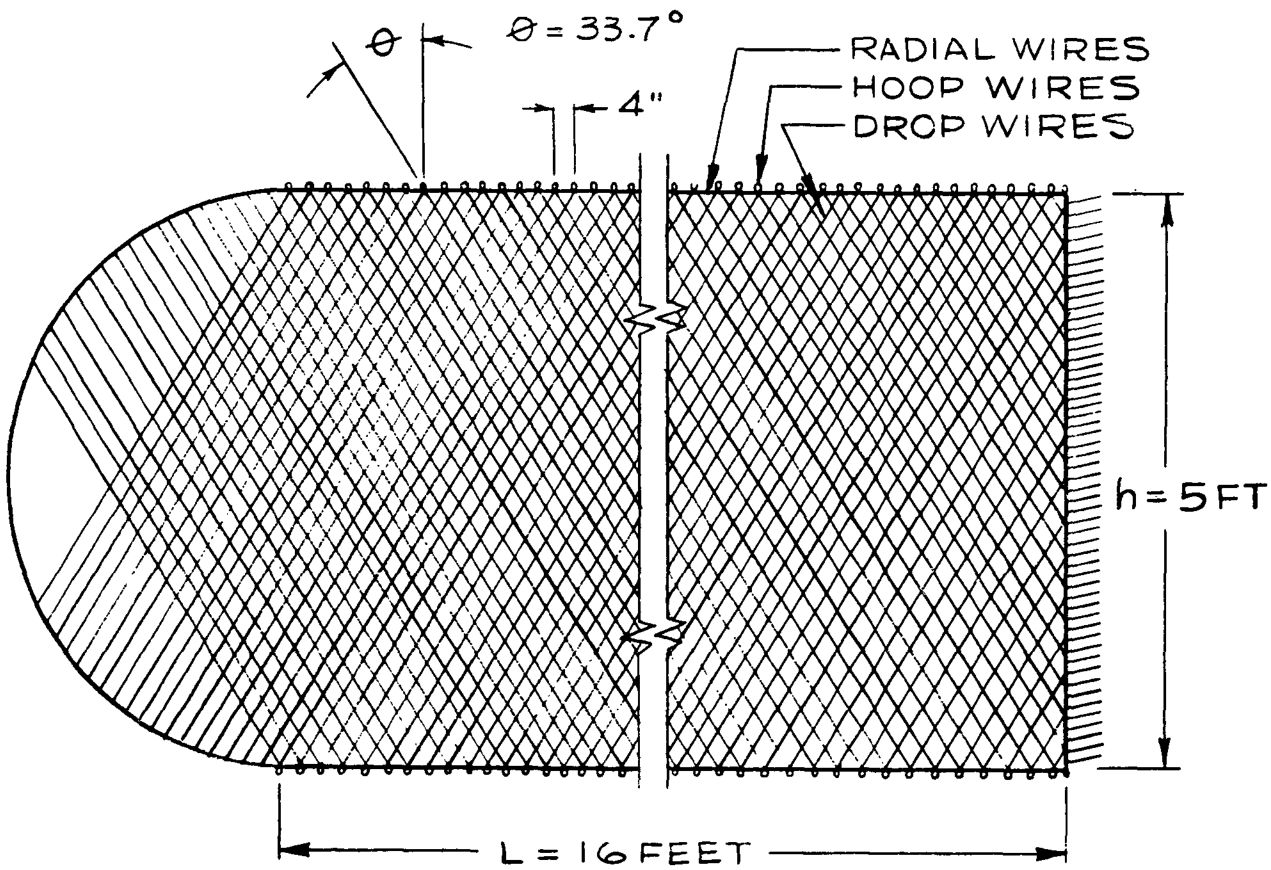

Figure 1-2. One Radial Truss

along the length of the hub and adequate tie off at the tip of the beam to obtain complete efficiency of the slanted drop wires.

2. Loads

Consider the loaded area supported by one radial beam. This trapezoidal area is divided into a rectangle of area, A_r, of width, $b = \pi$, and length, L; and a triangle of area, A_Δ, of altitude, $Z = H\pi$, and base, L. Then, from Figure 1-1, the running load per foot on the beam is

$$w_r = (\pi/12)\gamma = 0.262\gamma \text{ lb/ft} \tag{1-1}$$

and

$$w_\Delta = \frac{2\pi r - 8\pi}{(96)}\gamma = \frac{\pi(r-4)}{48}\gamma \text{lb/ft},$$

or in terms of x,

$$w_\Delta = \frac{\pi(16-x)}{48}\gamma = 0.0656(16-x)\gamma \text{lb/ft} \tag{1-2}$$

where γ = unit weight in lb/ft^2.

a. Unit Weight Estimate

For 1/2 in. of 5-pcf foam,	$\gamma_f = 0.2 \text{ lb/ft}^2$
Assume that weight of reflective surface is	$\gamma_c = 0.07 \text{ lb/ft}^2$
Steel hoop wires at 4-in. spacing (2 sides), where A_c = cross-sectional area of one wire in in.^2,	$\gamma_h = 20.4 A_c \text{ lb/ft}^2$
Fabric required to contain inflation gas is assumed equal to hoop wire weight, or	$\gamma_n = 20.4 A_c \text{ lb/ft}^2$
Estimating 15 percent of $(\gamma_h + \gamma_n)$ for seams,	$\gamma_s = 6.2 A_c \text{ lb/ft}^2$
Total,	$\gamma = 47 A_c + 0.27 \text{ lb/ft}^2$ (1-3)

b. Unit Beam Weight Estimation

Two radial wires, $w_r = 24(0.283)\ A_c$ $= 7\ A_c$ lb/ft

Drop wires, $w_d = (20)\ (2/\sin 33.7^o)\ (0.283)\ A_d$ $= 123\ A_d$ lb/ft

Drop wire connections (estimated as 5 percent drop wire weight), $w_c = 0.05\ (123\ A_d)$ $= 6\ A_d$ lb/ft

Total unit truss weight, w_t, $= 129\ A_d + 7\ A_c$ lb/ft (1-4)

c. Inertia Loads. For the specified acceleration of $6^o/\sec^2$ and for the truss ($\alpha = 6\pi/180 = 0.1.05$ rad/sec^2), the inertia loads, by Equations 1-1 and 1-2, are

$$w_{rg} = (0.262)\ (0.105/32.2)\ (20 - x)\gamma \quad (1\text{-}5)$$
$$= 0.000855\ (20 - x)\gamma\ \text{lb/ft},$$

$$w_{\Delta g} = (0.0656)\ (0.105/32.2)\ (20 - x)\ (16 - x)\gamma \quad (1\text{-}6)$$
$$= 0.000214\ (20 - x)\ (16 - x)\gamma\ \text{lb/ft},$$

and

$$w_{tg} = (0.105/32.2)\ (20 - x)\ w_t = 0.00326(20 - x)\ w_t\ \text{lb/ft}. \quad (1\text{-}7)$$

The antisymmetrical loading condition is now considered. The beam is divided into 2-foot increments, and the combined concentrated normal and tangential loads on each increment are determined in Table 1-1 by considering the approximate slope at each increment for a paraboloid of focal length, f = 14.3 ft (see Figure 1-3).

The parabola is defined by

$$r^2 = 4fy = 4(14.3)y = 57.2y. \quad (1\text{-}8)$$

The slope is

$$\phi = \tan^{-1}\ (r/28.6). \quad (1\text{-}9)$$

Table 1-1. Combined Normal and Tangential Loads

1 x	2 Approx r	3 ϕ	4 $P_{w\Delta}$ (by Eq 1-2)	5 P_{1g}	6 P_t = 5 cos 3	7 P_{n1g} = 5 sin 3	8 P_n = 7 + Eq 1-5, 1-6, and 1-7
0	19	$33^\circ 37'$	1.968γ	$2w_t + 2.492\gamma$	$1.665w_t + 2.075\gamma$	$1.11w_t + 1.385\gamma$	$1.234w_t + 1.54\gamma$
2	17	$30^\circ 45'$	1.705γ	$2w_t + 2.229\gamma$	$1.72w_t + 1.92\gamma$	$1.025w_t + 1.14\gamma$	$1.136w_t + 1.264\gamma$
4	15	$27^\circ 42'$	1.443γ	$2w_t + 1.967\gamma$	$1.775w_t + 1.745\gamma$	$0.93w_t + 0.915\gamma$	$1.028w_t + 1.011\gamma$
6	13	$24^\circ 28'$	1.181γ	$2w_t + 1.705\gamma$	$1.823w_t + 1.55\gamma$	$0.828w_t + 0.706\gamma$	$0.913w_t + 0.778\gamma$
8	11	$21^\circ 3'$	0.918γ	$2w_t + 1.442\gamma$	$1.87w_t + 1.35\gamma$	$0.719w_t + 0.518\gamma$	$0.791w_t + 0.570\gamma$
10	9	$17^\circ 29'$	0.655γ	$2w_t + 1.179\gamma$	$1.91w_t + 1.135\gamma$	$0.6w_t + 0.354\gamma$	$0.659w_t + 0.389\gamma$
12	7	$13^\circ 46'$	0.393γ	$2w_t + 0.917\gamma$	$1.94w_t + 0.89\gamma$	$0.477w_t + 0.219\gamma$	$0.523w_t + 0.239\gamma$
14	5	$9^\circ 55'$	0.131γ	$2w_t + 0.655\gamma$	$1.97w_t + 0.645\gamma$	$0.345w_t + 0.113\gamma$	$0.377w_t + 0.124\gamma$
16							
					$\Sigma = 14.63w_t + 11.3\gamma$		$\Sigma = 6.661w_t + 5.915\gamma$

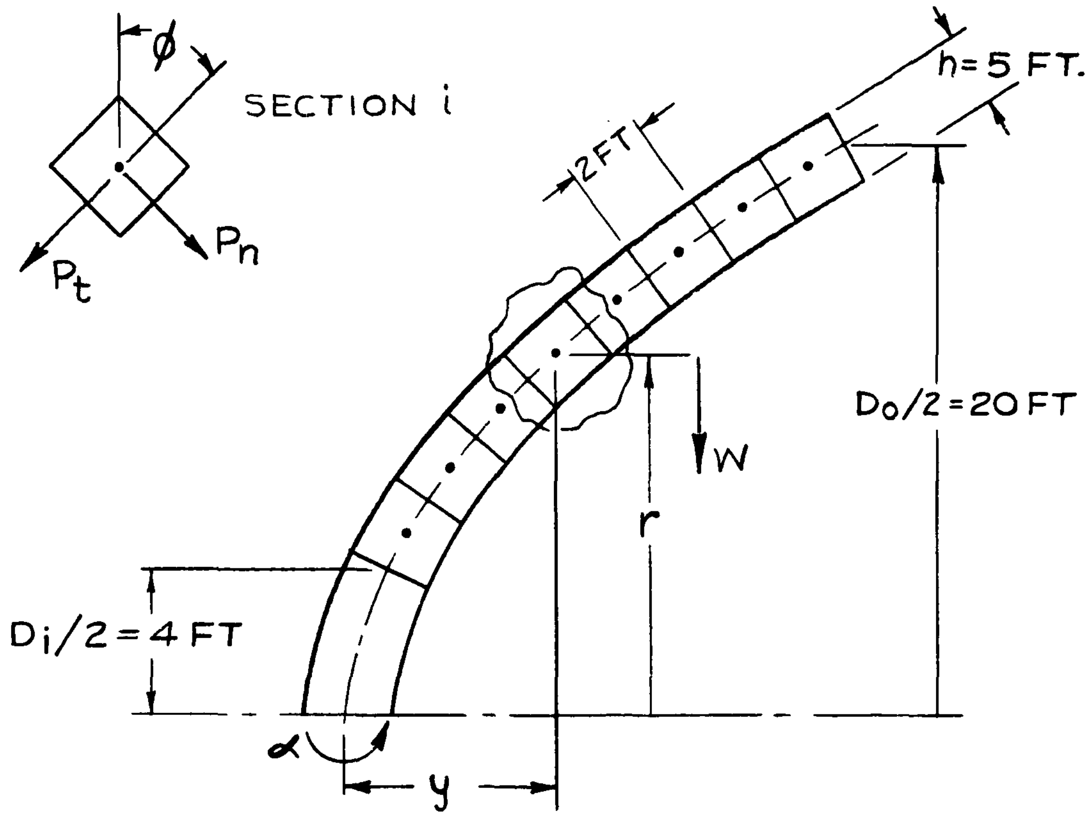

Figure 1-3. Antisymmetrical Loading of Critical Radial Beam

3. Deflections

The wire diameters will first be determined on the basis of bending and shear deflections due to the normal loads for the specified allowable tip deflection of 0.03 inch. The tangential loads (or axial loads) will then be applied to the deflected beam, and new deflections will be determined. The added deflection due to this column effect will be small; otherwise the axial loads would be in the same order of magnitude as the critical buckling load for the column. Hoop stiffness is neglected.

The moments (M_n), area of the moments (A_{M_n}), and moments of the area of the moments ($M_{A_{M_n}}$) due to the normal loads of Table 1-1 are determined in Table 1-2.

The bending deflection at the tip of the beam is

$$\Delta_{bt} = \frac{\Sigma M_{A_{M_n}}}{E_c I} = \frac{3456}{E_c A_c h^2} (4316.6 w_t + 4587.6 \gamma) \text{ in.} \quad (1\text{-}10)$$

or

$$\Delta_{bt} (E_c A_c h^2) \times 10^{-6} = 14.9 w_t + 15.9 \gamma \quad (1\text{-}11)$$

where

h = in.,

A_w = in.^{2},

E_c = psi,

w_t = lb/ft,

and

γ = lb/ft^2 .

Table 1-2. Bending Deflection Calculations

1 x	2 M_n	3 A_{M_n}	4 $M_{A_{M_n}}$
0	0	$1.234w_t + 1.54\gamma$	$1.645w_t + 2.06\gamma$
2	$1.234w_t + 1.54\gamma$	$6.072w_t + 7.424\gamma$	$18.716w_t + 22.272\gamma$
4	$4.838w_t + 5.884\gamma$	$15.444w_t + 18.387\gamma$	$77.22\ w_t + 91.935\gamma$
6	$10.606w_t + 12.503\gamma$	$28.921w_t + 33.414\gamma$	$202.447w_t + 233.898\gamma$
8	$18.315w_t + 20.911\gamma$	$46.043w_t + 51.578\gamma$	$414.387w_t + 464.202\gamma$
10	$27.728w_t + 30.667\gamma$	$66.319w_t + 72.049\gamma$	$729.509w_t + 792.539\gamma$
12	$38.591w_t + 41.382\gamma$	$89.227w_t + 94.107\gamma$	$1159.951w_t + 1223.39\gamma$
14	$50.636w_t + 52.725\gamma$	$114.217w_t + 117.156\gamma$	$1713.255w_t + 1757.34\gamma$
16	$63.581w_t + 64.431\gamma$		
			$\Sigma = 4316.630w_t + 4587.636\gamma$

The shear deflection of a standard, cantilevered AIRMAT beam (drop threads normal to the skins) with a concentrated load at the free end is

$$\Delta_s = PL/pbh \text{ (in.)} \tag{1-12}$$

where

P = concentrated tip load (lb),

p = inflation pressure (psi),

L = length of the beam (in.),

b = width of the beam (in.),

and

h = depth of the beam (in.).

For an AIRMAT with slanted drop threads as shown in Figure 1-2, the shear stiffness, say C, is greatly increased above the stiffness pbh of Equation 1-12. The shear stiffness for this construction is given in Reference 16 for a beam of unit width (b = 1 in.) as

$$C = ph + 2mnh\, A_d E_d \sin^2 \theta \cos \theta \text{ lb/in.} \tag{1-13}$$

where

A_d = area of a drop thread (in.^{2}),

θ = angle between drop thread and normal to the surface,

2n = total number of drop threads per unit length,

and

m = number of drop threads across the unit width.

For the radial beams, an average width of $b = 5\pi/2 = 7.85$ inches is taken for the pressure term of Equation 1-13, and is an adequate approximation since this term is very small compared to the second term. Also, in the second term, the product mb is unity for the radial beam. Substituting the above, along with θ = 33.7^o, into Equation 1-13 yields

$$C = 7.85\, ph + 2(0.256)nh\, A_d E_d \text{ lb,} \tag{1-14}$$

or neglecting the first term (slightly conservative),

$$C \approx \frac{nh}{2} A_d E_d \text{ lb.} \tag{1-15}$$

The shear deflection of each 2-foot increment under the load, P_n, at its mid-span is

$$d\Delta_s = \frac{2P_n L}{nhA_d E_d} \text{ (feet)}$$

$$= \frac{2P_n}{nhA_dE_d} \text{ (feet) for } L = 1 \text{ foot,} \tag{1-16}$$

and the tip deflection is then

$$\Delta_{st} = \frac{24}{nhA_dE_d}\left[\Sigma P_n + 2(i - 1) P_{n_1} + 2(i - 2) P_{n_2} + \ldots 2P_{n_i} - 1\right] \tag{1-17}$$

where

$i = 8$ for 8 increments of 2 feet each.

Substituting for P_n values for Table 1-1 into Equation 1-17,

$$\Delta_{st}(E_dA_d\, nh) = 1526\, w_t + 1546\gamma. \tag{1-18}$$

Substituting for w_t and γ from Equations 1-3 and 1-4 along with $n = 1/4$, $h = 60$, and $E_c = E_d = 29 \times 10^6$ for steel into Equations 1-11 and 1-18 yields

$$\Delta_{bt} \times 10^3 = 18.41\, A_d/A_c + 0.0411\, 1/A_c + 1.00 \text{ in.} \tag{1-19}$$

and

$$\Delta_{st} \times 10^3 = 0.1916\, A_c/A_d + 0.00096\, 1/A_d + 0.4525 \text{ in.} \tag{1-20}$$

The total primary deflection for the particular case of equal cover ply and drop wires ($A_d = A_c = A$) is

$$\Delta \times 10^3 = (\Delta_{bt} + \Delta_{st}) \times 10^3 = 20.054 + 0.04206/A.$$

Solving for A,

$$A = \frac{0.04206}{\Delta \times 10^3 - 20.054} \text{ (in.}^2\text{)} \tag{1-21}$$

and the diameter is

$$d = \sqrt{0.0536/\Delta \times 10^3 - 20.054}\ . \tag{1-22}$$

The required wire diameters for allowable tip deflections of 0.03, 0.05, 0.5, and 1 inch are calculated in Table 1-3. Also given are the corresponding minimum bend radii (ρ) to prevent yielding based on F_{ty} = 100 psi and given by

$$\rho = (Ed)/(F_{ty}) \text{ (for a circular section)}, \tag{1-23}$$

or

$$\frac{\rho}{d} = \frac{29 \times 10^6}{0.2 \times 10^6} = 145. \tag{1-24}$$

Table 1-3. Required Wire Diameters for Primary Allowable Tip Deflection (Neglecting Beam Column Effects) for $d_c = d_d = d$ and Minimum Bend Radii

1 Allowable, Δ (in.)	2 $d^2 = \frac{0.0536}{\Delta \times 10^3 - 20.054}$ (in.^{2})	3 d (in.)	4 $\rho = 145d$ (in.)
0.03	0.005389	0.0734	10.64
0.05	0.00179	0.0423	6.13
0.5	0.0001117	0.0106	1.54
1	0.0000547	0.0074	1.07

The above values are plotted in Figure 1-4, along with the required cover ply wire diameters, d_c, for several other values of the ratio, $k = d_d/d_c$. The obtainable k values are governed by fabrication and packagability limitations and strength requirements.

Beam column effect, for simplicity, considers only the case of Δ = 1 in. and k = 1. Then from Figure 1-4, $d_c = d_d$ = 0.0074 in. The corresponding unit weights are from Equations 1-3 and 1-4.

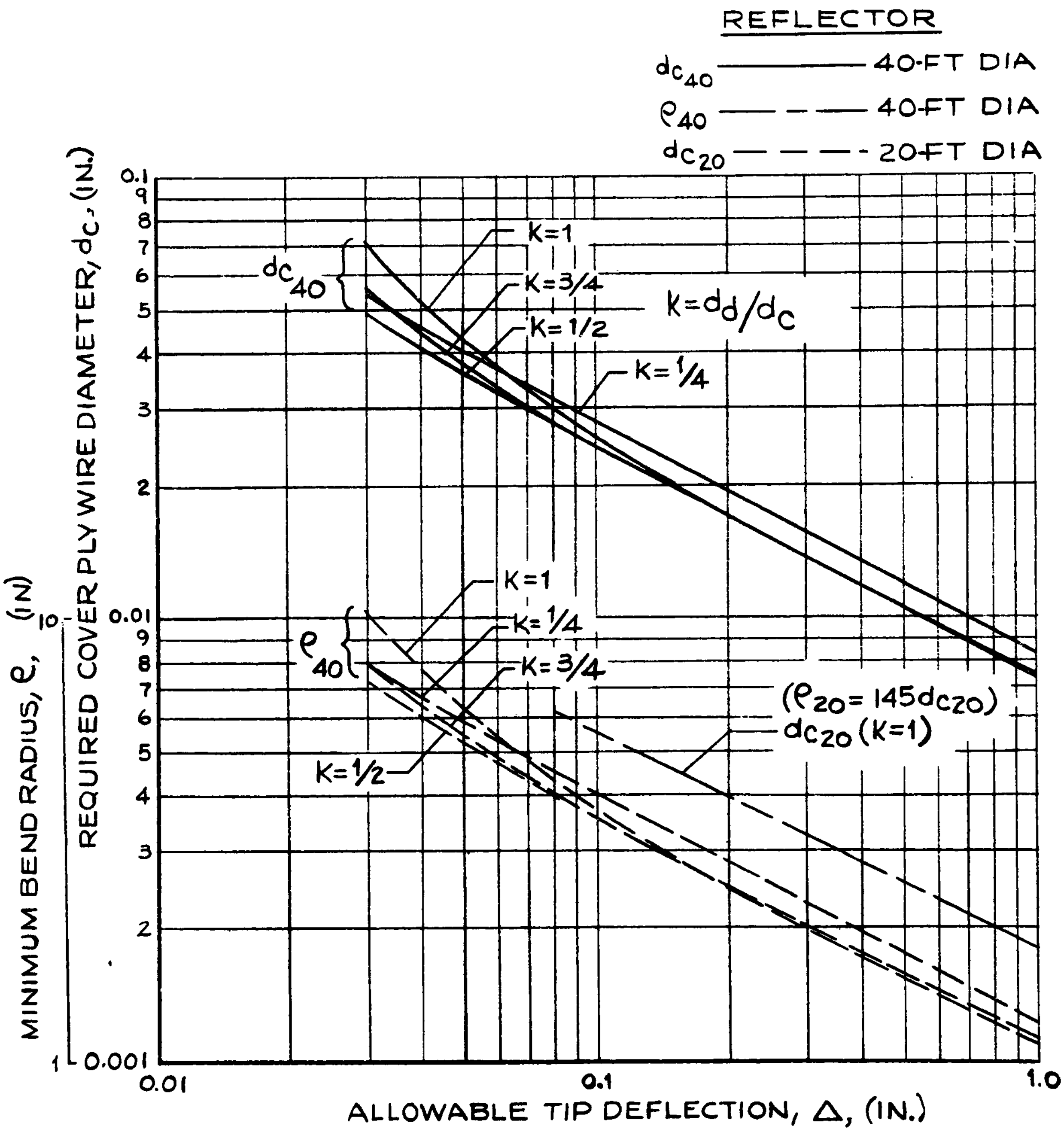

Figure 1-4. Required Cover Ply Wire Diameter and Minimum Bend Radius versus Allowable Tip Deflection for Values of the Drop Wire Diameter to Cover Wire Diameter Ratio, k

$$\gamma = (47)\,(\pi/4)\,(0.0074)^2 + 0.27 = 0.272 \text{ lb/ft}^2$$

and

$$w_t = (129 + 7)\,(\pi/4)\,(0.0074)^2 = 0.00585 \text{ lb/ft.}$$

The above values are substituted into the expressions of column 6 and 8 of Table 1-1, and column 3 of Table 1-2, and recorded in Table 1-4. The deflected curve is determined, the moments due to the axial loads, M_{P_t}, and finally the added tip deflection, Δ_{at}, are calculated in Table 1-4. Again, Equations 1-10 and 1-17 are used to obtain bending and shear deflections. Substituting E = 29 x 10^6, n = 1/4, h = 60, and A = $\pi/4(0.0074)^2$ = 43.0 x 10^{-6} into Equations 1-10 and 1-17 yields

$$\Delta_b = \frac{3456\ \Sigma M_{A_m}}{(29)\,(43.0)\,(3600)} = 0.770 \times 10^{-3}\ \Sigma M_{A_n}, \tag{1-25}$$

$$\Delta_s = \frac{(24)\,(4)\ \Sigma P_n}{(60)\,(43.0)\,(29)} = 1.283 \times 10^{-3},$$

and

$$\times \left[\Sigma P_n + 2(i-1)\,P_{n_2} + \ldots 2\,P_{n_i} - 1\right], \tag{1-26}$$

where

i = 8 for 8 increments of 2 feet each.

The additional tip deflection is (by Equations 1-25 and 1-26)

$$\Delta' = \Delta_b' + \Delta_s' = (0.770 \times 10^{-3})(13.62)$$

$$+(1.283 \times 10^{-3})\,(0.01844 + 0.17674) = 0.0107 \text{ in.} \tag{1-27}$$

This added deflection is only 1 percent of the primary deflection (1 inch) for the case considered and indicates that these secondary deflections may be neglected for the other cases of Figure 1-4.

Table 1-4. Secondary Deflection Calculations (Beam Column Effect)

(1) x	(2) P_t from (6) of Table 1-1 (lb)	(3) P_n from (8) of Table 1-1 (lb)	(4) Δ_s = 1.283 x 10^{-3} [ΣP_n + Eq 1-26 (in.)	(5) A_{M_n} from (3) of Table 1-2	(6) $\Sigma M_{A_{M_n}}$	(7) Δ_b = 0.770 x 10^{-3} $\Sigma M_{A_{M_n}}$ (in.)	(8) $\Delta = \Delta_s + \Delta_b$ (4) + (7) (in.)	(9) Slope = tan ϕ' ≈ sin ϕ'	(10) cos ϕ'	(11) P_t' = (2) (10) ≈ (2) (lb)	(12) P_n' = (2) (9) (9) (11) (lb)	(13) M_n'	(14) A_{M_n}'	(15) $M_{A_{M_n}'}$
0	0.5741	0.4260	0.02291	0.426	1272.955	0.98018	1.003	0.00704	1	0.5741	0.00404	0	0.00404	0.0054
2	0.5323	0.3505	0.02236	2.055	1053.843	0.81146	0.834	0.00704	1	0.5323	0.00375	0.00404	0.01991	0.0597
4	0.4850	0.2810	0.02082	5.092	837.212	0.64465	0.665	0.00679	1	0.4850	0.00329	0.01587	0.05061	0.2530
6	0.4322	0.2170	0.01848	9.258	627.728	0.48335	0.502	0.00638	1	0.4322	0.00276	0.03474	0.09440	0.6608
8	0.3781	0.1597	0.01549	14.299	432.594	0.33310	0.349	0.00567	1	0.3781	0.00214	0.05966	0.14914	1.3423
10	0.3172	0.1097	0.01202	19.985	261.017	0.20098	0.213	0.00458	1	0.3172	0.00145	0.08948	0.21237	2.3361
12	0.2534	0.0681	0.00821	26.119	123.724	0.09527	0.103	0.00308	1	0.2534	0.00078	0.12289	0.28142	3.6585
14	0.1870	0.0359	0.00417	32.535	32.535	0.02505	0.029	0.00121	1	0.1870	0.00023	0.15853	0.35371	5.3056
16			0		0	0	0					0.19518		
											Σ = 0.01844			Σ = 13.6214

C. TWENTY-FOOT DIAMETER REFLECTOR

The effect of the beam length, L, may be quickly estimated on the basis of bending deflections, since the shear deflections are essentially negligible for the slanted drop thread construction in the range of allowable tip deflections of from about 0.1 to 1 inch, observed in Figure 1-4 and columns 4 and 7 of Table 1-4.

In order to quickly compare a 20-foot diameter reflector with the 40-foot diameter reflector, the same rectangular loaded area on one beam is used by choosing (for the 20-foot reflector) a hub diameter, D_i = 4 ft, along with 48 radial beams.

Then, from Equations 1-1 and 1-2,

$$w_r = 0.262\,\gamma \text{ lb/ft} \tag{1-28}$$

and

$$w_\Delta = (\pi/24)\,(8 - x)\gamma = 0.1312(8 - x)\,\gamma \text{ lb/ft.} \tag{1-29}$$

The unit loads, γ and w_t, are again given by Equations 1-3 and 1-4.

The inertia loads to be compared to those of Equations 1-5 through 1-7 become

$$w_{rg} = 0.000855(10 - x)_\gamma \text{ lb/ft,} \tag{1-30}$$

$$w_{\Delta g} = 0.000428(8 - x)\gamma \text{ lb/ft,} \tag{1-31}$$

and

$$w_{tg} = 0.00326(10 - x)\,w_t \text{ lb/ft.} \tag{1-32}$$

Assuming the same parabolic shape as in Figure 1-3 and holding all other parameters for the bending stiffness (EI) constant, the relative tip deflections are determined for the deflection formulas in Figure 1-5.

CASE I

INERTIAL LOADING

$$\frac{120\,\Delta\,EI}{KL^5} = 8L + 9e \qquad (1\text{-}33)$$

CASE II

TRIANGULAR AREA GRAVITATIONAL LOADING

$$\frac{\Delta EI}{w_0} = \frac{11}{120} L^4 \qquad (1\text{-}34)$$

CASE III

RECTANGULAR AREA GRAVITATIONAL LOADING

$$\frac{\Delta EI}{w} = \frac{1}{8} L^4 \qquad (1\text{-}35)$$

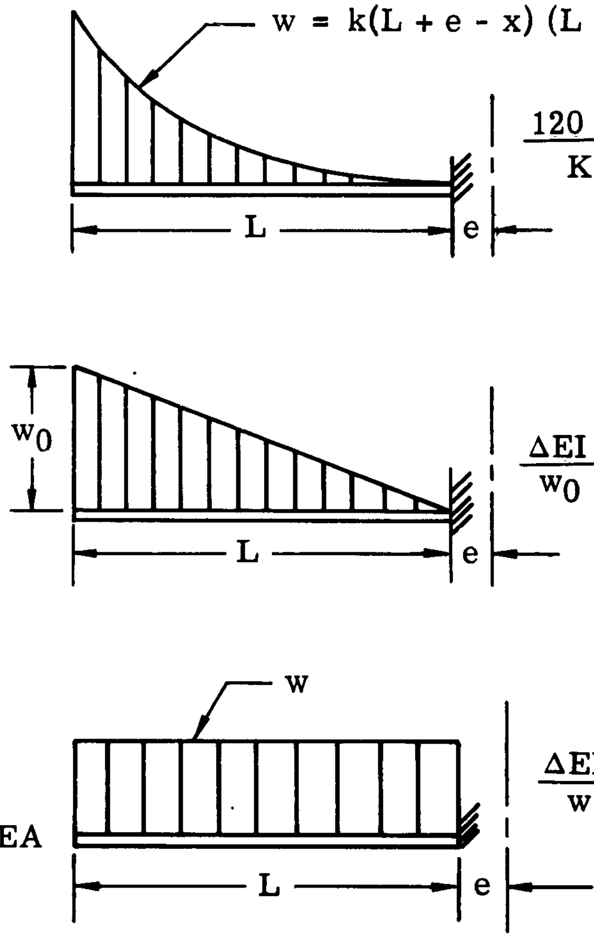

Figure 1-5. Typical Simple Beam Loadings

D. RELATIVE DEFLECTION FOR THE 40-FOOT REFLECTOR

Substitution of the loading for the 40-foot reflector into the previous bending deflection equations yields the following:

Equations 1-1, 1-4, and 1-35,

$$EI\Delta_{wr} = \frac{0.262}{8} \gamma L^4 \qquad (1\text{-}36)$$

$$EI\Delta_{wt} = \frac{w_t}{8} L^4 \,. \qquad (1\text{-}37)$$

Equations 1-2 and 1-34,

$$EI\Delta_{w_\Delta} = \frac{11(0.0656)}{120} \gamma L^5 . \tag{1-38}$$

Equations 1-5, 1-7, and 1-34,

$$EI\Delta_{w_{rg}} = \frac{11(0.000855)}{120} \gamma (L + e) L^4 \tag{1-39}$$

and

$$EI\Delta_{w_{tg}} = \frac{11(0.00326)}{120} w_t (L + e) L^4 . \tag{1-40}$$

Equations 1-6 and 1-33,

$$EI\Delta_{w_{\Delta g}} = \frac{0.000214}{120} \gamma (8L + 9e) L^5 . \tag{1-41}$$

Substituting L = 16 ft and e = 4 ft into Equation 1-36 then 1-41 along with Equations 1-3 and 1-4 for the case of $A_c = A_d = A$ and combining yields

$$EI\Delta = 8861\gamma + 8584 w_t = 1,584,000A + 2,392. \tag{1-42}$$

E. RELATIVE DEFLECTION FOR THE 20-FOOT REFLECTOR

Substitution of Equations 1-1, 1-4, and 1-19 through 1-32 into the deflection formulas along with L = 8 ft and e = 2 ft, for the case of $A_c = A_d = A$, yields

$$EI\Delta = 541.0\gamma + 524.2 w_t = 96,718A + 146. \tag{1-43}$$

F. REQUIRED COVER PLY WIRE DIAMETER

For the same modulus, beam depth, and allowable deflection, Equations 1-42 and 1-43 may be equated after the substitution of $EI = EAh^2/2$ to obtain

$$1,584,000 + \frac{2,392}{A_{40}} = 96,700 + \frac{146}{A_{20}} \tag{1-44}$$

where A_{40} and A_{20} are the required cross-section areas of the cover ply wire for the 40-foot and 20-foot diameter reflectors respectively.

Then

$$A_{20} = \frac{146\ A_{40}}{1,487,300\ A_{40} + 2,392}, \text{ or the required diameter is} \tag{1-45}$$

$$d_{20} = \sqrt{\frac{146\ d_{40}^2}{1.168,100\ d_{40}^2 + 2,392}} . \tag{1-46}$$

Equation 1-46 is also plotted in Figure 1-4 for values of d_{40} taken from Figure 1-4 in the range $0.1 < \Delta < 1$, where shear deflections are negligible. Also, as an added assist in using the curves in Figure 1-4, it must be recognized that the wire sizes given by the curves are based on 96 radial wires. If additional radial wires are provided, the diameter of the wires is reduced, since it is actually the total cross-sectional area of the wires that is required rather than the actual size of the wire. For this same reason, the ordinate giving the minimum bend radius also does not apply except when only 96 radial wires are used. In most practical applications more than 96 wires would be used. The 96 number was only used as one of the initial simplifying assumptions.

Goodyear Aerospace Corp, Akron, Ohio. ON ADVANCED ANTENNA DESIGN TECHNIQUES by D. D. Collins and J. C. Bell Jr., GER 11246. Report No. 4, Final Report, June 62 - Sept 63. 320p incl. illus. (Contract DA-36-039 SC-90746) DA Project No. 3A99-12-001.

Unclassified Report

Space vehicle antenna and ground-based tracking antenna system parameters are studied, establishing requirements as design goals. Various types of antenna configurations consisting of 12 space and 22 ground-based antenna concepts are investigated to meet established requirements. Those concepts appearing most desirable for meeting these requirements are evaluated and compared. One space antenna and two ground-based antennas, determined as the most promising, are studied from the standpoints of *detail design, structural* and mechanical aspects, and performance. New material applications are investigated, and new manufacturing techniques are developed. Three scale models are

(over)

UNCLASSIFIED

1. Antennas - Design-development, reflectors, materials.
2. Antennas - Performance.
3. Antennas - Configuration, parabolic, Cassegrain.
4. Antennas, Reflectors, inflatable, expandable.

I. Antenna Advanced Design Techniques - Space and Ground.
II. Collins, D. D. and Bell, J. C. Jr.
III. U.S. Army Electronics R&D Lab, Fort Monmouth, N. J.
IV. Contract DA-36-039 SC-90746.

UNCLASSIFIED

Goodyear Aerospace Corp, Akron, Ohio. ON ADVANCED ANTENNA DESIGN TECHNIQUES by D. D. Collins and J. C. Bell Jr., GER 11246. Report No. 4, Final Report, June 62 - Sept 63. 320p incl. illus. (Contract DA-36-039 SC-90746) DA Project No. 3A99-12-001.

Unclassified Report

Space vehicle antenna and ground-based tracking antenna system parameters are studied, establishing requirements as design goals. Various types of antenna configurations consisting of 12 space and 22 ground-based antenna concepts are investigated to meet established requirements. Those concepts appearing most desirable for meeting these requirements are evaluated and compared. One space antenna and two ground-based antennas, determined as the most promising, are studied from the standpoints of detail design, structural and mechanical aspects, and performance. New material applications are investigated, and new manufacturing techniques are developed. Three scale models are

(over)

UNCLASSIFIED

1. Antennas - Design-development, reflectors, materials.
2. Antennas - Performance.
3. Antennas - Configuration, parabolic, Cassegrain.
4. Antennas, Reflectors, inflatable, expandable.

I. Antenna Advanced Design Techniques - Space and Ground.
II. Collins, D. D. and Bell, J. C. Jr.
III. U.S. Army Electronics R&D Lab, Fort Monmouth, N. J.
IV. Contract DA-36-039 SC-90746.

UNCLASSIFIED

Goodyear Aerospace Corp, Akron, Ohio. ON ADVANCED ANTENNA DESIGN TECHNIQUES by *D. D. Collins and* J. C. Bell Jr., GER 11246. Report No. 4, Final Report, June 62 - Sept 63. 320p incl. illus. (Contract DA-36-039 SC-90746) DA Project No. 3A99-12-001.

Unclassified Report

Space vehicle antenna and ground-based tracking antenna system parameters are studied, establishing requirements as design goals. Various types of antenna configurations consisting of 12 space and 22 ground-based antenna concepts are investigated to meet established requirements. Those concepts appearing most desirable for meeting these requirements are evaluated and compared. One space antenna and two ground-based antennas, determined as the most promising, are studied from the standpoints of detail design, structural and mechanical aspects, and performance. New material applications are investigated, and new manufacturing techniques are developed. Three scale models are

(over)

UNCLASSIFIED

1. Antennas - Design-development, reflectors, materials.
2. Antennas - Performance.
3. Antennas - Configuration, parabolic, Cassegrain.
4. Antennas, Reflectors, inflatable, expandable.

I. Antenna Advanced Design Techniques - Space and Ground.
II. Collins, D. D. and Bell, J. C. Jr.
III. U.S. Army Electronics R&D Lab, Fort Monmouth, N. J.
IV. Contract DA-36-039 SC-90746.

UNCLASSIFIED

Goodyear Aerospace Corp, Akron, Ohio. ON ADVANCED ANTENNA DESIGN TECHNIQUES by D. D. Collins and J. C. Bell Jr., GER 11246. Report No. 4, Final Report, June 62 - Sept 63. 320p incl. illus. (Contract DA-36-039 SC-90746) DA Project No. 3A99-12-001.

Unclassified Report

Space vehicle antenna and ground-based tracking antenna system parameters are studied, establishing requirements as design goals. Various types of antenna configurations consisting of 12 space and 22 ground-based antenna concepts are investigated to meet established requirements. Those concepts appearing most desirable for meeting these requirements are evaluated and compared. One space antenna and two ground-based antennas, determined as the most promising, are studied from the standpoints of detail design, structural and mechanical aspects, and performance. New material applications are investigated, and new manufacturing techniques are developed. Three scale models are

(over)

UNCLASSIFIED

1. Antennas - Design-development, reflectors, materials.
2. Antennas - Performance.
3. Antennas - Configuration, parabolic, Cassegrain.
4. Antennas, Reflectors, inflatable, expandable.

I. Antenna Advanced Design Techniques - Space and Ground.
II. Collins, D. D. and Bell, J. C. Jr.
III. U.S. Army Electronics R&D Lab, Fort Monmouth, N. J.
IV. Contract DA-36-039 SC-90746.

UNCLASSIFIED

UNCLASSIFIED

designed, fabricated, and evaluated, demonstrating the feasibility of the selected concepts. Evaluation indicates that the folding metallic petal space antenna is structurally and mechanically feasible, practical to manufacture, capable of being deployed in space, and capable of performance comparable to a rigid close-tolerance parabolic reflector. Evaluation of the inflatable paraboloid and inflatable lenticular ground-based antenna models demonstrates their capability of providing quickly erectable, lightweight, packageable antennas that will retain the desired parabolic shape when pressurized. Limited packaging and inflation tests show that these inflatable antennas can be packaged into a relatively small volume and reinflated and still retain their original contour with no damage to the reflective surface.

UNCLASSIFIED

UNCLASSIFIED

designed, fabricated, and evaluated, demonstrating the feasibility of the selected concepts. Evaluation indicates that the folding metallic petal space antenna is structurally and mechanically feasible, practical to manufacture, capable of being deployed in space, and capable of performance comparable to a rigid close-tolerance parabolic reflector. Evaluation of the inflatable paraboloid and inflatable lenticular ground-based antenna models demonstrates their capability of providing quickly erectable, lightweight, packageable antennas that will retain the desired parabolic shape when pressurized. Limited packaging and inflation tests show that these inflatable antennas can be packaged into a relatively small volume and reinflated and still retain their original contour with no damage to the reflective surface.

UNCLASSIFIED

UNCLASSIFIED

designed, fabricated, and evaluated, demonstrating the feasibility of the selected concepts. Evaluation indicates that the folding metallic petal space antenna is structurally and mechanically feasible, practical to manufacture, capable of being deployed in space, and capable of performance comparable to a rigid close-tolerance parabolic reflector. Evaluation of the inflatable paraboloid and inflatable lenticular ground-based antenna models demonstrates their capability of providing quickly erectable, lightweight, packageable antennas that will retain the desired parabolic shape when pressurized. Limited packaging and inflation tests show that these inflatable antennas can be packaged into a relatively small volume and reinflated and still retain their original contour with no damage to the reflective surface.

UNCLASSIFIED

UNCLASSIFIED

designed, fabricated, and evaluated, demonstrating the feasibility of the selected concepts. Evaluation indicates that the folding metallic petal space antenna is structurally and mechanically feasible, practical to manufacture, capable of being deployed in space, and capable of performance comparable to a rigid close-tolerance parabolic reflector. Evaluation of the inflatable paraboloid and inflatable lenticular ground-based antenna models demonstrates their capability of providing quickly erectable, lightweight, packageable antennas that will retain the desired parabolic shape when pressurized. Limited packaging and inflation tests show that these inflatable antennas can be packaged into a relatively small volume and reinflated and still retain their original contour with no damage to the reflective surface.

UNCLASSIFIED

DISTRIBUTION LIST

Address	Copy No.
Chief of Research and Development OCS, Department of the Army Washington 25, DC	1
Commanding General US Army Electronics Command ATTN: AMSEL-AD Fort Monmouth, New Jersey	2-4
Director, US Naval Research Laboratory ATTN: Code 2027 Washington 25, DC	5
Commanding Officer and Director US Navy Electronics Laboratory San Diego 52, California	6
Headquarters, Electronic Systems Division ATTN: ESRR & ESSD L.G. Hanscom Field Bedford, Massachusetts	7-8
Commander, Defense Documentation Center (formerly ASTIA) ATTN: TIPCR Cameron Station, Bldg 5, 5010 Duke Street Alexandria 4, Virginia	9-12
Commanding Officer US Army Electronics Research and Development Laboratory ATTN: Director of Research/Engineering Fort Monmouth, New Jersey	13
Commanding Officer US Army Electronics Research and Development Laboratory ATTN: Technical Documents Center Fort Monmouth, New Jersey	14

DISTRIBUTION LIST (Continued)

Address	Copy No.
Missiles and Space Division Lockheed Aircraft Corporation ATTN: Technical Information Center 3251 Hanover Street Palo Alto, California	15
Fairchild Stratos Corporation ATTN: Librarian Hagerstown, Maryland	16
National Aeronautics and Space Administration Spacecraft Systems and Projects Division ATTN: Mr A. Kampinsky, Code 621 Goddard Space Flight Center Greenbelt, Maryland	17
Commanding General US Army Satellite Communications Agency ATTN: AMXSC-5 Fort Monmouth, New Jersey	18-19
Commanding Officer US Army Electronics Research and Development Laboratory ATTN: SELRA/NRA (Mr. F.J. Triolo) Fort Monmouth, New Jersey	20-21
General Electric Company Ordnance Department ATTN: Mr. Paul Blasangame Pittsfield, Massachusetts	22
Commanding Officer US Army Electronics Research and Development Laboratory ATTN: SELRA/LNR (Marine Corps Liaison Office) Fort Monmouth, New Jersey	23